Università degli Studi di Genova

Doctorate School in

Sciences and Technologies of

Chemistry and Materials

Doctorate in Chemical Sciences and Technologies

XXX CYCLE

Thermodynamic modeling of multicomponent alloy systems for the simulation of bulk Co alloys and related Coatings

Yao Wang

Tutor: **Prof. Gabriele Cacciamani**

Abstract

Co-based alloys received much attention because of its outstanding physical and chemical properties; however industrial applications as a high temperature material are limited by insufficient strength. The addition of alloying elements offer the opportunity for a considerable improvement, which makes Co-based alloys possibly become promising candidates for the next generation of superalloys.

To extend the temperature application range of high temperature materials metallic coatings are applied to protect the substrate, extend the working time and improve the working temperature.

In the present work, thermodynamic databases describing C-Co-Cr-Ni-Ta-W bulk alloys and Al-Co-Cr-Ni-Y alloy coatings were developed, which can be used for materials design of bulk superalloys and bond coat, respectively. To this end appropriate phase models were selected for all the phases appearing in the systems and especially for the Laves, Sigma, Mu and R phases, with particular attention to the consistency between thermodynamics and crystal structure.

Two important ternary subsystems Co-Cr-Ni and Co-Cr-Ta were completely assessed while other systems were partially taken from literature and possibly adapted to our models until the whole C-Co-Cr-Ni-Ta-W database was built. As a result, several multi-component commercial alloys involving C, Co, Cr, Ni, Ta and W can be simulated.

As for the coatings database, all the binary and ternary subsystems of the Al-Co-Cr-Ni-Y system were critically reviewed on the basis of the available literature. Then thermodynamic descriptions of binary systems taken from the literature were reviewed and refined if necessary. For each phase the model selection procedure is discussed in detail. A single Gibbs energy equation is used to model the order/disorder relation between ordered $L1_2$ and its disordered structure A1, as well as between ordered B2 and its disordered structure A2. The energy of vacancies in the A2 phase is adjusted to enhance its rationality. The Al-Co-Cr, Al-Co-Ni, Al-Cr-Ni, Al-Co-Y, Al-Cr-Y, Al-Ni-Y and Co-Ni-Y systems are modeled using the CALPHAD approach. Phase equilibria in the Al-rich corner are also considered during the optimization. According to the comparison, very good agreement between calculated results and experimental data is obtained. Based on the previous work, some extrapolations and brief discussions about the Al-Co-Cr-Ni quaternary system are performed. Satisfactory agreement between the calculations and experimental results are obtained, unless the stability range of the σ phase is slightly underestimated.

A reliable and self-consistent thermodynamic database for the Al-Co-Cr-Ni-Y multicomponent system is firstly obtained. As a conclusion a short analysis of the influence of Y addition on the Al-Co-Cr-Ni phase relations is presented based on the results of our calculations.

The thermodynamic descriptions of the C-Co-Cr-Ni-Ta-W and Al-Co-Cr-Ni-Y systems developed in this work can be used to support the design of new alloying compositions for bulk alloys and related coatings. Moreover they also play an important role in the kinetic simulation of the interactions occurring at the joint between coatings and bulk alloys when in service.

Acknowledgements

I would like to express my sincere gratitude to my advisor Prof. Gabriele Cacciamani for his motivation and guidance in my Ph.D. study and related research. It has been an honor to be his Ph.D. student and I benefit a lot from the joy and enthusiasm he has for the scientific research. Without his patient instruction and expert guidance, the completion of this thesis would not have been possible.

I would also like to express a very special thank to Prof. Paola Riani, who gave me much guidance in the experiment research with patient.

I would like to thank group members: Sofia Gambaro, Giacomo Roncallo, Marlena Ostrowska and Saverio Sitzia. I felt very honored to work with them. I also would like to thank the administrative staff in the department, who gave me the help in the past three years.

I would also like to thank my Chinese friends in Genoa: Anda Liu, Tianwen Qi, Shi Zhang, Yin Shen, Mengying Yan, Renyong Tu, Tao Li and Xue Bai. Thank all of you for bringing a lot of fun and help for me.

I should finally owe my gratitude to my family. Words cannot express how grateful I am to my parents and sister for their love and encouragement during my study career.

Contents

1. Introduction

Superalloys are defined as a kind of materials which can withstand loading at elevated temperature (above 600 °C). They have been widely used as critical structural materials in aircraft engines, blades, gas turbines, chemical processes and so on.

The mechanical properties of materials at high temperature usually are pretty different from those at room temperature because of the thermal effect. The larger grains and accelerated creep deformation caused by the high temperature causes a lower strength compared to the room temperature. In most demanding applications metals are subjected to several thermal cycles under high pressure for a long period. In order to survive, superalloys are supposed to have a higher melting point, excellent corrosion, oxidation, thermal creep and fatigue resistance as well as good mechanical strength.

They were firstly manufactured in the 1940s by military engineers to satisfy the high strength and high temperature resistance needed in jet engines. Then they have been widely utilized by engine and energy industries. In principle superalloys consist of one major element from Group VIIIB and some minority alloying elements. Based on chemical compositions, the superalloys are classified as Fe-based, Co-based or Ni-based alloys. The elements Co and Ni have higher melting point than Fe and their alloys are able to survive above 800°C. The major stable phases in the Co or Ni rich superalloys are listed as the following:

1) Gamma (γ) it is the continuous matrix with the face-centered-cubic (fcc, cF4-Cu, A1) structure. Pure Ni presents only the fcc structure while an allotropic transformation makes cobalt to adopt the fcc structure above 422 °C and the hcp below. The dissolution of appropriate elements in γ phase possibly improves its strength. Typical elements selected as addictions are Cr, Al, Mo, W and so on. It's worth to mention that Co can become an alloying element in the Ni-based alloys and vice versa.

2) Gamma prime (γ') is an ordered (cP4-$AuCu_3$, $L1_2$) crystal structure coherently precipitating from the fcc matrix. It is considered as a very important strengthening phase. Considering the order-disorder relationship between γ and γ', the small mismatch and the chemical compatibility make γ' homogeneously distributed among the matrix. In addition, γ' is pretty ductile. The volume fraction of γ' with the composition Ni_3(Al, Ti) in the Ni-based alloys can reach up to 70 %.

3) Topologically Close-Packed (TCP) phases are intermetallic phases characterized by a densely packed structure. Typical examples are the Laves phases (with formula AB_2), Sigma phase (AB), and Mu phase (A_6B_7) phase. In the formula A represents an element on the left side of the Mn group in the periodic table (such as Cr, V and so on) and B represents an elements on the right side of the Mn group such as Fe, Co, Ni and so on. TCP phases can form during heat treatment or during service, showing a needle-like or plate-like shape. They are generally very brittle and detrimental to the performance of materials. There are two main reasons for their harmful function: they

waste the strengthening elements in a useless form and they can trigger the crack due to their brittle character.

4) Carbides: Carbon, with an amount of 0.05-0.2 wt.%, can combine at high temperature with reactive and refractory elements to form carbides such as TaC, TiC and WC. During heat treatment or service, they decompose and lower carbides such as $M_{23}C_6$ and M_6C, are formed, possibly located on the grain boundaries. Normally C atoms occupy the interstitial site of the crystal structure. In the Ni-based alloys, more than one metallic element is contained in the $M_{23}C_6$ [1].

Among the previous mentioned phases, γ' is regarded as the main strengthening phase and offers the excellent high temperature performance of superalloys. In reality, Ni-based superalloys are the dominant high-temperature materials, although Co-based have a higher melting temperature, because of the existence of γ'-Ni_3Al. However, the industrial need for service temperatures beyond the ability of Ni-based alloys [2], makes Co-based alloys still regarded as a promising supplement.

Traditional Co-based superalloys show relatively limited strength at high temperatures due to the lack of the strengthening mechanism based on γ'. Without the existence of γ', Co-based alloys can only be intensified by carbides ($M_{23}C_6$, M_7C_3 and so on) and solid solutions. Through the interaction with carbides and fcc phase, the dissolution of moderate quantities of additional metallic elements can improve the strength. In 2006 Sato et al. [3], while investigating two isothermal sections of the Al-Co-W system at 900 and 1000 °C, found a ternary compound $Co_3(Al,W)$ with the $L1_2$ structure, being stable at 900°C and precipitating in the γ cobalt matrix with strong coherency. Their observations are considered as a milestone in the development of superalloys. The discovery of γ'-$Co_3(Al,W)$ makes Co-based alloys become a great promising candidate of the next generation high temperature materials with improved high-temperature properties, though these new alloys are still far from applications due to the limited stability of this ternary phase.

As previously mentioned, the Co-based alloys with respect to the Ni- or Fe-based ones, have higher melting points and flatter stress-rupture curves, better hot-corrosion resistance in gas turbine atmospheres, better weldability and thermal fatigue resistance. On the contrary they show lower strength, ductility and fracture toughness. With some additional metallic elements a series of commercial Co-based alloys such as ECY768, FXS414, Mar-M302 and so on, have been developed and successfully applied in the hot sections of gas turbines.

The physical performance and chemical component of superalloys are degrading with the increasing exposure time. The serving temperature is obviously limited by the melting point of superalloys, which is usually less than around 1327 °C. The further improvements of the temperature capability of superalloys become very tough. The idea to add a layer on the surface of Ni-based superalloys was firstly practiced in the 1960s [4]. The existence of the coatings on the surface of high temperature materials tend to protect the substrate and extend the working time. For this destination, two forms of protective coating designed for turbine application have been widely used: diffusion aluminide coatings and MCrAlY (M=Ni, Co, or Ni-Co)

overlay coatings.

Diffusion aluminide coatings can be formed on the surface based on the deposition of aluminum by chemical vapor deposition and heat treatment. Finally the covered alumina layer improves highly the resistance to oxidation. For greater resistance to oxidation and corrosion, the MCrAlY overlay coatings are invented with higher cost. They have the advantage of a greater flexibility of coating compositions over the diffusion coatings.

In order to meet the requirement of higher temperature, thermal barrier coatings are designed. At first they mainly consist of the ceramic layer. By their natural low thermal conductivity, the ceramic layers can act as a good thermal insulation to lower the temperature of the metallic substrate. The difference in the thermal expansion coefficients between superalloys substrate and ceramic coatings causes the formation of thermal stresses during the service, which leads to the final failure. For overcoming this trouble, a kind of bond layer is considered as a transition from the substrate to the ceramic coating; therefore thermal barrier coatings are eventually accepted to comprise two layers: a diffusion aluminide or MCrAlY bond coating and a ceramic top coating.

Figure 1-1 shows the different types of coatings relating to the corrosion resistance and Oxidation resistance [5]. Among these selections, CoCrNiAlY coatings present relatively good overall performance.

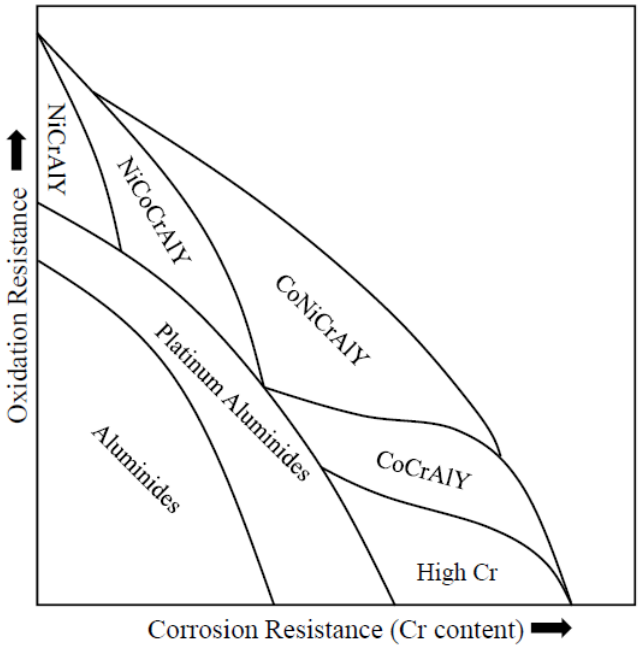

Fig. 1-1 The coatings types relating to the corrosion resistance and oxidation resistance

In view of the development of new alloys or improvement of the traditional ones, a detailed description of thermodynamic properties and phase equilibria of the involved multi-component systems is fundamental. This work is interested in the development of the reliable thermodynamic database of Co-based bulk alloys and coatings.

Many binary and ternary systems formed by the main alloying elements, namely Co, Cr, Ni, W, Ta, C, Al, Ti, Mo, etc., have already been modelled in literature or have been included in commercial databases. In both cases however there are difficulties and drawbacks: thermodynamic assessments reported in literature are typically performed by different authors, which often use different thermodynamic models for the same phase in different systems. This makes very difficult or even impossible to merge interaction parameters from different assessments in a single multi-component thermodynamic database. Moreover, owing to well reproduced phase equilibria, thermodynamics is often poorly defined and the adopted interaction parameters fail to give reliable higher order extrapolations.

On the other hand, commercial databases, while self-consistent, are usually reliable only in restricted composition ranges. Moreover thermodynamic models introduced several years ago have not been improved because a change would require a complete re-assessment of all the systems included in the database. So the development of a new self-consistent thermodynamic database for Co-based alloys with improved phase models is highly advisable.

1.1 Co-based bulk alloys

As an interested bulk superalloy, the C-Co-Cr-Ni-Ta-W system is selected as one of the research targets in the current work, since carbides are the main strengthening mechanism and refractory elements take effect in the solid-solution hardening. W and Ta are the main elements to form the carbides. A few amount of Cr could improve the resistance of corrosion during the service. However with adding metals in the superalloys, the unwanted phases (sigma, mu and so on) degrading the performance possibly become stable if the quantity of each additional element is not appropriately controlled. Theoretical simulations by using the thermodynamic database can predict phase constitutions at the interested compositions and temperatures. The target of this work is to construct a thermodynamic database of C-Co-Cr-Ni-Ta-W system. Several steps are taken to implement it. Firstly relevant literatures are collected and then carefully reviewed. In the basis of the critical evaluation, the models of phases involved need be selected. By combining the descriptions in the literature and the key assessment on the parameters of binary systems and ternary systems, the database of this multicomponent system is obtained. Among a quite large amount of binary and ternary subsystems in this six multi-component system, the Co-Cr-Ni and Co-Cr-Ta systems are optimized in the present work, which is a part of the thermodynamic modelling of C-Co-Cr-Ni-Ta-W system.

1.2 CoNiCrAlY coatings

The phase organizations partly determined by alloy compositions play an important role in the material properties. In general Al-Co-Cr-Ni alloys are accepted as the main coatings of superalloys and small amount of Y addition is useful to improve oxide scale adherence. Among four types of stable phases in the Co and Ni-based alloys above mentioned, several phases are beneficial for the properties while some are detrimental in the service period. Co and Ni are the major elements in the high temperature materials. The mixture of Co and Ni with the appropriate additional amount of Al, Cr and Y make the coatings reach the overall good performance. However it becomes very difficult to analyze the change of phases caused by each element without simulations if there are more than four components in the alloys. The reliable thermodynamic database can be used to calculate the stable phases and their quantities in advance, which is a good start to determine the additional amount of each element.

The objective is to investigate the Al-Co-Cr-Ni-Y system and its subsystems with CALPHAD approach and establish a reliable thermodynamic database to support the design of CoNiCrAlY coatings.

In order to actualize it, firstly all the binary subsystems will be systematically reviewed according to the available literatures and then some of them will be revised or optimized based on the evaluation, and then they are ternary subsystems. Liquid, solid solutions A1, A2 and A3, ordered $L1_2$ and B2 as well as the intermetallic compounds are well described with the critical consideration of their models. After that quaternary systems are evaluated. Finally a reliable and self-consistent of thermodynamic database of the Al-Co-Cr-Ni-Y multi-component system is obtained. On this basis several calculations of the alloys are released.

2. The CALPHAD approach

In the early 20th century, phase diagrams firstly are calculated by using the sample models. Since 1970s, the computer technologies and the thermodynamic theories have both been highly improved. The computer-coupling of phase diagram and thermochemistry known as CALPHAD (an abbreviation of the CALculation of PhAse Diagrams [6, 7]) method was proposed by Kaufman and then gradually developed by several researchers. This is a semi-empirical method to calculate phase diagrams under equilibrium conditions, partly relying on experimental data. By combining experimental determinations and thermodynamic simulations, it drastically decreases the need of experiments during phase diagram investigations. Based on the CALPHAD approach the Gibbs energies of the phases are expressed as a function of temperature and composition. Usually the effect of the pressure is ignored in the intermetallic systems. Other thermodynamic quantities (eg. enthalpy, entropy, heat capacity) can be derived from the Gibbs energy. Some important thermodynamic relations regarding the Gibbs energy are shown in the following:

Gibbs energy G: $G = H - TS$ (2-1)

Enthalpy H: $H = G - T \bullet \frac{\partial G}{\partial T}$ (2-2)

Entropy S: $S = -\left(\frac{\partial G}{\partial T}\right)_{P,Ni}$ (2-3)

Heat capacity C_P: $C_P = \left(\frac{\partial H}{\partial T}\right)_P = T \bullet \left(\frac{\partial S}{\partial T}\right)_P = -T \bullet \left(\frac{\partial^2 G}{\partial T^2}\right)_{P,Ni}$ (2-4)

By extrapolating the thermodynamic descriptions of the binary and ternary subsystems, quaternary system can be preliminarily calculated. If necessary, a few parameters are added. In principle, the extrapolations could reproduce most of the phase equilibria when the descriptions of the subsystems are reliable. The thermodynamic descriptions can reach good accuracy with limited experimental data. Then, compared to a traditional experimental approach, this method offers a high-efficiency way to explore phase equilibria of multicomponent systems.

Figure 2-1 presents the detailed flow chart of the CALPHAD method [8]. As previously mentioned, the target is to determine the Gibbs energy functions of phases. The analytical model of the Gibbs energy of each phase is selected on the basis of crystal structure and chemical components. There are several adjustable parameters in the Gibbs energy functions, which need to be determined with the aid of reliable experimental data. In principle, experiments on phase equilibria and thermodynamic quantities are collected and then critically evaluated on the basis of the information about the experimental procedure adopted. Moreover the thermodynamic data obtained by first-principles calculations are also considered as input during the

assessment. When the optimization process is completed, the calculated parameters are compiled into a thermodynamic database, which can be used for the calculation of higher order systems.

The calculated phase and property diagrams based on the obtained thermodynamic database are a common and useful tool to accelerate the process of new materials design. It's well known that pure elements as structural materials hardly fulfill the industrial requirements. Then small amounts of alloying elements are added in the matrix in order to improve the material properties. Taking Co-alloys as an example, up to 8 alloying elements are found in the Co matrix of the MAR-M302 commercial alloys [9]. What's more the thermodynamic database is the necessary input of the phase field simulations and kinetic diffusion calculations.

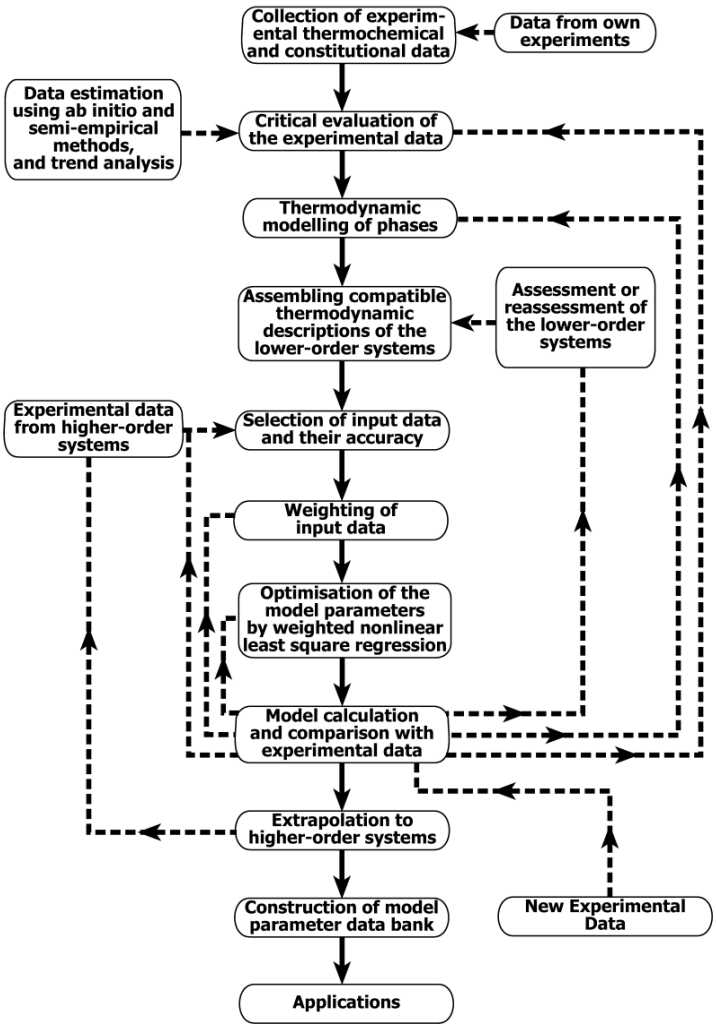

Fig. 2-1 The flowchart of CALPHAD method [8]

At current, there are several commercial softwares for performing the CALPHAD task, such as Thermo-Calc [10], Pandat [11], Factsage [12] and so on. Essentially these softwares combine phase models and thermodynamic equilibrium calculations to calculate phase equilibria at different conditions, as well as the metastable phase constitutions.

Thermo-Calc software, used in the present work, was first released by KTH in 1981. It's widely employed for phase diagram simulations. It can handle multicomponent systems with up to 40 elements, 1000 species and many different solution or stoichiometric phases. The workflow of Thermo-Calc is provided in Figure 2-2. It is composed of several modules and each of them has its own specialized function.

The current work has been performed using the Thermo-Calc software and the assessment part has been done by means of the optimization module PARROT [13] which works by minimizing the sum of the squared differences between experimental and calculated values. Phase diagrams are calculated with the POLY-3 module of the software package Thermo-Calc.

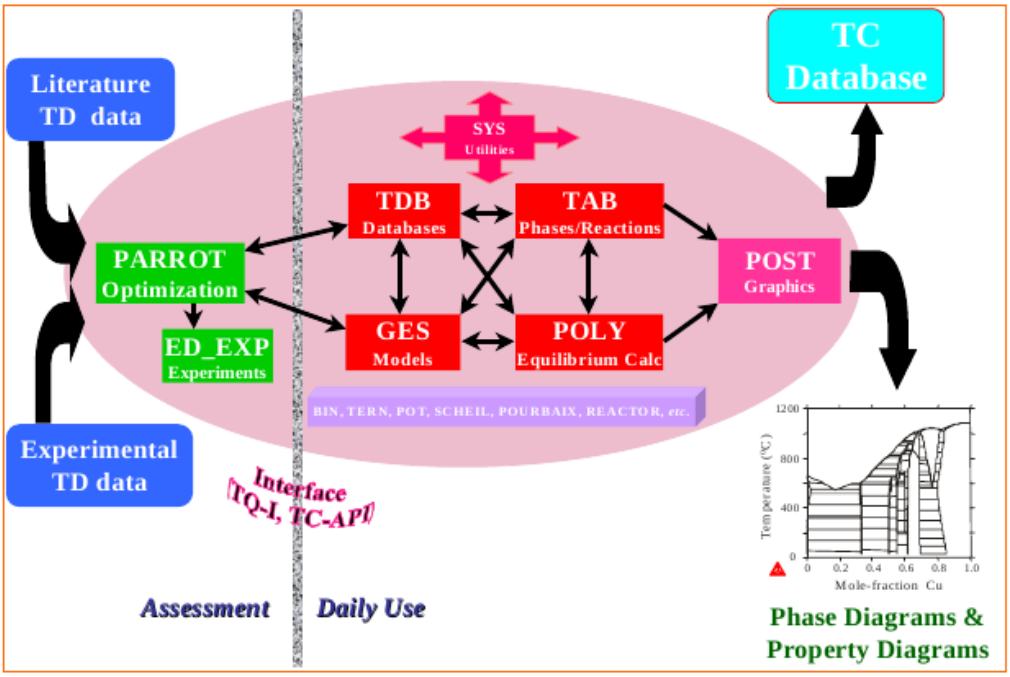

Fig. 2-2 The workflow of Thermo-Calc software taken from Thermo-Calc user's guide

3 Thermodynamic models

3.1 Common phase models

The Gibbs energy of a phase ϕ can be expressed as the sum of a few terms:

$$G^{\phi} = {}^{ref}G^{\phi} + {}^{id}G^{\phi} + {}^{ex}G^{\phi} + {}^{mag}G^{\phi} \tag{3-1}$$

${}^{ref}G^{\phi}$, the reference term, is the Gibbs energy of the mechanical mixing of the constituents. ${}^{id}G^{\phi}$, the ideal mixing term, represents the effect of the ideal configurational entropy of mixing on the Gibbs energy. ${}^{ex}G^{\phi}$ is the excess Gibbs energy, accounting for the difference between ideal solution and real solution. ${}^{mag}G^{\phi}$ represents the contribution of magnetic ordering.

The selection of most appropriate thermodynamic model is one of the key steps to build a reliable thermodynamic database. In the selection of the optimal thermodynamic model for each phase, it is necessary to consider the crystal structure, chemical composition, magnetic transition, ordered-disorder phase change and other information. The following is a brief introduction to the thermodynamic models involved in this database. The crystallographic data of all stable phases and their adoptive models in the C-Co-Cr-Ni-Ta-W and Al-Co-Cr-Ni-Y systems are summarized in Table 3-1 and Table 3-2, respectively.

3.1.1 Pure elements

In the case of a pure element, second and third terms of eq. (3-1) are missing and any dependence on composition of course disappears. Eq. (3-1) becomes:

$$G^{\phi} = {}^{ref}G^{\phi} + {}^{mag}G^{\phi} \tag{3-2}$$

with

$${}^{ref}G^{\phi}(T) = A^{\phi} + B^{\phi}T + C^{\phi}T\ln T + D^{\phi}T^{2} + \cdots \tag{3-3}$$

and

$${}^{mag}G^{\phi} = RT \cdot f(\tau) \cdot \ln(\beta(x)+1) \tag{3-4}$$

where A, B, C, D,… are empirical parameters taken from the PURE database by SGTE [14]. They are referred to the Standard Element Reference (SER) state, i.e. the stable phase at 10^5 Pa and 25 °C.

The magnetic term in the eq. (3-4) is based on the model introduced by Inden [15] and subsequently adapted by Hillert and Jarl [16]. β is the average magnetic moment per mole of atoms in Bohr magnetons, τ is the ratio T/T_C (T_C= critical temperature for magnetic ordering), and $f(\tau)$ is a polynomial expression obtained by expanding Inden's description of the magnetic heat capacity into a power series of τ.

3.1.2 Stoichiometric Compounds

Stoichiometric compounds refer to phases which do not show any solubility. They are modelled by an n-sublattice model with each sublattice occupied by only

one element. As in the case of pure elements, mixing terms of the Gibbs energy are missing. In this case eqs. (3-5) become:

$$G^{\phi} = \sum_i x_i G_i^{SER}(\mathrm{T}) + {}^{form}G^{\phi}(T) \qquad (3\text{-}5)$$

Where $G_i^{SER}(T)$ is the Gibbs energy of the pure component *i* in its standard element reference state (SER), being referred to the stable phase at 10^5 Pa and 25 °C and ${}^{form}G^{\phi}(T)$ is the Gibbs energy of formation of the compound expressed, as a function of temperature, according to eq. (3-3). This equation is used in case heat capacity is not available and then two parameters A and B from eq. (3-3) are needed. The assumption that the Gibbs energy of formation of compound linearly depends on temperature means that heat capacity of formation is equal to zero. This approach is called Neumann-Kopp rule and it is most probably used for all intermetallic phases in the reviewed work.

In case when heat capacity of stoichiometric phase A_aB_b (ϕ) is known, the following equation is used:

$$G^{\phi} - a\,{}^{0}H_A^{\phi} - b\,{}^{0}H_B^{\phi} = f(T)$$

with the reference to 25 °C and f(T) described by eq. (3-3). In this case parameters C and D related to heat capacity are also used.

3.1.3 Disordered solutions

In the simplest case of random mixing, as in the liquid or in the fcc, bcc and hcp solid solutions, only one sublattice is needed and the three main terms of eq. (3-1) a

$${}^{ref}G^{\phi} = \sum_i x_i G_i^{\phi}$$

$${}^{id}G^{\phi} = RT\sum_i x_i \ln x_i$$

$${}^{ex}G^{\phi} = {}^{ex2}G^{\phi} + {}^{ex3}G^{\phi} + \cdots \qquad (3\text{-}6)$$

where: x_i is, at the same time, the site fraction in the unique sublattice and the overall mole fraction of component *i*. $G_i^{\phi}(T)$ is the Gibbs energy of the pure component *i* in the φ phase (eq. (3-2)), ${}^{ex2}G^{\phi}$ and ${}^{ex3}G^{\phi}$ are the binary and ternary excess terms, respectively. They are expressed as:

$${}^{ex2}G^{\phi} = \sum_{i=1}^{n-1}\sum_{j=i+1}^{n} x_i x_j \sum_v {}^{v}L_{i,j}^{\phi}(T)(x_i - x_j)^v \qquad (3\text{-}7)$$

and

$${}^{ex3}G^{\phi} = \sum_{i=1}^{n-2}\sum_{j=i+1}^{n-1}\sum_{k=j+1}^{n} x_i x_j x_k (u_i L_i^{\phi}(T) + u_j L_j^{\phi}(T) + u_k L_k^{\phi}(T)) \qquad (3\text{-}8)$$

respectively, with:

$$u_i = x_i + \frac{1 - x_i - x_j - x_k}{3}, u_j = x_j + \frac{1 - x_i - x_j - x_k}{3}, u_k = x_k + \frac{1 - x_i - x_j - x_k}{3} \tag{3-9}$$

$L^{\phi}(T)$ in eqs. (3-7) and (3-8) are empirical parameters whose temperature dependence is similar to that $G^{\phi}(T)$ given in eq. (3-3), i.e.:

$$L^{\phi}(T) = A^{\phi} + B^{\phi}T + C^{\phi}T\ln T + D^{\phi}T^2 + \cdots \tag{3-10}$$

In general only parameters A and B are used in eq. (3-10) when information about excess heat capacity of mixing is not known.

For a binary phase with magnetic ordering the composition dependence of ${}^{mag}G^{\phi}$ (eq. (3-4)) results from the composition dependence of T_C and β, which are expressed by a Redlich–Kister series expansion:

$$T_C^{\phi}(x) = x_A T_C^{\phi}(A) + x_B T_C^{\phi}(A) + x_A x_B \sum_{i=0\cdots n} {}^{i}T_C^{\phi}(x_A - x_B)^i$$
$$\beta_C^{\phi}(x) = x_A \beta^{\phi}(A) + x_B \beta^{\phi}(A) + x_A x_B \sum_{i=0\cdots n} {}^{i}\beta^{\phi}(x_A - x_B)^i \tag{3-11}$$

where ${}^{i}T_C^{\phi}$ and ${}^{i}\beta^{\phi}$ are expansion parameters to be evaluated on the basis of the experimental information available.

3.1.4 Ordered solid solutions

Ordered solid solutions are binary or higher order intermediate phases showing more or less extended solubility ranges. Similarly to compounds each component element occupies a preferential site, but mixing of different elements in the same site is allowed, as well as the appearance of vacancies. A typical example may be an ordered binary solution represented by a two-sublattice model where each sublattice is mainly occupied by one component but its substitution by the other element is allowed. Then both elements can occupy both sublattices.

Whenever more components are allowed to mix in two or more sublattices the Gibbs energy is expressed as a function of the site fractions. Site fractions obey the conditions:

$$\sum_i y_i^{(s)} = 1$$
$$\frac{\sum_s n^{(s)} y_i^{(s)}}{\sum_s n^{(s)}(1 - y_{VA})} = x_i \tag{3-12}$$

where $n^{(s)}$ are the stoichiometric coefficients relating the sublattices. Notice that eqs. (3-12) have been formulated assuming that vacancies (VA) can also be included in one or more sublattices. This accounts for a second solubility mechanism, namely vacancy formation in one or more sublattices.

Equations (3-5) become:

$$
\begin{aligned}
{}^{ref}G^{\phi} &= \sum_{i}\sum_{j}\cdots\sum_{k} y_i^{(1)} y_j^{(2)} \cdots y_k^{(s)} G^{\phi}_{i:j:\ldots:\mathrm{k}} \\
{}^{id}G^{\phi} &= \frac{1}{\sum_{s} n^{(s)}} RT \sum_{s}\sum_{i} n^{(s)} y_i^{(s)} \ln y_i^{(s)} \\
{}^{ex}G^{\phi} &= {}^{ex2}G^{\phi} + {}^{ex3}G^{\phi} + \ldots = \sum_{s}\sum_{i}\sum_{j} y_i^{(s)} y_j^{(s)} \sum_{r\neq s}\sum_{k} y_k^{(r)} L^{\phi}_{i,j:\ldots:k}(T) + \ldots + {}^{ex3}G^{\phi} + \ldots
\end{aligned}
\tag{3-13}
$$

where $G^{\phi}_{i:j:\ldots:k}$ in ${}^{ref}G^{\phi}$ are the Gibbs energies of all the so-called "end members", the stoichiometric compounds (either stable, metastable or unstable) formed when only one constituent is present in each sublattice. $L^{\phi}_{i:j:\ldots:k}(T)$ in ${}^{ex2}G^{\phi}$ are binary interaction parameters corresponding to the mixing of components *i* and *j* on the sublattice *s* while the other sublattices are singly occupied. More terms can be added to ${}^{ex2}G^{\phi}$, corresponding to simultaneous mixing on two sublattices while the remaining sublattices are singly occupied. ${}^{ex3}G^{\phi}$ accounts for the possible interactions of three elements in a given sublattice.

3.1.5 Solid solutions with an order/disorder relation

A special case, relatively frequent in intermetallic systems, occurs when ordered phases may be related to a disordered one. In Al-Co-Cr-Ni-Y system, this is the case of the $L1_2$ phase (cP4, Cu_3Au type) related to the disordered Fcc_A1 structure, and the B2 phase (cP2, CsCl type) related to the disordered Bcc_A2 structure.

Ordered and disordered structures can transform to each other by a first order as well as a second order transformation. Such a behavior may be modeled by introducing one single Gibbs energy expression for both ordered and disordered phases. The ordering state will depend on the occupation of the different sublattices. Such kind of treatment can not only decrease the number of parameters but also make the functions a physical meaning.

Ansara et al. [17, 18] developed a single Gibbs energy function to describe both the ordered and disordered phases and this model has been successfully utilized in the assessment of the Al-Ni system. The function is shown as the following:

$$
G_m = G_m^{dis}(x) + G_m^{ord}(\mathrm{y}_1, \mathrm{y}_2) - \mathrm{G}_m^{ord}(x)
$$

$G_m^{dis}(x)$ represents the Gibbs energy of the disordered state. It has the same mathematical expression as the correspondent disordered phase. $G_m^{ord}(\mathrm{y}_1, \mathrm{y}_2)$, a contribution of the ordered state, is described by the sub-lattice model. $\mathrm{G}_m^{ord}(x)$ is the Gibbs energy of the disordered state to the ordered phase. In the disordering situation, the site fractions $\mathrm{y_i}$ and mole fractions x must be equal and then the last two terms cancel each other. Some relations are developed to fulfill the constraint.

At first the two-sublattice (2SL) model is chosen to describe the ordered phases. Four-sublattice model is able to give a more physical simulation of the crystal structure; however the end-members are quickly increasing with the increasing number of elements in the multi-component system. It brings some inconvenient effect in the application. The two-sublattice is easier to handle. In the current

assessment, the 2SL is considered for the ordered phases. In both cases a number of constraint and relations between end members and interaction parameters can be introduced. Such relations, which have already been discussed in the papers by Dupin et al. [19] are also adopted in this work.

3.1.5.1 A1/$L1_2$ transition

The lattices of A1 and $L1_2$ are presented in Fig. 3-1. In the cubic lattice of A1 phase, one atom is located in the corners of the unit cell and three atoms occupy the face centers. The four sites are equivalent and atoms mix randomly in these sites. However, in the lattice of the $L1_2$ phase shown in the Fig. 3-1, the sites on the corners and face centers are not equivalent and are occupied by different atoms.

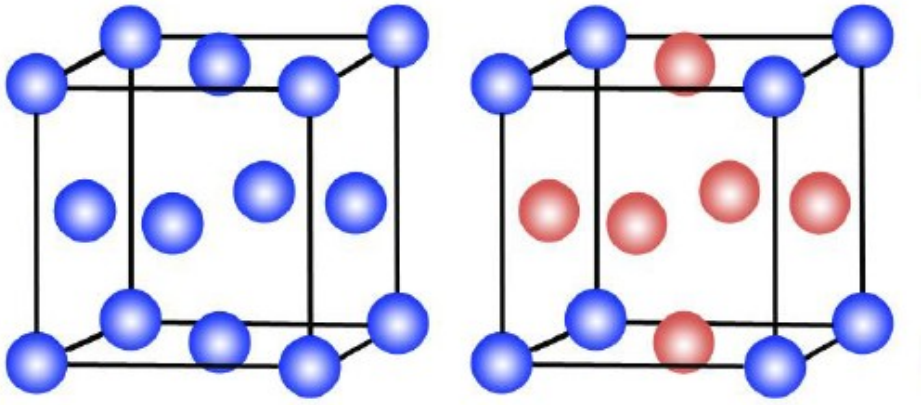

Fig. 3-1 Unit cells of the A1 (left) and $L1_2$ (right) phase

To model the phases in the disordered-ordered transition with a single Gibbs energy function, a four-sublattice model (4SL) $(A, B\ldots)_{0.25}(A, B\ldots)_{0.25}(A, B\ldots)_{0.25}(A, B\ldots)_{0.25}$ was developed and used in several binary and ternary metal systems. When only disordered A1 and ordered $L1_2$ phase are found in the system, 4SL can be converted into a two sublattice model (2SL) $(A, B\ldots)_{0.75}(A, B\ldots)_{0.25}$. The conversion can reduce the number of parameters and easily carry out in the mutlicomponent system. In principle the 4SL model can describe ordered A1 forms such as $L1_2$ and $L1_0$ (A_2B_2) while 2SL can only model the $L1_2$ ordering. However the number of parameters to be determined is quickly increased when the 4SL model is applied to high-order system.

In the present work the single lattice model (A, B…) is selected to model the A1 phase, while a 2SL model is adopted for the $L1_2$ phase, since only the disordered A1 and ordered $L1_2$ phases exist in the target multicomponent system. The following equations have been introduced by Dupin et al. [19] between parameters employed in modeling the $L1_2$ phase in binary, ternary and quaternary systems when 2SL is utilized. The constraints can make sure the disordered state is always possible.

In A-B binary system

$${}^{0}G_{A:B}^{L1_2} = G_{A_3B}$$

$${}^{0}G^{Ll_2}_{B:A} = G_{AB_3}$$

$${}^{0}L^{Ll_2}_{A,B:A} = -1.5*G_{AB_3} + 1.5*G_{A_2B_2} + 1.5*G_{A_3B}$$

$${}^{0}L^{Ll_2}_{A,B:B} = 1.5*G_{AB_3} + 1.5*G_{A_2B_2} - 1.5*G_{A_3B}$$

$${}^{1}L^{Ll_2}_{A,B:A} = 0.5*G_{AB_3} - 1.5*G_{A_2B_2} + 1.5*G_{A_3B}$$

$${}^{1}L^{Ll_2}_{A,B:B} = 1.5*G_{AB_3} + 1.5*G_{A_2B_2} - 0.5*G_{A_3B}$$

$${}^{0}L^{Ll_2}_{*:A,B} = {}^{0}L^{Ll_2}_{A,B}$$

$${}^{1}L^{Ll_2}_{*:A,B} = {}^{1}L^{Ll_2}_{A,B}$$

$${}^{0}L^{Ll_2}_{A,B:*} = 3*{}^{0}L^{Ll_2}_{A,B}$$

$${}^{1}L^{Ll_2}_{A,B:*} = 3*{}^{1}L^{Ll_2}_{A,B}$$

In the A-B-C ternary system

$$\begin{aligned}{}^{0}L^{Ll_2}_{A,B,C:A} = {} & +G_{AB_3} - 1.5*G_{A_2B_2} - 1.5*G_{A_3B} + G_{A_3C} - 1.5*G_{A_2C_2} \\ & - 1.5*G_{A_3C} - 1.5*G_{ABC_2} - 1.5*G_{AB_2C} + 6*G_{A_2BC}\end{aligned}$$

$$\begin{aligned}{}^{0}L^{Ll_2}_{A,B,C:B} = {} & -1.5*G_{AB_3} - 1.5*G_{A_2B_2} + G_{A_3B} + G_{B_3C} - 1.5*G_{B_2C_2} \\ & - 1.5*G_{B_3C} - 1.5*G_{ABC_2} + 6*G_{AB_2C} - 1.5*G_{A_2BC}\end{aligned}$$

$$\begin{aligned}{}^{0}L^{Ll_2}_{A,B,C:C} = {} & -1.5*G_{AC_3} - 1.5*G_{A_2C_2} + G_{A_3C} - 1.5*G_{BC_3} - 1.5*G_{B_2C_2} \\ & + G_{B_3C} + 6*G_{ABC_2} - 1.5*G_{AB_2C} - 1.5*G_{A_2BC}\end{aligned}$$

$${}^{0}L^{Ll_2}_{A,B:C} = -1.5*G_{A_3C} - 1.5*G_{B_3C} + 1.5*G_{AB_2C} + 1.5*G_{A_2BC}$$

$${}^{0}L^{Ll_2}_{A,C:B} = -1.5*G_{A_3B} - 1.5*G_{BC_3} + 1.5*G_{ABC_2} + 1.5*G_{A_2BC}$$

$${}^{0}L^{Ll_2}_{B,C:A} = -1.5*G_{AB_3} - 1.5*G_{AC_3} + 1.5*G_{ABC_2} + 1.5*G_{AB_2C}$$

$${}^{1}L^{Ll_2}_{A,B:C} = -0.5*G_{A_3C} + 0.5*G_{B_3C} - 1.5*G_{AB_2C} + 1.5*G_{A_2BC}$$

$${}^{1}L^{Ll_2}_{A,C:B} = -0.5*G_{A_3B} + 0.5*G_{BC_3} - 1.5*G_{ABC_2} + 1.5*G_{A_2BC}$$

$${}^{1}L^{Ll_2}_{B,C:A} = -0.5*G_{AB_3} + 0.5*G_{AC_3} - 1.5*G_{ABC_2} + 1.5*G_{AB_2C}$$

In the quaternary system A-B-C-D system

$$\begin{aligned}{}^{0}L^{Ll_2}_{A,B,C:\mathrm{D}} = {} & +G_{A_3D} + G_{B_3D} + G_{C_3D} - 1.5*G_{AB_2C} - 1.5*G_{A_2BC} - 1.5*G_{AC_2D} \\ & - 1.5*G_{BC_2D} - 1.5*G_{A_2CD} - 1.5*G_{B_2CD} + 6*G_{ABCD}\end{aligned}$$

$$
\begin{aligned}
{}^{0}L^{L1_2}_{A,B,D:C} = &+G_{A_3C}+G_{B_3C}+G_{CD_3}-1.5*G_{AB_2C}-1.5*G_{A_2BC}-1.5*G_{ACD_2}\\
&-1.5*G_{A_2CD}-1.5*G_{BCD_2}-1.5*G_{B_2CD}+6*G_{ABCD}
\end{aligned}
$$

$$
\begin{aligned}
{}^{0}L^{L1_2}_{A,C,D:B} = &+G_{A_3B}+G_{BC_3}+G_{BD_3}-1.5*G_{ABC_2}-1.5*G_{A_2BC}-1.5*G_{ABD_2}\\
&-1.5*G_{A_2BD}-1.5*G_{BCD_2}-1.5*G_{BC_2D}+6*G_{ABCD}
\end{aligned}
$$

$$
\begin{aligned}
{}^{0}L^{L1_2}_{B,C,D:A} = &+G_{AB_3}+G_{AC_3}+G_{AD_3}-1.5*G_{ABC_2}-1.5*G_{AB_2C}-1.5*G_{ABD_2}\\
&-1.5*G_{AB_2D}-1.5*G_{ACD_2}-1.5*G_{AC_2D}+6*G_{ABCD}
\end{aligned}
$$

Where some functions used in the above equations are defined in the following:

$$G_{A_3B}=3*U_{AB}$$

$$G_{A_2B_2}=4*U_{AB}$$

$$G_{AB_3}=3*U_{AB}$$

$$G_{A_2BC}=2*U_{AB}+2*U_{AC}+U_{BC}$$

$$G_{AB_2C}=2*U_{AB}+2*U_{BC}+U_{AC}$$

$$G_{ABC_2}=2*U_{BC}+2*U_{AC}+U_{AB}$$

$$G_{ABCD}=U_{AB}+U_{AC}+U_{AD}+U_{BC}+U_{BD}+U_{CD}$$

$$U_{ii}=0$$

In the previous equations, U_{ij} is the bonding energy between the pair i-j composed by different atoms (the letter i and j symbol the elements A, B,…..).

3.1.5.2 A2/B2 transition

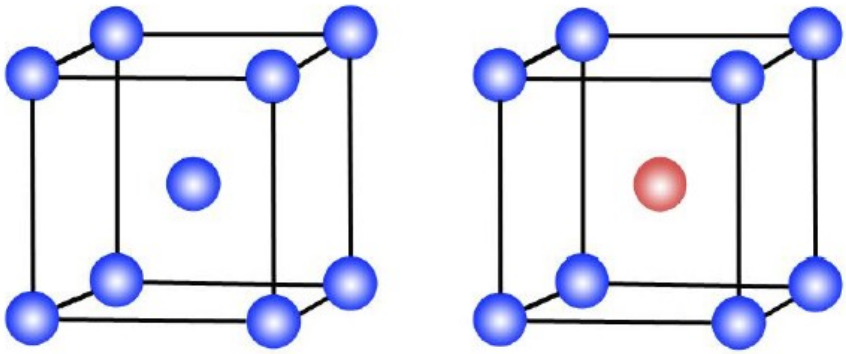

Fig. 3-2 Unit cells of the A2 (left) and B2 (right) phase

Fig 3-2 shows the lattices of A2 and B2 phases. There is one atom in the center and one atom in the corner of the cubic unit cell. These two sites are not identical in B2 while there are in A2. Therefore in the case of A2/B2 ordering, we can assume for B2 a 2SL model, (A, B,…Va)$_{0.5}$(A, B…. Va)$_{0.5}$. It becomes equivalent to the single sublattice model of A2, (A, B, ….. Va)$_1$ when there is no ordering effect. Since the two sublattices of B2 phase are equivalent and have the same number of sites, the following assumptions are utilized:

$${}^0G^{B_2}_{A:B} = {}^0G^{B_2}_{B:A}$$

$${}^0L^{B_2}_{A,B:\mathrm{C}} = {}^0G^{B_2}_{\mathrm{C}:A,B}$$

$${}^0L^{B_2}_{A,B,C:\mathrm{D}} = {}^0G^{B_2}_{D:A,B,C}$$

Studies show that there are a few thermal vacancies in the ordered B2 phase. Then Va need to be taken into account in the B2 sublattices. Since the order-disorder model requires the consistence between constituents of the disorder and order phase, Va must be introduced in the sublattice of A2, which brings some extra parameters. Nevertheless the reference Gibbs energy G^{A2}_{Va} is not recorded in the accepted unary database by SGTE. At current several detailed discussions on this parameters have been published and some values are also recommended. The current consensus within the CALPHAD community is that a largely positive value should be assigned, but there is still no agreement about its value.

Firstly the Gibbs energy of vacuum in A2 G^{A2}_{Va} was set to zero by Dupin and Sundman [19] in the development of a thermodynamic database for Ni-base superalloys. Their determination was easily understood because the vacancy means nothing. However in 2014 Dinsdale et al. [20] demonstrated that setting G^{A2}_{Va} to 0 or negative in the compound energy formalism is unreasonable, resulting in the unwanted catastrophic stability of the phase. After discussing the effects on the total Gibbs energy of various values for G^{A2}_{Va}, finally Dinsdale et al. suggested 30T as the recommendation. In the same year Franke [21] found that G^{A2}_{Va} must be larger than a limiting value $(\ln 2 - 1/2)RT$ and recommended a value only slightly above this limit 0.2RT. Recently Guan and Liu [22] developed a physical model which is able to give a physical definition of the Gibbs energy of the full-vacant end-member within the CALPHAD approach. The model parameters are related to quantities that can be calculated by first-principles or measured experimentally. It was thought to solve the long-standing controversy in modeling the vacancies in solids. However the model is far from being introduced in the current thermodynamic database due to its complexity. So this proposal is not considered anymore.

No matter which remedy is employed, obviously the modification will imply a change of the A2 phase region. Peng et al. [23], in order to compensate this modification of phase diagram, proposed to include a term -0.2·RT into the coefficients of the A2 phase when G^{A2}_{Va} revised to 0.2RT, which has been successfully done in the Al-Ni database. In the current work, the quantity suggested

by Franke is selected and the trick used by Peng et al. [23] is adopted in the thermodynamic modeling of Al-Co-Cr-Ni-Y system.

Moreover similar to G_{Va}^{A2}, the improper interaction parameters $G_{*,Va}^{A2}$ between Va and the host atom also bring some change of phase stability, such as the unreasonable concentration of vacancy as well as the melting point when the A2 phase is the stable phase. A large, positive and temperature independent value is recommended in this case. For the reasonability the amount of Va in each host atom with A2 structure will calculated based on the parameters from literature. The parameter $G_{\mathrm{Y},Va}^{A2}$ is determined in the present work to make sure that the concentration of Va in the A2 phase is less than 0.01 at.%.

3.2 Selected models in this work

All the phases included in the C-Co-Cr-Ni-Ta-W and Al-Co-Cr-Ni-Y systems and modeled in the present work are separately listed in Table 3-1 and 3-2, where crystal structure information and sublattice models are also reported.

The selection of the most appropriate phase model for each phase has been based on a series of criteria which can be summarised as follows:

1) Consistency between crystallographic structure and thermodynamic model in terms of correspondence between crystallographic sites and thermodynamic sublattices.

2) Minimisation of the number of different sublattices (no more than three or four) in order to reduce the number of end-members and parameters to be evaluated.

3) Merging in a single sublattice of all crystallographic sites which are similar in terms of coordination number and geometry, occupation, etc.

4) Capability to reproduce the experimentally determined homogeneity ranges of the phases.

Finally, in the case of multi-sublattice models, sublattices have been ordered according to the decreasing coordination of the corresponding crystallographic sites. As an example, the model for the $MgCu_2$ type structure is (CN16 site)1 (CN12 site)2, while, for the Al_2Cu structure, it is (CN15 site)2 (CN10 site)1.

In the following section, for each group of phases present in the database, the selection of the most appropriate sublattice model will be illustrated and discussed. The unit cells of the most important solution phases are shown in Fig. 3-3.

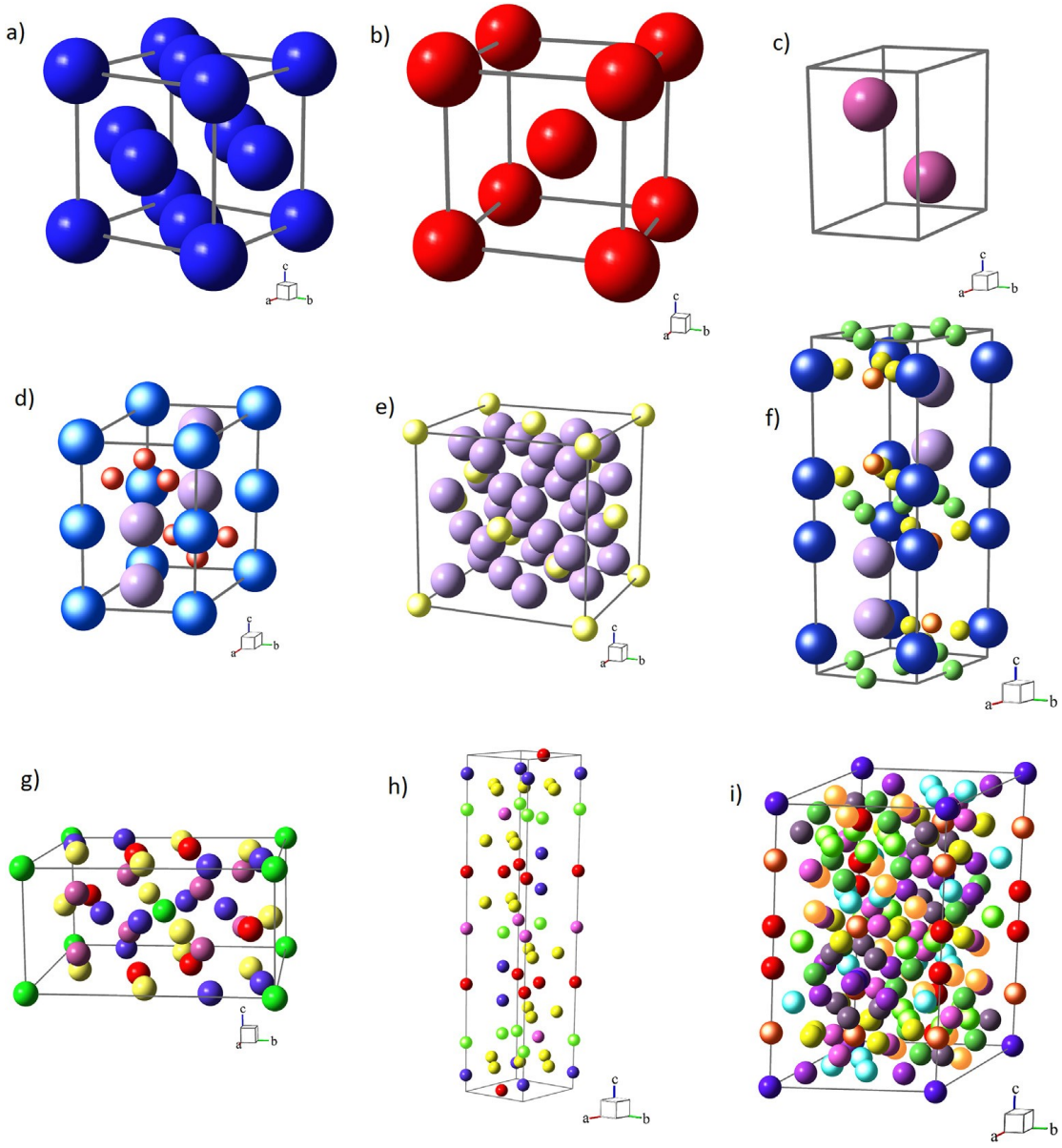

Fig. 3-3 Unit cells of the most important solid solution phases modeled in this work. Different colors correspond to different crystallographic sites; larger diameters indicate positions with larger coordination. a) cF4 - Cu fcc A1; b) cI2 - W bcc A2; c) hP2 - Mg hcp A3; d) hP12 - $MgZn_2$ C14; e) cF24 - $MgCu_2$ C15; f) hP24 - $MgNi_2$ C36; g) tP30 - CrFe sigma; h) hR39 - W_6Fe_7 mu; I) hR159 - $Co_5Cr_2Mo_3$ R.

3.2.1 Phases A1, A2, A3 and Liquid

A1 (*cF*4 – Cu), A2 (*cI*2 – W) and A3 (*hP*2 – Mg) are characterised by the occupation of a single crystallographic site where all the metallic species mix randomly: namely position 4*a* in the *Fm*-3*m* space group for A1, position 2*a* in the *Im*-3*m* space group for A2, and position 2*c* in the $P6_3/mmc$ space group for A3, respectively. Moreover, small atoms such as carbon or vacancy can occupy octahedral interstices, which correspond to the 4*b*, 6*c* and 2*d* positions in A1, A2 and A3, respectively. Then, for these phases, a two-sublattice model (see Table 3-1) has been

adopted with the first sublattice corresponding to the metallic site and the second one to the interstitial site, usually empty, but possibly partially occupied by C in the C-Co-Cr-Ni-Ta-W system. In term of the A1, A2 and A3 phases in the Al-Co-Cr-Ni-Y system, the interstitial sublattice is neglected and only one lattice (see Table 3-2) has been taken to represent the metallic site.

3.2.2 Graphite

Graphite has been described as a single component phase. No metal has been considered to dissolve in it.

3.2.3 Laves phases

C14 (*hP*12 – $MgZn_2$), C15 (*cF*24 – $MgCu_2$) and C36 (*hP*24 – $MgNi_2$) have been modelled by the same two-sublattice model with 1:2 ratio (see Table 3-1). For C15 the two sublattices correspond to the 8*a* and 16*d* Wyckoff positions of *Fd*-3*m* resulting in the model $(8a)_1$ $(16d)_2$. For C14 and C36 crystallographic positions with similar coordination number and geometry have been merged in the same sublattice, resulting in the models $(4f)_1$ $(2a+6h)_2$ and $(4e+4f^I)_1$ $(4f^{II}+6g+6h)_2$, respectively. For all of them any metallic element can occupy both sublattices, but the first one is preferentially occupied by larger atoms (namely Ta), while the second one is mainly occupied by smaller elements (namely Co and Cr).

3.2.4 Sigma phase

The crystal structure of the σ phase (*tP*30 – CrFe) is characterised by the occupation of five Wyckoff positions in the $P4_2/mnm$ space group: 2*a*, 4*f*, $8i^I$, $8i^{II}$, 8*j*. Then, a thermodynamic model fully consistent with the crystal structure would require the introduction of five sublattices. However, in view of the implementation of a multi-component database, it is advisable to keep as low as possible the number of different sublattices, in order to reduce the number of end-members to be evaluated. Then, in order to reduce the number of thermodynamic sublattices, we referred to the thorough structural analysis carried out by Joubert [24]. According to this analysis all metallic elements can enter each position and the phase is never completely ordered, but larger elements tend to preferentially occupy positions 4*f*, $8i^I$ and 8*j*, with coordination 15, 14, 14, respectively, while smaller elements prefer positions 2*a* and $8i^{II}$ with coordination 12. As for the site occupations, the site fraction of a specific element as a function of the overall composition tends to be the same in $8i^I$ and 8*j* as well as in 2*a* and $8i^{II}$. Then, as already proposed by [24], the most appropriate sublattice model for σ is $(4f)_2$ $(8i^I+8j)_8$ $(2a+8i^{II})_5$ with first and second sublattices mainly occupied by larger (A) elements (Ta and W in our case) and the third sublattice mainly occupied by the smaller (B) ones (Co and Ni). Cr, due to its intermediate dimensions, can play both roles, depending on the partner. This gives rise to a theoretical stoichiometry A_2B when all sublattices are singly occupied by the appropriate element.

It is worth mentioning that, before the Joubert's work, a different model, $(8j)_8$

$(4f)_4$ $(2a+8i^I+8i^{II})_{18}$, had been introduced and widely used in thermodynamic databases. As a consequence many authors still use it in order to be consistent with older assessments.

3.2.4 Mu phase

For the μ phase (*hR*39 – W_6Fe_7) the same criteria already adopted for the σ phase have been applied and, based on the structural analysis carried out by Joubert and Dupin [25], the four-sublattice model $(6c^I+6c^{II})_4$ $(6c^{III})_2$ $(3a)_1$ $(18h)_6$ has been adopted. First two sublattices are mainly occupied by larger (A) atoms (namely Ta and W), while the other two are mainly occupied by smaller (B) ones (Co, Ni), resulting in a theoretical stoichiometry A_6B_7. As in the case of the σ phase, Cr has an intermediate behaviour, depending on the partner elements.

Different models used in literature for this phase are $(6c^I+6c^{II})_4$ $(6c^{III}+3a)_3$ $(18h)_6$ [26] and $(6c^I+6c^{II})_4$ $(6c^{III})_2$ $(3a+18h)_7$ [26]. However, according to the experimentally determined site occupations, site 3*a* cannot be associated to any other and a four-sublattice model is needed.

3.2.5 R phase

The R phase (*hR*159 – $Co_5Cr_2Mo_3$ type) has a complex structure with 159 atoms in the hexagonal unit cell. They are distributed in 11 different crystallographic sites with coordination (CN) ranging between 12 and 16. It has been modelled with 3 sublattices by collecting in the same sublattice crystallographic sites with similar CN: $(CN16)_8$ (CN14 and CN15)$_{18}$ $(CN12)_{27}$ i.e.

$(6c^{II}+18f^{VIII})_8$ $(18f^{V}+18f^{VI}+18f^{VII})_{18}$ $(3b+6c^{I}+18f^{I}+18f^{II}+18f^{III}+18f^{IV})_{27}$.

Then it has been assumed that CN16 sublattices are mainly occupied by larger (A) atoms (in our case W), CN12 sublattices are mainly occupied by smaller (B) ones (Co, Cr), while in CN14 and CN15 sites both A and B atoms mix with similar probability.

The resulting model in the C-Co-Cr-Ni-Ta-W system is then: $(W)_8$ (Co, Cr, W)$_{18}$ (Co, Cr)$_{27}$.

Table 3-1 C-Co-Cr-Ni-Ta-W phases: summary of crystal structures and sublattice models. Crystal data are taken from the website Atomwork

Phase name	Pearson symbol Space group Prototype	Selected model
Liquid	- - - - - -	$(C, Co, Cr, Ni, Ta, W)_1$
A1	*cF*4 – Cu *Fm*-3*m*	$(\mathbf{Co}, Cr, \mathbf{Ni}, Ta, W)_1$ $(C, \mathbf{Va})_1$
A2	*cI*2 – W *Im*-3*m*	$(Co, \mathbf{Cr}, Ni, \mathbf{Ta}, Va, \mathbf{W})_1$ $(C, \mathbf{Va})_3$
A3	*hP*2 – Mg $P6_3/mmc$	$(\mathbf{Co}, Cr, Ni, Ta, W)_1$ $(C, \mathbf{Va})_{0.5}$
GRAPHITE	*hP*4 – C-graphite $P6_3/mmc$	$(C)_1$
C14 $TaCo_2$, $TaCr_2$	*hP*12 – $MgZn_2$ $P6_3/mmc$	$(Co, Cr, Ni, \mathbf{Ta})_1$ $(\mathbf{Co}, \mathbf{Cr}, Ni, Ta)_2$
C15 $TaCo_2$, $TaCr_2$	*cF*24- $MgCu_2$ *Fd*-3*m*	$(Co, Cr, Ni, \mathbf{Ta})_1$ $(\mathbf{Co}, \mathbf{Cr}, \mathbf{Ni}, Ta)_2$
C36 $TaCo_2$	*hP*24 – $MgNi_2$ $P6_3/mmc$	$(Co, \mathbf{Ta})_1$ $(\mathbf{Co}, Ta)_2$
SIGMA σ(Co,Cr)	*tP*30 – CrFe $P4_2/mnm$	$(Co, \mathbf{Cr}, Ni, Ta, \mathbf{W})_2$ $(Co, \mathbf{Cr}, Ni, Ta, \mathbf{W})_8$ $(\mathbf{Co}, Cr, \mathbf{Ni}, Ta, W)_5$
MU μ(Ta,Co), μ(W,Co) μ(Ta,Ni)	*hR*39 – W_6Fe_7 *R*-3*m*	$(\mathbf{Ta}, \mathbf{W})_4$ $(Co, Cr, Ni, \mathbf{Ta}, \mathbf{W})_2$ $(\mathbf{Co}, Cr, \mathbf{Ni}, Ta, W)_1$ $(\mathbf{Co}, Cr, \mathbf{Ni})_6$
R_PHASE R(Co,W) rt R(Co,Cr,W)	*hR*159 – $Co_5Cr_2Mo_3$ *R*-3	$(W)_8$ $(Co, Cr, W)_{18}$ $(Co, Cr)_{27}$
AL2CU_TYPE Ta_2Co, Ta_2Ni	*tI*12 – Al_2Cu *I*4/*mmc*	$(Co, Ni, \mathbf{Ta})_2$ $(\mathbf{Co}, \mathbf{Ni}, Ta)_1$
MOSI2_TYPE $TaNi_2$	*tI*6 – $MoSi_2$ *I*4/*mmm*	$(Cr, Ni, \mathbf{Ta})_1$ $(\mathbf{Cr}, \mathbf{Ni}, Ta)_2$
NBPT3_TYPE $TaNi_3$ ht	*mP*16 – $NbPt_3$ $P2_1/m$	Model $(2e^{I}+2e^{II})_1$ $(2e^{III}+2e^{IV}+4f^{I}+4f^{II})_3$ $(Ni, \mathbf{Ta})_1$ $(\mathbf{Ni}, Ta)_3$
TIAL3_TYPE $TaNi_3$ rt	*tI*8 – $TiAl_3$ *I*4/*mmm*	Model $(2a)_1$ $(2b+4d)_3$ $(\mathbf{Ta})_1$ $(\mathbf{Ni})_3$
MG3CD_TYPE WCo_3, $Ta(Co,Ni)_3$	*hP*8 – Mg_3Cd $P6_3/mmc$	$(Co, Ni, \mathbf{W}, \mathbf{Ta})_1$ $(\mathbf{Co}, \mathbf{Ni}, W, Ta)_3$
NBNI8_TYPE $TaNi_8$	*tI** 	$(Ta)_1$ $(Ni)_8$

TA2CO7_TYPE Ta_2Co_7	*hR36* – Ta_2Co_7 *R-3m*	$(Ta)_2$ $(Co)_7$
MONI4_TYPE WNi_4	*tI*10 – $MoNi_4$ *I4/m*	$(W)_1$ $(Ni)_4$
MOPT2_TYPE $CrNi_2$	*oI*6 – $MoPt_2$ *Immm*	$(Cr)_1$ $(Ni)_2$
WNI	*oP*112 – MoNi $P2_12_12_1$	$(W)_1$ $(Ni)_1$
W2NI	*tI*96 – W_2Ni *I*4	$(W)_2$ $(Ni)_1$
WC	*hP*2 – WC *P-6m2*	$(W)_1$ $(C)_1$
MC TaC, WC	*cF*8 – NaCl *Fm-3m*	(Cr, **Ta**, **W**)$_1$ (**C**, Va)$_1$
M2C Ta_2C, W_2C	*hP*3 – CdI_2 *P3m1*	(Cr, **Ta**, **W**)$_1$ (**C**, Va)$_{0.5}$
M4C W_3NiC	*cP*5 – Fe_4N *Pm-3m*	$(W)_3$ $(Ni)_1$ $(C)_1$
M6C Co_2Ta_4C, Co_2W_4C Ni_2W_4C	*cF*112 – CFe_3W_3 *Fd-3m*	(Co, Cr, Ni)$_2$ (Ta, W)$_2$ (Co, Cr, Ni, Ta, W)$_2$ $(C)_1$
M12C Co_6W_6C, Ni_6W_6C	*cF*104 – CMo_6Ni_6 *Fd-3m*	(Co, Ni)$_6$ $(W)_6$ $(C)_1$
M7C3 Cr_7C_3	*oP*40 – Mn_7C_3 *Pmna*	(**Co**, **Cr**, **Ni**, W)$_7$ $(C)_3$
M3C2 Cr_3C_2	*oP*20 – Cr_3C_2 *Pmna*	(**Co**, **Cr**, **Ni**, W)$_3$ $(C)_2$
M23C6 $Cr_{23}C_6$	*cF*116 – $Cr_{23}C_6$ *Fm-3m*	(Co, Cr, Ni)$_3$ (Co, Cr, Ni, W)$_{20}$ $(C)_6$

3.2.6 Other binary intermetallics

3.2.6.1 Phases with solubility

A number of binary intermetallic phases with appreciable solubility ranges are present in the systems. They are: Ta_2Co and Ta_2Ni, $TaNi_2$, HT-$TaNi_3$, LT-$TaNi_3$, WCo_3 and $Ta(Co,Ni)_3$ in the C-Co-Cr-Ni-Ta-W system, Co_2Al_5, Co_2Al_9, Co_4Al_{13}, YCo_4Al_{13}, $CoAl_3$, $NiAl_3$, Ni_3Al_4, Ni_2Al_3, Cr_5Al_8-H, Cr_5Al_8-L, Cr_7Al_{45}, CoY_3 and NiY_3, Ni_4Y, NiY, CoY, $Co_{17}Y_2$ and $Ni_{17}Y_2$, Co_5Y and Ni_5Y, Co_7Y_2 and Ni_7Y_2, Co_3Y and Ni_3Y, Al_2Y and Co_2Y and Ni_2Y, in the Al-Co-Cr-Ni-Y system. All of them have been modelled with two sublattices, applying the same procedure already illustrated for the Laves phases. See Table 3-1 and 3-2 for more details.

3.2.6.2 Phases without solubility

Many binary intermetallic phases which do not show any appreciable solubility ranges in the binary and ternary systems as well as in the higher order systems have been modelled as binary (two-sublattices) stoichiometric phases without relation to their crystal structures which, in some cases, are not completely known. They are: $TaNi_8$, Ta_2Co_7, WNi_4, $CrNi_2$, WNi, W_2Ni in C-Co-Cr-Ni-Ta-W system and $CrAl_5$, Cr_4Al_{11}, Ni_5Al_3, Al_2Y_3, AlY_2, α-Al_3Y, β-Al_3Y, Co_3Y_2, Co_7Y_6, Co_3Y_4, Co_5Y_8, Ni_2Y_3 in the Al-Co-Cr-Ni-Y system.

3.2.7 Ternary phases

Several ternary phases starting inside isothermal sections have been experimentally determined in several ternary systems, mainly found in the Al-Co-Cr-Ni-Y system. For easily read and marked on the phase diagrams, each compound is called after the stable composition set as well as an extra Greek letter here. The same character with the distinctive subscript symbols these intermetallic phases stable found in the same system. There are three in Al-Cr-Ni: Cr_2NiAl_8 (τ_1), $Cr_{.11}Ni_{.09}Al_{.80}$ (τ_2) and $Cr_{.15}Ni_{.03}Al_{.82}$ (τ_3); three in Al-Co-Ni: DAlCoNi (θ_1), XAlCoNi (θ_2) and Y2AlCoNi (θ_3); five in Al-Co-Y: Al_7Co_2Y (ψ_1), $Al_9Co_3Y_2$ (ψ_2), Al_2CoY (ψ_3), $(Al, Co)_2Y$ (ψ_4) and $(Al,Co)_3Y_2$ (ψ_5); twelve in Al-Ni-Y: $Al_{23}Ni_6Y_4$ (φ_1), Al_9Ni_3Y (φ_2), Al_4NiY (φ_3), Al_3NiY (φ_4), $Al_7Ni_3Y_2$ (φ_5), Al_3Ni_2Y (φ_6), Al_2NiY (φ_7), $AlNiY$ (φ_8), $AlNi_2Y_2$ (φ_9), $Al_2Ni_6Y_3$ (φ_{10}), $AlNi_3Y_2$ (φ_{11}) and $AlNi_8Y_3$ (φ_{12}); three in Al-Cr-Y: $Al_{20}Cr_2Y$ (ε_1), Al_8CrY (ε_2) and Al_8Cr_4Y (ε_3); one in Co-Ni-Y: $Co_3Ni_2Y_5$ (δ). The models for the above mentioned phases will be discussed in the following section as two parts.

3.2.7.1 Phases with solubility

The compounds with some homogeneity range are considered as ordered solid solutions. They are Cr_2NiAl_8, DAlCoNi, XAlCoNi, Y2AlCoNi, $Co_3Ni_2Y_5$ and $Al_{20}Cr_2Y$.

As for Cr_2NiAl_8 phase, since the crystallographic structure is not clear, it is modelled as $(Al, Cr, Ni)_8(Al, Cr, Ni)_2(Al, Cr, Ni)_1$ in consideration of its solubility.

DAlCoNi is a typical quasicrystalline decagonal phase. Because of the complicated crystal structure, this phase couldn't be described by using any simplified unit. Based on the elemental compositions, the final model is $(Al)_{14}(Al, Co, Ni)_1(Co, Ni)_5$, In the case of XAlCoNi phase, All Al sites with same coordination number or point symmetry are classified into one sublattice and the sites occupied by Co and Ni with similar coordination number or point symmetry are grouped into one sublattice. Thus the resulting model is $(Al)_{0.75}(Co, Ni)_{0.25}$. A similar strategy is applied to Y2AlCoNi phase, therefore the $Al_{69.2}Co_{15.4}(Co, Ni)_{15.4}$ has been employed.

$Al_{20}Cr_2Y$ (ε_1) was firstly described as the three-lattice model $(Al)_{20}(Cr)_2(Y)_1$ for simplification and later was modified to the four-sublattice model $(Al)_{18}(Al, Cr)_2(Cr)_2(Y)_1$, which will be discussed in detail in section 5.2.5.2. The remaining

three phases are (Al, Co)$_2$Y having MgZn$_2$ (C14) structure already discussed, Co$_3$Ni$_2$Y$_5$ with MoB described by a two-sublattice model (Co, Ni)$_1$(Y)$_1$ and (Al, Co)$_3$Y$_2$ which has been modelled as (Al, Co)$_3$(Y)$_2$ due to the undetermined crystallographic sites.

3.2.7.2 Phases without solubility

The compounds without solubility are treated as stoichiometric phases. Taking $Cr_{0.11}Ni_{0.09}Al_{0.80}$ as an example, the adopted model is three sublattices with only one element in each sublattice and the used proportion is based on the phase composition, resulting in the model $(Al)_{0.8}(Cr)_{0.11}(Ni)_{0.09}$. A similar strategy is used for all the intermetallics without homogeneity range. All of them are presented in Table 3-2.

Table 3-2 Al-Co-Cr-Ni-Y phases: summary of crystal structures and sublattice models

Phase name	Pearson symbol Space group Prototype	Selected model
Liquid	- - - - - -	(Al, Co, Cr, Ni, Y)$_1$
A1,fcc, (Al), (Ni), (Co)	*cF*4 - Cu *Fm*$\bar{3}$*m*	(Al, **Co**, Cr, Ni**,** Y)$_1$
A2, bcc, (Cr)	*cI*2 - W *Im*$\bar{3}$*m*	(Al, Co, Cr, Ni, Y, Va)$_1$
A3, hcp (Co), (Y)	*hP*2 - Mg *P6$_3$/mmc*	(Al, Co, Cr, Ni, Y)$_1$
L1$_2$, Ni$_3$Al	*cP*4 - Cu$_3$Au *Pm*$\bar{3}$*m*	(Al, Co, Cr, Ni, Y)$_{0.75}$(Al, Co, Cr, Ni, Y)$_{0.25}$ Disordered contribution from A1
B2, NiAl, CoAl	*cP*2- CsCl *Pm*$\bar{3}$*m*	(Al, Co, Cr, Ni, Y, Va)$_{0.5}$(Al, Co, Cr, Ni, Y, Va)$_{0.5}$ Disordered contribution from A2
Co$_4$Al$_{13}$	--	(Co, Ni)$_4$(Al)$_{13}$
YCo$_4$Al$_{13}$	--	(Co, Ni)$_{4.9}$(Al)$_{15.1}$
CoAl$_3$	*mC*34 – Os$_4$Al$_{13}$ *P2/m*	(Co, Ni)$_1$(Al)$_3$
Co$_2$Al$_5$	*hP*28 - Co$_2$Al$_5$ *P6$_3$/mmc*	(Co, Ni)$_2$(Al)$_5$
Co$_2$Al$_9$	*mP*22 - Co$_2$Al$_9$ *P2$_1$/a*	(Co, Ni)$_2$(Al)$_9$
CrAl$_4$	*hR*574 -μMnAl$_4$ *P6$_3$/mmc*	(Cr)$_1$(Al, Va)$_4$
CrAl$_5$	*mP*48 - CrAl$_5$ *P2*	(Cr)$_1$(Al)$_5$
Cr$_2$Al	*tI*6 - MoSi$_2$ *I4/mmm*	(Al, Cr)$_2$(Al, Cr)$_1$

Cr_4Al_{11}	*aP*15 - Mn_4Al_{11} $P\bar{1}$	$(Cr)_4(Al)_{11}$
Cr_5Al_8-H, γ-H	*cI*52 - Cu_5Zn_8 $I4\bar{3}m$	(**Cr**, Ni)$_2$(Al, **Cr**, Ni)$_3$(**Al**, Cr)$_2$(Al)$_6$
Cr_5Al_8-L, γ-L	*hR*26 - Cr_5Al_8 $R\bar{3}m$	(**Cr**, Ni)$_5$(Al, **Cr**, Ni)$_5$(**Al**, Cr)$_4$(Al)$_{12}$
Cr_7Al_{45}	*mC*104 - V_7Al_{45} *C2/m*	(**Cr**, Ni)$_7$(Al)$_{45}$
Ni_5Al_3	*oC*16 - Pt_5Ga_3 *Cmmm*	(Ni)$_5$(Al)$_3$
$NiAl_3$	*oP*16 - CFe_3 *Pnma*	(Co, Ni)$_1$(Al)$_3$
Ni_3Al_4	*cI*112 – Ni_3Ga_4 $Ia\bar{3}d$	(Co, Ni)$_3$(Al)$_4$
Ni_2Al_3	*hP*5 – Ni_2Al_3 $P\bar{3}m1$	(Al)$_3$ (Al, Co, Cr, Ni)$_2$ (Co, Ni, Va)$_1$
$CrNi_2$	*oI*6 - $MoPt_2$ *Immm*	(Cr, Ni)$_1$(Cr, Ni)$_2$
Sigma, σ	*tP*30 - σCrFe $P4_2/mnm$	(Al, Co, Cr, Ni)$_2$(Al, Co, Cr, Ni)$_8$(Al, Co, Cr, Ni)$_5$
Al_2Y_3	*tP*20 - Al_2Zr_3 $P4_2/mnm$	(Al)$_2$(Y)$_3$
AlY_2	*oP*12 - Co_2Si-b *Pnma*	(Al)$_2$(Y)$_1$
MY AlY, CoY	*oS*8 - TlI *Cmcm*	(Al, Co)$_1$(Y)$_1$
αAl_3Y	*hR*8 - $SnNi_3$ $P6_3/mmc$	(Al)$_3$(Y)$_1$
βAl_3Y	*hR*36 - Pb_3Ba $R\bar{3}mh$	(Al)$_3$(Y)$_1$
Co_3Y_2	- *cP* – ---	(Co)$_3$(Y)$_2$
Co_7Y_6	--- ---	(Co)$_7$(Y)$_6$
Co_3Y_4	*hP*22 – $Ho_6Co_{4.5}$ $P6_3/m$	(Co)$_3$(Y)$_4$
Co_5Y_8	*mP*52 – Co_5Y_8 $P2_1/c$	(Co)$_5$(Y)$_8$
M_7Y_2 Co_7Y_2, Ni_7Y_2	*hR*54 – Gd_2Co_7 $P6_3/mmc$	(Al, Co, Ni)$_7$(Y)$_2$
MY_3 CoY_3, NiY_3	*oP*16 - Fe_3C *Pnma*	(Co, Ni)$_1$(Y)$_3$
$M_{17}Y_2$	*hP*38 – Th_2Ni_{17}	(Al, Co, Ni, Y)$_{17}$(Co, Ni, Y)$_2$

$Co_{17}Y_2$, $Ni_{17}Y_2$	*P6₃/mmc*	
M_5Y Co_5Y, Ni_5Y	*hP*6 – $CaCu_5$ *P6/mmm*	$(Al, Co, Ni, Y)_5(Co, Ni, Y)_1$
Ni_2Y_3	*tP*80 – Ni_2Y_3 *P4₁2₁2*	$(Ni)_2(Y)_3$
Ni_4Y	*hR*- -	$(Co, Ni)_4(Y)_1$
NiY	*oP*8 - FeB *Pnma*	$(Co, Ni)_1(Y)_1$
θ_1, DAlCoNi	*P10/mmm*	$(Al)_{14}(Al, Co, Ni)_1(Co, Ni)_5$
θ_2, XAlCoNi	*oI*96 *Immm*	$(Al)_9(Co)_2(Co, Ni)_2$
θ_3, Y2AlCoNi	*mS*26 *C2/m*	$(Al)_3(Co, Ni)_1$
τ_1, Cr_2NiAl_8	*-P6₃/m-*	(**Al**, Cr, Ni)$_8$(Al, **Cr**, Ni)$_2$(Al, Cr, **Ni**)$_1$
τ_2, $Cr_{.11}Ni_{.09}Al_{.80}$	*P2₁* or *P2₁/m*	$(Al)_{0.8}(Cr)_{0.11}(Ni)_{0.09}$
τ_3, $Cr_{.15}Ni_{.03}Al_{.82}$	*R*3 or $R\bar{3}$	$(Al)_{0.82}(Cr)_{0.15}(Ni)_{0.03}$
ψ_1, Al_7Co_2Y	o - -	$(Al)_7(Co)_2(Y)_1$
ψ_2, $Al_9Co_3Y_2$	*oS*56 - $Y_2Co_3Ga_9$ *Cmcm*	$(Al)_9(Co)_3(Y)_2$
ψ_3, Al_2CoY	*oS*16 – $MgCuAl_2$ *Cmcm*	$(Al)_2(Co)_1(Y)_1$
ψ_4, AlCoY	*hP*12 – $MgZn_2$ *P6₃/mmc*	$(Al, Co)_2(Y)_1$
ψ_5, $AlCo_2Y_2$	---	$(Al, Co)_3(Y)_2$
φ_1, $Al_{23}Ni_6Y_4$	*mC*66 – $Al_{23}Ni_6Y_4$ *C2/m*	$(Al)_{23}(Ni)_6(Y)_4$
φ_2, Al_9Ni_3Y	*hR*99 – $DyNi_3Al_9$ *R32*	$(Al)_9(Ni)_3(Y)_1$
φ_3, Al_4NiY	*oC*24 – Al_4NiY *Cmcm*	$(Al)_4(Ni)_1(Y)_1$
φ_4, Al_3NiY	*oP*20 – Al_3NiY *Pnma*	$(Al)_3(Ni)_1(Y)_1$
φ_5, $Al_7Ni_3Y_2$	*hP*	$(Al)_7(Ni)_3(Y)_2$
φ_6, Al_3Ni_2Y	*hP*18 – Al_3Ni_2Y *P6/mmm*	$(Al)_3(Ni)_2(Y)_1$
φ_7, Al_2NiY	*oC*16 – $CuMgAl_2$ *Cmcm*	$(Al)_2(Ni)_1(Y)_1$
φ_8, AlNiY	*hP*9 – Fe_2P $P\bar{6}2m$	$(Al)_1(Ni)_1(Y)_1$
φ_9, $AlNi_2Y_2$	*oI*10 – Mo_2NiB_2 *Immm*	$(Al)_1(Ni)_2(Y)_2$
φ_{10}, $Al_2Ni_6Y_3$	*cI*44 – $Ce_3Ni_6Si_2$ *Im3m*	$(Al)_2(Ni)_6(Y)_3$

φ_{11}, $AlNi_3Y_2$	*hP*12 – $MgZn_2$ *P6₃/mmc*	$(Al)_1(Ni)_3(Y)_2$
φ_{12}, $AlNi_8Y_3$	*hP*24 – Ce_3Co_8Si *P6₃/mmc*	$(Al)_1(Ni)_8(Y)_3$
ε_1, $Al_{20}Cr_2Y$	*cF*184 – $Mg_3Cr_2Al_{18}$ $Fd\bar{3}m$	$(Al)_{18}(Al, Cr)_2(Cr)_2(Y)_1$
ε_2, Al_8CrY	hexag	$(Al)_8(Cr)_1(Y)_1$
ε_3, Al_8Cr_4Y	*tI*26 – $CeMn_4Al_8$ *I4/mmm*	$(Al)_8(Cr)_4(Y)_1$
δ, $Co_3Ni_2Y_5$	*tI*16 – BMo *I4₁/amd*	$(Co, Ni)_1(Y)_1$

4. The C-Co-Cr-Ni-Ta-W system

Up to 15 binary and 20 ternary subsystems need to be assessed while constructing the thermodynamic database of the six-component system. As a portion of this massive task, Co-Cr-Ni and Co-Cr-Ta ternary systems as well as their binary subsystems have been thermodynamically assessed in this work. They will be thoroughly presented in this section. Then databases developed in this work have been combined with those developed by colleagues in order to obtain the multicomponent database able to simulate phase equilibria in selected commercial alloys. Several simulations of the interested alloys are presented based on the database at the end of this section. The corresponding parameters of Co-Cr-Ni and Co-Cr-Ta systems are listed in the Appendix.

4.1 Binary systems

4.1.1 Co-Cr system

Experimental investigations of the Co-Cr phase equilibria have been critically evaluated by Ishida and Nishizawa [27] in 1990. Their assessment was merely based on experimental information of Allibert et al. [28]. At high temperature Co-Cr is a simple eutectic system, but in the solid state more complex equilibria appear. A tricritical point and a miscibility gap are formed between the ferromagnetic and the paramagnetic A1 solid solutions, investigated by Oikawa et al. [29]. The hcp solid solution also forms a miscibility gap between the Co terminal solution and a Cr richer stability range. Moreover the σ phase forms congruently at about 1283 °C in the Cr-rich side.

This binary system has been optimized by several authors including Kusoffsky et al. [30], Oikawa et al. [29], Vrestal et al. [31] and Li et al. [32]. Phase relations calculated according to both Kusoffsky and Oikawa can reproduce reasonably well the experimental data: Oikawa results seem more accurate in the Co-rich part of the phase diagram and in the thermodynamic functions but cannot reproduce the congruent transformation of the σ phase. Both authors adopted the traditional $(Co)_8(Cr)_4(Co,Cr)_{18}$ sublattice model for σ, while it was described by a five sublattice model $(Co,Cr)_2(Co,Cr)_4(Co,Cr)_8(Co,Cr)_8(Co,Cr)_8$ in the recent work of Li et al. [32] who used first principle calculations to evaluate the enthalpies of formation of all end-members. In principle this is the best choice when the consistency between thermodynamics and crystal structure is considered. However, in view of the implementation of a multi-component database, the use of a five-sublattice model implies the evaluation of too many end-members. Therefore, in the present work the parameters calculated by Oikawa et al. [29] have been adopted but the σ phase has been reassessed in order to be consistent with the model selected and to better reproduce its congruent transformation. The calculated Co-Cr phase diagram using the present thermodynamic description is shown in Fig. 4-1.

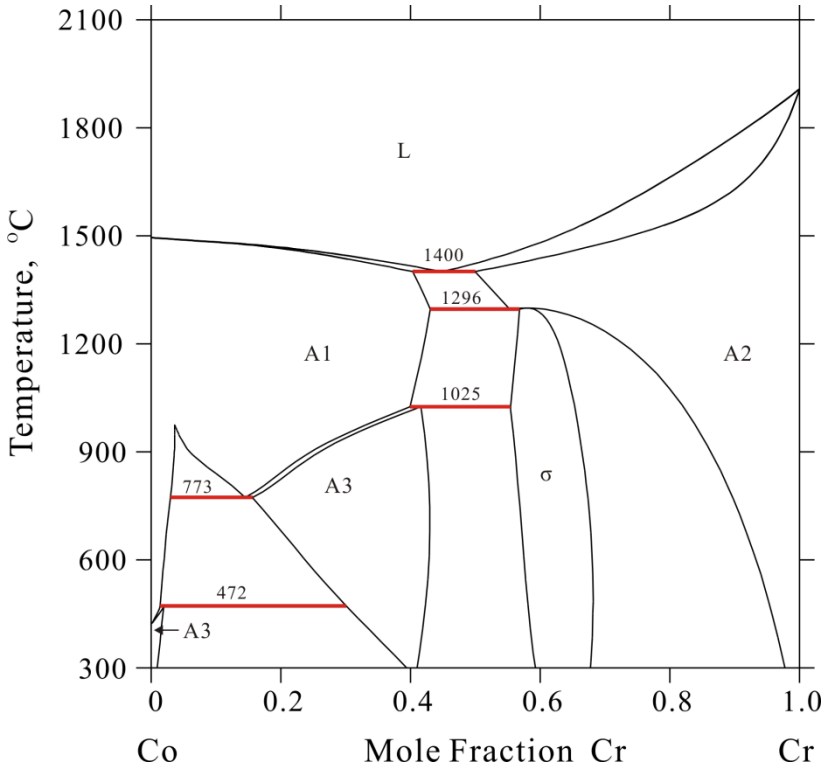

Fig. 4-1 Co-Cr phase diagram calculated in this work

4.1.2 Co-Ni system

Co and Ni show complete solubility both in the liquid and in the A1 phases. The Co-Ni system has been critically assessed and optimized by Fernandez-Guillermet [33] and its interaction parameters have been adopted in all subsequent assessments involving Co and Ni. Then they have been used also in this work. The Co-Ni phase diagram calculated in this work is shown in Fig. 4-2.

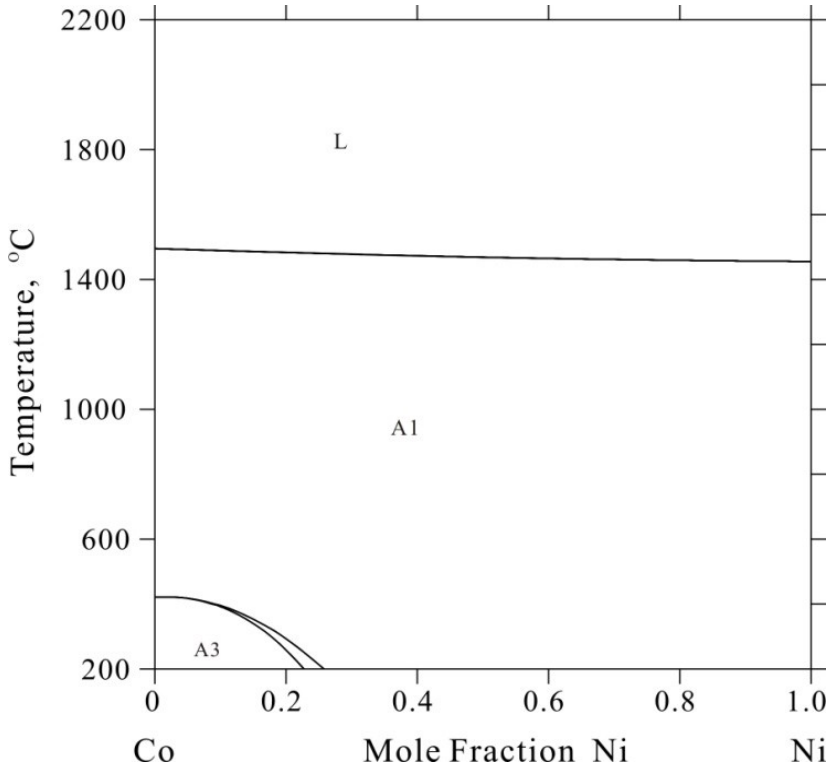

Fig. 4-2 Co-Ni phase diagram calculated in this work

4.1.3 Cr-Ni system

The Cr-Ni system at high temperature is a simple eutectic system and phase equilibria are well known. At temperatures lower than about 627 °C an intermediate phase ($CrNi_2$) forms peritectoidally and, in the Ni-rich side, magnetic ordering gives rise to a tricritical point and a miscibility gap in the A1 phase. For a critical discussion of the Cr-Ni experimental investigations we refer to the recent work by Xiong [34].

The Cr-Ni system was firstly assessed by Gustafson [35] using a subregular solution model for all the assessed phases (liquid and terminal solid solutions). Later Lee et al. [36] reassessed the system just in order to obtain a satisfactory description of C-Cr-Ni. Both of them can reproduce phase diagrams and thermodynamic data satisfactorily. Compared to the first assessment, the latter shows a more negative value of the Gibbs energy of the A1 phase. Subsequently the $CrNi_2$ phase, which is stable below 583 °C, was included in the reassessment works of Turchi et al. [37], Chan et al. [38] and Xiong [34]. In the present work the modelling by Gustafson [35] is accepted with the addition of the $CrNi_2$ phase whose interaction parameters have been taken from Chan et al. [38]. The Cr-Ni phase diagram calculated in this work is shown in Fig. 4-3.

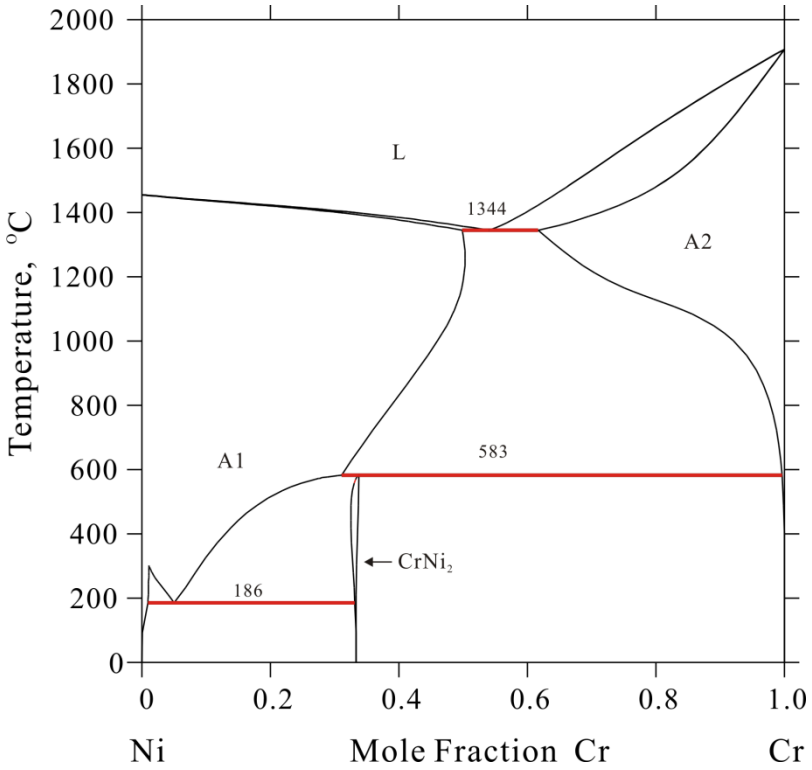

Fig. 4-3 Cr-Ni phase diagram calculated in this work

4.1.4 Co-Ta system

The stable phases in the Co-Ta binary system are: liquid, A1, A2, A3, the C14, C15 and C36 Laves phases, Ta_2Co_7, Ta_2Co and μ phase. Literature data have been critically revised by Garg [39]. The thermodynamic modelling first performed by Liu and Chang [40] has been recently revised by Shinagawa et al. [26]. The Liu's work, though older than Shiganawa's, seems to produce more accurate extrapolations, possibly thanks to a simpler modelling. Moreover, the phase model used by Shinagawa et al. for the μ phase is not consistent with the model adopted in this work. On the other hand, Liu and Chang did not reproduce accurately the solid solubility of all intermediate phases and used arbitrary values for the unary end-members of the Laves phases because, at that time, ab initio values were not available. Then the Liu's interactions parameters for the liquid phase are adopted and all the solid phases are reassessed by introducing, for the end-members of the Laves phases, the ab-initio energies calculated by Sluiter [41]. The Co-Ta phase diagram calculated in this work is shown in Fig. 4-4.

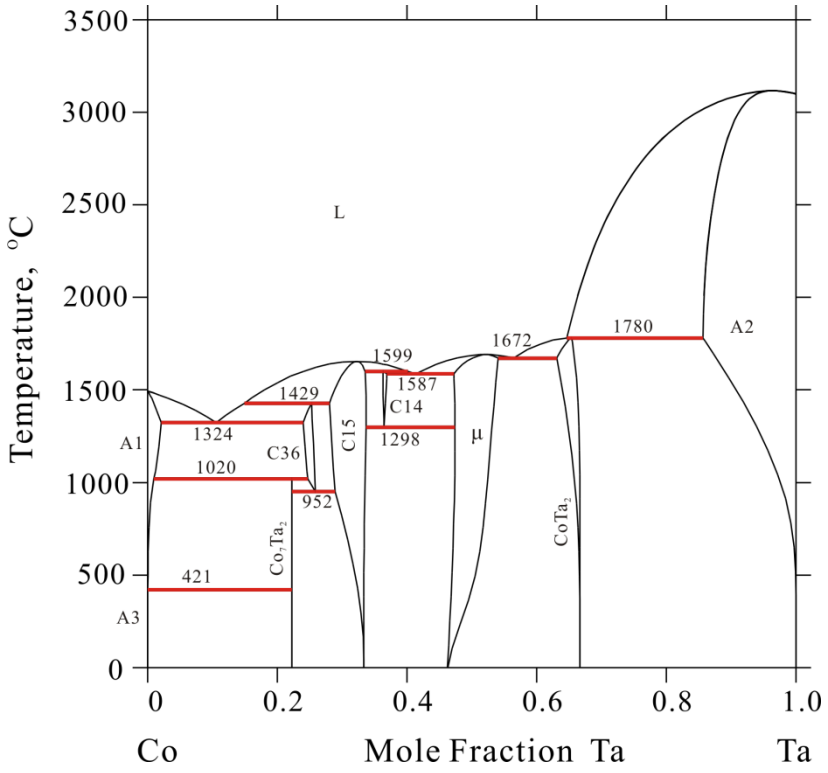

Fig. 4-4 Co-Ta phase diagram calculated in this work

4.1.5 Cr-Ta system

The Cr-Ta system is characterized by a single intermediate phase Cr_2Ta with two allotropic forms: C14 at high temperature and C15 at low temperature. Literature data have been critically reviewed by Venkatraman and Neumann [42], and no more recent phase diagram data have been found in the literature. Thermodynamic modelling of this system has been done by Dupin and Ansara [43]. Their parameters have been adopted in this work, but for the pure element end-members of the Laves phases values calculated ab-inition by Sluiter [44] have been preferred to the arbitrary values used by Dupin and Ansara. This required a complete re-evaluation of the mixing parameters of the Laves phases. The Cr-Ta phase diagram calculated in this work is shown in Fig. 4-5.

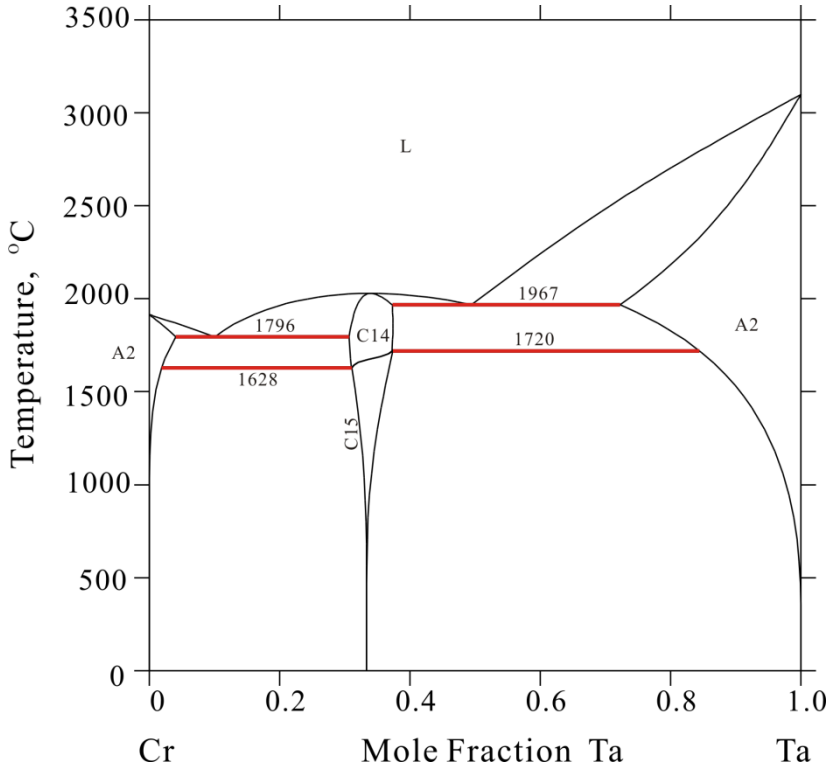

Fig. 4-5 Cr-Ta phase diagram calculated in this work

4.2 Ternary systems

4.2.1 Co-Cr-Ni system

4.2.1.1 Review

Co-Cr-Ni phase diagram has been experimentally studied by several authors. Elsea and McBride [45] studied the influence of nickel additions upon the transformation and precipitation reactions occurring in the Cobalt-rich Cobalt-chromium alloys. Unfortunately their investigation was based on a Co-Cr phase diagram not consistent with the currently accepted version. Rideout et al. [46] firstly investigated the isothermal section at 1200 °C using optical microcopy (OM) and X-ray diffraction (XRD). The same section was also investigated by Xu and Jin [47] using diffusion couple (DC) approach. The 800 °C isothermal section was determined using OM, XRD and SEM-EPMA by Zhmurko et al. [48]. Recently Omori et al. [49] investigated isothermal phase equilibria at several temperatures between 750 and 1300 °C by DSC and SEM-EPMA. In addition, the phase boundaries due to the magnetically induced phase separation in the fcc and hcp phases were also observed at 750, 800 and 850 °C by the DC method. According to their experimental results, σ, A1 and A2 phases could form a three-phase region below 1200 °C at least. In the isothermal section at 1300 °C only A1 and A2 are stable.

The only thermodynamic data available are from Kubaschewski and Hack [50] who measured the heat of formation of 15 alloy samples in the fcc and bcc ranges of

stability at 1250 °C using an adiabatic high temperature calorimeter. They also determined the heats of transformation from sigma to bcc at different compositions. Their data, resulting from small differences between large heat quantities (one measured and one calculated from literature data) are probably affected by large uncertainty.

The Co-Cr-Ni ternary system has been assessed by Yang et al. [51] ignoring the magnetic transformation in the Co-rich region and enthalpy measurements from [50]. They adopted the binary Co-Cr, Co-Ni and Cr-Ni parameters by Oikawa et al [29], Fernandez-Guillermet [33] and Gustafson et al. [35], respectively and used the traditional model $(Co,Ni)_8(Cr)_4(Co,Cr,Ni)_{18}$ for the σ phase. Recently Liu et al. [52] reassessed this ternary system while implementing a new thermodynamic database for the Al-Co-Cr-Ni system but did not improve the model of the σ phase.

In this work, mainly due to the different model adopted for the σ phase, the Co-Cr-Ni system has been completely reassessed taking in special consideration phase equilibria recently determined by Omori et al. [49].

4.2.1.2 Results and Discussions

Considering the character of the available isothermal sections, the optimization started from the A1 phase in order to fit the magnetic effect in the Co-rich corner. On the basis of the Gibbs energy of A1, the interaction parameters of A2 and A3 were preliminarily evaluated. After that the end-members of the σ phase were adjusted so that it could extend into the ternary system with the right homogeneity range. If necessary, the interaction parameters were also moderately added. Finally, all ternary parameters were re-optimized simultaneously to reproduce all accepted experimental results.

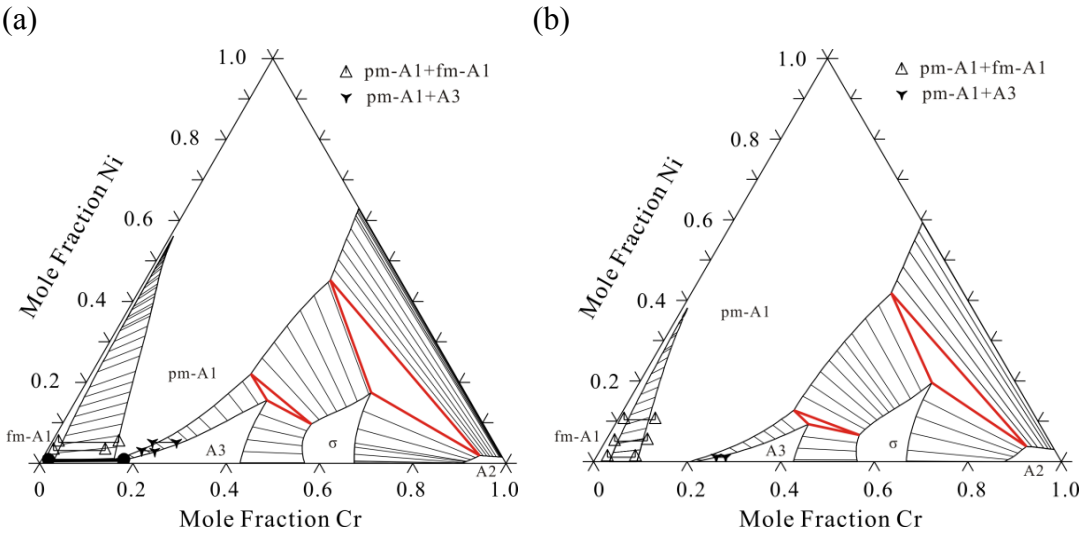

Fig. 4-6. The calculated isothemal sections at Co-rich region in Co-Cr-Ni system at (a) 750 °C (b) 850 °C compared with the experimental data from Omori et al. [49]

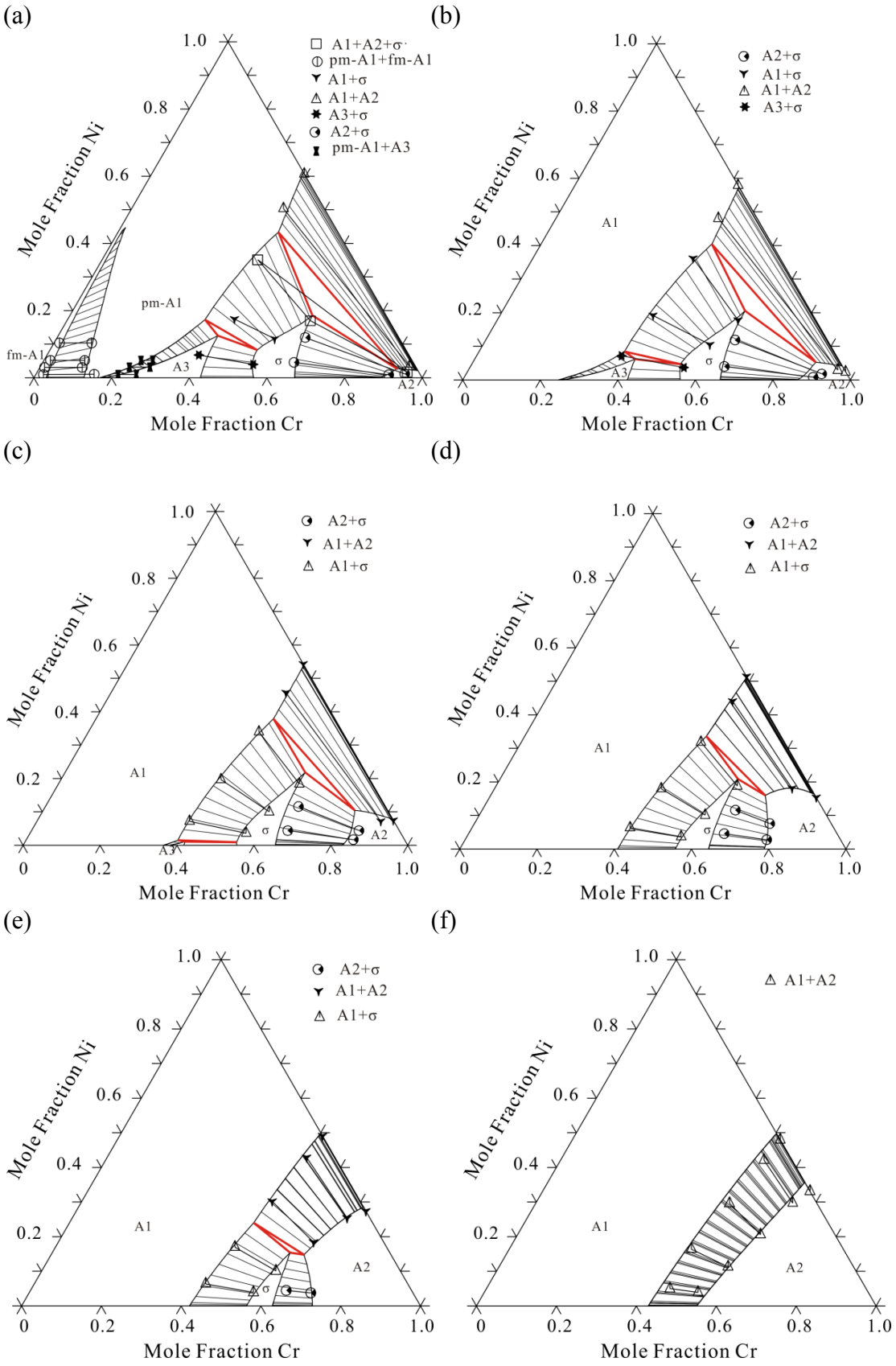

Fig. 4-7 Calculated isothermal sections of Co-Cr-Ni system at (a) 800 °C, (b) 900°C, (c) 1000 °C, (d) 1100 °C, (e) 1200 °C and (f) 1300 °C compared with the experimental data from Omori et al. [49]

Fig. 4-6 show the calculated isothermal sections of the Co-Cr-Ni system at 750 and 850 °C using the present thermodynamic descriptions in comparison with magnetic transformations experimentally determined by Omori et al. [49]. In the Co-rich corner the magnetically induced phase separation of fcc phase is noticed, whose influence on phase equilibria increases with the decreasing temperature.

Fig. 4-7 present the calculated isothermal sections at 800, 900, 1000, 1100, 1200 and 1300 °C in the whole composition range and compared with the experimental data by Omori et al. [49]. The σ phase has some solubility when extending from binary to ternary system, which has been well depicted in the present optimization.

4.2.2 Co-Cr-Ta system

4.2.2.1 Review

The Co-Cr-Ta system was experimentally investigated by a few authors. Drapier et al. [53] detect the fcc-Co phase boundary at 1200 °C by XRD. According to the partial isothermal section, the solubility of fcc-Co phase at 1200°C is ~34 wt.% (36.9 at.%) Cr in the Co-Cr side and ~12 wt.% (4.25 at.%) Ta in the Co-Ta side. Haour et al. [54] studied the Co-base eutectic reactions by preparing samples around the Co-15 wt.%Cr-13 wt.%Ta composition and observing the microstructure. Without the help of a compositional analysis, the results by Haoer et al. were considered unreliable. More recently, Zhao et al. [55] investigated the isothermal sections at 1100, 900 and 800°C. Specimens were annealed at 1100, 900 and 800 °C for 120, 140 and 150 days, respectively, then they were quenched and analysed by backscattered electron (BSE), wavelength dispersive X-ray (WDX) and XRD. The complete isothermal sections of the Co-Cr-Ta system at 1100, 900 and 800 °C were determined based on the analysis results. No ternary compounds were found. A large solubility of Cr was detected in the μ phase. The C14 phase with a wide homogeneity range was detected at temperature below its stability limits in Co-Ta and Cr-Ta binary systems, in the range 4 to 61 at.% Cr and 24 to 41 at.% Ta. A small amount of Ta was found to dissolve in the (αCo), (εCo) and (Cr) phases. Actually the shape of the reported solid solutions looks very irregular and poses some doubts about their reliability. In particular the ternary extension of the Ta-based bcc solid solution reported by Zhao et al. seems very improbable.

No thermodynamic assessment was found in literature. Then the system has been modelled and assessed, mainly based on the available experimental results by Zhao et al. and Drapier et al.

4.2.3.2 Results and Discussions

In Fig. 4-8 the Co-Cr-Ta isothermal sections at 800, 900 and 1100 °C calculated in this work are compared to the experimental data by Zhao et al.. The calculated results can fit generally well the experimental phase equilibria with some discrepancies affecting the homogeneity regions of bcc-Ta and C14 phase.

As for the bcc-Ta, we may observe that Cr solubility in the (Ta) phase is very

limited in the Cr-Ta binary, while a relatively large amount of Cr (up to 19.4 at.%) is reported to dissolve in (Ta) in the ternary region, However, the maximum solubility of Co in (Ta) is around 1.5 at.%, which is the same as that in the Co-Ta side. The Cr solubility in (Ta) may have been overestimated in the experimental results. That may be the reason why the bcc-(Ta) experimental solubility region cannot be reproduced by the calculated results.

Similarly, it was not possible to reproduce the phase boundary of C14 phase close to the Ta-rich side although a mass of hard-work have been done.

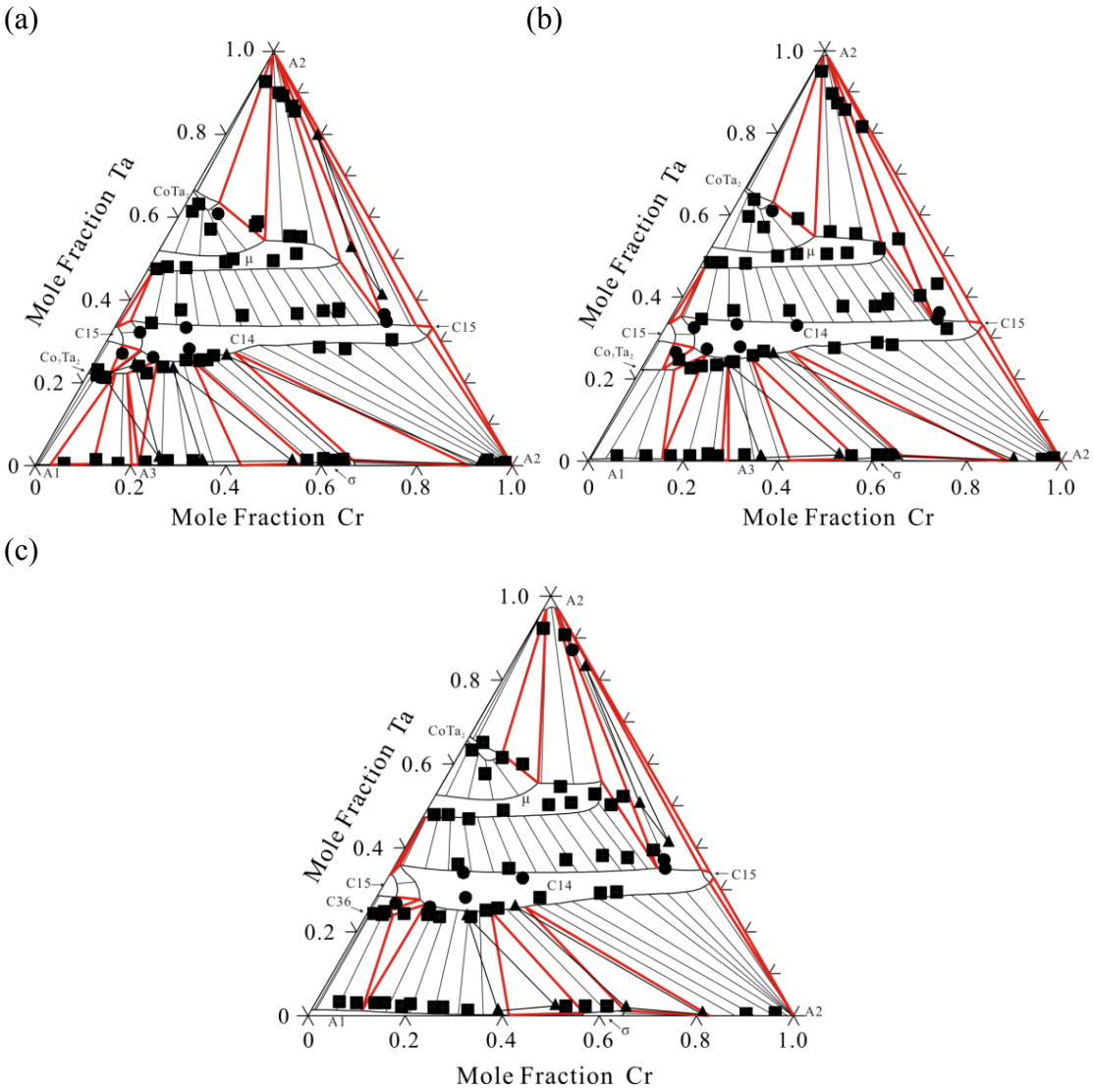

Fig. 4-8 Calculated Co-Cr-Ta isothermal sections at (a) 800 °C (b) 900°C, and (c) 1100 °C compared with the experimental data, single phase (●), tie-line (■), three-phase (▲)

4.3 Other binary and ternary systems

As above mentioned, the assessments of the remaining subsystems in the C-Co-Cr-Ni-Ta-W system have been implemented by the colleagues. Here the particular texts on each system are omitted and Table 4-1 summarizes the main

knowledge of this portion. The adopted models of phases have been presented in the Section 3 in detail.

Table 4-1 Summary of the references for the binary and ternary subsystems in the C-Co-Cr-Ni-Ta-W

Systems	Reference	Comments
C-Co	Kaplan [56]	
C-Cr	Khvan et al. [57]	
C-Ni	Gabriel et al. [58]	Revision of the metastable A2 parameters
C-Ta	Frisk and Guillermet [59]	TaC and Ta_2C described separately
C-W	Gustafson [60]	WC and W_2C described separately
Co-W	Kaplan et al. [61]	Revision of phase μ model
Cr-W	Gustafson [35]	
Ni-Ta	Zhou et al. [62]	Revision of phase μ model
Ni-W	Guillermet et al. [63]	Revision of phases μ, WNi_4 and W_2Ni
Ta-W	Guo et al. [64]	
C-Co-Cr	Kaplan et al. [65]	
C-Co-Ni	Guillermet [66]	
C-Co-Ta	Dumitrescu et al. [67]	Modification to compensate the different Co-Ta
C-Co-W	Markström et al. [68]	
C-Cr-Ni	Luoma [69]	Slight revision of the A1 phase
C-Cr-W	Gustafson [60]	
C-Cr-Ta	Sha et al. [70]	
C-Ni-Ta	Cui and Jin [71]	
C-Ni-W	Wang et al. [72]	Revision of phase M_4C
C-Ta-W	Frisk [73]	
Co-Cr-W	Kaplan et al. [61]	Revision of phases σ and μ
Co-Ni-Ta	Assessed by this group	
Co-Ni-W	Zhu et al. [74]	Revision of phases A3 and μ
Co-Ta-W	Extrapolation	
Cr-Ni-Ta	Dupin and Ansara [75]	
Cr-Ni-W	Gustafson [76]	Revision of phases σ
Cr-Ta-W	Kaufman et al. [77]	
Ni-Ta-W	Extrapolation	

4.4 Discussions and Conclusions

The thermodynamic database of C-Co-Cr-Ni-Ta-W system (SuperCo database) is finally established through the combination of the current work and the cooperation.

By means of the present database several multi-component commercial alloys can be simulated. In particular those mentioned in Table 4-2: FSX-414 (missing constituents B and Fe), Mar-M302 (missing constituents B and Fe), Mar-M509 and ECY-768 (they became equivalent when Zr, Ti and Al are missing), and Stellite 31. For all of them, equilibrium phase fractions calculated as a function of temperature are reported in Figs. 4-9 (a to d). Notice that in the multi-component alloys considered some phases may be stable at different compositions, as in the case of the phases hcp and sigma in the ECY-768 alloy where, at 350 °C two hcp phases are stable with compositions 57.05 Co, 29.40 Cr, 13.54 Ni, 0.000036 Ta, 0.000043 W, 0.00017 C and 83.11 Co, 0.74 Cr, 16.15 Ni, 0.00033 Ta, 4.5×10^{-8} W, 7.8×10^{-8} C, respectively, in mass%. Similarly, in the same alloy, at 300 °C two sigma phases are stable with compositions 45.06 Co, 42.35 Cr, 12.58 Ni, 4.1×10^{-8} Ta, 0.0074 W, 0.0 C and 42.89 Co, 23.65 Cr, 5.47×10^{-4} Ni, 2.5×10^{-10} Ta, 3.35 W, 0.0 C, respectively, in mass%.

Table 4-2 Composition (mass%) of selected Co-based alloys. Elements considered in the SuperCo database are in bold.

Alloy	***Co***	***Cr***	***Ni***	***W***	*Mo*	***Ta***	*Zr*	***C***	*Ti*	*Al*	*B*	*Other*
FSX-414	Bal.	29.5	10.5	7	–	–	–	0.25	–	–	0.012	2 Fe
Stellite 21	Bal.	28	2	–	5.5	–	–	0.3	–	–	–	–
Mar-M302	Bal.	21.5	–	10	–	9	–	0.85	–	–	0.005	0.75 Fe
Mar-M509	Bal.	23.4	10	7	–	3.5	0.45	0.6	0.23	–	–	–
ECY-768	Bal.	23	10	7	–	3.5	–	0.6	0.23	0.18	–	–
Haynes-188	Bal.	22	22	14.5	–	–	–	0.1	–	–	–	< 3 Fe, 0.9 La
Stellite 31	Bal.	20	10	15	–	–	–	0.1	–	–	–	–

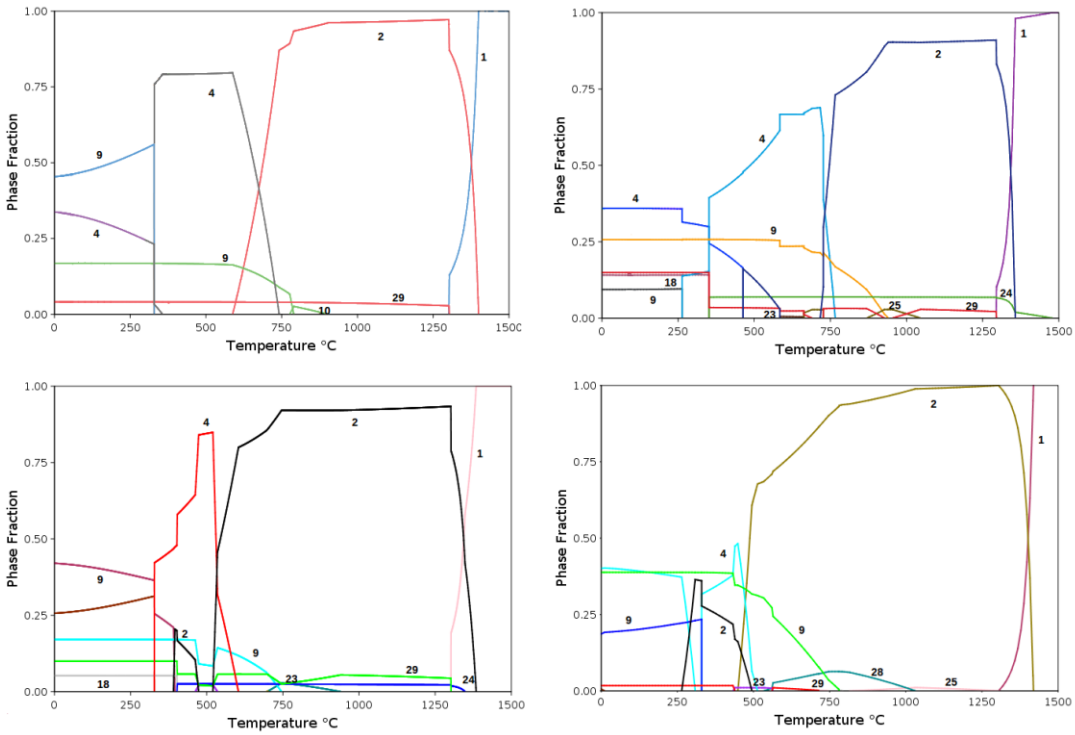

Fig. 4-9 Computed equilibrium phase fractions as a function of temperature for selected Co based alloys: a) FSX-414 (missing constituents B and Fe); b) Mar-M302 (missing constituents B and Fe); c) Mar-M509 and ECY-768 (equivalent when Zr, Ti and Al are missing); d) Stellite. (1-Liquid, 2-A1, 4-A3, 9-σ, 10- μ, 18-Ta_2Co_7, 23-WC, 24-MC, 25-M_2C, 28-$M_{12}C$, 29- M_7C_3)

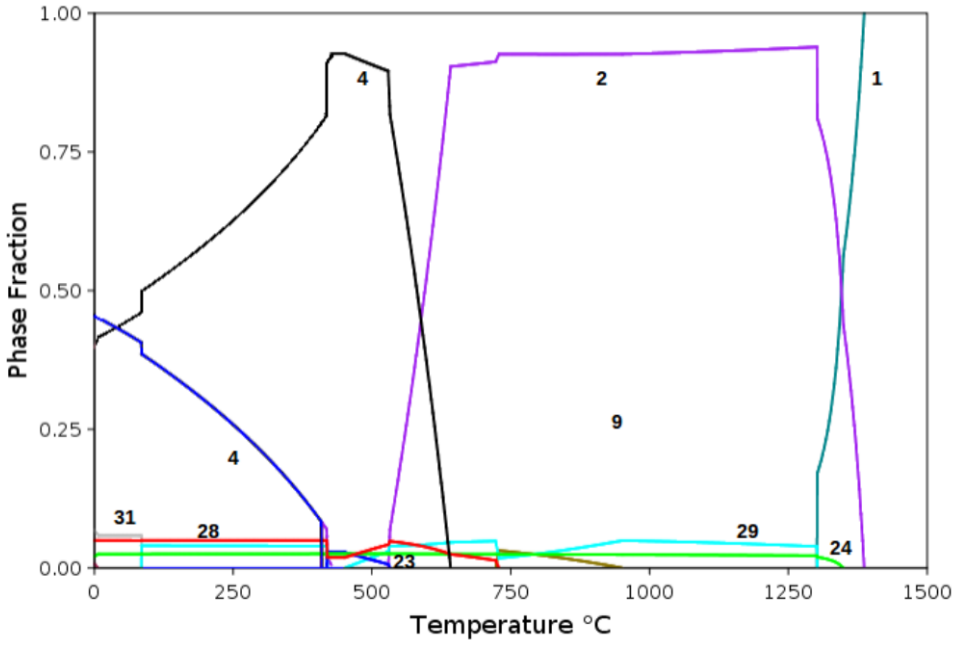

Fig. 4-10 Phase fractions versus temperature for the ECY-768 alloy computed by suspending all intermetallic phases. (1-Liquid, 2-A1, 4-A3, 9-σ, 23-WC 24-M_2C 28-$M_{12}C$ 29-M_7C_3, 31- $M_{23}C_6$)

Notice however that, in real alloys, the mobility of the metallic atoms in the solid state is very slow and solid state formation of intermetallics is inhibited. As an example in Fig. 4-10 the phase constitution as a function of temperature of alloy ECY-768 has been calculated suspending all intermetallics but keeping carbides.

Recently Vacchieri et al. [78] demonstrated that the fcc to hcp transformation in an ECY-768 alloy occurs at about 650 °C only when catalysed by thermal or mechanical stress.

The role of the minor alloying elements in stabilising or destabilising specific phases can be discussed with reference to Figs. 4-11 a and b where, for the ECY-768 alloy, isoplethal sections are reported as a function of the Ta and W content, respectively. It may be observed that the hcp phase is slightly stabilised by an increasing Ta content, while it is slightly destabilised by an increased W content.

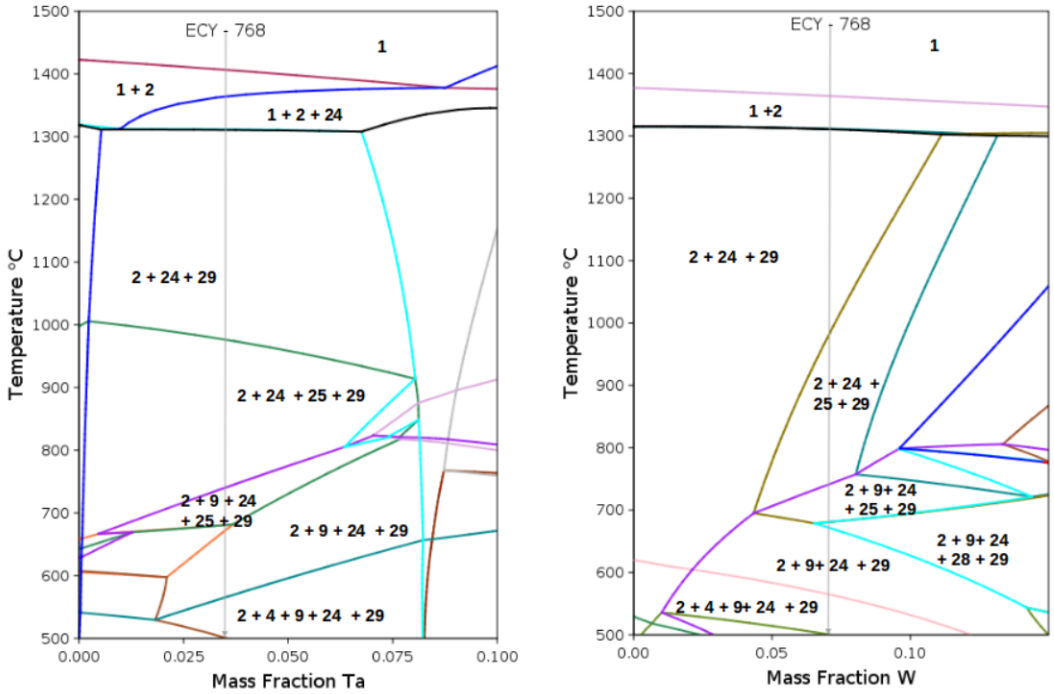

Fig. 4-11 Vertical sections of the Co-Cr-Ni-Ta-W-C system at the composition of the ECY-768 alloy as a function of the a) Ta and b) W composition. (1-Liquid, 2-A1, 4-A3, 9-σ, 23-WC, 24-MC, 25-M_2C, 28-$M_{12}C$, 29- M_7C_3)

These two examples demonstrate that the present database, though limited to only six elements, may be successfully used to predict behaviour and characteristics of multi-component alloys of interest for technological applications.

5. The Al-Co-Cr-Ni-Y system

There are 10 binary sub-systems and 10 ternary sub-systems in the target multi-component system. With the purpose of constructing a reliable thermodynamic database, all the binary and ternary sub-systems have been assessed or adapted from the previous assessments reported in literature, depending on the review of the available information. The detailed discussion on each sub-system will be systematically reported in this section. The complete set of thermodynamic parameters is given in the Appendix B.

5.1 Binary systems

5.1.1 Al-Co system

A detailed critical evaluation of the Al-Co system was presented by Grushko and Cacciamani [79] based on the available literature data. The thermodynamic modeling was reported by McAlister[80], Dupin and Ansara [81], Stein et al.[82]. In order to investigate melting behavior and homogeneity range of the B2 phase, Stein et al. [82] prepared a series of Al-Co alloys in the composition range 30-60 at.% Co and then analyzed them by differential thermal analysis (DTA), SEM and EPMA. As a result the melting temperature of the B2 phase was found to be 1673 °C, significantly 45 °C higher than the value (1628 °C) mentioned by Dupin and Ansara. Moreover the Al-Co system was reassessed by taking into account this new result and keeping the same phase models used by Dupin and Ansara. After that, Priputen et al. [83] reinvestigated experimentally phase relationships in the vicinity of Co_4Al_{13} family of phases. Several alloys between 20 and 23 at.% Co were prepared and annealed for 330h at various temperatures between 1070 and 1150 °C. XRD, DSC and SEM with EDXS were utilized. As a result six phases belonging to the Co_4Al_{13} family were found: $CoAl_3$, Y_1-Co_4Al_{13}, Y_2-Co_4Al_{13}, M-Co_4Al_{13}, O-Co_4Al_{13} and O'-Co_4Al_{13}. Small homogeneity ranges were found for O'-Co_4Al_{13}, Y_1-Co_4Al_{13}, M-Co_4Al_{13} and Co_4Al_{13} above 1000 °C. Y_1-Co_4Al_{13} was found to become stable at higher temperature and to transform into M-$Al_{13}Co_4$ by a quasipolytypic reaction. The temperature was proposed to be around 1077 °C. Y_2-Co_4Al_{13} resulted to be metastable. Maybe a transition reaction between O-Co_4Al_{13} and O'-Co_4Al_{13} take place below 1000 °C. At last revised Al-Co phase diagram in the composition range 20-29 at.% Co above 1000 °C was established. For the sake of simplification, Dupin and Ansara treated the stable phases of the Co_4Al_{13} family as a single stoichiometric phase named Co_4Al_{13} (at 23.53 at.% Co). In the current work, the parameters from Stein et al. [82] are considered and adjusted to fit the experimental data by Priputen et al.[83]. Moreover, in this work, a new phase named Y-Co_4Al_{13} is added at 24.5 at.% Co to describe Y_1-Co_4Al_{13} and M-Co_4Al_{13}. It is formed by a peritectic reaction at 1129°C. The quasi-polytypic transformation between the Y-Co_4Al_{13} and M-Co_4Al_{13} was omitted due to the uncertain temperature.

Moreover, in order to be consistent with our previous work [84], the Gibbs energy of vacancies in A2 phase has been changed to 0.2·RT and consequently, to the

interaction parameters between pure element and Va, a term -0.2·RT was added, as suggested by Peng et al.[23]. Obviously this change shifts the B2 phase boundaries. Then in order to keep the original equilibria, the parameters of the phases close to B2 have been adjusted slightly. The Al-Co phase diagram according to the present calculation is presented in Fig. 5-1.

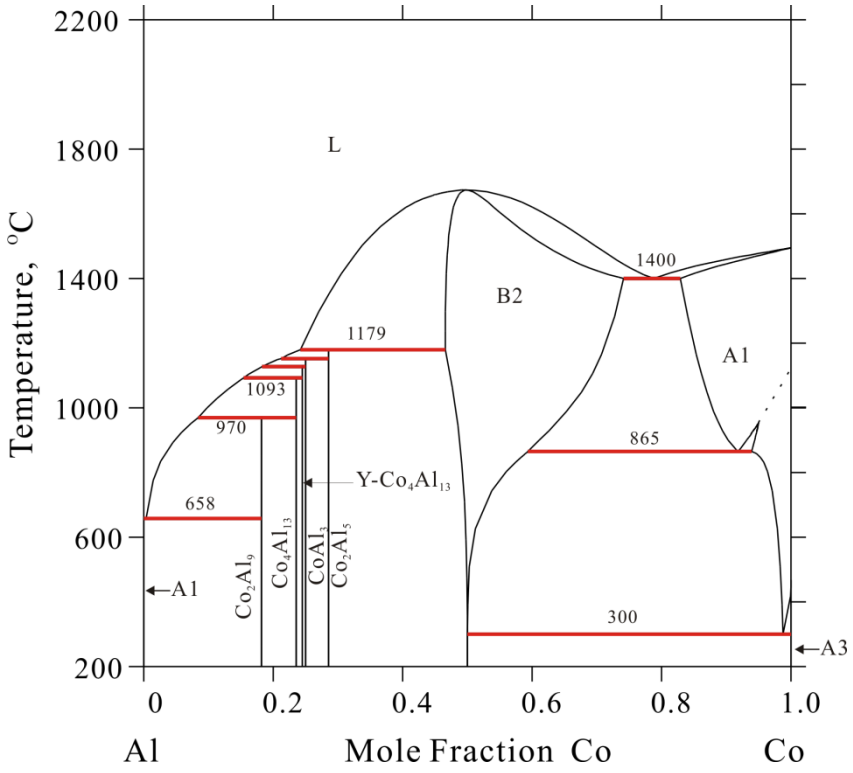

Fig. 5-1 Al-Co phase diagram calculated in this work

5.1.2 Al-Cr system

In the Al-Cr system, a number of intermetallic compounds have been reported, some of which were confirmed repeatedly, i.e. Cr_7Al_{45}, $CrAl_4$ and Cr_2Al. Cr_4Al_{11} was first observed by Grushko et al. [85], forming by a peritectoid reaction between $CrAl_4$ and Cr_5Al_8-L at about 700-800 °C. This phase was not confirmed by Hu et al.[86] who critically reviewed literature data and did selected XRD experiments. Later Wu et al. [87] investigated the Cr_4Al_{11} phase by making Al/Cr composite films. These samples were characterized by metallographic microscopy (LOM), SEM, transmission electron microscopy (TEM), spherical aberration corrected transmission electron microscopy (Cs-TEM) and DTA. According to Wu et al. [87] this phase forms at 829 °C. In this work the results from Grushko et al. [85] are preferred, because his investigations of binary Al-Cr and ternary Al-Cr-Ni systems [88, 89] are mutually consistent. The formation of this phase is then set around 750 °C.

Some controversies still exist about the stable phases in the composition range from 30 to 42 at.% Cr. Four different phases denoted by the Cr_5Al_8 base stoichiometry exist in the Al-Cr phase diagram reported by Chen [90] while only Cr_5Al_8-H and

Cr_5Al_8-L are considered to be stable by Grushko et al.[85]. No controversy affects the Cr-rich part of the phase diagram where Cr_2Al decomposes congruently in the solid state.

The Al-Cr binary system was reviewed and modeled by many authors [86, 91-94]. Cr_5Al_8-H (cI52 - Cu_5Zn_8 type) and Cr_5Al_8-L (hR26 - Cr_5Al_8 type) phases were both treated as line compounds by both Saunders and Rivlin [91], and Ansara et al.[92]. The results of Saunders and Rivlin [91] were used in the Al-Cr-Ni assessment by Dupin et al. [95]. In the more recent work of Tokunaga et al. [93], a single Cr_5Al_8 solution phase was utilized to describe both Cr_5Al_8-H and Cr_5Al_8-L phases in the composition range between about 30 and 42 at.% Cr. Liang et al. [94] reassessed this binary system considering the homogeneity range and the allotropic transformation of the Cr_5Al_8 phase. However the selected models for Cr_5Al_8-H and Cr_5Al_8-L were not based on their crystal structures. In order to improve the thermodynamic description of the system, Hu et al. [86] produced a new reassessment. In this work the assessment of Hu et al. [86] has been adopted because it is a recent one and phase models adopted for the Cr_5Al_8-H and Cr_5Al_8-L phases are more consistent with their crystal structures. In addition, we introduced the Cr_4Al_{11} phase, according to the experimental investigation of Grushko et al. [85].

The Al-Cr phase diagram calculated in this work is shown in Fig. 5-2.

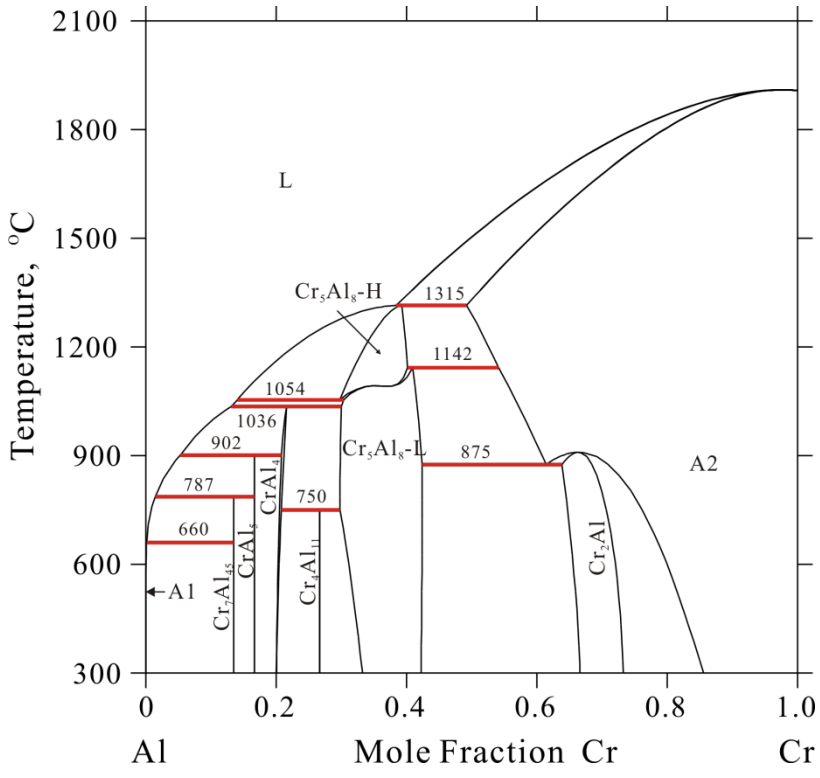

Fig. 5-2 Al-Cr phase diagram calculated in this work

5.1.3 Al-Ni system

The Al-Ni system has long been investigated experimentally in great detail. It is characterized by the high stability of the NiAl (B2) phase, which melts congruently at a temperature much higher than the average of the constituent elements. The most investigated phase, due to its technological importance, is Ni_3Al ($L1_2$), whose decomposition occurs at about 1367 °C. For a summary and a critical assessment of the literature data on this system we refer to Saltykov et al. [96]. After that no new relevant experimental data have been reported in literature about Al-Ni phase equilibria, while Chen et al. [97] measured heat capacity of $NiAl_3$ either at low (-271-50 °C) and high (310-800 °C) temperatures.

The Al-Ni system has earlier been assessed by Du and Clavaguera [98], Huang and Chang [99], Ansara et al. [17] and subsequently improved by Dupin et al. [95], Zhang et al. [100]. Du and Clavaguera [98] didn't consider the ordering in the fcc phase, meanwhile they used the associate model to describe the thermodynamic properties of the liquid phase. The ordered and disordered phases were modeled separately in the work of Huang and Chang [99]. Ansara et al. [17] and Dupin et al. [95] used the substitutional solution model for liquid, bcc and fcc phases and the order-disorder relations with a two sublattice model were applied to the ordered bcc phase (NiAl) and the order fcc phase (Ni_3Al). The remaining two phases, $NiAl_3$ and Ni_5Al_3 were treated as stoichiometric. Later Oates et al. [101] suggested to select 60 kJ/mol (instead of 0 kJ/mol used by Dupin et al. [95]) for the lattice stability of the pure vacancy end-member in the NiAl phase. Zhang et al. [100] improved the assessment of Huang and Chang by introducing the cluster site approximation for the evaluation of the stability of stable and metastable fcc ordered phases. More recently, based on new experiments about heat capacity of $NiAl_3$ phase, Chen et al. [97] reassessed this binary system but did not use order/disorder relations for the fcc and bcc phases. The parameters from Dupin et al. [95] are preferably adopted in the present work because they are more consistent with the other binary subsystems. In addition we introduced the Ni_3Al_4 phase, first reported by Ellner et al. [102] and subsequently investigated by several authors [103, 104]. In particular, this phase which decomposes peritectoidally at 702 °C, can be considered a derivative of the B2 structure with an ordered set of vacancy sites, as determined by Ellner et al. [102]. Its stability was evaluated by Shi et al. [105] using first-principles calculations and these values are adopted in the present work. The Al-Ni phase diagram according to the present calculation is reported in Fig. 5-3.

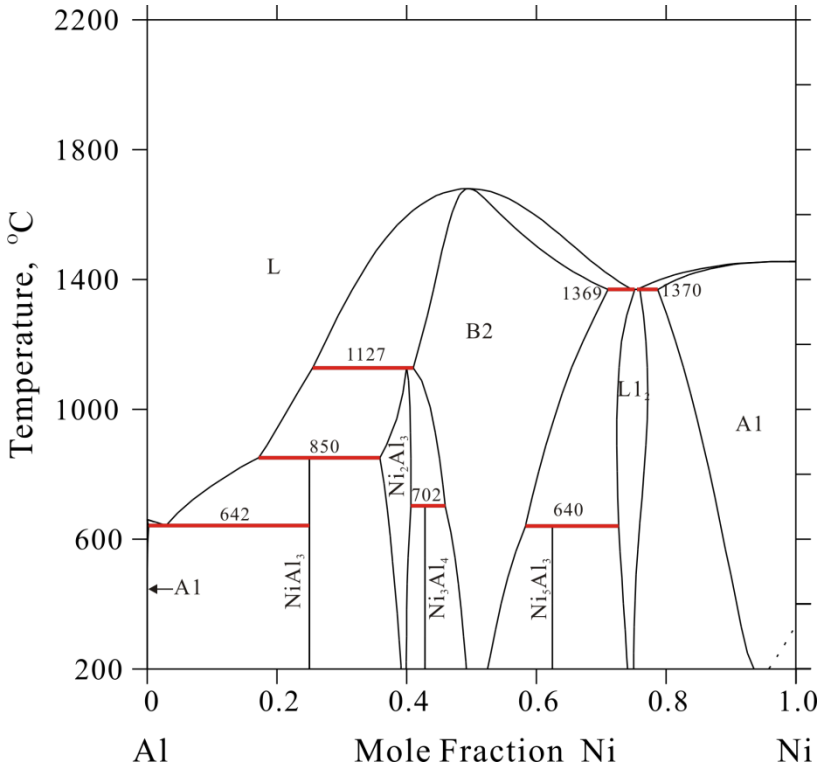

Fig. 5-3 Al-Ni phase diagram calculated in this work

5.1.4 Al-Y system

A critical review of the literature about the Al-Y system was carried out by Gschneidner and Calderwood [106] in 1989 and the phase diagram there reported is generally accepted. Later for the sake of improving it, Liu et al. [107] analyzed 16 alloys prepared by arc-melting with the support of inductively coupled plasma mass spectrometer (ICP-MS), OM, DTA, XRD and SEM-EDS. The ICP-MS results indicate that the actual compositions were close to the nominal ones. So far the Al-Y phase diagram was completely constructed. At atmospheric pressure, there are ten stable phases. Besides Liquid, A1, A2 and A3 phases, six intermetallic compounds α-Al_3Y, β-Al_3Y, Al_2Y, AlY, Al_2Y_3 and AlY_2 exist. The Al_2Y and Al_2Y_3 melt congruently at 1490 °C and 1105 °C, respectively. β-Al_3Y, AlY and AlY_2 are formed via peritectic reactions.

The Al-Y has been successively optimized by several authors [92, 108-110]. Considering the limit of previous assessments and new experimental data, Liu et al. [109] reoptimized the Al-Y system over the whole composition and temperature and the calculated results fit well with the experimental data. A two-sublattice mode (Al, $Y)_2$(Al, $Y)_1$ was utilized for Al_2Y phase and other intermetallic compounds were modeled as stoichiometric phases. Later Kang et al. [110] also developed the thermodynamic modeling of this binary system by using the Modified Quasichemical Model for the liquid phase. Because the selected models by Kang et al. are inconsistent with the present work, the parameters published by Liu et al. [109] will be adopted after refinement of the Al_2Y phase. Considering it has a very narrow

homogeneity, the Al_2Y is revised to be a stoichiometric phase. The calculated Al-Y phase diagram is presented in the Fig. 5-4.

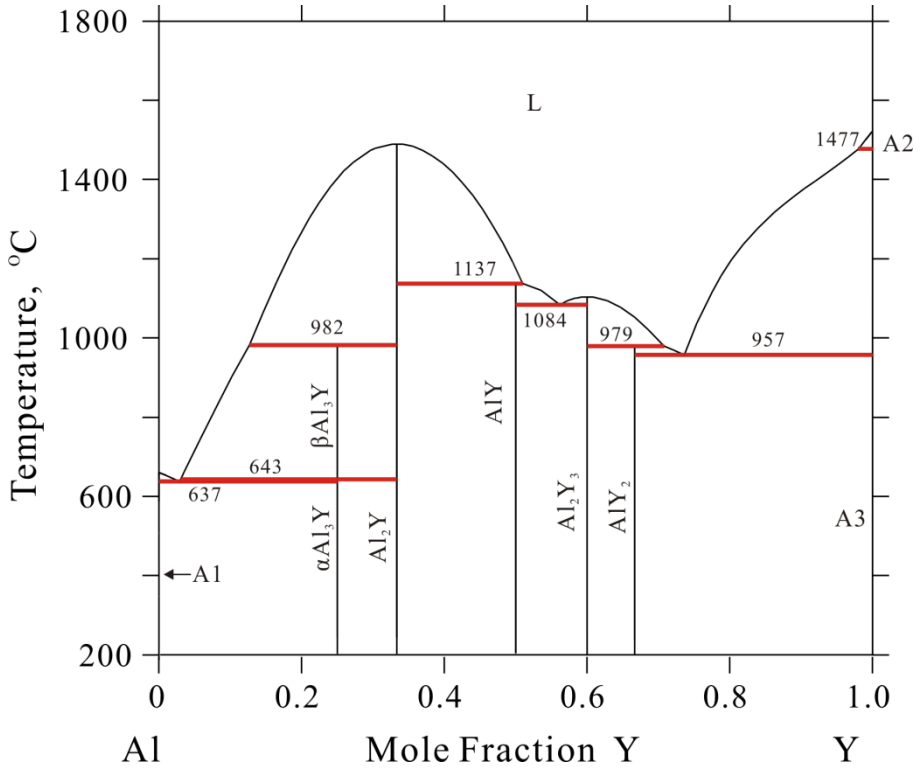

Fig. 5-4 Al-Y phase diagram calculated in this work

5.1.5 Co-Y system

A critical evaluation of the Co-Y diagram up to 1990 has been performed by Wu and Chuang [111]. Later Okamoto [112] updated it based on the new experimental work of Wu et al. [113]. The most recent evaluation was produced by Okamoto [114]. At atmospheric pressure, there are eleven intermediate compounds in the Co-Y system, including $Co_{17}Y_2$, Co_5Y, Co_7Y_2, Co_3Y, Co_2Y, Co_3Y_2, Co_7Y_6, CoY, Co_3Y_4, Co_5Y_8 and CoY_3.

Du et al. [115] optimized this binary system by means of the CALPHAD approach. Based on the crystallographic description of the phases $Co_{17}Y_2$ and Co_5Y, a three-sublattice model $(Co_2, Y)_1(Co_2, Y)_2Co_{15}$ was selected to describe both of them. Other intermediate phases treated as stoichiometric compounds are modeled by using two sublattices without mixture. Later, Golumbfskie and Liu [116] further investigated the Co-Y system with the contribution of first-principles calculations. The enthalpies of formation of five stable intermetallic phases and the end-members of the Co_5Y phase were estimated. Therefore Golumbfskie and Liu reassessed this system and the calculations fit well with the experimental data and first-principles results. The $Co_{17}Y_2$ and Co_5Y phases were described separately as the $(Y, Co_2)_1(Y, Co_2)_2(Co)_{15}$ and $(Y, Co_2)_1(Co)_4(Co, Va)$, which could be easily extrapolated to the high-order systems. Unfortunately a reversed miscibility gap of liquid phase appears

above 3100 °C in the calculated phase diagram, which should be avoided at low temperature.

Most of the parameters published by Golumbfskie and Liu [116] have been adopted in the present optimization after refinement. The models for $Co_{17}Y_2$ and Co_5Y phases are modified as the $(Co, Y)_{17}(Co, Y)_2$ and $(Co, Y)_5(Co, Y)_1$, respectively. In order to destabilize the unwanted miscibility gap, the parameters for the liquid phase are readjusted. All the revisions are made on the premise that all the calculations for the Co-Y system lead to the same results as the original dataset by Golumbfskie and Liu. The corresponding Co-Y phase diagram is shown in Fig 5-5.

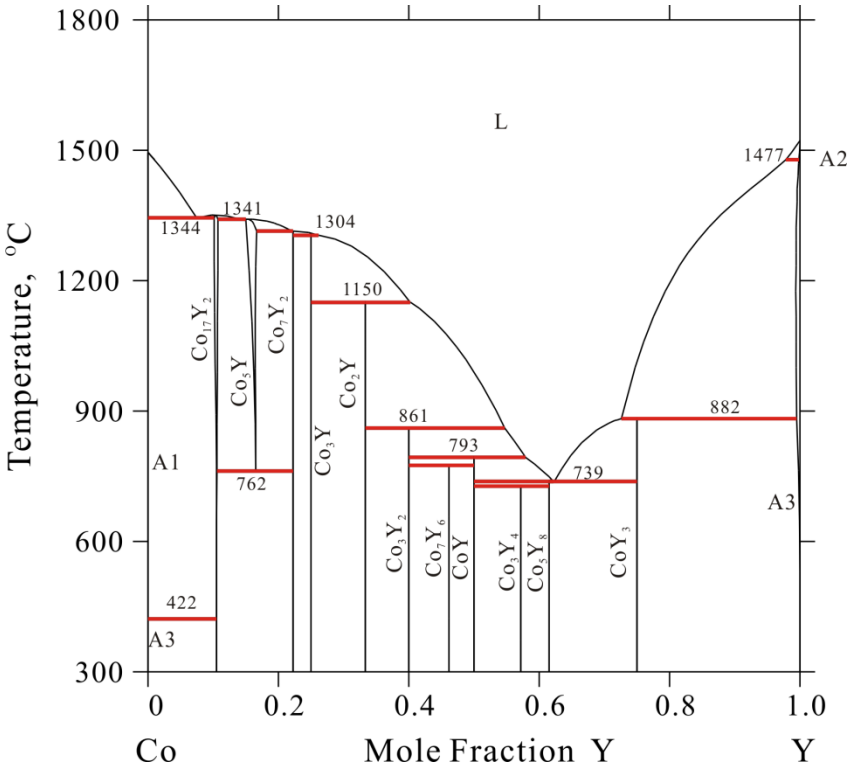

Fig. 5-5 Co-Y phase diagram calculated in this work

5.1.6 Cr-Y system

Cr-Y is a simple system without any intermetallic compound. Okamoto [117] firstly released a literature review on the Cr-Y system. The experimental studies on phase equilibria by Terekhova et al. [118] are largely restricted in the Cr-rich side and the invariant reactions. Two invariant reactions are detected: one eutectic point at 1315±7 °C with 79.65 at.% Y among A2, A3 and Liquid phases and one monotectic point involving Liquid and A2 at 1760±25 °C with 9.36 at.% Y. Both the solubilities of Y in the (Cr) terminal solution and Cr in (Y) are very limited. Chan et al. [119] has developed the CALPHAD modeling of this binary system based on the evaluation of experimental data available in the literature. In the calculated phase diagram, in addition to the previous invariant reactions, a possible catatectic reaction ($\beta Y \rightleftarrows L+\alpha Y$) is predicted in the Y-rich corner. The evaluation given by Chan et al. is totally

accepted and the assessed parameters are mainly considered with several modifications of A2 because of the new additional Va in the A2 phase in the current work. The revised thermodynamic descriptions can reproduce the experimental results and the calculated Cr-Y phase diagram is presented in Fig. 5-6.

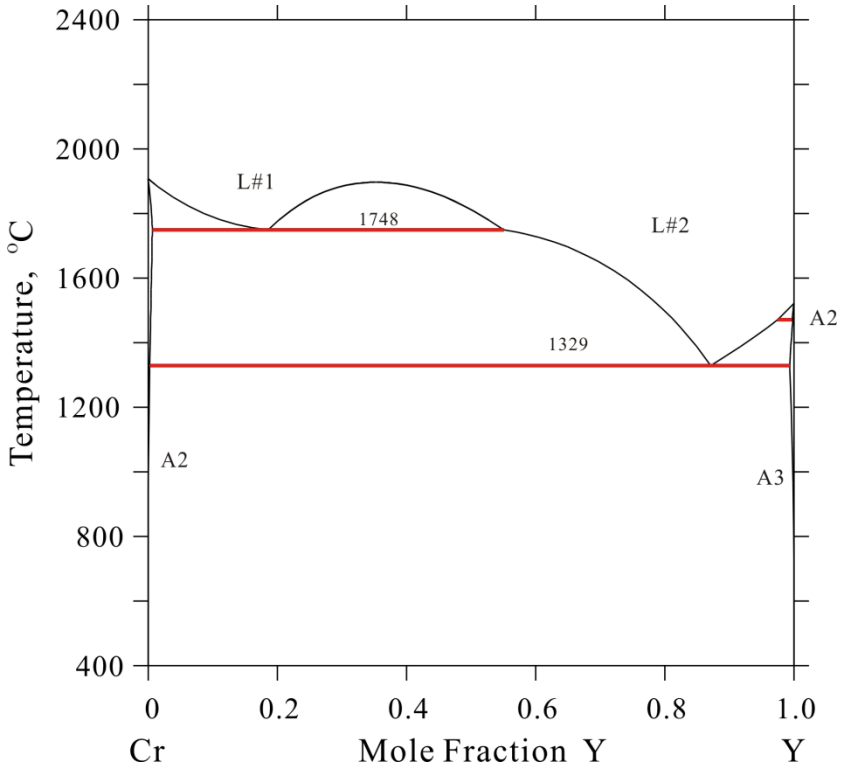

Fig. 5-6 Cr-Y phase diagram calculated in this work

5.1.7 Ni-Y system

Experimental investigations of the Ni-Y phase equilibria have been critically evaluated by Nash et al. [111] in 1990. No solubilities were found in the terminal solid solutions and intermetallic compounds $Ni_{17}Y_2$, Ni_5Y, Ni_4Y, Ni_7Y_2, Ni_3Y, Ni_2Y, NiY, Ni_2Y_3 and NiY_3. Most of them are formed through peritectic reactions. Ni_4Y and NiY melt congruently at 1430 and 1070 °C, respectively.

The CALPHAD thermodynamic modeling of this system was firstly carried out by Du and Zhang [120] and Mezbahul-Islam and Medraj [121]. Phase relations calculated according to both sets of parameters can reproduce reasonably well the experimental data. All the binary compounds were treated as stoichiometric phases. The main difference was in the model for Liquid selected by them: solution model in [120] and modified quasichemical model in [121].

For compatibility with our database, parameters from Du and Zhang will be adopted, while the models of the intermetallic compounds $Ni_{17}Y_2$ and Ni_5Y are revised as $(Ni, Y)_{17}(Ni, Y)_2$ and $(Ni, Y)_5(Ni, Y)_1$ to be consistent with $Co_{17}Y_2$ and Co_5Y phases having the same structure.

The Ni-Y phase diagram calculated in this work is shown in Fig. 5-7.

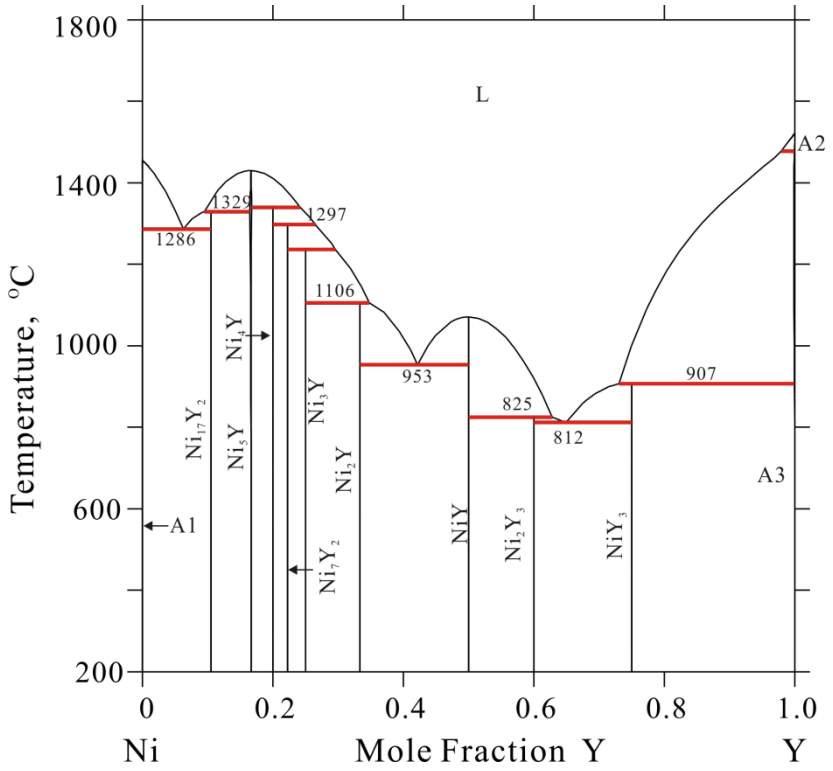

Fig. 5-7 Ni-Y phase diagram calculated in this work

5.2 Ternary systems

Thermodynamic investigations on the sub-ternary systems in the Al-Co-Cr-Ni-Y system will be separately discussed in the following, including the literature review and final calculations. The selected models of phases have been presented in Table 3-2.

5.2.1 Al-Co-Cr system

5.2.1.1 Review

The literature involving phase equilibria and thermodynamic data of the Al-Co-Cr system will be carefully reviewed in the present work. The available experimental investigations focus on the Co-Cr rich region and no studies on the phase relation of the Al-rich region exist. Moskvitina et al. [122] studied the Al-Co-Cr and established the isothermal section in the Co-Cr rich region at 900 °C. Ishikawa et al. [123] investigated phase relationships and ordering reactions in the Al-lean portion of the Al-Co-Cr system over a temperature range of 1000-1350 °C, combining equilibrated alloys and the diffusion couple method. Pure Co (99.9 at.%), Cr (99.6 at.%) and Al (99.7 at.%) were taken to manufacture the samples by induction melting in a Al_2O_3 crucible under the protection of Ar. The annealing treatment of these samples was operated at 1000 °C for 1200h, 1200°C for 168h, 1300 °C for 6h and 1350 °C for 3h, separately. The analyses after annealing were carried out by optical microstructure, SEM with EDS. In order to determine the A2/B2 phase transition,

TEM was performed on the diffusion couples. Finally isothermal sections of Al-Co-Cr system at 1000, 1200, 1300 and 1350 °C were partially established. The main phases in these investigated regions include the A1, A2, B2 and σ. The compositions of the three-phase region A1+B2+σ were successfully confirmed at 1000 °C. The miscibility gap island appeared in the central part of triangle at all the investigated temperatures, which was caused by the present of the A2/B2 ordering reaction. The shape of this region was ellipsoidal. The area increased as the decrease of temperature. Shown as the dashed line, the boundary of A1 phase at 1350 °C was not clear.

Later Liu et al. [124] prepared four samples containing the main elements Al, Co and Cr with a very small amount of Y by arc melting to study the phase relationship of Al-Co-Cr system. These alloys were sealed in a vacuum quartz capsules, and then annealed at 1150 °C for 48h. After that pretreated samples slowly cooled down to the interested temperatures. They were kept at 900, 1000 and 1100 °C for 500h, 200h and 100h, respectively, and then followed by quenching in the water. Phase analyses were done with the support of XRD and EPMA. The three-phase region A1+B2+σ was detected as well as their compositions at 900, 1000 and 1100 °C. B2 phase has a relatively wide stability region. Due to the little quantities of the element Y in the samples, the intermetallics containing Y have precipitated and presented as the bright part. Compositional analysis by EPMA indicated that two types of Co-rich yttrium compounds were found, having ~7 at.% Y and ~9 at.% Y with 18-25 at.% Cr and 7-14 at.% Al. The crystal structure of these phases could not be determined by XRD because of the low volume fractions. Beyond that, Liu et al. [124] didn't release more information about these two compounds. Based on their experimental results and the available literature, the Al-Co-Cr system was optimized by Liu et al. with the aid of first-principles calculation. End members of σ phases and enthalpies of mixing of A1, A2, $L1_2$ and B2 at some compositions are simulated by method of the first-principles calculation. The three-lattice model with the ration 2:4:9 describes the σ phase. The parameters of binary systems are taken from Al-Co by Dupin and Ansara [125], Al-Cr by Saunder and Rivlin [91] and Co-Cr by Oikawa et al. [29]. Experimental results reported by Ishikawa et al. [123] and Moskvitina et al. [122] are also considered in their optimization.

Ishikawa et al. [123] and Liu et al. [124] both investigated phase equilibria of Al-Co-Cr system at 1000 °C. Their results are consistent with each other. In the present work, the ratio of three sublattices for the phase σ is revised to 2:8:5. The Al-Co-Cr system will be reassessed with respect to the different parameters of binary systems and the new model of σ. The experimental data by Moskvitina et al. [122], Ishikawa et al. [123] and Liu et al. [124] are used in the present work. The end members of σ estimated on the first-principles calculation by Liu et al. are not considered because of the distinctive model. The results of A1 and $L1_2$, A2 and B2 from Liu et al. by using SQS solution are utilized for comparison with the calculation.

5.2.1.2 Results and discussions

Fig. 5-8 shows the calculated isothermal sections of the Al-Co-Cr system at 900,

1000, 1100 and 1300 °C compared to experimental data. All the available experimental investigations concentrate on the Al-lean region of Al-Co-Cr system, involving A1, A2, A3, B2 and σ phases. The optimizations in the Al-lean region are done by using the available experiments, while the phase diagrams in the Al-rich corner are extrapolated due to the lack of experimental data. The current calculated results can reproduce well the experimental data. The three-phase region A1+B2+σ is stable at 900, 1000 and 1100 °C. The areas of A2 and B2 phases become larger with the increasing temperature. The calculated enthalpies of mixing for A1 and $L1_2$ phases along x(Al)=0.25 with simulated data are presented in the Fig. 5-9 and Fig. 5-10 presents the enthalpies of mixing for A2 and B2. These calculations can be accepted under the consideration of error ranges.

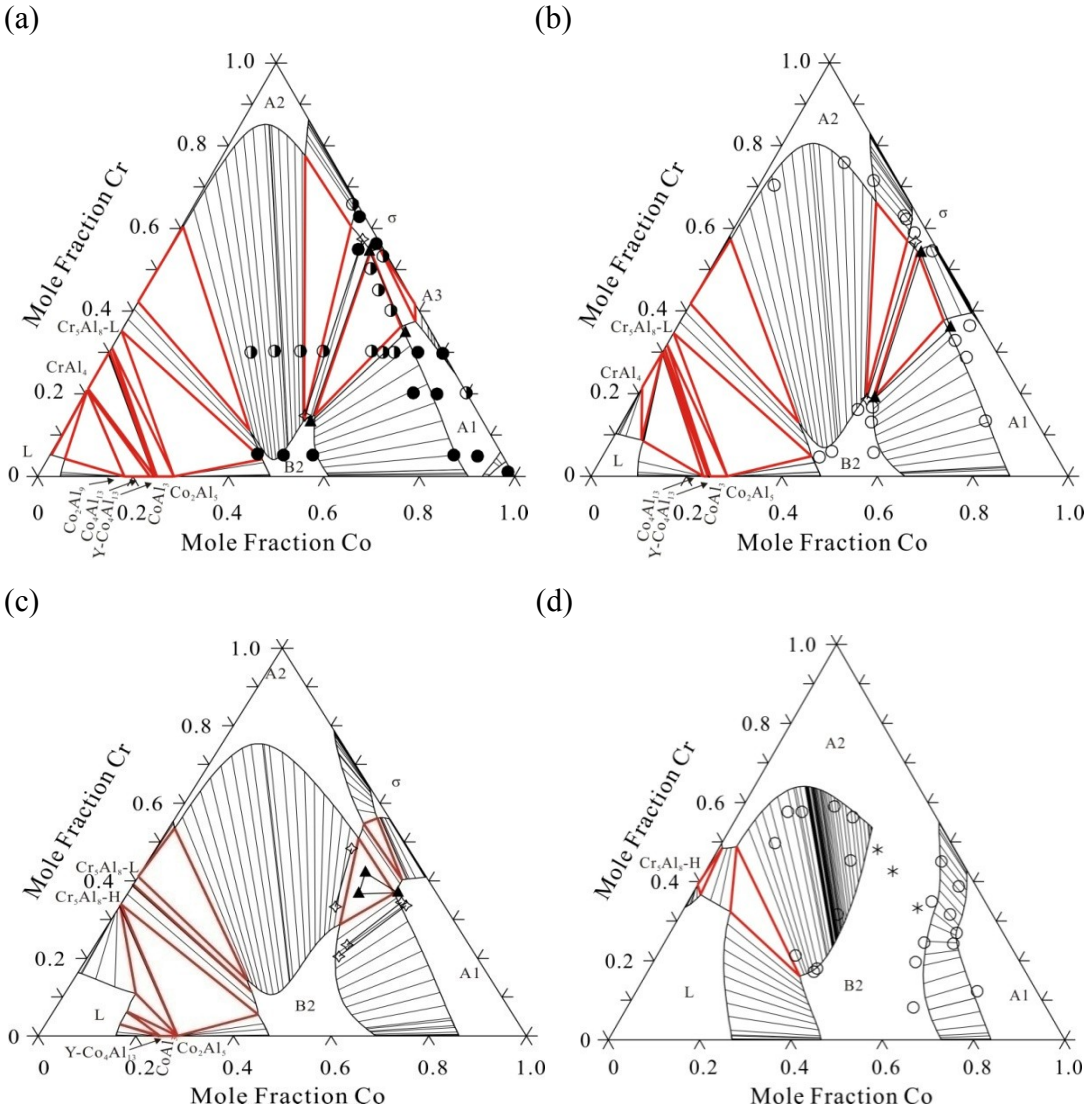

Fig. 5-8 Calculated isothermal sections of Al-Co-Cr system at (a) 900, (b) 1000, (c) 1100 and (d) 1300 °C, compared to the experimental data. single phase (●) and two phases (◑) by Moskvitina et al. [122], tie-line (○), order-disorder transition (✳) by Ishikawa et al. [123], two phases (✧) and three phase (▲) by Liu et al. [124]

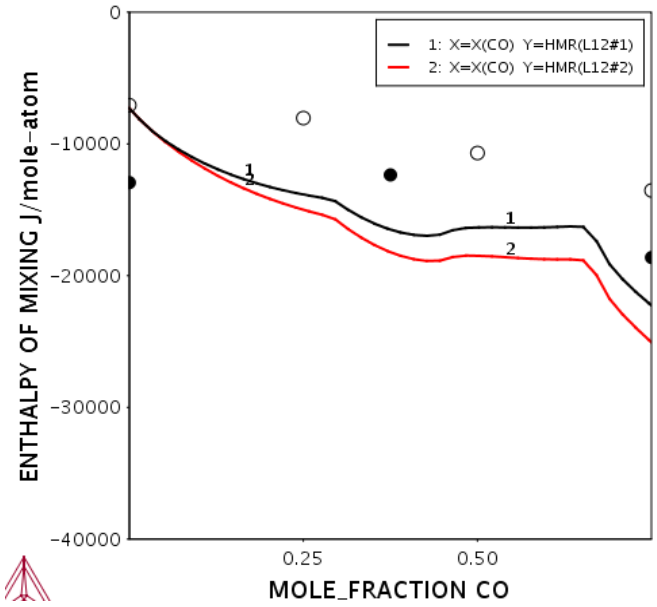

Fig. 5-9 the calculated enthalpies of mixing for A1 (L12#1) and $L1_2$ (L12#2) phases compared to the simulated data from Liu et al. [124]. Reference states are taken as A1 for Al, Co and Cr.

(a) (b)

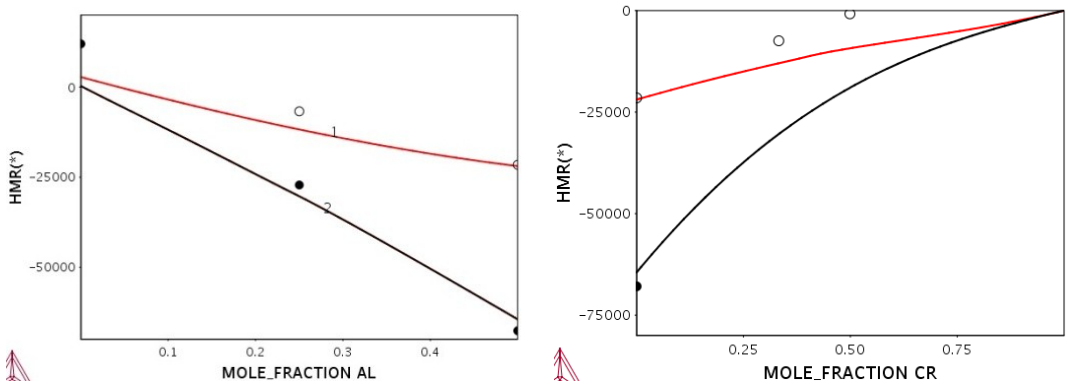

Fig. 5-10 Calculated enthalpies of mixing for A2 (red line) and B2 (black line) phases compared to the simulated data from Liu et al. [124] at 298K. (a) x(Co)=0.5; (b) x(Al)=x(Co). Reference states are taken as A2 for Al, Co and Cr.

5.2.2 Al-Co-Ni system

5.2.2.1 Review

Velikanova et al. [126] published a detailed evaluation of the Al-Co-Ni system based on the literature available before 2004. Phase relationships in the Co-Ni rich part between A1, $L1_2$ and B2 at 900, 1000, 1100, 1200 and 1300 °C were determined by several authors [127-130]. A three-phase region A1+B2+$L1_2$ was speculated according to the tie-lines in the neighboring two-phase fields. Bai [131] firstly measured the detailed phase compositions of three phases in this region by using equilibrated alloys. Recently, Zhu et al. [132] use SEM and EPMA to investigate

phase equilibria in the Co-rich part of the Co-Al-X (X=W, Mo, Nb, Ni and Ta) ternary systems using two sets of diffusion multiples (Ni-Co-CoAl-Cr-Mo-Nb-Ta-W and Ni-Co-NiAl-Si-Zr). As a result, isothermal sections in the Co-rich part of Al-Co-Ni system at 800 and 900 °C were constructed and some tie-lines determined in the A1+$L1_2$, A1+B2 and $L1_2$+B2 phase regions were presented. All the above mentioned investigations about A1, $L1_2$ and B2 phases are consistent with each other except slight distinctions in phase compositions.

As for the Al-rich region, isothermal sections at 600, 730, 850, 900, 1050, 1100 and 1170 °C were investigated by Gödecke et al. [133] who also determined the liquidus projection and the full reaction scheme. A considerable solubility of Co was found in the binary compounds $NiAl_3$, Ni_2Al_3 and Ni_3Al_4, respectively. Almost 5 at.% Ni can dissolve in the Co_2Al_9 and Co_2Al_5. Gödecke et al. reported that a phase named Y_1 was the ternary solid solution of the binary high-temperature phase Y_1-Co_4Al_{13} stable at 1050 °C. Three ternary compounds named DAlCoNi (θ_1), XAlCoNi (θ_2) and Y2AlCoNi (θ_3) were detected by Gödecke et al. [133]. The decagonal θ_1 phase was reported with a relatively large homogeneity range from about 70 to 73 at.% Al and 5 to 24.5 at.% Ni. It is formed from the melt. The θ_2 phase is formed by the four-phase reaction Y_1-Co_4Al_{13}+θ_1+Co_2Al_9 $\rightleftarrows$ θ_2 and was found stable at a composition around Al_9Co_2Ni. θ_3 was identified as a line compound between Co and Ni at constant Al.

Since a series of detailed experimental results are published and the experimental process seems reliable, the results by Gödecke et al. [133] will be utilized as experimental basis for the present assessment.

It's worth to mention that a ternary compound named W was firstly found in an $Al_{72.5}Co_{20}Ni_{7.5}$ alloy annealed at 950 °C by Hirage et al. [134]. This phase is very close to the decagonal phase τ_1. A deeper investigation of the W phase was conducted in 2009 by Katrych and Steurer [135]. They studied phase equilibria in the Co-rich region, in the range from 0 to 11 at.% Ni and from 68 to 74 at.% Al at temperatures of 800, 900 and 1000 °C. Alloys at composition around the W phase were annealed at 800, 900 and 1000 °C for 80, 18-80 and 80h, respectively. The samples were analyzed by XRD and SEM with EDX. The phase transition temperatures were obtained by using DTA. The investigations indicated that the W phase is a high-temperature phase which was stable at 900 and 1000°C and metastable at temperatures lower than 800 °C. It was found to melt incongruently at approximately 1070°C while its formation temperature was not investigated. The ternary compounds θ_1, θ_2 and θ_3 will be taken into account in the present assessment, while the W phase is ignored due to the doubts still affecting its stability range.

A number of vertical sections have been experimentally established for this system: at x(Al)= 0.75 and 0.78 by Gödecke and Ellner [136], at x(Al)= 0.8, 0.85, 0.925 and 0.97 by Gödecke [137], at x(Al)=0.575, 0.65, 0.70 by Gödecke et al.[104], at x(Al)=0.70, 0.715 and 0.725 by Scheffer et al. [138], at x(Ni)= 0.19 by Gödecke et al. [104] and x(Ni)= 0.1 and 0.13 by Scheffer et al. [138]. These vertical sections will be used for comparison in the present work.

As for thermodynamic data, the enthalpies of formation were measured at 850 °C

by Rzyman [139] and Kek et al. [140], at x(Ni)=0.75 and x(Al)=0.75, respectively. Grün et al. [141] investigated the enthalpy of formation of B2 phase at 42 and 50 at.% Al and 800 °C. Moreover Albers et al. [130] studied thermodynamic properties of selected alloys at 1200 °C along the section at x(Ni)/x(Al)=3. The excess chemical potential defined as $RTLnf_i$ (i=Al, Co, Ni) was measured by Albers et al. [130].

Dupin [142], Liu et al. [52] and Wang et al. [143] separately reported the thermodynamic assessments of the Al-Co-Ni system which included a critical evaluation of the experimental data.

The first Al-Co-Ni thermodynamic description done by Dupin [142], was limited to the phase relationships between A1, $L1_2$ and B2 phases.

Phase relationships in the Co-Ni rich region of the Al-Co-Ni system were modeled by Liu et al. [52] by combining first-principles calculations and CALPHAD approach. The experimental data in the Al-rich corner, however, were omitted. The parameters for the Al-Co, Al-Ni and Co-Ni subsystems were taken from Dupin and Ansara [81], Ansara et al. [144] and Fernandez-Guillermet [33], respectively. Two-sublattice model was separately utilized to describe the A1/$L1_2$ and A2/B2 phases.

Later Wang et al. [143] developed a thermodynamic database which can describe the Al-Co-Ni system in the whole composition range. The parameters of the binary systems were taken from Dupin and Ansara [81] for Al-Co, Sundman and Dupin [145] for Al-Ni and Fernandez-Guillermet [33] for Co-Ni. The compound DAlCoNi was simplified as a line compound at constant Al. Four-sublattice model was proposed for the A1/$L1_2$ phases based on the reassessment of Al-Ni reported by Sundman and Dupin. The workload becomes quite heaver when the system having the four-sublattice model is used to develop the database of the high-order system. At current, the two-sublattice is still considered, which makes it practicable for the whole work. The homogeneity range of DAlCoNi will be considered in the current work since the region is appreciable large.

5.2.2.2 Results and Discussions

Considering the complexity of the present system, the assessment procedure was carried out in two steps. Firstly, thermodynamic data and phase relations between $L1_2$, A1 and B2 phases in the Ni-rich portion were optimized to fit the experimental results. Secondly, experimental data in the Al-rich side were considered. DAlCoNi was first introduced as a line compound and subsequently treated as a multi-sublattice solid solution to reproduce its homogeneity range.

Calculated phase equilibria are compared to experimental tie lines or tie triangles in several isothermal sections between 600 and 1300 °C, namely at 600, 730, 800, 850, 900, 1000, 1050, 1100, 1170, 1200 and 1300 °C. Most of the experimental data can be well reproduced by the present model with a few acceptable discrepancies.

A comparison between calculated isothermal sections and selected experimental data mainly concerning phase relationships between A1, $L1_2$ and B2 phase in the Co-Ni side at 800, 900, 1000 and 1200 °C, is shown in Fig. 5-11. B2 phase has a

continuous wide homogeneity region extending between NiAl and CoAl. In the isothermal section at 800 °C, a little discrepancy between the calculation and experimental work by Zhu et al. [132] results about the para- to ferro-magnetic transition of A1. The reported sections indicate that the current calculated results can reproduce the available experimental data satisfactorily.

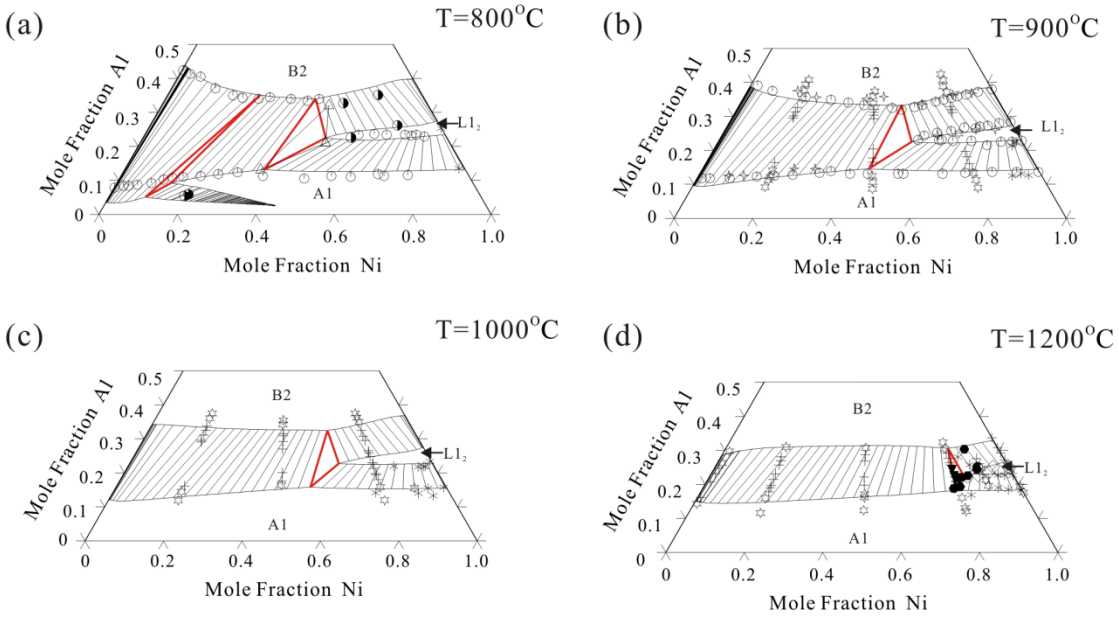

Fig. 5-11 The calculated Al-Co-Ni isothermal sections in the Co-Ni rich region at different temperatures compared with experimental data: single phase(✡), two-phase (┼), three-phase(▼) by Schramm[127]; Jia et al.[128](✳); single phase(◇), two-phase (◐), tie-line(⬣) by Alber et al. [130]; Kai et al. [129](✧); Zhu et al.[132](◷); tie-line (◑), three-phase (△) by Bai [131].

Fig. 5-12 presents isothermal sections at 730, 850, 1050 and 1100 °C in the Al-rich region compared to the experimental data by Gödecke et al. [133]. θ_1 phase located in the central part of the section, shows an appreciable solubility and complex relations with other phases. Based on the comparison with experiments the current description involving the ternary compounds θ_1, θ_2 and θ_3 is satisfactory. Notice that Ni_3Al_4 and $NiAl_3$ are stabilized in the ternary system by Co additions above the stable range in the Al-Ni binary. The only disagreement between the present calculations and experiments is about three phase regions B2+θ_3+Ni_3Al_4 (B2+Co_2Al_5+Ni_3Al_4 according to experiments) at 730 °C.

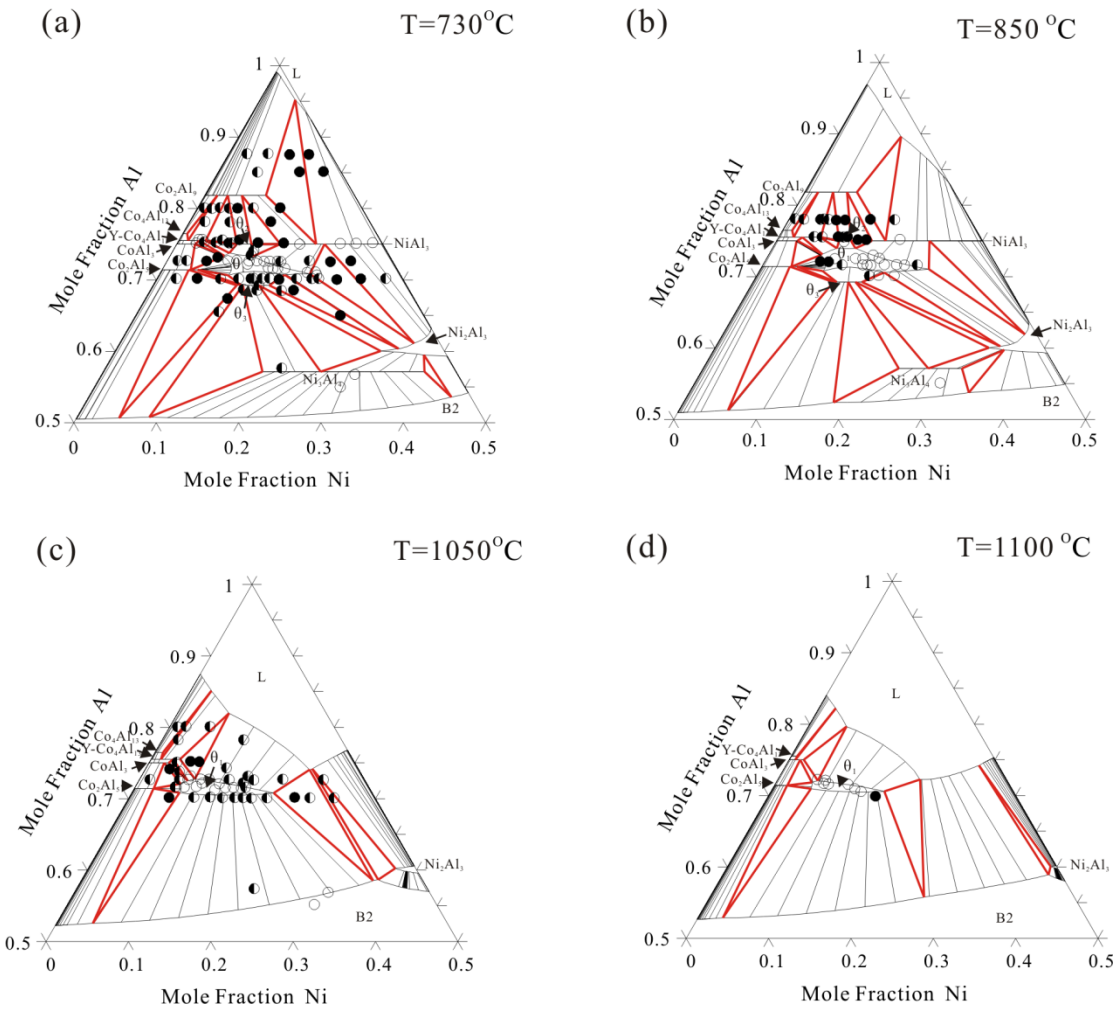

Fig. 5-12 Calculated isothermal sections in Al-rich region at different temperatures compared with experimental data by Gödecke et al.[133] single-phase (○), two phases (◐) and three phase (●).

Figs.5-13 a) to d) show the calculated vertical sections at w(Ni):w(Co)=9:1, 8:2, 5:5 and 2:8 in the Al-poor side, while Figs. 5-13 e) to h) show sections at constant x(Al)= 0.65, 0.7, 0.85 and x(Ni)=0.19 compared with the experimental results by Schramm [127] and Gödecke et al. [104], respectively. Current calculations have a considerable agreement with the experimental data reported in the sections.

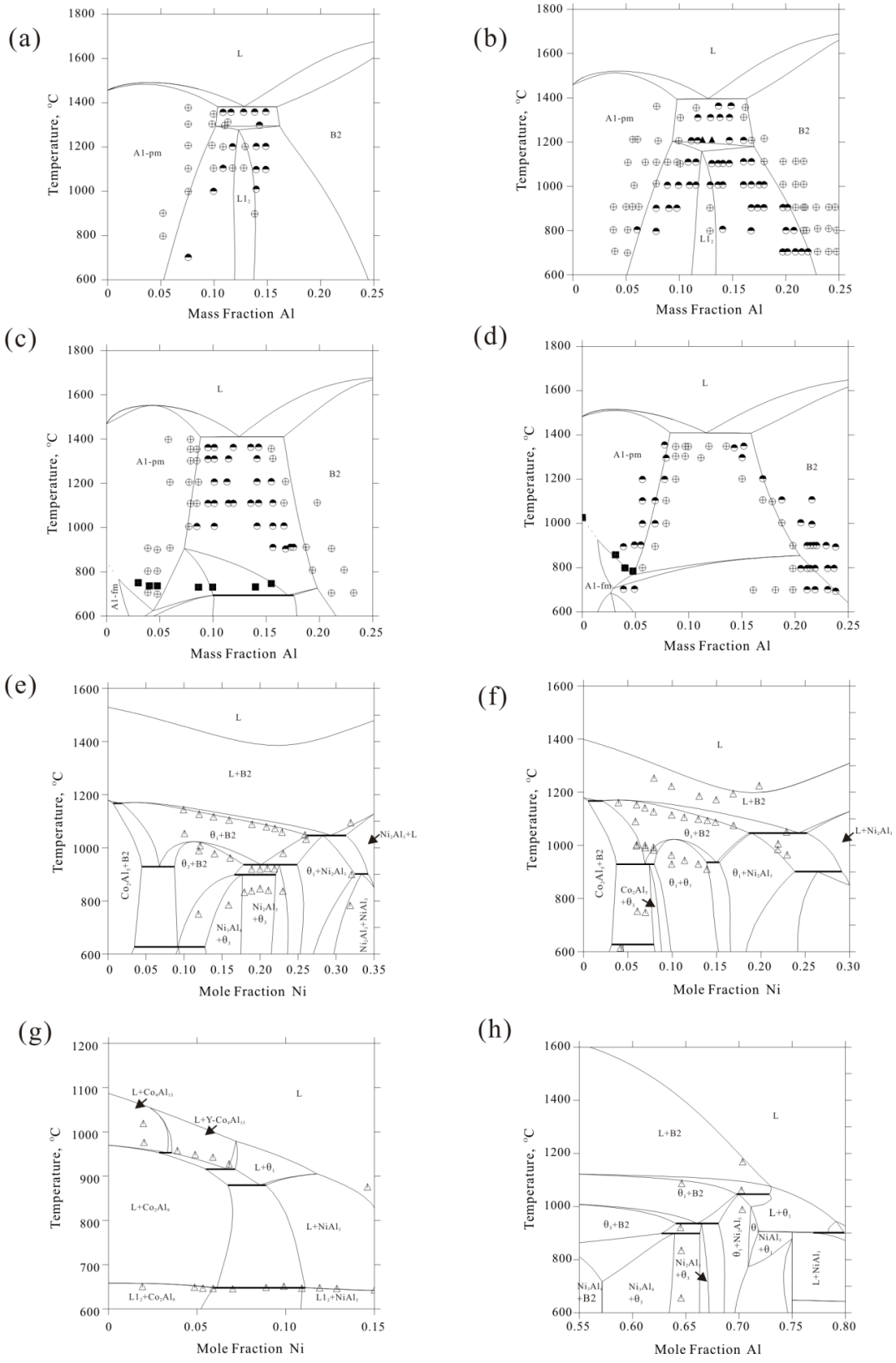

Fig. 5-13 Calculated vertical sections at (a) w(Ni):x(Co)=9:1, (b) w(Ni):x(Co)=8:2, (c) w(Ni):x(Co)=1:1, (d) w(Ni):x(Co)=2:8, (e) x(Al)=0.65, (f) x(Al)=0.7, (g) x(Al)=0.85 and (h) x(Ni)=0.19 compared to experimental data: single phase (⊕), two-phases (◓), three-phases(▲) by Schramm [127]; DTA heating (△) by Gödecke et al. [104].

Fig. 5-14 presents the calculated projection of the mono-variant liquidus lines over the whole composition range and Table 5-1 lists all the invariant reactions involving liquid phase compared to the available experimental results [133]. According to the liquidus projection, most reactions are located in the Al-rich region. The calculated reaction types and temperatures mostly fit the experimental data well, while some discrepancy exits in the reaction type involving L, τ_1, $NiAl_3$ and Ni_2Al_3. The calculated transition reaction type replaces the peritectic equilibrium speculated by Gödecke et al.[133]. A Scheil reaction scheme is shown in Fig. 5-15.

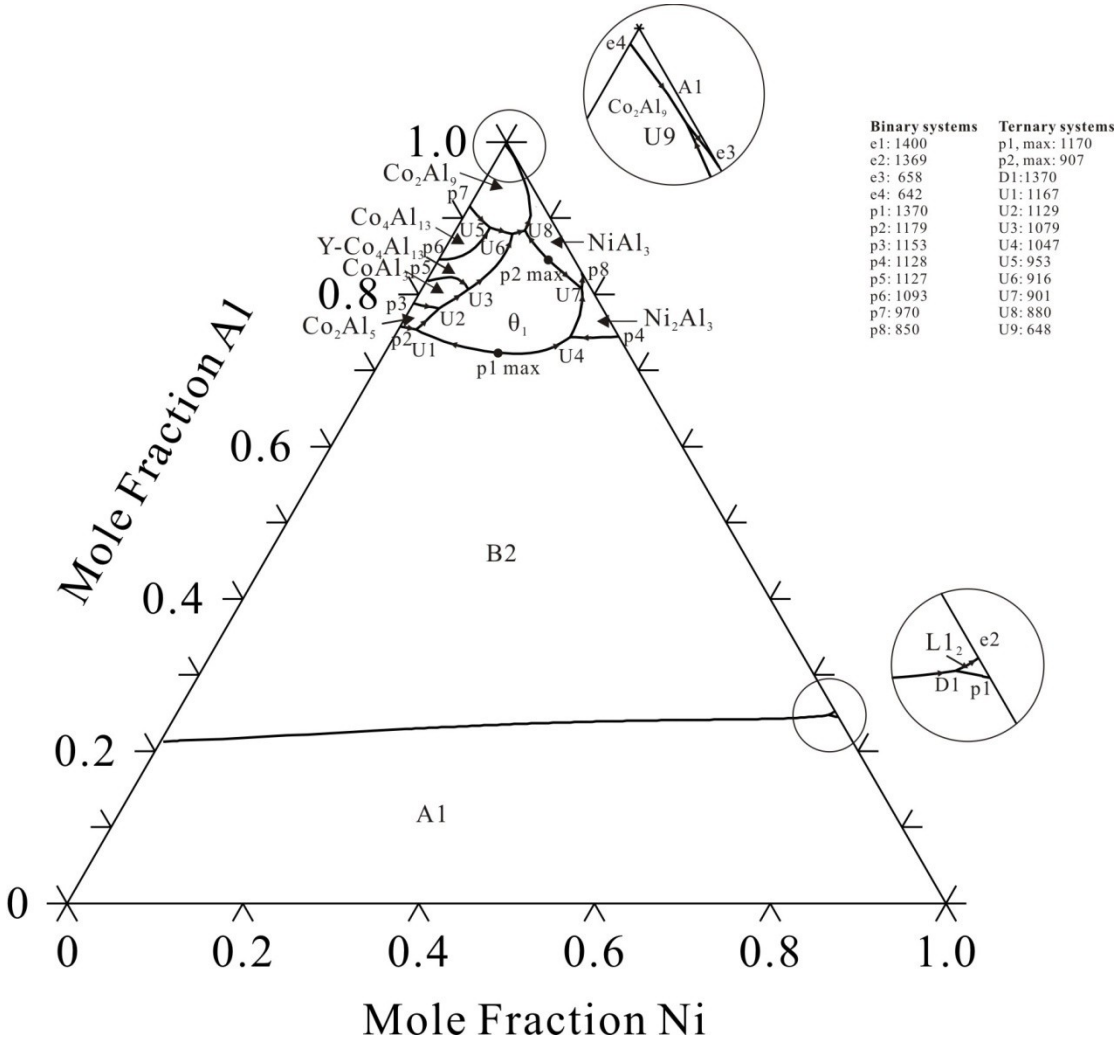

Fig. 5-14 Calculated projection of the mono-variant liquidus lines of the Al-Co-Ni system over the whole composition range in the present work

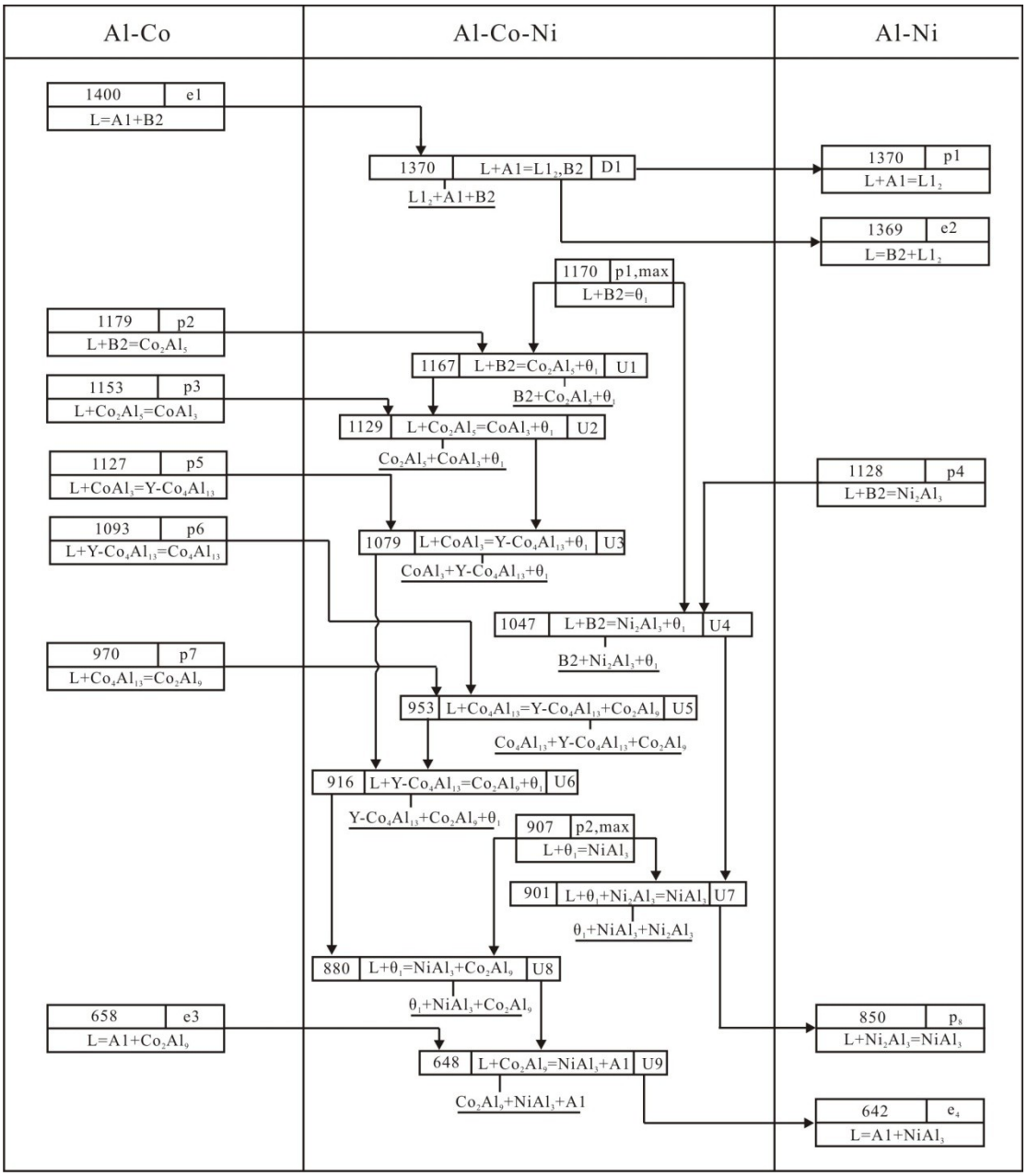

Fig. 5-15 Scheil reaction scheme of the Al-Co-Ni system

Table 5-1 Comparisons between calculated and experimental invariant reaction temperatures in the Al-Co-Ni system

Type	Invariant equilibrium	Temperature (°C)	Reference
p1 max	L+ B2 ⇄θ_1	1170	Calc.
		1175	Exp. [133]
p2 max	L+θ_1 ⇄ $NiAl_3$	907	Calc.
		-	-
D1	L+A1 ⇄ $L1_2$,B2	1370	Calc.
		-	-
U1	L+B2 ⇄ Co_2Al_5+θ_1	1167	Calc.
		1160	Exp. [133]
U2	L+Co_2Al_5 ⇄ $CoAl_3$+θ_1	1129	Calc.
		1136	Exp. [133]
U3	L+ $CoAl_3$ ⇄ Y-Co_4Al_{13}+θ_1	1079	Calc.
		1080	Exp. [133]
U4	L+ B2 ⇄ Ni_2Al_3+θ_1	1047	Calc.
		1048	Exp. [133]
U5	L+ Co_4Al_{13} ⇄Co_2Al_9+ Y-Co_4Al_{13}	953	Calc.
		950	Exp. [133]
U6	L+ Y-Co_4Al_{13} ⇄ Co_2Al_9+τ_1	916	Calc.
		906	Exp. [133]
U7	L+θ_1 ⇄ $NiAl_3$+ Ni_2Al_3	901	Calc.
	L+θ_1 + Ni_2Al_3⇄ $NiAl_3$	900	Exp. [133]
U8	L+θ_1 ⇄ $NiAl_3$+ Co_2Al_9	880	Calc.
		888	Exp. [133]
U9	L+ Co_2Al_9 ⇄ $NiAl_3$+ $L1_2$	648	Calc.
		643	Exp. [133]

The calculated enthalpy of formation of alloys along x(Ni)=0.75 and x(Al)=0.25 at 850 °C is presented in Fig. 5-16, as well as the measured results by Rzyman [139] and Kek et al.[140]. The comparison indicates that the thermodynamic parameters are reliable Fig. 5-17 shows the calculated enthalpy of formation of B2 phase along x(Al)=0.42 and 0.5 at 800 °C compared with the experimental data [141]. Moreover, the calculated activities of Co and Ni at 1200 °C along x(Ni)/x(Al)=3 with experimental data from [130] is presented in Fig. 5-18. These comparisons support the reliability of the present thermodynamic description.

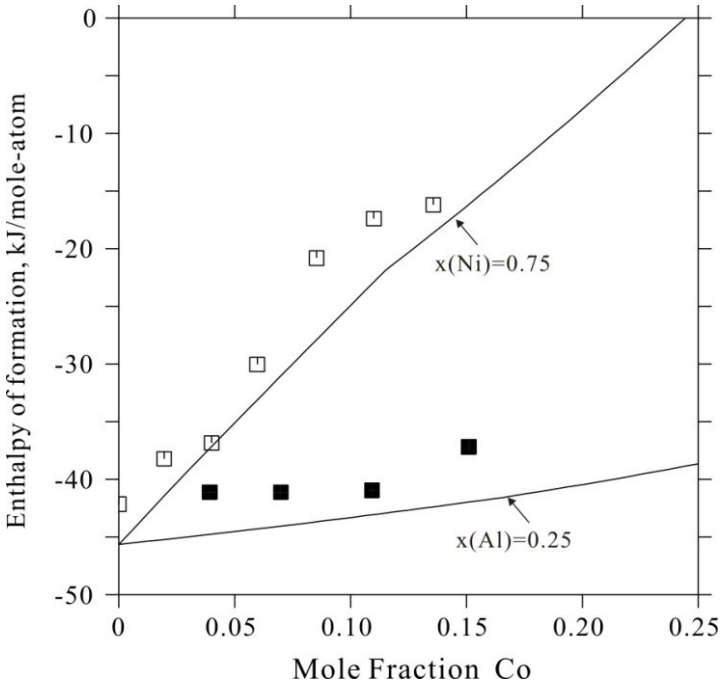

Fig. 5-16 calculated enthalpy of formation of alloys along x(Ni)=0.75 and x(Al)=0.25 at 850 °C compared to experimental data by Rzyman [139](□) and Kek et al. [140](■)

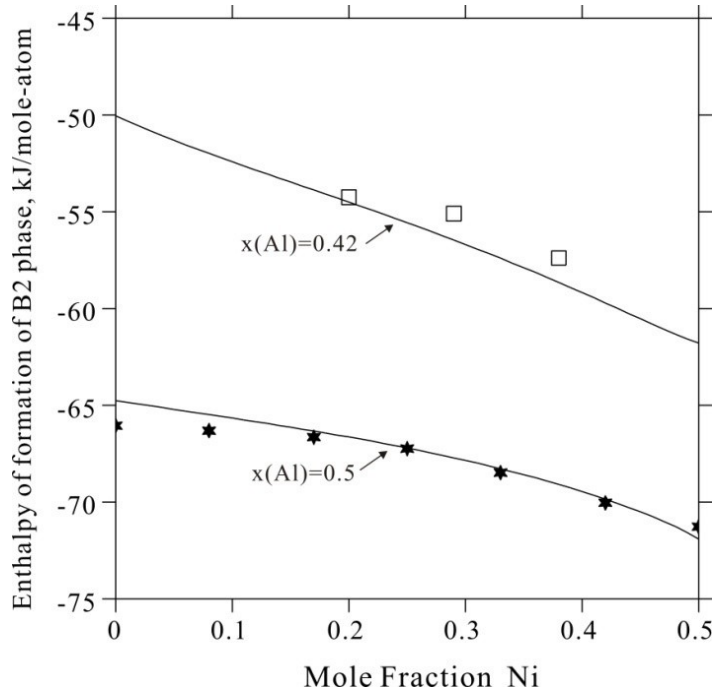

Fig. 5-17 Calculated enthalpy of formation of B2 phase along x(Al)=0.42 and 0.50 at 800 °C compared to experimental data by Grün et al. [141] (□, ✱).

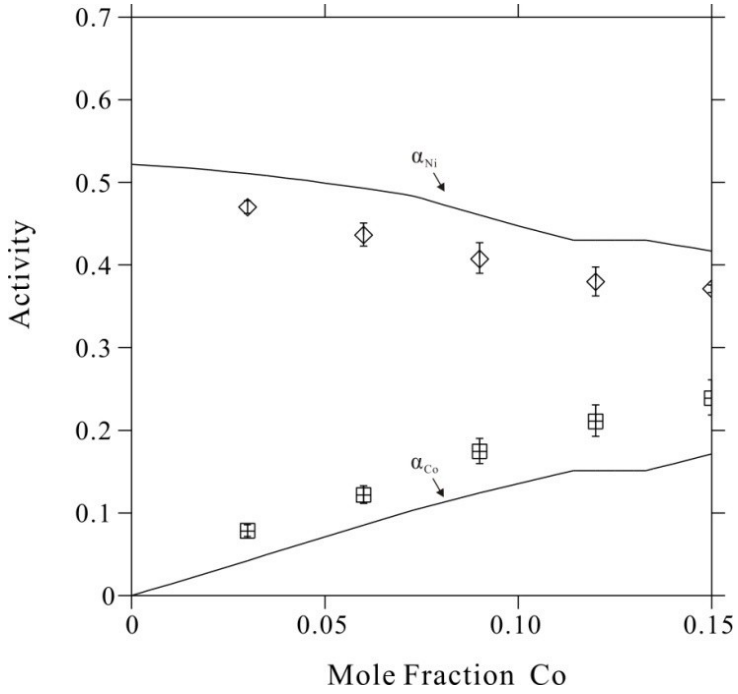

Fig. 5-18 Calculated activity of Co and Ni along x(Ni)/x(Al)=3 at 1200 °C compared to experimental data by Albers et al.[130] (⊞, ◇).

Based on a critical review of the available literature, the Al-Co-Ni system was modeled over the entire composition and temperature range according to the CALPHAD method. The liquid phase and the terminal solid solutions A1, A2 and A3 were modeled using a regular solution model while all other phases were described using sublattice models. Two sublattices were introduced for the ordered $L1_2$ and B2 phases. Calculated results have been compared to experimental phase equilibria and thermodynamic data. From the above comparisons it can be seen that a satisfactory agreement has been obtained between calculations and experiments. A self-consistent thermodynamic description of Al-Co-Ni system is obtained, which can be accepted for the modeling of higher order system.

5.2.3 Al-Cr-Ni system

5.2.3.1 Review

Phase relations in the Al-Cr-Ni system have been investigated by many authors. Most of earlier researches paid more attention to the Ni-rich region, due to its relevance for applications. However, the information about the Al-rich part is scarce.

In 2004 Velikanova et al. [126] made a critical evaluation considering all the available literature up to 2003: several isothermal sections in Ni-rich region and a number of vertical sections were presented, in addition to selected thermodynamic data. We refer to this paper for the description and discussion of the older literature data, while papers published after 2003 will be presented and discussed in this work.

Phase equilibria of Ni-rich region at 1150 °C were investigated by Kitajima et al. [146] using annealed ternary alloys and diffusion couples. The solubility ranges of B2 and $L1_2$ as well as a number of B2-A2 (Cr), B2-$L1_2$, B2-A1 and $L1_2$-A1 tie lines were determined. Maximum Cr solubility was found to be about 9 at.% in Ni_3Al and 17 at.% in NiAl.

The Ni-Cr rich part (at x(Al)<0.5) of the 1200 °C isothermal section was investigated by Cutler [147] using diffusion multiples together with SEM imaging and EPMA. He determined several tie-lines between the A1, A2, $L1_2$, and B2 phases. It is worth mentioning that the two-phase fields fcc+$L1_2$ and $L1_2$+B2 determined by Cutler at 1200 °C are systematically richer in Ni than the accepted binary Al-Ni equilibria.

Several studies have been reported in literature about ternary phases and ternary solubilities of binary Al-Cr phases in the Al-rich part of the system [88, 89, 148, 149]. In particular, isothermal sections and invariant reactions have been studied by Weitzer et al. [149] and by Grushko et al. [88, 89]. Owing some disagreement between the older investigations, the most recent ones [88, 89, 149] seem to agree about the existence of three ternary compounds, one of which with an appreciable solid solubility.

In particular Weitzer et al. [149] constructed a tentative liquidus projection of Al-Cr-Ni system at ≥50 at% Al using XRD, energy dispersive X-ray analysis (EDXA), DTA up to 1500 °C and metallography. He also proposed a partial reaction scheme and established phase relations in the Al-rich part at 700 °C. For the ternary phase labeled τ_1, whose crystal structure was previously determined by Sato et al. [148], a wide composition range was reported. This phase was found to form incongruently at 1036 °C from Liquid and Cr_5Al_8-L. Another two ternary compounds τ_2 and τ_3 were also found to be stable at 700 °C. According to [149] τ_2 melts incongruently into Liquid, τ_1 and Ni_2Al_3, while τ_3 decomposes in the solid state at 976K.

Grushko et al. [88] investigated the Al-Cr-Ni ternary compounds as well as the ternary solubilities of the binary phases. The ternary extensions of the binary Al-Cr phases were found to be: 2 at.% Ni for Cr_7Al_{45}, up to 1 at.% Ni for $CrAl_4$ and $CrAl_5$ and up to 3 at.% Ni for Cr_5Al_8. As for Al-Ni, the binary $NiAl_3$ phase dissolves around 1 at.% Cr and Ni_2Al_3 up to ~3 at.% Cr. Ternary solubilities lower than 1 at.% will be omitted in the present modeling.

Moreover Grushko et al. [89] detected the same ternary compounds as Weizter et al. [149]. Through DTA examinations, τ_1 was found to form at ~1030 °C, in good agreement with Weizter et al. [149]. τ_2 phase was found to be stable below 835 °C around the $Al_{80}Ni_9Cr_{11}$ composition, with a limited solubility. τ_3 phase was found to be stable at 700 and 800 °C in a limited composition range around $Al_{82}Ni_3Cr_{15}$. Another ternary phase named ε was detected by Grushko to be stable in a small temperature range around 1000 °C, but it was not observed by Weitzer et al. [149]. Due to uncertainty about nature and stability range of this phase, it will not be considered in this work.

Several isothermal sections in the Al-rich region have been investigated by Grushko et al. [88, 89] at 700, 800, 900, 1000 and 1150 °C. There are some

disagreements between the results by Weitzer et al. [149] and Grushko et al. [89]: the compositions of all the ternary phases reported by Grushko et al. are richer in Al than those reported by Weitzer et al., while τ_2 and τ_3 are reported as line compounds by Weitzer et al. and with some solid solubility by Grushko et al.. Moreover in the isothermal sections at 700 °C, the three phase fields $NiAl_3$+τ_2+ Ni_2Al_3 and τ_1+τ_2+ Ni_2Al_3 are detected by Weitzer et al. [149], while $NiAl_3$ +τ_1+ Ni_2Al_3 and τ_1+τ_2+$NiAl_3$ are found in the work by Grushko et al. [89]. Discrepancies between Weitzer et al. and Grushko et al. are also due to the different choice about the accepted binary Al-Cr phases: four different Cr_5Al_8 phases according to Weitzer and only two, according to Grushko. Moreover there are some differences in the temperature stability ranges of τ_2 and τ_3.

Since a series of detailed experimental result are published and the experimental process seems more reliable, the results by Grushko et al. [88, 89] will be utilized as the experimental basis for the present assessment. Due to the very limited solubility, phases τ_2 and τ_3 are modeled as line compounds in this work.

As for the vertical section of between NiAl and Cr, there is a maximum eutectic reaction between L, A2 and B2 phases. Merchant and Notis [150] released a very detailed review about experimental results based on the available literature. Several authors have investigated this eutectic reaction, giving different compositions for the eutectic point. It seems that only Kornilov and Mints [151] reported the reaction temperature as 1445 °C, determined by means of thermal and microscopic analysis, assisted by hardness and resistivity measurements. However their samples contained Cr of relatively low purity (99.96 at.% Cr or 97 at.% Cr plus 2.5 at.% Al, 0.3at.%Si and 0.5 at.% Fe). Moreover the Cr melting point taken by Kornilov and Mints was 1828 °C, almost 80 °C lower than the accepted one, which can be considered a consequence of a low purity Cr. Merchant and Notis [150] concluded that it was likely that NiAl-Cr maximum eutectic lied in the vicinity of about 34 at.% Cr and about 1445 °C. Rogl [152] evaluated this system and accepted the estimated temperature and composition from Merchant and Notis [150]. He deduced that the maximal solid solubility at 1025, 1150 and 1200 °C was much larger than previously claimed by Kornilov and Mints [151], Bagarystskiy [153] and redrew the vertical section. Unfortunately, the composition of eutectic point shown in the figure in [152] was not the same as the one listed in the table. In 2004, Velikanova et al. [154], while updating the Rogl's work, didn't accept the composition and temperature of this eutectic reaction, possibly considering that it was not sufficiently supported by reliable data. In 2008, Weitzer et al. [149] reported this reaction at 1433 °C without indication of the composition. Due to the low purity of the Cr used in [151], the results from Weitzer et al. are considered more reliable. Then, the data from [151] are not used for this assessment.

A thermodynamic assessment of the Al-Cr-Ni system has been performed by Huang and Chang [155], based on the experimental data available at that time, using a substitutional solution model for the liquid, bcc and fcc phases and a two sublattice model for $L1_2$, (Al, Cr, Ni)$_{.25}$(Al, Cr, Ni)$_{.75}$ and B2 (Al, Cr, Ni)$_{0.5}$(Cr, Ni, Va)$_{0.5}$. No

ternary solubility was considered for the remaining Al-Ni and Al-Cr phases and no ternary phase was introduced. As for the binary subsystems, the assessments by Saunders and Rivlin [91], Huang and Chang [99], and Lee [36] were adopted for Al-Cr, Al-Ni and Cr-Ni, respectively.

In 2001 Dupin et al. [95] remodeled the system by improving the assessment previously developed in the Dupin's thesis [142]. In that work a single equation was used for the description of couples of phases related by order/disorder transformations, i.e. A1 and $L1_2$ as well as A2 and B2. Dupin et al. [95] focused the new assessment on the Ni-rich part of the system (the Cr-Ni-NiAl region) by modeling only the liquid, A1, $L1_2$, A2 and B2 phases.

Later Cao et al. [156] used the cluster/site approximation to model the disordered and ordered fcc phases, as an extension of their similar calculation previously developed for Al-Ni [100]. Even in this work the Al-rich part of the system was neglected.

In terms of thermodynamic data, Maciag and Rzyman [157, 158] used solution calorimetry to measure enthalpy of formation of Al-Ni-Cr alloys in the $Ni_{75}Al_{25}$-$Ni_{85}Cr_{15}$ (at 600 °C) [157] and $Ni_{75}Al_{25}$-$Ni_{75}Cr_{25}$ (at 600, 723 and 877 °C) [158] sections. Then, by observation of the change in slope of the enthalpy curves as a function of composition, they determined the $L1_2$/$L1_2$+A1 and $L1_2$+A1/A1 phase boundaries in the mentioned sections. It's worth to mention that the enthalpies of formation from [158] are in good agreement with accepted values on the Al-Ni side while on the Ni_3Cr side they are significantly higher than the accepted ones. For this reason the enthalpy of formation data by [157, 158] will not be used for the present assessment.

Moreover, $L1_2$/$L1_2$+A1 and $L1_2$+A1/A1 phase boundaries determined by [158] are compared with other experimental results [159-162] in the Ni_3Al-Ni_3Cr vertical section. It may be observed that the stability region of $L1_2$ phase according to [158] is much smaller than that based on direct investigation of quenched samples [159-162].

Partial and integral enthalpies of mixing of ternary liquid alloys have been determined by Saltykov et.al [163] by high temperature isoperibolic calorimetry at 1445-1458 °C. These results will be taken in this work.

Kek et al. [164] measured the enthalpy of formation of ternary alloys at the $Cr_5Ni_{72}Al_{23}$, $Cr_8Ni_{70}Al_{22}$ and $Cr_{12}Ni_{67}Al_{21}$ compositions by solution calorimetry at room temperature. Based on X-ray and metallographic analyses authors concluded that only $L1_2$ phase was stable in the measured samples. Dupin et al. [95] however, pointed out that the agreement between calculations and experiments was better when considering also A1 and A2 as possible equilibrium phases at the investigated compositions. So the experiment values from [164] will not be used for the optimization, but only for comparison with calculated results. Oforka and Argent [165] derived the molar Gibbs energy of the phases in the three-phase fields $L1_2$+A1+B2 and A1+B2+A2 at 1150 °C from activity measurements. These will be used for comparison with the calculated results of this work.

5.2.3.2 Results and Discussions

The similar strategy used in the Al-Co-Ni system is also accepted during the optimized procedure of the Al-Cr-Ni system, therefore the detailed steps are omitted here.

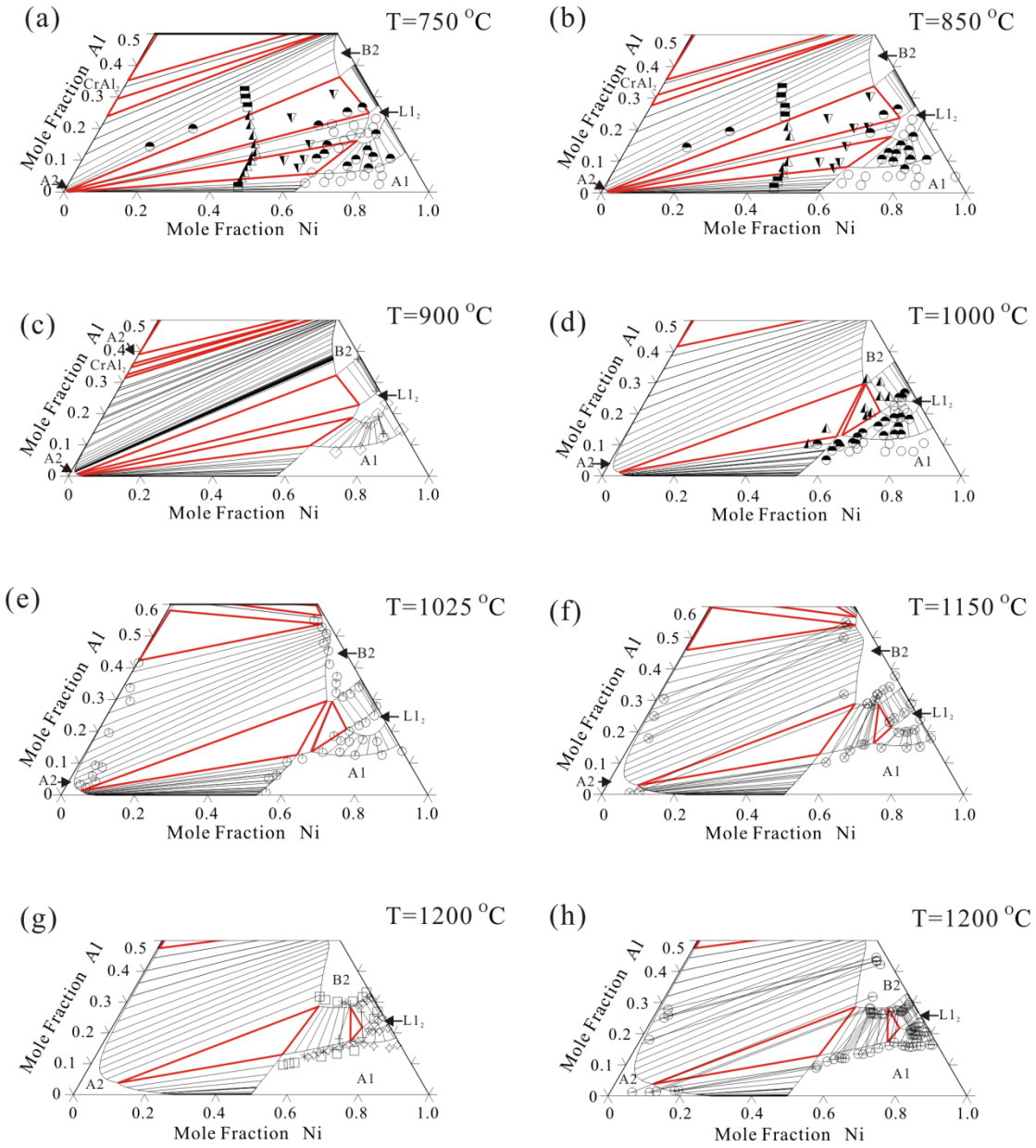

Fig. 5-19 The calculated Al-Cr-Ni isothermal sections in the Cr-Ni rich region at different temperatures compared with experimental data: single phase (○), two phases (◓) and three phases (▼), by Taylor and Floyd [159]; two phases (⬒) and three phases (◭), by Goretsky [166]; tie-line by Jia et al. [167] (+), Brozh et al. [168] (◇), DeLancrolle and Seigle [169] (⏀), Kitajima et al. [146] (⊗), Carol [170] (□), Yeung et al. [171] (✳), Qiao [172] (✧), Culter [147] (⊖)

Calculated phase equilibria are compared to experimental tie lines or tie triangles in several isothermal sections between 700 and 1300 °C, namely at 700, 750, 850, 900,

1000, 1025, 1100, 1150, 1200, 1300 °C. Most of the experimental data can be well reproduced by the present model with a few acceptable discrepancies.

A comparison between calculated isothermal sections and selected experimental data mainly concerning phase relationships between (Ni), $L1_2$ and B2 in the Ni-rich region, is shown in Fig. 5-19. It may be observed that it was not possible to fit the solubility limit of the Ni-rich fcc phase at all the reported temperatures, especially at 1150 °C. At this temperature the calculated phase boundary is at fairly higher Al concentration than the experimental points, but a better agreement with ternary data would conflict with the accepted binary equilibria.

Fig. 5-20 presents the isothermal sections at lower temperatures in the Al-rich region, where the τ_1 phase exists with an appreciable solubility region, and two more ternary phases τ_2 and τ_3 are stable. The calculated phase equilibria are consistent with the experimental results by Grushko et al. [88, 89]: all phase relations correspond. There is only some minor discrepancy about the extent of the homogeneity region of τ_1, mainly because τ_2 and τ_3 have been approximated as stoichiometric phases. According to our calculation τ_1 phase decomposes above 1150 °C.

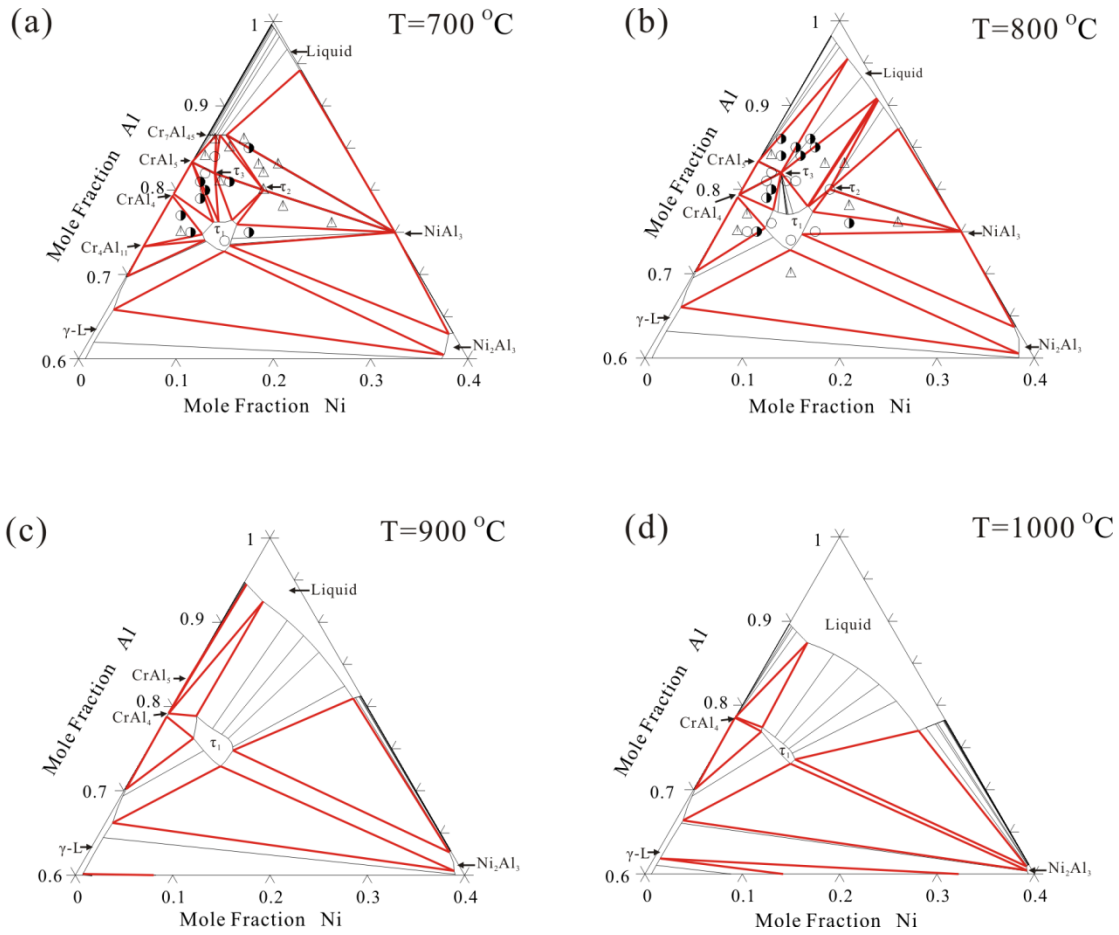

Fig. 5-20 Calculated isothermal sections in Al-rich region at different temperatures compared with experimental data by Grushko et al. [88, 89] single-phase (○), two phases (◑) and three phase (◬).

Fig. 5-21 shows the calculated vertical sections at x(Al):x(Ni)=1:1 and x(Ni)=0.75, in comparison with experimental values. In Figure 6(a) we can notice that the A2 solubility region is larger than experimental results by [151, 153]. However it is consistent with isothermal solubility data by Oforka and Argent [165] (at 1150 °C), De Lancrolle and Seigle [169] (at 1025 °C), and Cutler [147] (at 1200 °C), as already observed also by Rogl [152]. More experiments are needed to better define the boundary of the A2 solid solution in the Cr rich region. Figure 5-21(b) presents phase relationships between A1, $L1_2$ and liquid in the 75 at% Ni vertical section. We can notice that the A1 solubility limit is well defined and consistently calculated, while about the boundary of the $L1_2$ homogeneity region larger uncertainty exist ant it is impossible to reproduce all the experimental results.

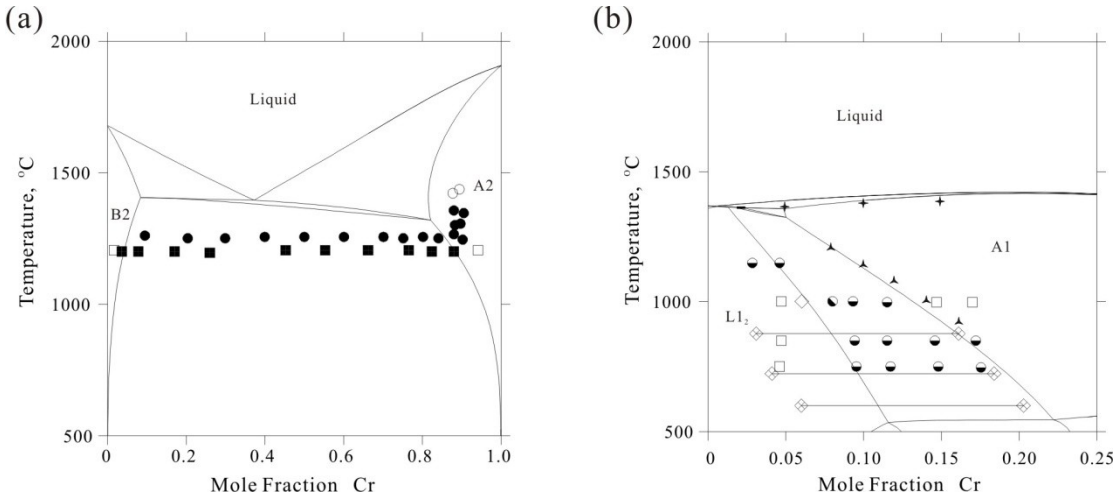

Fig. 5-21 Calculated vertical sections at (a) (Al):x(Ni)=1:1 and (b) x(Ni)=0.75 compared to experimental data by Kornilov and Mints [151] single phase (□), two phases (■), Bagaryatskiy [153] single phase (○), two phases (●), Maciag and Rzyman [157] (⊗), Taylor and Floyd [159] single phase (□), two phases (◒), Ochiai et al. [160] single phase (◇), two phases (◒), Hong et al. [161](⮝), and David [162](✦).

In Fig. 5-22 the vertical sections at x(Cr)=0.05, 0.1 and 0.15 are reported. It can be noticed that, in this case, there is poor agreement between experimental liquidus points from different authors [162, 173], with differences in the order of about 50 °C. Having no reason to exclude any of the literature sources, in agreement with the previous assessment by Dupin et al. [95], we considered all of them and, consequently, our calculated liquidus lies between these points.

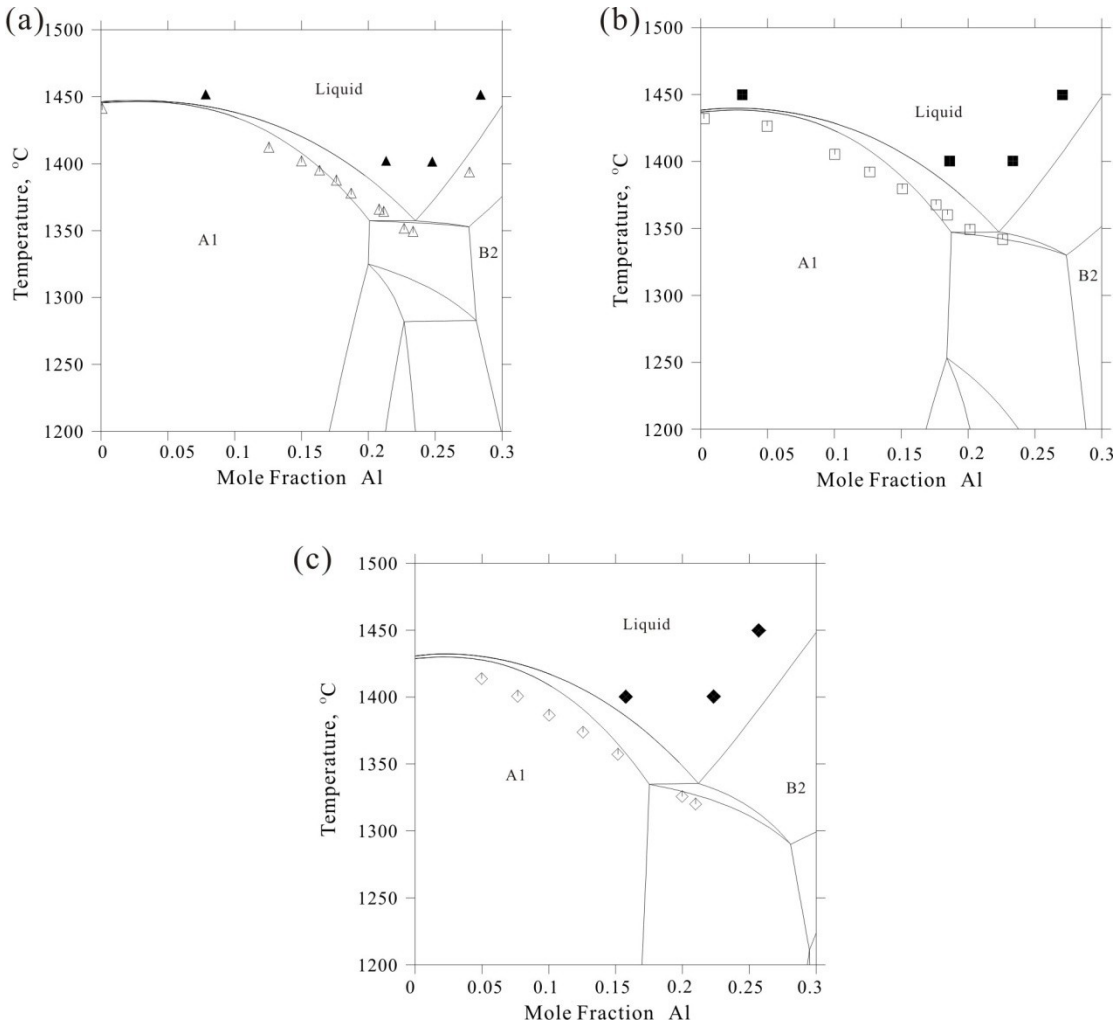

Fig. 5-22 Calculated Al-Cr-Ni vertical sections at (a) x(Cr)=0.05, (b) x(Cr)=0.10 and (c) x(Cr)=0.15 compared to experimental liquidus temperatures, by Kornilov and Mints [151] (▲, ■, ◆), David [162] (△, □, ◇), Sung and Poirier [174] (+)

The calculated fcc solvus curves at different Al compositions are compared to experimental data [161] in Fig. 5-23. The calculated results fit well at higher constant Al while become less good in the low Al part. The difference between the experimental data and calculated results starts from the Al-Ni boundaries. Curves at higher Al content (namely at 17 and 15 at.% Al) are consistent with the accepted Al-Ni binary system, while at lower Al composition they become more and more inconsistent (a difference of almost 60 °C exists at 13 at.% Al). Possibly the discrepancies may be due to the difficulty of reaching equilibrium during DTA measurements at lower temperatures. Then in this work only higher temperature data were taken into account. The calculated results can reproduce the experiments within acceptable accuracy.

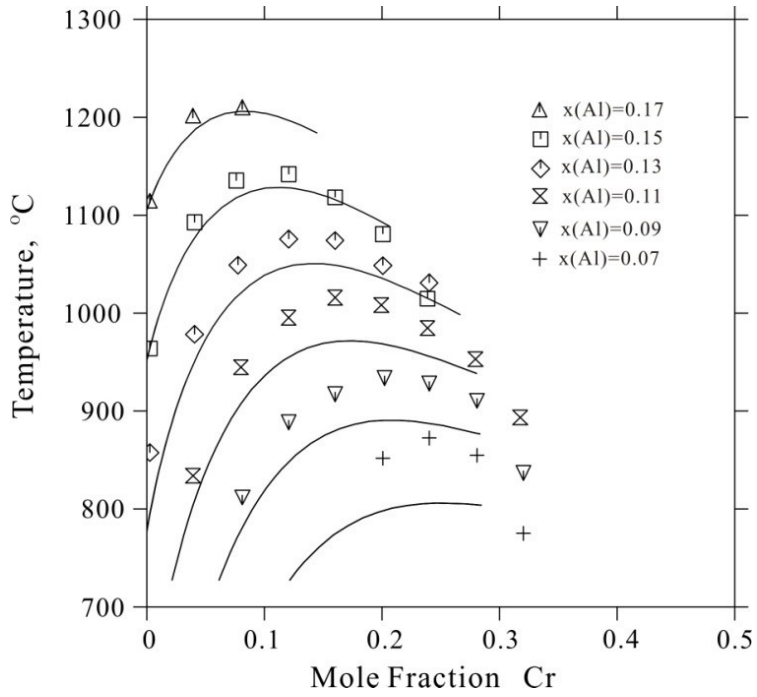

Fig. 5-23 Calculated solvus curves (A1-A1+$L1_2$ phase boundary) in several vertical sections at constant Al composition compared to experimental data by Hong et al. [161].

The calculated liquidus surface is reported in Fig. 5-24 and all the invariant reactions involving liquid are listed in Table 5-2 where they are compared to experimental results, mainly from Weitzer et al. [149]. The same invariant reactions are also shown in the form of a Scheil reaction scheme in Fig. 5-25.

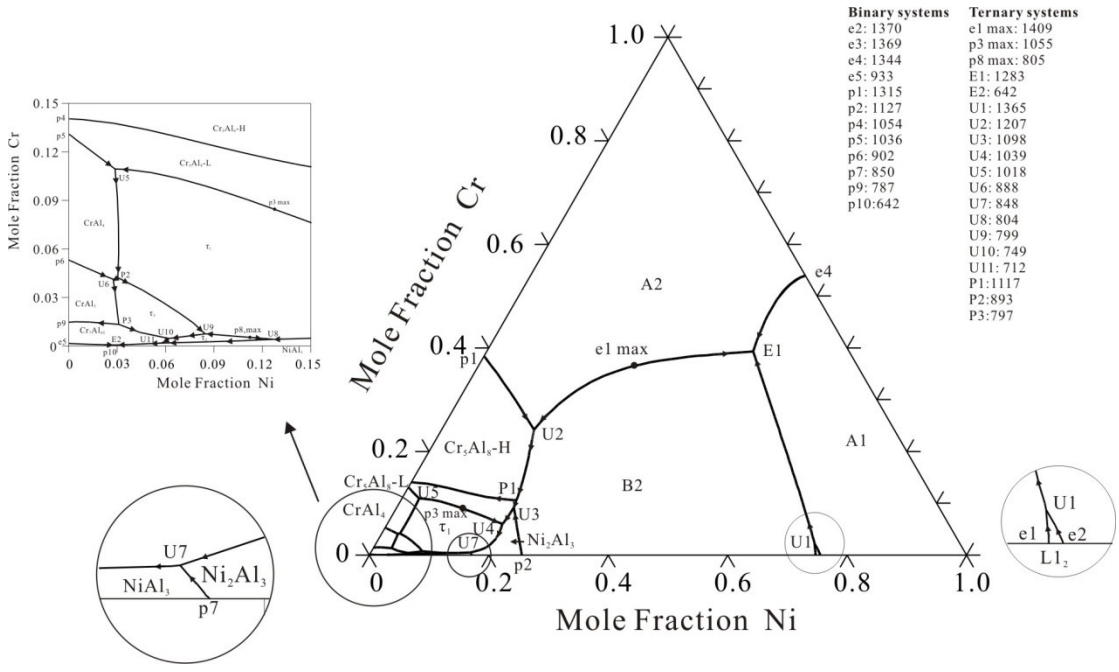

Fig. 5-24 Calculated monovariant liquidus lines and primary solidification ranges of the Al-Cr-Ni system in the present work

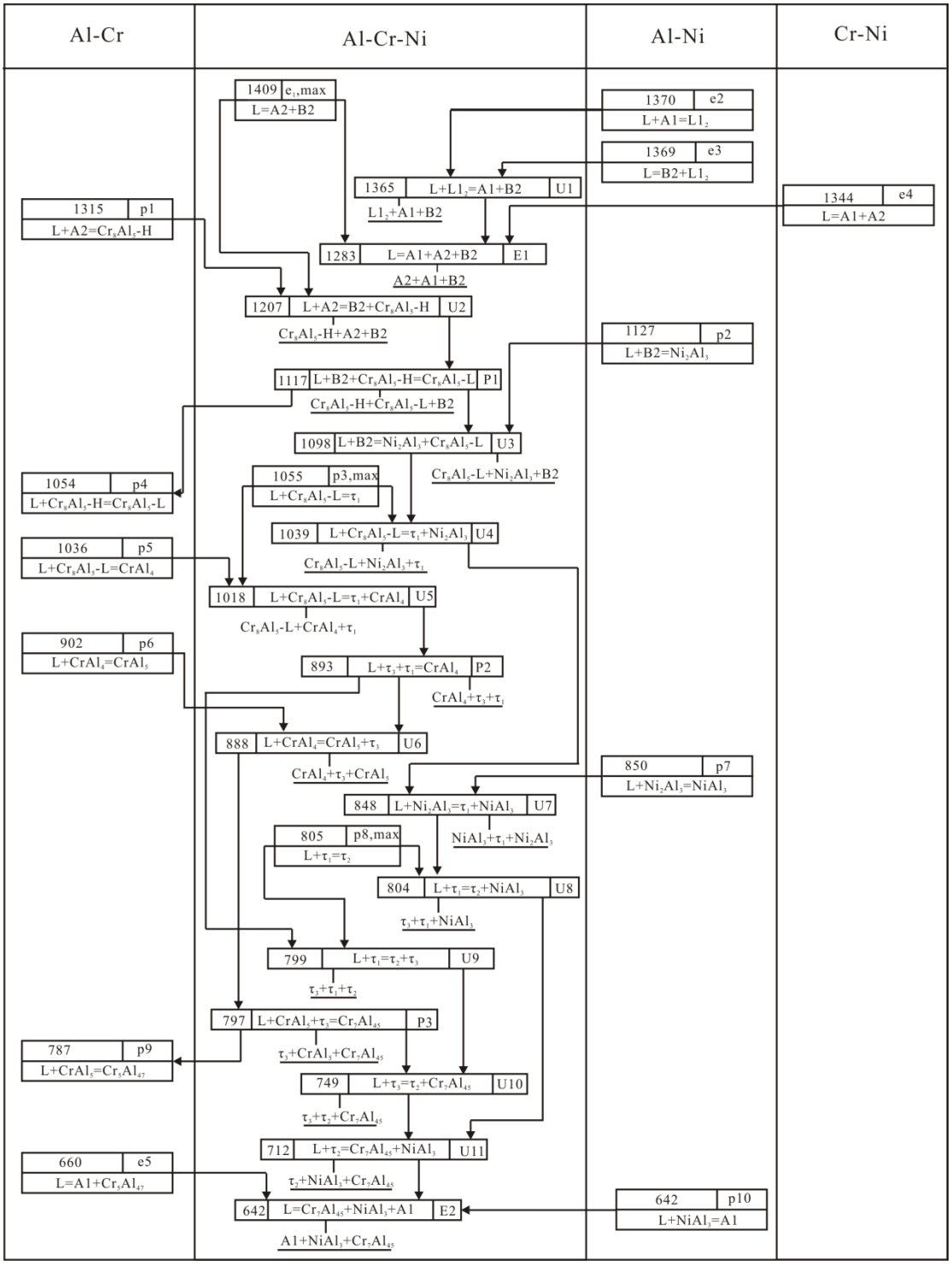

Fig. 5-25 Scheil reaction scheme of the Al-Cr-Ni system

About the liquidus surface we can observe that very few experimental data have been reported in literature and further investigations would be useful. However, more information is available about invariant equilibria. In this case a general good agreement has been obtained, unless there are some differences between selected

invariant temperatures or invariant reactions. It seems that further investigations are needed to reach a better agreement between experiments and calculations, especially in the Al rich corner where a more complex system of invariant equilibria close to each other is present.

Table 5-2 Comparisons between calculated and experimental invariant reaction temperatures in the Al-Cr-Ni system

Type	Invariant equilibrium	Temperature °C	Reference
e1 max	L ⇄ A2+B2	1409	Calc.
		1433	Exp. [149]
		1445	Exp. [151]
p3 max	L+ Cr_5Al_8-L ⇄ τ_1	1055	Calc.
p8 max	L+τ_1 ⇄ τ_2	805	Calc.
U1	L+$L1_2$ ⇄ A1+B2	1365	Calc.
		1341	Exp. [149]
		1341±10	Exp. [159]
E1	L ⇄ A1+A2+B2	1283	Calc.
		1289	Exp. [149]
		1320±10	Exp. [159]
		1300	Exp. [151]
U2	L+A2 ⇄ B2+ Cr_5Al_8-H	1207	Calc.
		1155	Exp. [149]
P1	L+B2+ Cr_5Al_8-H ⇄ Cr_5Al_8-L	1117	Calc.
U3	L+B2 ⇄ Cr_5Al_8-L+ Ni_2Al_3	1098	Calc.
		1055	Exp. [149]
U4	L+ Cr_5Al_8-L ⇄ τ_1+ Ni_2Al_3	1039	Calc.
		1027	Exp. [149]
U5	L+ Cr_5Al_8-L ⇄ τ_1+ $CrAl_4$	1018	Calc.
		1023	Exp. [149]
P2	L+τ_3+τ_1 ⇄ $CrAl_4$	893	Calc.
U6	L+ $CrAl_4$ ⇄ $CrAl_5$+τ_3	888	Calc.
U7	L+ Ni_2Al_3 ⇄ τ_1+ $NiAl_3$	848	Calc.
U8	L+τ_1 ⇄ τ_2+ $NiAl_3$	804	Calc.
U9	L+τ_1 ⇄ τ_2+τ_3	799	Calc.
P3	L+ $CrAl_5$+τ_3 ⇄ Cr_7Al_{45}	797	Calc.
U10	L+τ_3 ⇄ τ_2+ Cr_7Al_{45}	749	Calc.
U11	L+τ_2 ⇄ $NiAl_3$+ Cr_7Al_{45}	712	Calc.
		714	Exp. [149]
E2	L ⇄ $NiAl_3$+ Cr_7Al_{45}+A1	642	Calc.
		639	Exp. [149]

Fig. 5-26 presents the enthalpy of mixing of the liquid phase at 1445 °C at different Al composition compared with the experimental data from [163]. Fig. 5-27 shows the calculated enthalpy of formation of alloys in the $Ni_{75}Al_{25}$ - $Ni_{75}Cr_{25}$ and $Ni_{75}Al_{25}$ - $Ni_{85}Cr_{15}$ sections at 600 °C compared to the experimental data from [157]. As already observed in section 5.2.3.1, there is good agreement between calculation and experiments in the region close to Ni-Al while difference becomes larger in the region close to Ni-Cr part, where data by [157] do not agree with the accepted values for the Ni-Cr binary system.

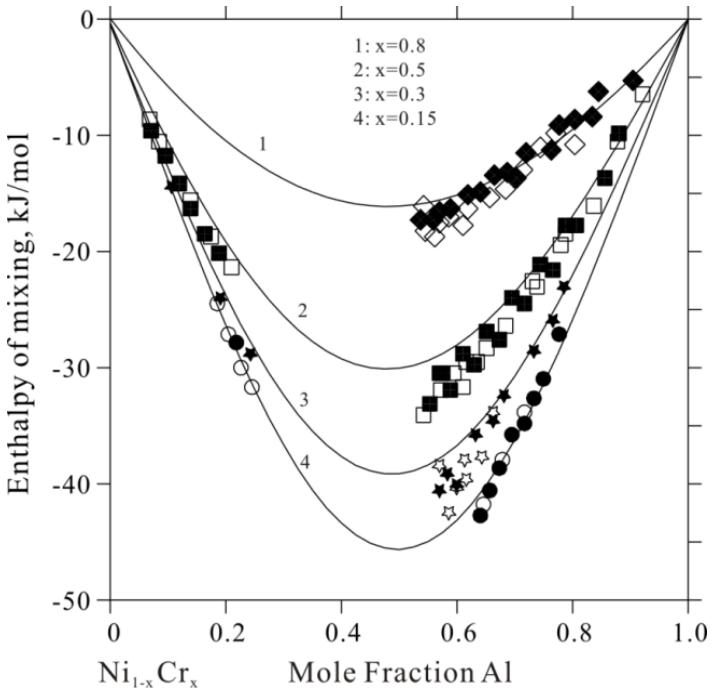

Fig. 5-26 Calculated enthalpy of mixing of the liquid phase at 1445 °C, along a series of $Ni_{1-x}Cr_x$-Al sections, compared to experimental data by Saltykov et al. [163]. Solid points and open points are from different equations respectively.

Table 5-3 compares the calculated molar Gibbs energy of the phases at 1150 °C with calculation from Dupin et al. [95] and experiments from [164]. Table 5-4 shows the calculated molar enthalpy of formation of solid alloys at some certain compositions with experiments from [175]. A general good agreement may be observed.

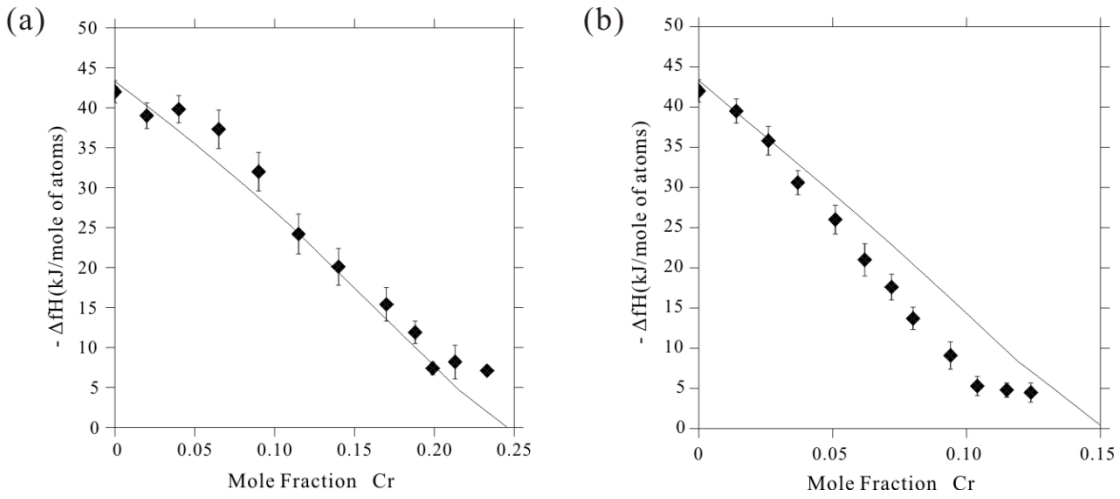

Fig.5-27 Calculated enthalpy of formation at 600 °C along the (a) $Ni_{75}Al_{25}$-$Ni_{75}Cr_{25}$ and (b) $Ni_{75}Al_{25}$-$Ni_{85}Cr_{15}$ sections compared to experimental data by Maciag and Rzyman [157].

Table 5-3 Molar Gibbs energy of formation of the phases involved in the three phase equilibria at 1150 °C in kJ/mol of atoms. Reference state is Al liquid, Cr bcc and Ni fcc at 1150 °C.

Equilibrium	phase	ΔG calc.		ΔG exp. from [165]
		This work	Dupin et al. [95]	
A1+$L1_2$+B2	A1	-26.1	-25.3	-24.9
	$L1_2$	-30.9	-31.1	-30.3
	B2	-37.3	-37.8	-34.7
A1+B2+A2	A1	-21.5	20.7	-23.6
	B2	-37.1	-38.3	-37.9
	A2	-5.2	-2.9	-9.2

Table 5-4 Calculated molar enthalpy of formation of the solid alloys studied by Kek et al. [164]. Reference state is Al fcc, Cr bcc and Ni fcc at room temperature.

Composition at %			Enthalpy of formation (kJ/mol of atoms)	
Al	Cr	Ni	Calculation this work	Exp [164]
23	5	72	-38.9	36.7±1.4
22	8	70	-37.3	-35.2±1.4
21	12	67	-35.6	-34.9±1.3

5.2.4 Al-Co-Y system

5.2.4.1 Review

Rykhal and Zarechnyuk [176] and Jiang et al. [177] have successively studied the phase relations of Al-Co-Y ternary system. The isothermal section with less than 33.3at.% Y at 600 °C was published by Rykhal and Zarechnyuk [176], According to this report, there were four ternary compounds namely Al_7Co_2Y, $Al_9Co_3Y_2$, Al_2CoY

and AlCoY. In 2004, Bodak [178] released a critical evaluation of this ternary system. Phase equilibria of Al-Co-Y are taken from the work by Rykhal and Zarechnyuk. Their results are revised respect to the newly evaluated Al-Co system and the compositions of compounds in the evaluation of Bodak.

This year Jiang et al. [177] investigated phase relations of Al-Co-Y system by the method of equilibrated alloys. Thirty alloys were prepared by act melting from high purity elements. Subsequently samples were sealed in evacuated quartz tubes filled with argon and annealed at 900 °C for 960h to reach equilibrium situation. Based on SEM, EPMA and XRD investigations, the isothermal section at 900 °C in the less than 66.7 at.% Y composition range has been successfully determined. There are 27 three-phase and 50 two-phase regions in the isothermal section. The previous mentioned four compounds were confirmed and a new ternary compound $AlCo_2Y_2$ was found to be stable at 900 °C. The crystal structure has been preliminarily determined. A relatively large amount of Al can dissolve into the Co-Y intermetallic compounds. However only few Co and Y are found in the Al-Y and Al-Co binary compounds, respectively, with the exception of Al_2Y, which dissolves up to 16 at.% Co at constant Y, meaning that the Co atom can replace the Al site in the crystal lattice of Al_2Y. The phase equilibria in the Y-rich region are not clear and are depicted by the dashed lines.

As mentioned above, Bodak has done some modifications on the isothermal section at 600 °C reported by Rykhal and Zarechnyuk. However the revised results still have some contradictions with the binary phase diagrams accepted in this work. The Co_5Y with a large solubility of Al is stable in the ternary system while it becomes unstable in the Co-Y boundary at 600 °C. A similar difference exists in the M_7Y_2 phase. Considering these discrepancies, the experimental results published by Rykhal and Zarechnyuk and then revised by Bodak are not accepted. In the present work the data reported by Jiang et al. are utilized in the assessment process. Materials Project website reports the enthalpy of formation of τ_3 based on first-principles calculation. Due to lack of the thermodynamic data, the value will be considered.

Al_7Co_2Y, $Al_9Co_3Y_2$ and Al_2CoY are treated as stoichiometric compounds, using the three-sublattice model. AlCoY with C15 crystal structure and $AlCo_2Y_2$ are described by using two-sublattice models $(Al, Co)_2(Y)_1$ and $(Al, Co)_3Y_2$, respectively. The detailed explanations of models can be found in the section 3.2.7 and summarized in Table 3-2.

5.2.5.2 Results and Discussions

Combining the experimental data and the selected models, the Al-Co-Y system has been optimized in the present work for the first time. A thermodynamic database is obtained. The isothermal sections at 600 and 900 °C are shown in the Fig. 5-28, where experimental results and calculated phase diagrams are compared. Five ternary compounds Al_7Co_2Y, $Al_9Co_3Y_2$, Al_2CoY, AlCoY and $AlCo_2Y_2$ are modeled in the current work. As previously stated, the isothermal section at 900 °C was selected as accepted experimental results while phase equilibria at 600 °C were only for

comparison. According to Fig. 5-28(a) the calculation could reproduce well the Al-Co-Y phase relations at 900 °C. The solubility ranges for AlCoY and $AlCo_2Y_2$ are well matched. The obtained parameters can be considered reliable

As for the Y-rich part, the extrapolated calculations are accepted since there is no experimental investigation available in literature.

(a)

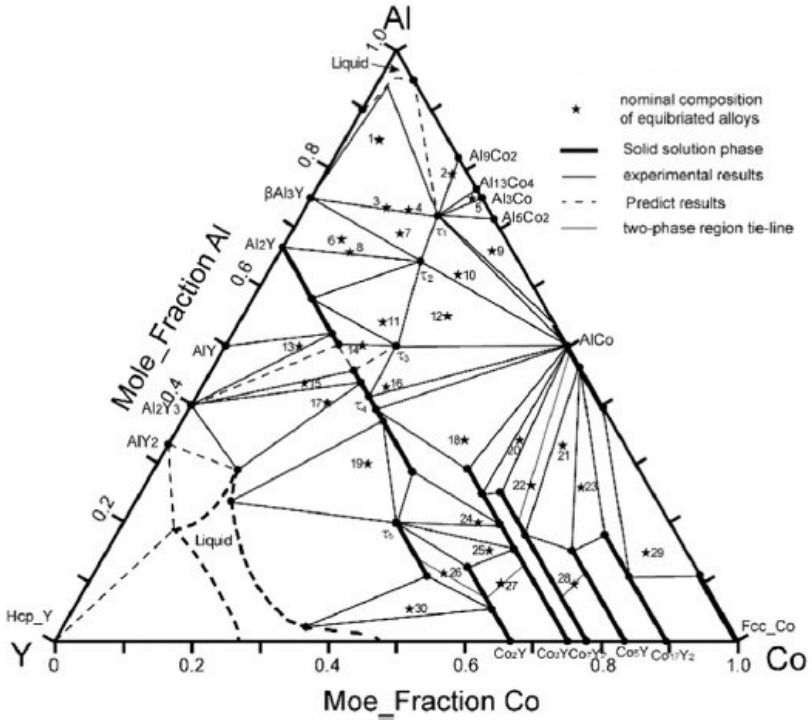

(b)

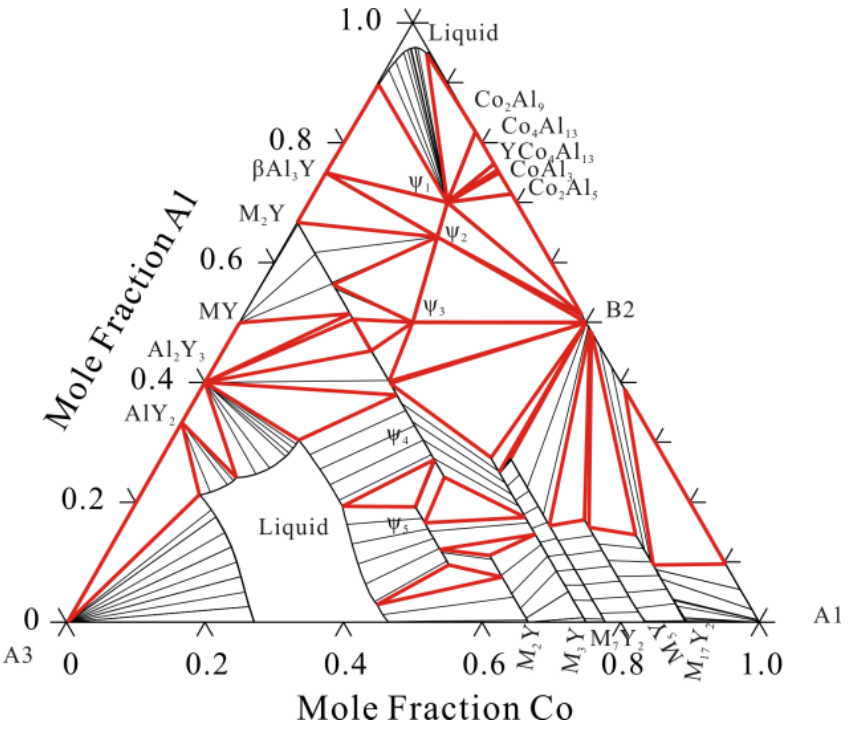

(c)

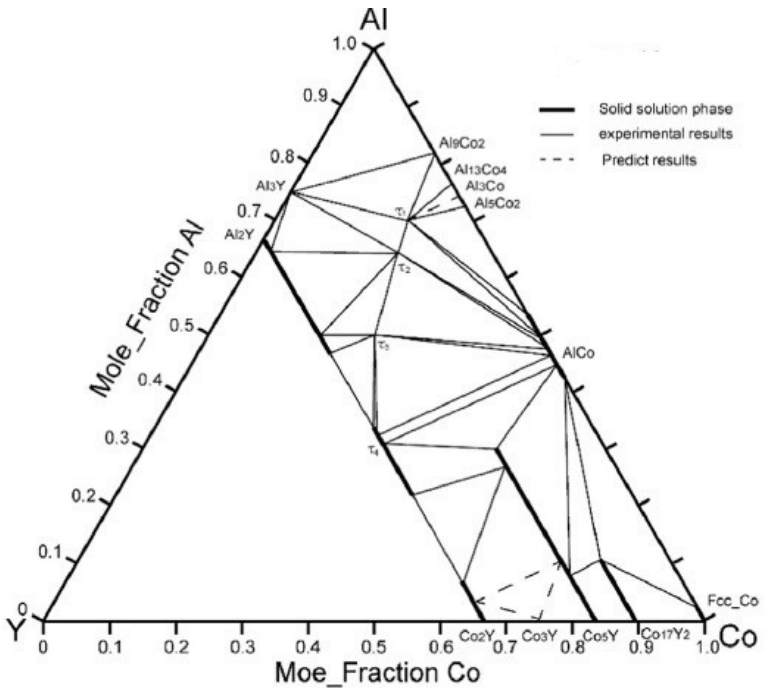

(d)

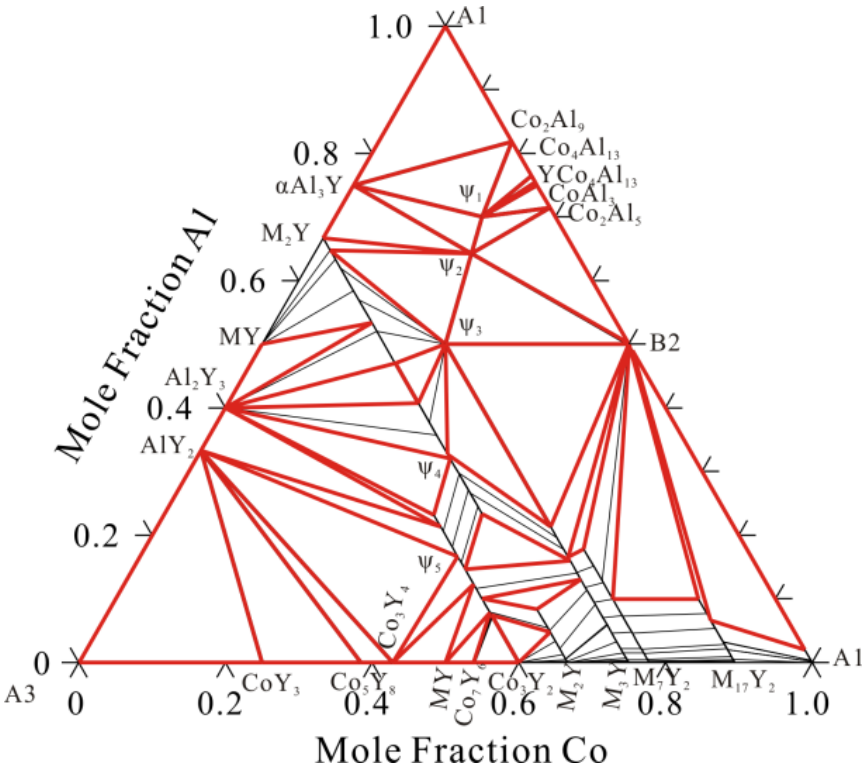

Fig. 5-28 Calculated isothermal sections of Al-Co-Y system based on (a) experiment at 900 °C by Jiang et al. [177], (b) calculations at 900 °C; (c) experiment at 600 °C revised by Bodak [178], (d) calculations at 600 °C

5.2.5 Al-Cr-Y system

5.2.5.1 Review

A detailed review of the Al-Cr-Y system has been given by Guzei [179] in 1991 on the basis of several experimental investigations. The partial isothermal sections at 500 °C experimentally constructed by Zarechnyuk et al. [180] was accepted in this evaluation. 53 alloys prepared from 99.99 % Al and Cr, 99.6 %Y by arc-melting in an argon atmosphere were annealed at 500 °C for 1000 h, followed by quenching in cold water. Three ternary compounds Al_8Cr_4Y, $Al_{20}Cr_2Y$ and Al_8CrY were confirmed to be stable in the Al-rich corner. The $Al_{20}Cr_2Y$ phase has a compositional extension parallel to the A-Cr boundary, while Al_8Cr_4Y and Al_8CrY are point compounds. As for the solubility in the binary phases, the third element hardly dissolves. Although three ternary compounds have been considered, there are still some uncertainties about their interactions with other phases, resulting in dash lines in the investigated region. With the help of limited experimental results, the thermodynamic description of the Al-Cr-Y system will be conducted in the present work.

5.2.5.2 Results and Discussions

Fig 5-29 shows the calculated isothermal sections at 500 °C using the present thermodynamic description in comparison with the experimental diagram from Guzei. The calculated phase relationships in the Y-rich side are based on the extrapolations. The homogeneity range of the ε_1 phase is ignored in the modeling, shown as (Al)20(Cr)2(Y)1. A good agreement is achieved between the calculations and experimental data, with the only exception of the $\varepsilon_1+\varepsilon_2+CrAl_4$ region which is not well described by the calculations. During the optimization, the ε_1 stability was tentatively set to be more negative; but with this choice the other phase equilibria containing ε_1 can't be well reproduced.

According to the shape of the singe phase region in the isothermal section at 500 °C, a small amount of Cr possibly replaces Al in its crystal site. This is initially omitted in our modelling for the sake of simplification. However this is likely to result in the improper description of phase relationships toward Cr-rich direction.

Then we firstly considered to add Cr in the Al-rich sublattice using the model (Al, Cr)20(Cr)2(Y)1, but it didn't work. After that, the model of this phase was carefully rechecked.

The crystal structure of the $Al_{20}Cr_2Y$ phase (cF184-$Al_{18}Mg_3Cr_2$) is characterised by the occupation of five Wyckoff positions in the Fd-3m space group: 8a, 16c, 16d, 48f and 96g. Al mainly occupies the 16c, 48f and 96g, Cr is in the 16d, and Y occupies the 8a. Then, a thermodynamic model fully consistent with the crystal structure would require the introduction of five sublattices. It is advisable to keep as low as possible the number of different sublattices, in order to reduce the number of end-members to be evaluated. Considering the solubility of Cr, the model is reset to the four sublattices (Al)18(Al, Cr)2(Cr)2(Y)1. The value of the previous assessed end-member is kept while the additional parameters in this new model are calculated

in order to fit all phase equilibria.

(a)

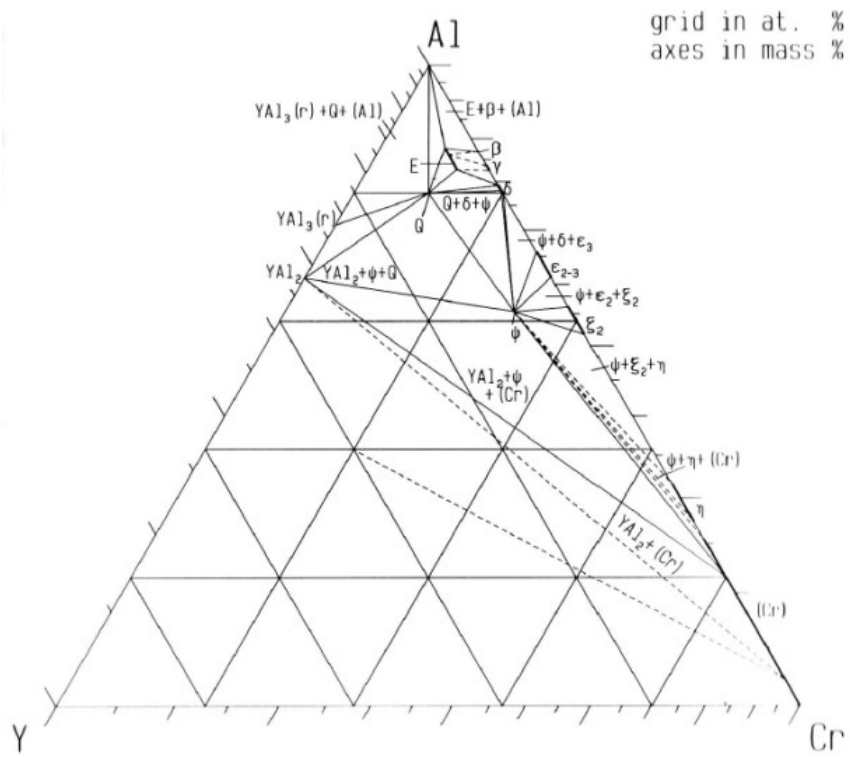

(b)

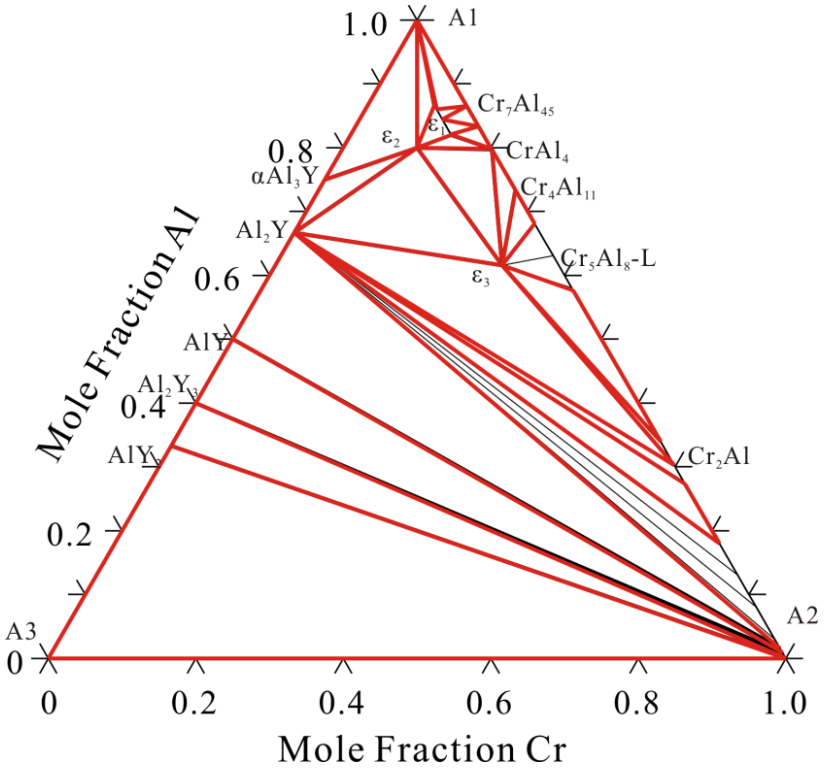

Fig. 5-29 Calculated isothermal sections of Al-Cr-Y system at 500 °C based on (a) experimental data from Guzei, (b) calculations using the present thermodynamic description.

5.2.6 Al-Ni-Y system

5.2.6.1 Review

Several investigations on the Y-poor region of Al-Ni-Y system have been carried out since 1960s, mainly concerning the intermediate phases, their crystal structures, magnetic properties and hydrogenation. Ferro et al. [181] released a critical evaluation on the basis of available literature. The partial isothermal sections reported by Rosen and Goebel [182] at 1000 °C and by Rykhal, and Zarechnyuk [183] at 800 °C in the region from 0 to 33.3 at.% Y are reproduced in this evaluation. Up to 10 ternary compounds $Al_{16}Ni_3Y$, Al_3Ni_2Y, $Al_7Ni_3Y_2$, Al_4NiY, $AlNi_8Y_3$, Al_2NiY, $Al_2Ni_6Y_3$, $AlNi_3Y_2$, AlNiY and $AlNi_2Y_2$ in the Y-poor region were determined. However the crystal structures and thermal stability ranges of several reported phases were still uncertain at the time.

Later, using different micrographic techniques, Raggio et al. [184] investigated the phase relationships in the region 60 to 100 at.% Al at 500 °C as well as the stabilities of ternary compounds previously suggested. Preparation and heat treatment of the samples were performed in a pure argon atmosphere, starting from the pure elements: Aluminium (99.999 mass%), nickel (99.99 mass%) and yttrium (99.9 mass%). The samples were synthesized by induction melting a mixture of small pieces of the components in alumina crucibles and then annealed at 500 °C for 2 weeks, followed by slow cooling. For alloys having lower aluminium content, an annealing at 800 °C for 2 or 4 weeks was carried out, followed by ice-water quenching. According to their analysis supported by XRD and EPMA, a partial isothermal section of Al-Ni-Y system at 500 °C is finally constructed by Raggio et al. [184]. Ternary compounds $Al_{23}Ni_6Y_4$ and Al_9Ni_3Y firstly identified by Gladyschevskii et al. and Al_4NiY have been confirmed. However $Al_{16}Ni_3Y$ is not observed. Two ternary tie-triangles A1+Al_3Ni+ $Al_{23}Ni_6Y_4$, and A1+Al_3Y+ $Al_{23}Ni_6Y_4$ and two ternary eutectic equilibria E1 around 96.5 at.% Al, 2.6 at.% Ni, 0.9 at.% Y and E2 around 96.0 at% Al, 1.0 at.% Ni 3.0 at.% Y have been identified in this region, while phase equilibria involving Al_4NiY and Al_9Ni_3Y are still incomplete.

The enthalpies of formation of $Al_{23}Ni_6Y_4$, Al_9Ni_3Y, Al_4NiY, Al_3Ni_2Y, Al_2NiY, $Al_2Ni_6Y_3$, AlNiY, $AlNi_2Y_2$ and $AlNi_8Y_3$ were investigated by Nash et al. [185] using experimental method and by Golumbfskie et al. [186] using first-principles calculations. Moreover Shin et al. [187] validated the crystal structures of 10 ternary compounds from first-principles calculation. Starting from the prototype, all the atoms were fully relaxed to minimize the total energy and then their space groups, lattice constants and atom positions were obtained. The mentioned calculated results showed good agreement with the available experiments.

Recently the two more intermetallic compounds have been reported. Matselko et al. [188] synthesized the alloy at $Al_6Ni_2Y_{0.67}$ by arc melting and its crystallographic structure was analyzed by X-ray powder diffraction resulting in hP11-2.33, space group P-6m2, a=0.418904(2), c=0.909816(6) nm, which can be decomposed into three kinds of layers. Benndorf et al. [189] mentioned that the Al_3NiY_{10} phase located

in the Y-rich corner with an ordered anti-Co_2Al_5 structure was synthesized by arc melting. Unfortunately without further experimental investigations, the stability ranges of $Al_6Ni_2Y_{0.67}$ and Al_3NiY_{10} phases can't be confirmed, therefore they wouldn't be considered in the current work. Until now the phase equilibria in the Y rich corner are still empty.

Considering the available literature about phase diagrams and thermodynamic data, Huang et al. [190] thermodynamically optimized the Al-Ni-Y system. The parameters of the binary subsystems are taken from Al-Ni [99], Al-Y [109] and Ni-Y [191]. As for phase models, these ternary compounds have been treated as the stoichiometric phases except for Al_3Ni_2Y showing some solubility range. Due to the different selections of parameters for binaries, the Al-Ni-Y system will be re-optimized in the present work. The partial isothermal sections at 500, 800 and 1000 °C and enthalpies of formations will be utilized to support the optimization.

5.2.6.2 Results and Discussions

The calculated isothermal sections of the Al-Ni-Y system at 500, 800 and 1000 °C have been presented in Fig. 5-30, as well as the experimental results for the comparison. The calculated phase equilibria are consistent with the available experimental data. Two calculated eutectic reactions are shown as E1: 96.9 at.%Al-2.8 at.%Ni-0.3 at. %Y at 640 °C and E2: 96.8 at.% Al, 0.5 at.%Ni-2.7 at. %Y at 635 °C, which are consistent with the compositions determined by experimental measurement [184]. This set of ternary parameters can be integrated into the multi-component thermodynamic database. Due to the lack of the experimental investigations, the phase relations on the Y-rich corner are shown based on the extrapolations of the current database.

(a)

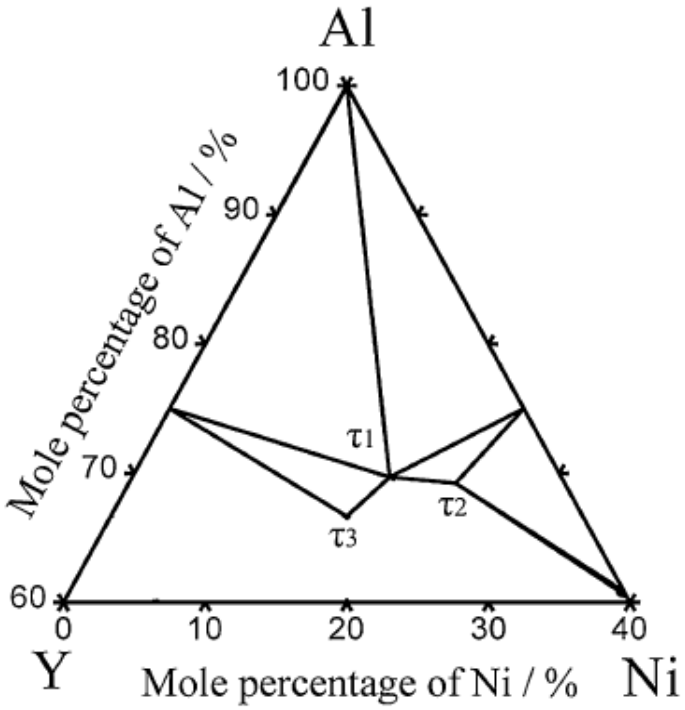
Al
100
90
80
70
60
Mole percentage of Al / %
τ1
τ2
τ3
0
10
20
30
40
Y
Mole percentage of Ni / %
Ni

(b)

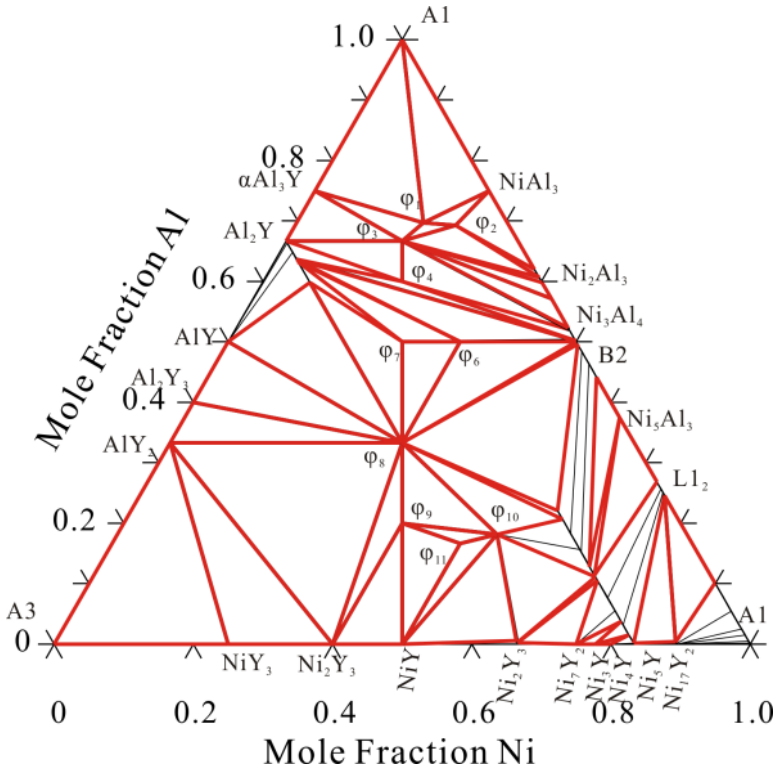
Al
1.0
0.8
0.6
0.4
0.2
0
A3
αAl3Y
Al2Y
AlY
Al2Y3
AlY3
NiAl3
Ni2Al3
Ni3Al4
B2
Ni5Al3
L12
φ1
φ2
φ3
φ4
φ6
φ7
φ8
φ9
φ10
φ11
NiY3
Ni2Y3
NiY
Ni2Y3
Ni7Y2
Ni3Y
Ni4Y
Ni5Y
Ni17Y2
Mole Fraction Al
Mole Fraction Ni
0
0.2
0.4
0.6
0.8
1.0

(c)

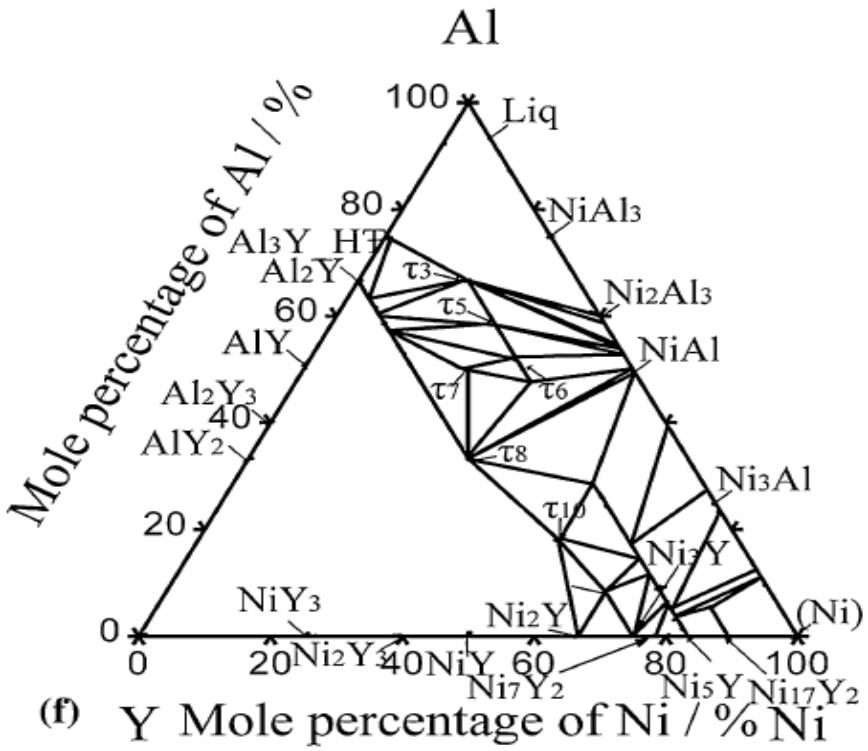
Al
Mole percentage of Al / %
100
80
60
40
20
0
Liq
NiAl3
Al3Y_HT
Al2Y
AlY
Al2Y3
AlY2
τ3
τ5
τ7
τ6
τ8
τ10
Ni2Al3
NiAl
Ni3Al
Ni3Y
NiY3
Ni2Y
(Ni)
0
20
Ni2Y3
40
NiY
60
Ni7Y2
80
Ni5Y
100
Ni17Y2
(f) Y Mole percentage of Ni / % Ni

(d)

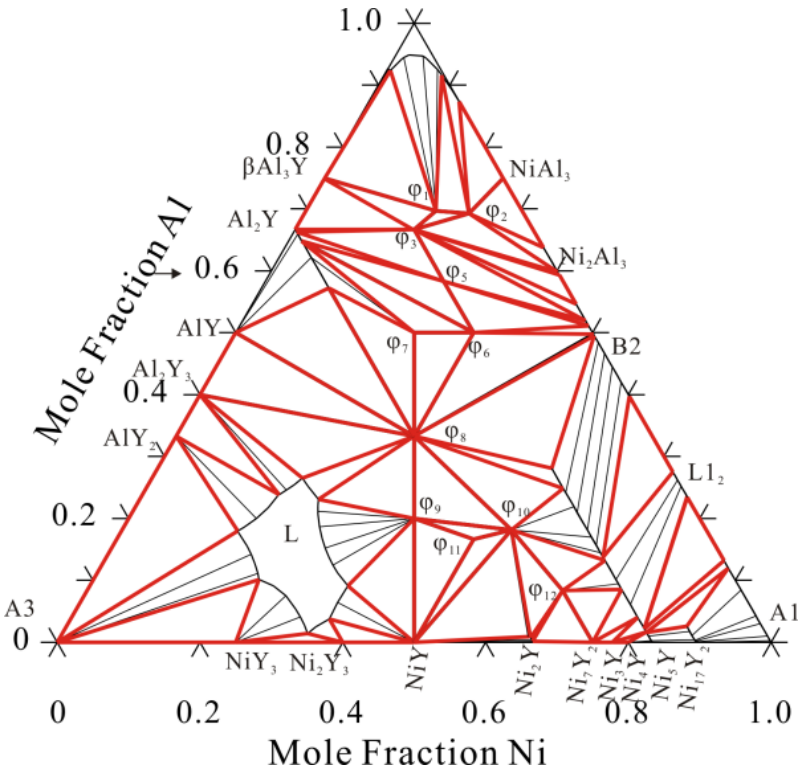
Mole Fraction Al
1.0
0.8
0.6
0.4
0.2
0
βAl3Y
Al2Y
AlY
Al2Y3
AlY2
A3
NiAl3
Ni2Al3
B2
L12
A1
L
φ1
φ2
φ3
φ5
φ6
φ7
φ8
φ9
φ10
φ11
φ12
NiY3
Ni2Y3
NiY
Ni2Y
Ni7Y2
Ni3Y
Ni4Y
Ni5Y
Ni17Y2
0
0.2
0.4
0.6
0.8
1.0
Mole Fraction Ni

(e)

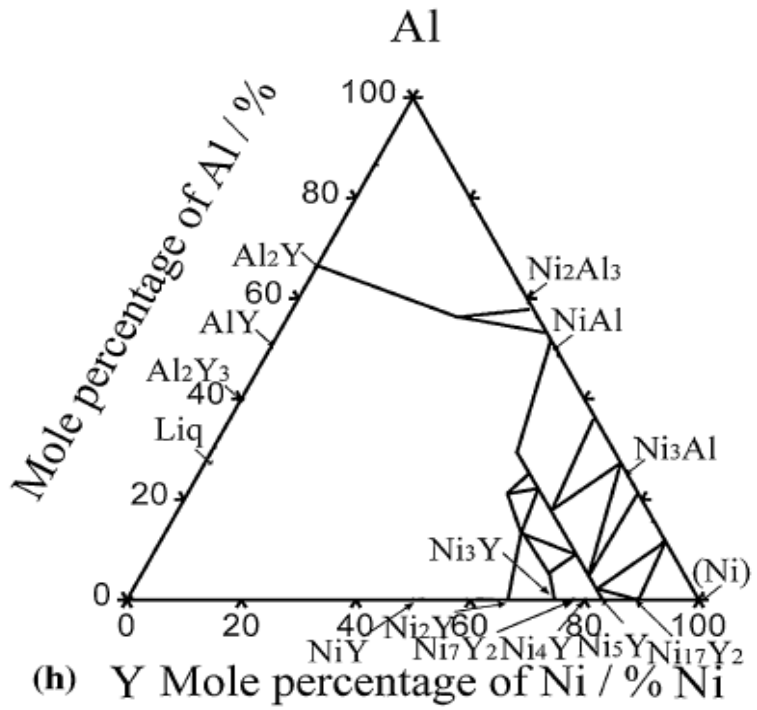

(f)

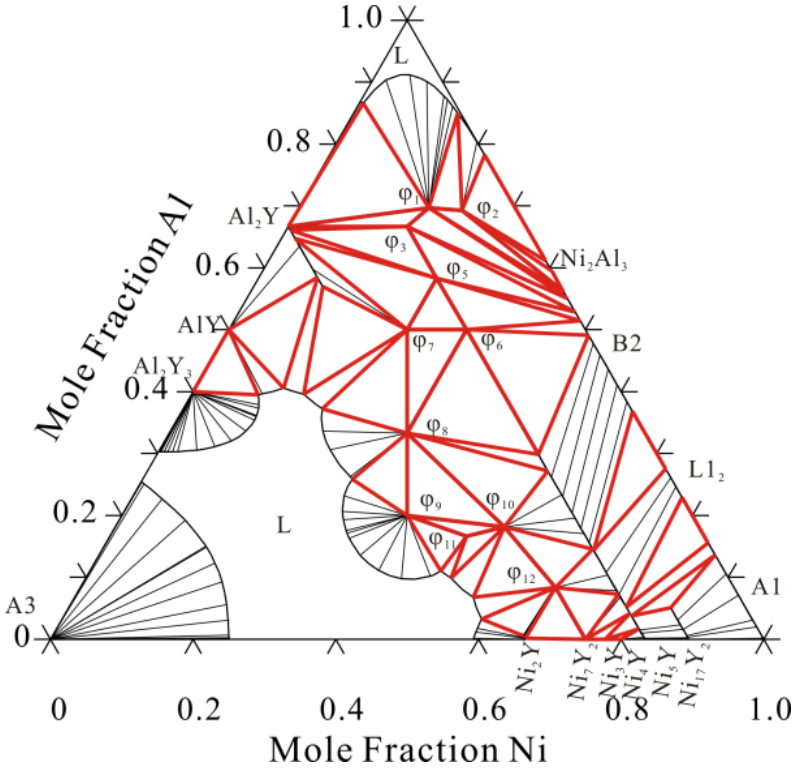

Fig. 5-30 Calculated isothermal sections of Al-Ni-Y system based on (a) experiment at 500 °C by Raggio et al. [184], (b) calculation at 500 °C; (c) experiment at 800 °C by Raggio et al. [184], (d) calculation at 800 °C, (e) experiment at 1000 °C by Rosen et al. [182], (f) calculation at 1000 °C

Enthalpies of formation of ternary compounds in the Al-Ni-Y system have been calculated in the present work. They are listed in Table 5-5 and compared to the values based on the experimental method by Nash et al. [185] and first-principles calculation by Golumbfskie et al. [186]. In general, the current calculations can keep in consistent with the available experimental and simulated results.

Table 5-5 Calculated enthalpies of formation of ternary intermetallic compounds in the Al-Ni-Y system compared to other sources

Phase	Enthalpies of formation, J/mol-atom		
	Present work	Exp. by Nash et al.	Cal. By Golumbfskie et al.
$Al_{23}Ni_6Y_4$ (φ_1)	-50600	-50600	-50800
Al_9Ni_3Y (φ_2)	-51246	-54000±800	-55300
Al_4NiY (φ_3)	-58015	-59800	-59400
Al_3NiY (φ_4)	-64278	--	--
$Al_7Ni_3Y_2$ (φ_5)	-58250	--	--
Al_3Ni_2Y (φ_6)	-60000	-62800±1500	-62600
Al_2NiY (φ_7)	-60000	-62800±2300	-65600
$AlNiY$ (φ_8)	-61698	-54100±900	-60500
$AlNi_2Y_2$ (φ_9)	-48000	-54100±900	-54800
$Al_2Ni_6Y_3$ (φ_{10})	-47273	-48500±1500	-55400
$AlNi_3Y_2$ (φ_{11})	-45833	--	--
$AlNi_8Y_3$ (φ_{12})	-38000	-37900±2500	-44300

5.2.7 Co-Cr-Y system

No experimental data has been found in the literature about phase equilibria and thermodynamic data of the Co-Cr-Y system, therefore it is calculated as an ideal extrapolation of the binary subsystems. A computed isothermal section at 1000 °C is reported in Fig. 5-31.

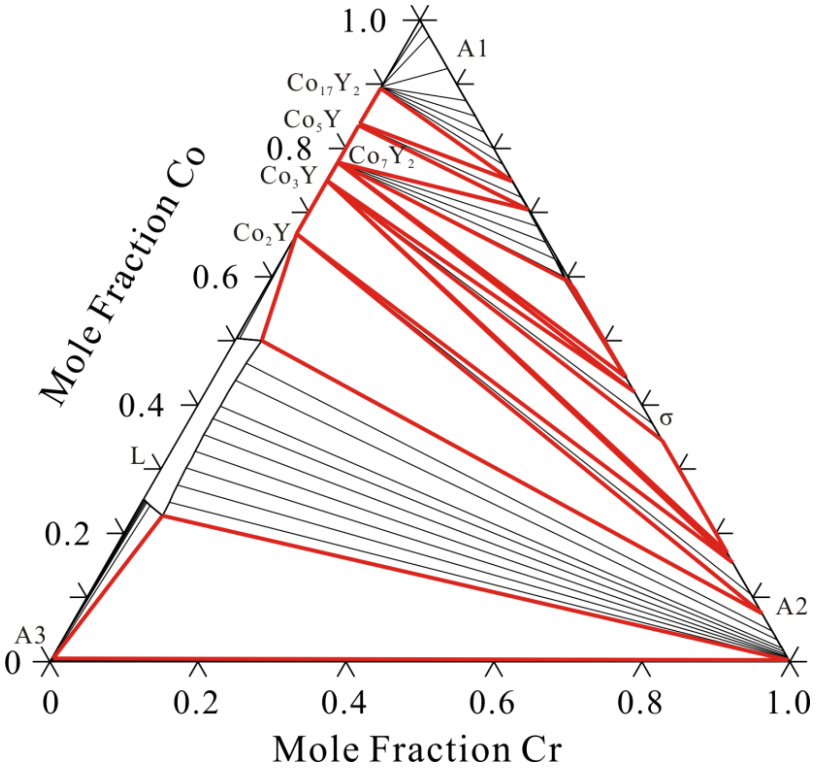

Fig. 5-31 Calculated isothermal section of Co-Cr-Y system at 1000 °C based on the extrapolation.

5.2.8 Co-Ni-Y system

5.2.8.1 Review

At current, isothermal sections of Co-Ni-Y system at 600, 800, 1000 and 1175 °C have been partly reported by several authors. Most of the investigations are located in the Co-Ni rich side. Kharchenko et al. [192] firstly investigated the Co-Ni-Y system by X-ray structural and microstructural analysis on 126 alloys utilized with the compositions up to 66.6 at.% Y. The samples with compositions below 33.3 at.% Y were annealed at 800 °C for 360 h and the alloys above 33.3 at.% Y were annealed at 600 °C for 360 h. All annealed alloys were quenched in cold water. Finally the isothermal sections up to 33.3 at.% Y at 800 °C and with more than 33.3 at.% Y at 600 °C were obtained. The partial isothermal section at 800 °C show a few continuous solid solutions between Co_5Y-Ni_5Y, Co_7Y_2-Ni_7Y_2, Co_3Y-Ni_3Y and Co_2Y-Ni_2Y phases. Due to the different crystal structure, $Co_{17}Y_2$ and $Ni_{17}Y_2$ don't form a continuous solution. Around 35 at.% Ni dissolves in $Co_{17}Y_2$ and about 10 at.% Co was detected in $Ni_{17}Y_2$. A ternary compound, with ideal composition $Co_3Ni_2Y_5$ was observed in the composition region between 20 and 40 at.% Co in the CoY-NiY section at 600 °C. It was found to in equilibrium with the Ni_2Y, NiY, CoY_3 and Co_3Y_4, forming four three-phase regions $Co_3Ni_2Y_5$+Ni_2Y+Co_3Y_4, $Co_3Ni_2Y_5$+ Ni_2Y+NiY, $Co_3Ni_2Y_5$ + NiY +CoY_3 and $Co_3Ni_2Y_5$ +CoY_3+Co_3Y_4. According to the single crystal X-ray studies, $Co_3Ni_2Y_5$ has the MoB tetragonal structure with 16 atoms per cell, space group $I4_1$. It needs to be pointed out that Ni_2Y_3, CoY, Co_2Y_3 and Co_5Y_8 phases were not reported

at 600 °C even though these phases existed in the Co-Y and Ni-Y systems.

By diffusion couples method, Xue et al. [193, 194] established the partial isothermal sections at 1000 and 1175°C supported by EPMA and SEM analysis. 99.9 mass% pure elements Co, Ni and Y were taken as the raw materials to manufacture two types of diffusion couples: Co/Ni/Y couples and Y/(Co,Ni). In the Co/Ni/Y couple, the bulk Y was sandwiched by two slabs of Ni and two pieces of Co, alternatively. The sample sealed in argon filled quartz capsules was annealed at 1000 °C for 15d to reach equilibrium. In order to obtain more information, (Co, Ni) alloys including four ratios 20:80, 40:60, 60:40 and 80:20 were prepared in the Y/(Co,Ni) couples. After similar treatment, these couples were annealed for 20 days at 1000 °C. The constitution and disposition of phases were determined with the help of EPMA and SEM equipments. The two mentioned isothermal sections were determined in the composition range at less than 40 at% Y while phase equilibria at more than 40 at % Y were still unclear. According to the accepted binary phase diagrams, there are several binary intermediate phases in the Co-Y and Ni-Y which correspond in composition and structure. Consequently, a series of $Y_m(Co, Ni)_n$ line compounds are formed in the Co-Ni-Y system, including the $Y(Co, Ni)_2$, $Y(Co, Ni)_3$, $Y_2(Co, Ni)_7$ phases which show continuous solubility between Co and Ni at 1000°C. Ten two-phase and three three-phase regions were reported and the detailed positions of three-phase regions were determined. At the higher temperature of 1175°C, phase equilibria above 33.3 at.% Y were not experimentally determined.

The boundaries of the isothermal sections at 1000 and 1175 °C released by Xue et al. are consistent with the accepted binary phase diagrams while the phase equilibria in the boundary side in the 600 °C section and above 33.3 at.% Y published by Kharchenko et al. [192] show several unfit part. It's very difficult to get the accurate results in the Y-rich side because the element Y is easily oxidized. In the present optimization, the work by Xue et al. and the isothermal section at 800 °C reported by Kharchenko et al. are accepted, while the 600 °C isothermal section with the composition above 33.3 at. % Y by Kharchenko et al. is rejected here.

5.2.8.2 Results and Discussions

The optimization work started from the comparison between the extrapolated ternary equilibria and the available experimental results. Based on the resulting differences, the interaction parameters for the binary phases with homogeneity range are firstly evaluated to fit the experimentally determined solubility. After reaching an approximate calculation, the ternary intermetallic $Co_3Ni_2Y_5$ modeled as $(Co, Ni)_1(Y)_1$ is introduced. Eventually all additional parameters were re-optimized simultaneously to reproduce all accepted experimental results.

Figs. 5-32 (a) to (c) compare the complete calculated isothermal sections at 800, 1000 and 1175 °C calculated using the present thermodynamic descriptions are compared to the experimental data. The calculations agree well with the available experimental results.

(a)

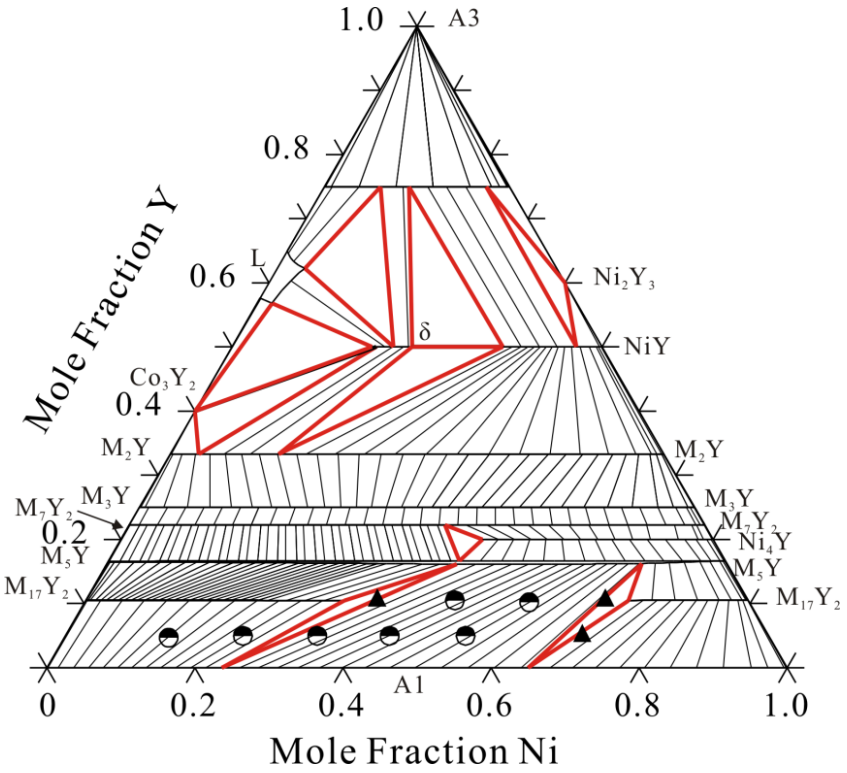
1.0
A3
0.8
0.6
L
Ni_2Y_3
δ
NiY
Co_3Y_2
0.4
M_2Y
M_2Y
M_7Y_2
M_3Y
M_3Y
0.2
M_2Y_3
Ni_4Y
M_5Y
M_5Y
$M_{17}Y_2$
$M_{17}Y_2$
A1
0
0.2
0.4
0.6
0.8
1.0
Mole Fraction Y
Mole Fraction Ni

(b)

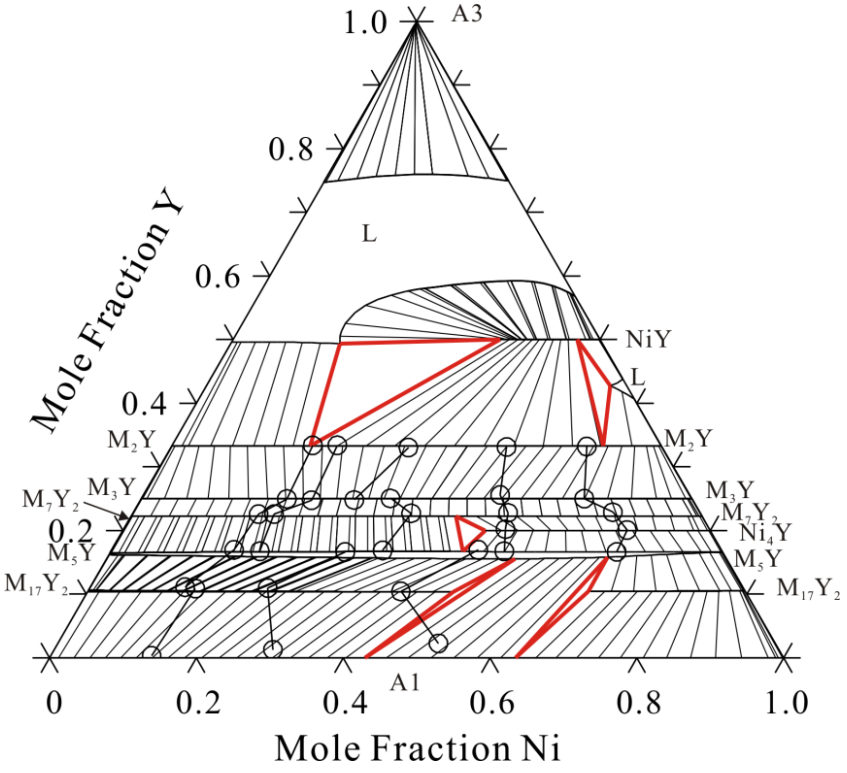
1.0
A3
0.8
L
0.6
NiY
L
0.4
M_2Y
M_2Y
M_7Y_2
M_3Y
M_3Y
0.2
M_2Y_3
Ni_4Y
M_5Y
M_5Y
$M_{17}Y_2$
$M_{17}Y_2$
A1
0
0.2
0.4
0.6
0.8
1.0
Mole Fraction Y
Mole Fraction Ni

(c)

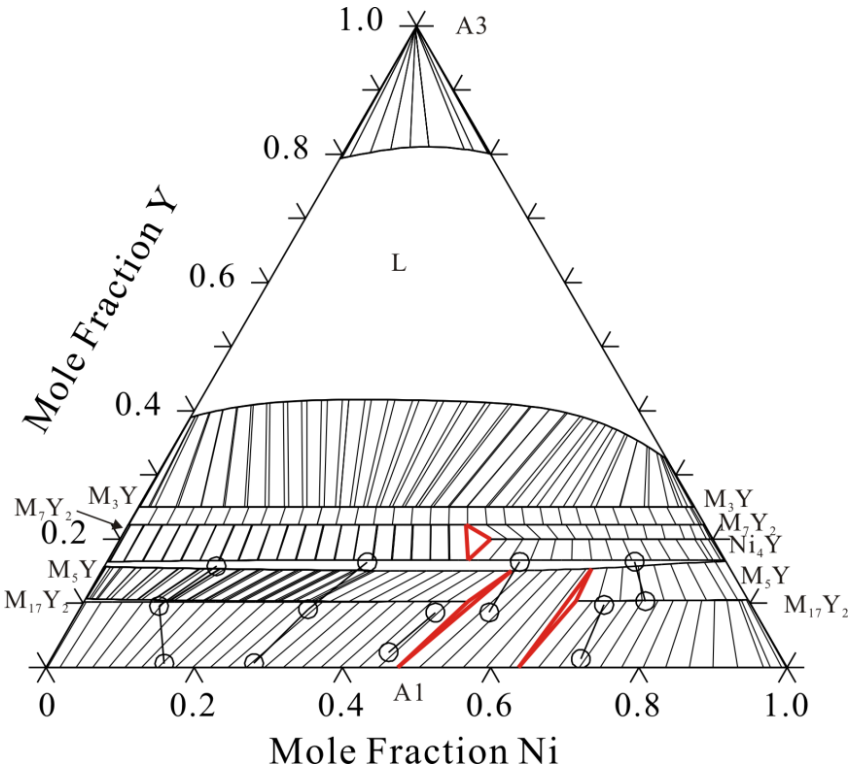

Fig. 5-32 Calculated isothermal sections of Co-Ni-Y system at (a) 800°C, (b) 1000 °C and (c) 1175 °C compared with the experimental data. two-phase (◓) and three-phase (▲) by Kharchenko et al. [192]. tie-line (○) by Xue et al. [193, 194]

5.2.9 Cr-Ni-Y system

Similarly to the Co-Cr-Y system, there are rarely any experimental investigations about phase relationships and thermodynamic data regarding the Cr-Ni-Y system. Only one phase, namely $CrNi_5Y_2$, was mentioned. Since there is no available information, the Cr-Ni-Y has been modeled as an ideal extrapolation of the binary subsystems selected in the present work. A computed isothermal section at 1100 °C is reported in Fig. 5-33.

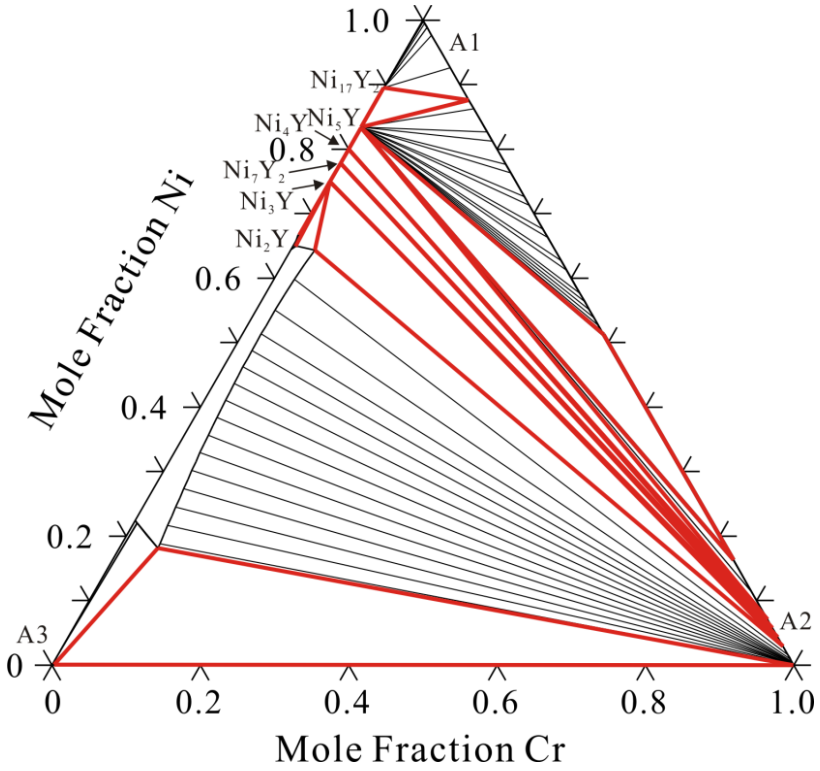

Fig. 5-33 Calculated isothermal sections of Cr-Ni-Y system at 1100 °C based on the extrapolation.

5.3 Quaternary systems

There are five quaternary subsystems in the Al-Co-Cr-Ni-Y quinary but only about Al-Co-Cr-Ni several experimental studies of phase equilibria of are reported in literature. In the following this quaternary system will be presented and discussed based on the available literature. As for the remaining three quaternary systems, the evaluation is missing due to the lack of relevant experimental data.

5.3.1 Review

With reference to the important industrial applications of Co- and Ni-based alloys, phase equilibria in the Al-Co-Cr-Ni system involving A1, $L1_2$, A2 and B2 phases have been experimentally and theoretically investigated by several authors.

Broz et al. [195, 196] and Bursik et al. [197] collectively implemented thermodynamic database for this quaternary system and performed a few experimental investigations to evaluate the reliability of the calculations. Broz et al. [195] melted five Al-Co-Cr-Ni alloys with Ni content close to 70 at.% in an induction furnace under Ar atmosphere. Samples were annealed at 900 °C for 650 h to reach a state close to the thermodynamic equilibrium and water quenched. The microstructure and compositions of individual phases were studied under the support of SEM with EDS and TEM. Four equilibrated alloys were located in the two-phase region A1+$L1_2$, and a fifth one, at Ni-8.8Al-9.5Cr-10.9Co, contained the single A1 phase. In the same year similar, similarly to [195], Broz et al. [196] prepared four quaternary samples at 70 at.% Ni and different contend of remaining elements to obtain a large volume ratio

of A1 and $L1_2$. After annealing at 1000 °C for 200 h, these samples were quenched in water. Both A1 single-phase and A1+$L1_2$ two-phase region were detected in the isothermal section at 1000 °C. According to their experimental results, the A1/A1+$L1_2$ boundary moves towards higher amount of aluminum with increasing temperature.

Later Bursik et al. [197] further investigated phase equilibria of the Al-Co-Cr-Ni system at 1000 and 1100 °C by using the same experimental approach as Borz et al. with the intention to cover a large composition range. Five samples with Ni content close to 60 at.% were separately annealed at 1000 °C for 112 h and 1100°C for 10 h, and then quenched in water. Based on SEM-EDX and TEM phase analyses, B2 phase was missing, while a phase marked as β' with lamellar shape and fine twins was found in some of the alloys. Its composition corresponded to the predicted compositions of B2 phase. Authors speculated that the appearance of β' was caused by the fast quenching from annealing temperature. There are two two-phase regions (A1+$L1_2$, $L1_2$+β') and one three-phase region (A1+$L1_2$+β') in the sections at 60 at.% Ni and 1000°C, while at 1100°C one single-phase (A1), two two-phase (A1+$L1_2$, A1+β') and two three-phase (A1+$L1_2$+β', A1+A2+β') regions were detected in the annealed samples. For the purpose of comparison with the calculations, the above mentioned β' phase directly corresponded to B2. The calculated phase relations agree reasonably well with most of their own experimental data. Some discrepancies existed in the samples located in the phase regions containing β'. However, the quaternary database used was just a simple combination of parameters of binary systems and Al-Cr-Ni [155]. Unfortunately, authors did not introduce phase models adopted and did not mention the source of the accepted interaction parameters.

In order to investigate the phase equilibria, Gheno et al. [198] prepared seven Al-Co-Cr-Ni samples with an additional 0.1 at.% Y by arc melting under Ar atmosphere. Samples were homogenized 6h at 1200 and 48h at 1150 °C, and finally they were vacuum encapsulated in quartz capsules and further annealed at 1150 °C for 48h, and slowly cooled to given temperatures. The final annealing was conducted at 900, 1100 and 1200 °C for 525, 100 and 50h, respectively, followed by water quenching. XRD and EPMA were chosen to implement phase analysis. All alloys exhibit a primary A1-B2 microstructure with the different precipitate A2, σ and $L1_2$. The attractive $L1_2$ phase precipitated in A1 was observed in the micrographs for the Cr-poor alloys. However its appearance could not be distinguished from A1 using XRD equipment and even accurate composition measurements by EPMA became tough because of too fine dispersion of the $L1_2$ particles. It's worth to mention that the β' phase detected by Bursik et al. was also found instead of B2 in the Cr-poor alloys at 1100 and 1200 °C. It's possibly formed by a diffusionless transformation during cooling. Moreover small amounts of Y-containing intermetallics caused by additional 0.1 at.% Y were observed in the microstructure. They were completely neglected during the phase identification and composition measurement.

Later, Liu [199] investigated the Al-Co-Cr-Ni phase equilibria by using theoretical methods in his thesis. The thermodynamic database was constructed according to the descriptions of binaries and ternary subsystems with the support of

DFT calculations. The Al-Co-Cr, Al-Co-Ni and Co-Cr-Ni ternaries modeled by Liu were combined with the Al-Cr-Ni parameters by Dupin et al. [95] to produce a preliminary extrapolation, mainly involving the $L1_2$, A2, A1, B2 and σ in the ternary sub-systems. All phase equilibria in the Al-rich corner of these ternary systems were ignored during the optimization. Liu realized that part of the Al-Co assessment was inappropriate and a revised thermodynamic description of Al-Co was performed based on the work by Dupin and Ansara [125], but they were not used in his database for the multicomponent system. A three-sublattice model with the ratio 2:4:9 was selected for the σ phase and the components selectively occupy some sublattices. The experimental results from Gheno et al. [198] are accepted for the comparison.

5.3.2 Results and Discussions

In principle the extrapolations based on combination of binary and ternary subsystems could reproduce well most of the experimental results if no quaternary compounds exist. In the current work, Al-Co-Cr-Ni is systematically described on the basis of the parameters of binary and ternary systems previously presented. In the following our results are compared to the mentioned experimental data.

To obtain a better thermodynamic description of the quaternary phase equilibria, only slight refinement is performed. In particular, a metastable $L1_2$ parameter is optimized to fit the boundary of $L1_2$ phase reported by Bursik et al.

Fig. 5-34 presents the calculated phase diagrams at x(Ni)=0.7 and 900 and 1000°C with the experimental data. The current results can reproduce the experimental data well. Fig. 5-35 shows the calculations at x(Ni)=0.6 and 1000 and 1100°C, compared to the experimental points. In most cases the calculated results show good agreement with experiment. A few discrepancies appear in the phase region close to the Al-Cr-Ni boundary. In the isothermal section at 1100°C and x(ni)=0.6, the experimental point close to the Al-Cr-Ni side (at 3.2 at.% Co) is located in the three-phase region β'+A2+A1, which is supposed to originate from Al-Cr-Ni boundary subsystem. However, according to the Al-Cr-Ni system, this three-phase field stabilizes at lower amount of Ni. The appearance of the metastable β' phase affects the distributions of elements at some level, and then causes some uncertainties about the remaining phase equilibria.

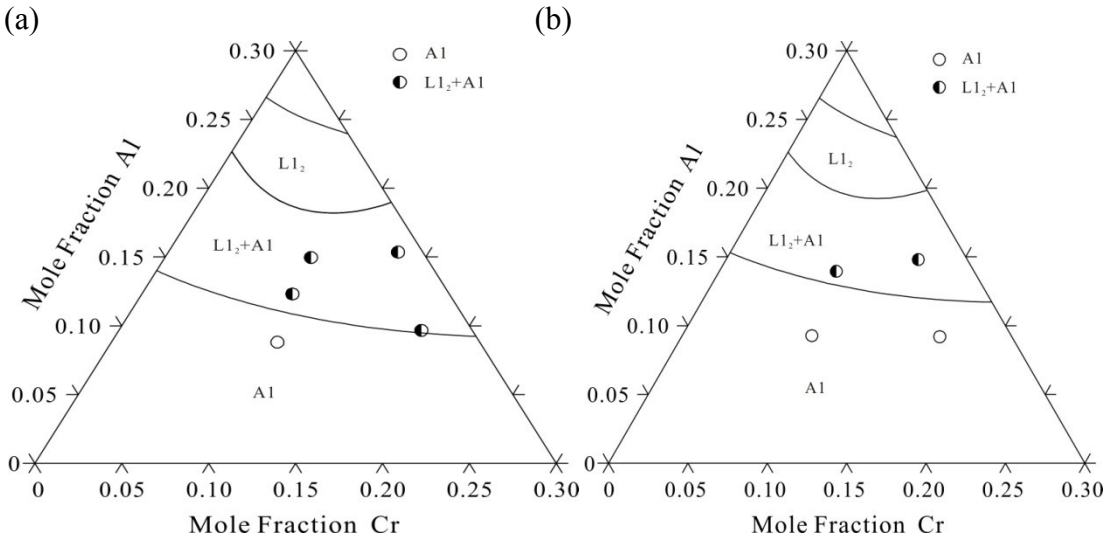

Fig. 5-34 Calculated phase diagram at x(Ni)=0.7 compared with experimental data by Broz et al. [195, 196] (a) T=900 °C and (b) T=1000 °C

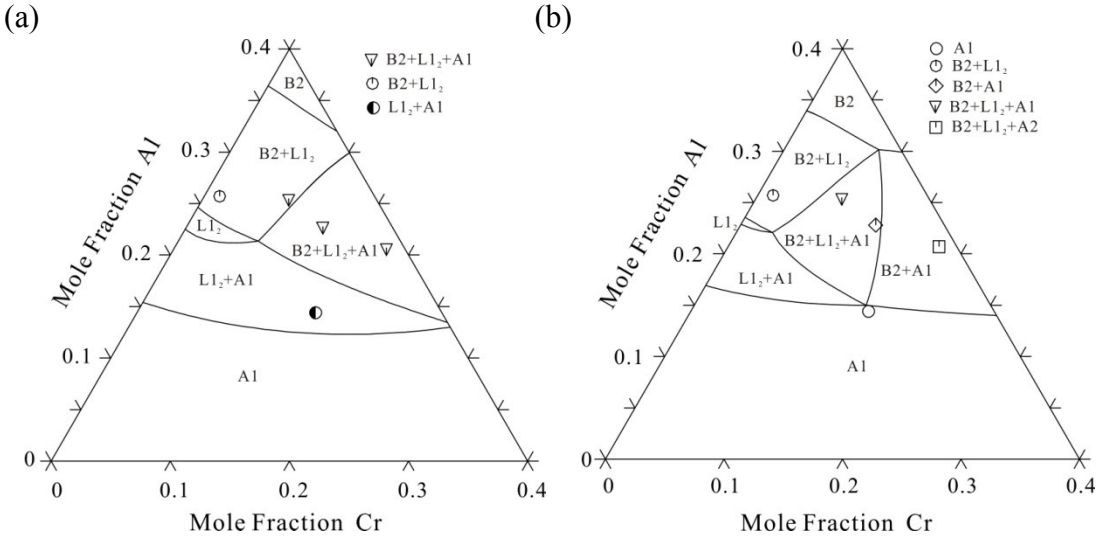

Fig. 5-35 Calculated phase diagram at x(Ni)=0.6 compared with experimental data by Bursik et al. [197], (a) T=1000 °C and (b) T=1100 °C

Figs. 5-36 (a) to (c) presents the phase diagram at 19 at.% Co and 900 °C, 1100 °C and 1200 °C compared to experimental results from Gheno et al.. The calculated phase equilibria at 30 at.% Co and the same temperatures are shown in Fig. 5-37. In general the present thermodynamic database could reproduce most of phase equilibria and phase compositions within the experimental uncertainty. The main discrepancy affects the transition reaction between σ and A2. According experiments, a four-phase region A1+A2+B2+σ exists in the alloy annealed at 1100 °C. The same alloy contains the A1, B2 and σ phase at 900 °C while it changes to the A1, B2 and A2 at 1200 °C. At current the transformation at intermediate temperature is not completely confirmed. The current calculations probably underestimate the stability

of σ phase, since it is absent in the calculated phase relation of this alloy at 1100 °C.

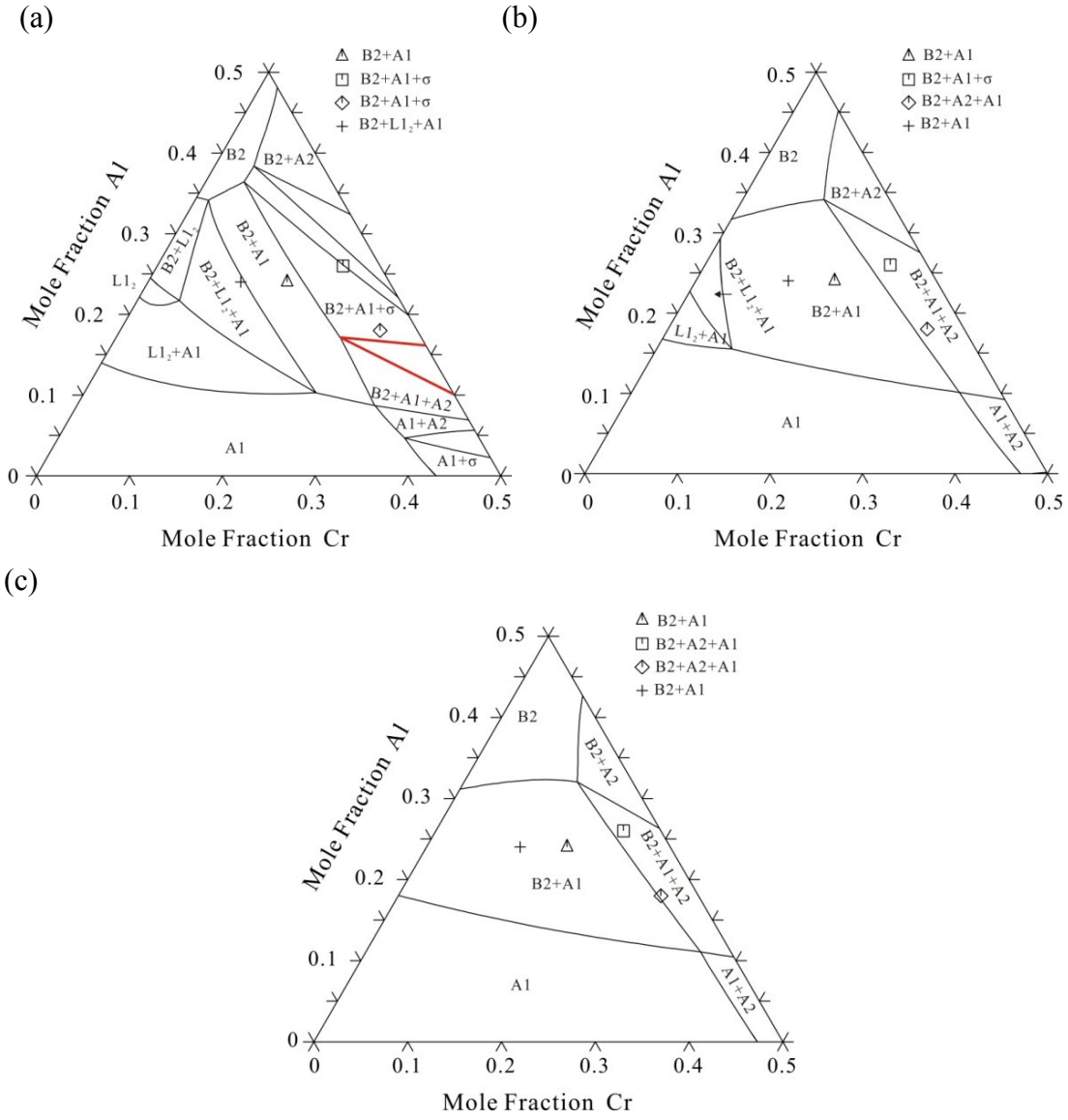

Fig. 5-36 Calculated phase diagrams of Al-Co-Cr-Ni system with 19 at.% Co at (a) 900 °C, (b) 1100 °C and (c) 1200 °C, compared to the experimental results from Gheno et al.

In theory this problem is possibly due to the σ parameters adopted in the subsystems. Since σ originates from the Co-Cr system and there is a small quantity of Al in the Al-Co-Cr and Ni in the Co-Cr-Ni in the ternary systems. According to the selected model, there are up to 64 σ end-members in the quaternary system and most of them cannot be adjusted on the basis of experiments because of correspond to metastable or unstable states not accessible experimentally. Although some attempts have been made, for the moment no better agreement was obtained.

More theoretical studies by using first-principles calculations in addition to experimental investigations are strongly expected for a better modeling of σ.

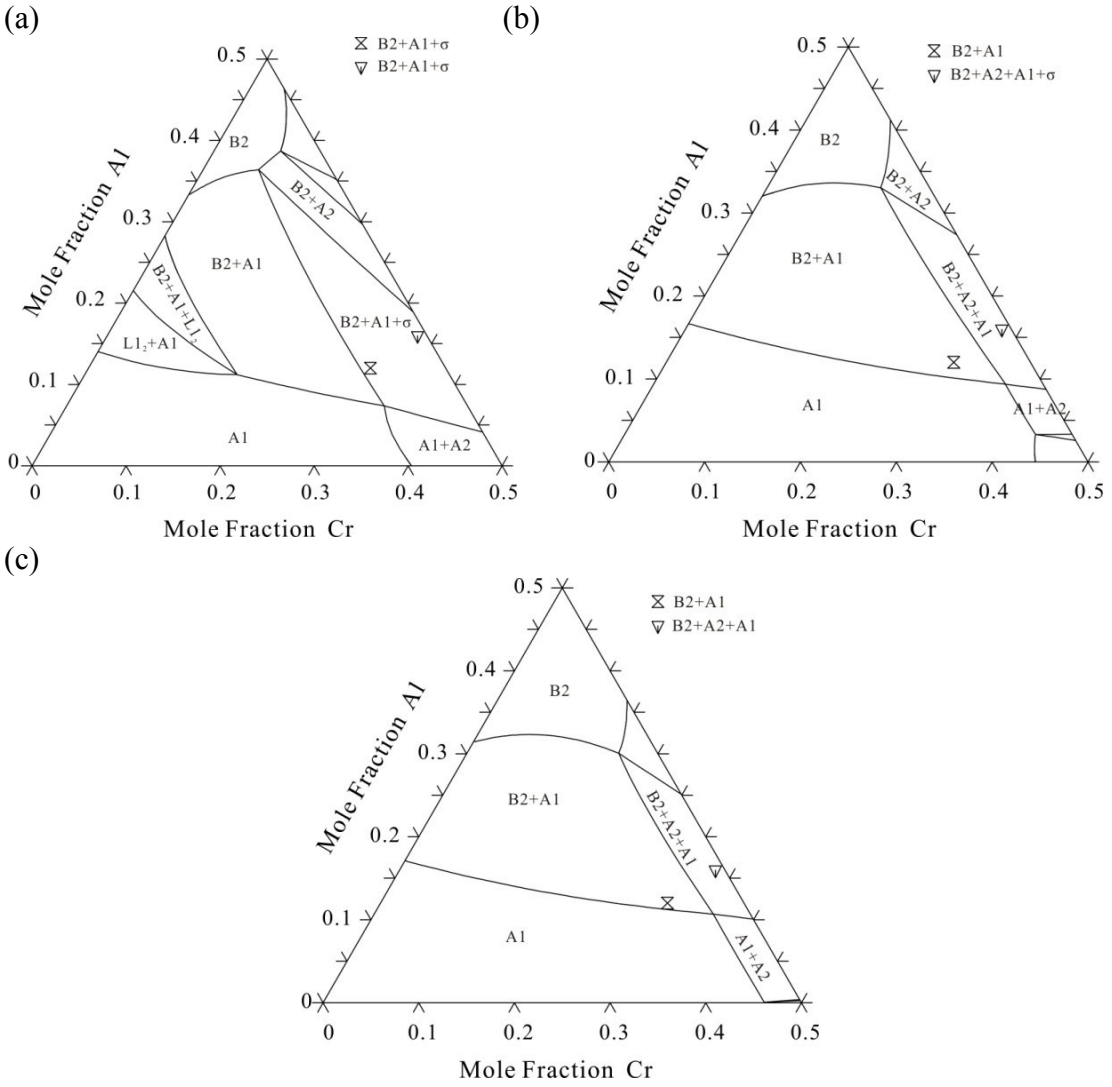

Fig. 5-37 Calculated phase diagrams of Al-Co-Cr-Ni system with 30 at.% Co at (a) 900 °C, (b) 1100 °C and (c) 1200 °C, compared to the experimental results from Gheno et al.

5.4 Discussions and Conclusions

A self-consistent thermodynamic database for the Al-Co-Cr-Ni-Y system was implemented in the present work. In particular, it's the first time that the component Y is systematically involved in the thermodynamic modeling of Al-Co-Cr-Ni-Y. Some predictions and discussions based on this database will be presented here.

According to Gheno's experimental investigations, a quite small amount of Y (0.1 at.%) is able to precipitate some Y-containing compounds. The influence of the alloying element Y on the phase constituent is discussed. To discuss this point the calculated phase fractions results as a function of temperature for the Co-23.2Ni-17.9Cr-12.7Al-0.53Y (wt.%) alloy are shown in Fig. 5-38. There are six main stable phases above 500 °C: Liquid, A1, B2, A3, σ and M_5Y. The primary phase is B2 and A1 forms at approximately 1340 °C. Then the presence of Y stabilizes the M_5Y intermetallic compound below around 1250°C.

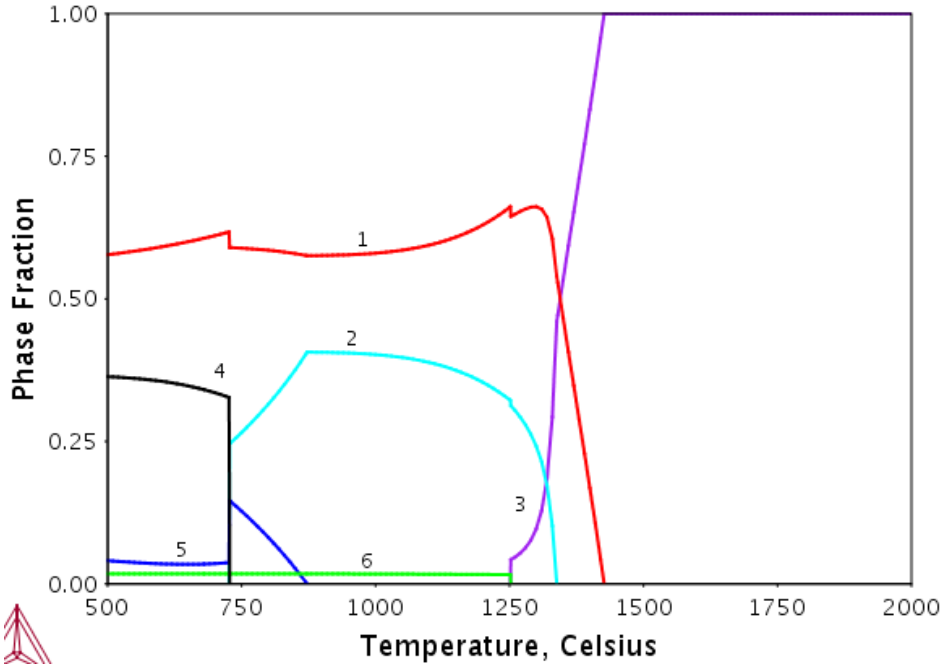

Fig. 5-38 Calculated equilibrium phase fractions as a function of temperature for Co-23.2Ni-17.9Cr-12.7Al-0.53Y (wt.%) alloy.(1- B2, 2-A1, 3-Liquid, 4-A3, 5- σ, 6-M_5Y)

Fig. 5-39 presents the calculated mole fractions of stable phases for the Co-23.2Ni-17.9Cr-12.7Al-Y (wt.%) at 900 °C as a function of the Y amount. Based on the simulation, the A1 amount decreases with increasing Y and M_5Y, while the quantity of the B2 phase is less influenced. The detrimental phase σ become stable at above 1.25 wt.% Y and its amount increases first and then reaches a maximum between around 5 wt.% and 8.5 wt.% Y. After that it decreases slowly with increasing Y.

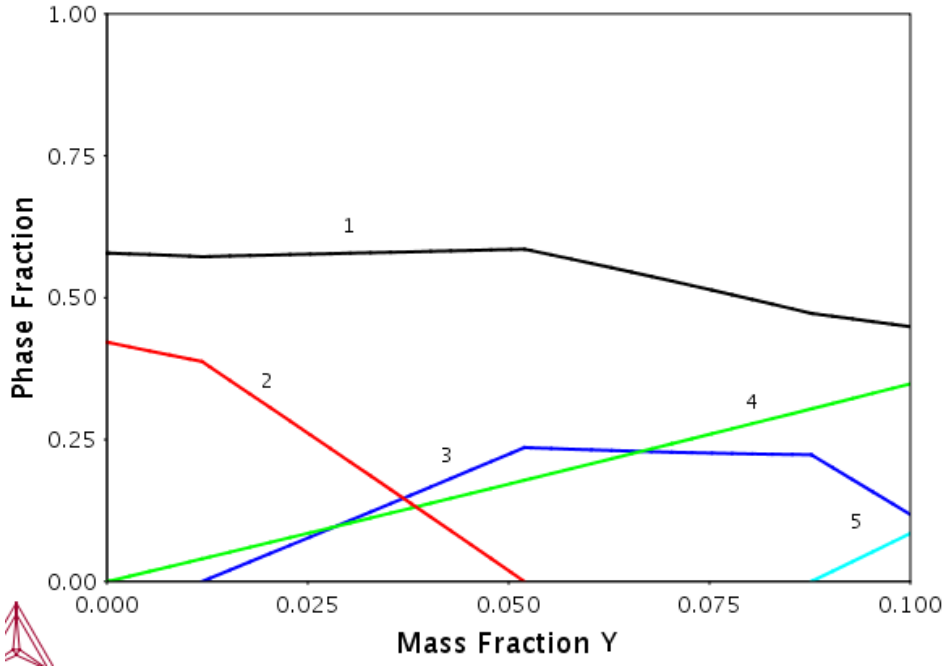

Fig. 5-39 Calculated equilibrium phase fractions as a function of amount Y at 900 °C for Co-23.2Ni-17.9Cr-12.7Al-Y (wt.%) alloy. (1- B2, 2-A1, 3- σ, 4- M_5Y, 5- A2)

6 Summary and Outlook

In this thesis, thermodynamic modeling of C-Co-Cr-Ni-Ta-W bulk alloys and Al-Co-Cr-Ni-Y coatings has been performed by means of the CALPHAD approach. Two important ternary subsystems Co-Cr-Ni and Co-Cr-Ta have been thermodynamically assessed for the implementation of C-Co-Cr-Ni-Ta-W bulk alloys database, while all the binary and ternary Al-Co-Cr-Ni-Y subsystems have been evaluated to build the coatings database on the basis of the available literature.

In chapter 1, the motivation of the current work is presented. Moreover a brief introduction of the advantages of the Co-based superalloys and coatings as well as the main stable phases involved are introduced.

Chapter 2 is dedicated to the CALPHAD approach. The introduction and the advantages of this method are briefly presented as well as the operating flowchart. Thermo-Calc software is adopted for performing the optimization.

Chapter 3 focuses on the existing thermodynamic phase models adopted in the CALPHAD approach. The generally accepted ones are shortly introduced, and then the phase models selected in this work for each phase are introduced and discussed. The A2 and B2 phases are modeled with a single Gibbs energy function as well as the A1 and $L1_2$ phases. In particular, the constraints applied in the modeling of $L1_2$ phase are listed in detail. Sigma phase is described by using a three-sublattice model with the ration 2:8:5, considering its crystallographic structure and the reasonable simplification.

In chapter 4 Co-Cr-Ni, Co-Cr-Ta and the corresponding binary subsystems are considered. Their thermodynamic assessments are presented, after a critical review of the available literature. The homogeneity ranges of Sigma and Laves phases experimentally determined are carefully considered. Satisfactory agreement is obtained in the whole composition range. The thermodynamic database of C-Co-Cr-Ni-Ta-W system (SuperCo database) is finally established through the combination of the current work with the assessment work performed by other students. Several simulations of commercial superalloys are presented at the end of this section.

Chapter 5 is devoted to the thermodynamic investigations of the Al-Co-Cr-Ni-Y system, starting from the critical evaluation of all binary subsystems on the basis of the available literature. Special attention is dedicated to the evaluation of the Gibbs energy of thermal vacancies in the A2 and B2 phases, which is set to 0.2RT. Then, the thermodynamic description of all ternary subsystems is developed. Al-Co-Ni and Al-Cr-Ni phase equilibria in the whole composition range are especially considered during the implementation of the whole database. In particular the homogeneity ranges of the ternary compounds θ_1 and τ_1 in the Al-rich corner are well reproduced. As for the ternary systems containing Y, the optimizations are focused on the Y-poor regions due to the lack of experimental literature in the Y-rich corner. A large number of ternary intermetallic compounds were experimentally confirmed and most of them are modelled as stoichiometric phases by using three sublattices. Very good agreement

between calculated results and experimental data is achieved, even if phase relations in the Y-rich regions are generally based on extrapolations since no reliable experimental data are available in the literature, partly due to the easy oxidation of Y.

In the same chapter selected quaternary Al-Co-Cr-Ni isothermal sections containing A1, $L1_2$, A2, B2 and σ phases are calculated and compared to experimental results. The current database can reproduce well most of the experimental data and the only discrepancy concerns the phase transition between A2 and σ phases at high temperature. In the end a short analysis on the influence of Y on the phase relations is presented.

In general the obtained thermodynamic database can provide a reliable description of phase equilibria. Therefore they can be used to support the selection of new alloying compositions or the simulations of the C-Co-Cr-Ni-Ta-W bulk alloys and Al-Co-Cr-Ni-Y coatings. Moreover they also play an important role in the prediction of the interactions occurring at the joints between coatings and bulk alloys, as a necessary thermodynamic background for kinetic simulations and phase field modeling.

There are more investigations worth to do in the future in order to further improve the thermodynamic descriptions based on the current work:

As reviewed in chapter 4.2.3.2, in the Co-Cr-Ta system the solubility region of bcc-Ta as proposed by the only existing experimental study seems improbable when compared to the binary phase diagrams. Therefore, more experimental work on the phase equilibria in the Ta-rich region should be considered in the future.

In the Al-Co-Cr-Ni quaternary system, the stability of the σ phase is possibly underestimated in the present work. In order to improve the modeling of this phase, more theoretical studies on the σ end members supported by first-principles calculations and further experimental investigations on the phase transition between A2 and σ are strongly expected.

Appendix A The thermodynamic dataset of the Co-Cr-Ta system

```
ELEMENT /-   ELECTRON_GAS              0.0000E+00  0.0000E+00  0.0000E+00!
ELEMENT VA   VACUUM                    0.0000E+00  0.0000E+00  0.0000E+00!
ELEMENT CO   A3                        5.8933E+01  0.0000E+00  0.0000E+00!
ELEMENT CR   A2                        5.1996E+01  4.0500E+03  2.3560E+01!
ELEMENT TA   A2                        1.8095E+02  5.6819E+03  4.1472E+01!


FUNCTION GLIQCO     298.15  +GHSERCO#+15085.037-8.931932*T-2.19801E-21*T**7;
     1768 Y
      -846.61+243.599944*T-40.5*T*LN(T); 6000 N !
FUNCTION GLIQCR     298.15 +GHSERCR#+24339.955-11.420225*T+2.37615E-21*T**7;
     2180 Y
      -16459.984+335.616316*T-50*T*LN(T); 6000 N !
FUNCTION GLIQTA     298.15  +21875.086+111.561128*T-23.7592624*T*LN(T)
     -.002623033*T**2+1.70109E-07*T**3-3293*T**(-1); 1000 Y
      +43884.339-61.981795*T+.0279523*T*LN(T)-.012330066*T**2
     +6.14599E-07*T**3-3523338*T**(-1); 3290 Y
      -6314.543+258.110873*T-41.84*T*LN(T); 6000 N !
FUNCTION GFCCCO     298.15  +427.591-.615248*T+GHSERCO#; 6000 N !
FUNCTION GFCCCR     298.15  +GHSERCR#+7284+.163*T; 6000 N !
FUNCTION GFCCTA     298.15  +GHSERTA#+16000+1.7*T; 6000 N !
FUNCTION ZERO       298.15  +0.0; 6000 N !
FUNCTION GBCCCO     298.15  +GHSERCO#+2938-.7138*T; 6000 N !
FUNCTION GHSERCR    298.15  -8856.94+157.48*T-26.908*T*LN(T)+.00189435*T**2
     -1.47721E-06*T**3+139250*T**(-1); 2180 Y
      -34869.344+344.18*T-50*T*LN(T)-2.88526E+32*T**(-9); 6000 N !
FUNCTION GHSERTA    298.15  -7285.889+119.139857*T-23.7592624*T*LN(T)
     -.002623033*T**2+1.70109E-07*T**3-3293*T**(-1); 1300 Y
      -22389.955+243.88676*T-41.137088*T*LN(T)+.006167572*T**2
     -6.55136E-07*T**3+2429586*T**(-1); 2500 Y
      +229382.886-722.59722*T+78.5244752*T*LN(T)-.017983376*T**2
     +1.95033E-07*T**3-93813648*T**(-1); 3290 Y
      -1042384.01+2985.49125*T-362.159132*T*LN(T)+.043117795*T**2
     -1.055148E-06*T**3+5.54714342E+08*T**(-1); 6000 N !
FUNCTION RGAS       298.15  +8.3144621; 6000 N !
FUNCTION GHSERCO    298.15  +310.241+133.36601*T-25.0861*T*LN(T)
     -.002654739*T**2-1.7348E-07*T**3+72527*T**(-1); 1768 Y
      -17197.666+253.28374*T-40.5*T*LN(T)+9.3488E+30*T**(-9); 6000 N !
FUNCTION GHCPCR     298.15  +GHSERCR#+4438; 6000 N !
FUNCTION GHCPTA     298.15  +GHSERTA#+12000+2.4*T; 6000 N !
FUNCTION GC14CO     298.15  +16400+GHSERCO#; 6000 N !
```

```
FUNCTION GC14CR    298.15 +28630+GHSERCR#; 6000 N !
FUNCTION GC14TA    298.15 +9350+GHSERTA#; 6000 N !
FUNCTION GC15CO    298.15 +19600+GHSERCO#; 6000 N !
FUNCTION GC15CR    298.15 +27290+GHSERCR#; 6000 N !
FUNCTION GC15TA    298.15 +10940+GHSERTA#; 6000 N !
FUNCTION GC36CO    298.15 +16400+GHSERCO#; 6000 N !
FUNCTION GC36TA    298.15 +10150+GHSERTA#; 6000 N !
FUNCTION GC36CR    298.15 +27750+GHSERCR#; 6000 N !
FUNCTION GBCCCR    298.15 +GHSERCR#; 6000 N !
FUNCTION GMU4TA    298.15 +11461.54+1.2923*T+GHSERTA#; 6000 N !
FUNCTION GMTACO    298.15 -525200+60*T; 6000 N !
FUNCTION GMCOTA2   298.15 +133081; 6000 N !
FUNCTION GMTACO3   298.15 -6500; 6000 N !
FUNCTION GMTACO4   298.15 +671970; 6000 N !
FUNCTION GMU4CR    298.15 +22400+1.2923*T+GHSERCR#; 6000 N !
FUNCTION GMU4CO    298.15 +10200+1.2923*T+GFCCCO#; 6000 N !
FUNCTION GSIGMACO  298.15 +4700+.25*T+GFCCCO#; 6000 N !
FUNCTION GSIGMACR  298.15 +13200+GHSERCR#; 6000 N !
FUNCTION GSIGMATA  298.15 +1900+GHSERTA#; 6000 N !
FUNCTION GHCPCO    298.15 +GHSERCO#; 6000 N !
FUNCTION GBCCTA    298.15 +GHSERTA#; 6000 N !
FUNCTION UN_ASS 298.15 +0; 300 N !

TYPE_DEFINITION % SEQ *!
DEFINE_SYSTEM_DEFAULT ELEMENT 2 !
DEFAULT_COMMAND DEF_SYS_ELEMENT VA /- !


PHASE LIQUID:L %  1  1.0  !
   CONSTITUENT LIQUID:L :CO,CR,TA :  !

  PARAMETER G(LIQUID,CO;0)              298.15 +GLIQCO#; 6000 N REF2 !
  PARAMETER G(LIQUID,CR;0)              298.15 +GLIQCR#; 6000 N REF2 !
  PARAMETER G(LIQUID,TA;0)              298.15 +GLIQTA#; 6000 N REF2 !
  PARAMETER G(LIQUID,CO,CR;0)           298.15 -12008.6239+2.2019*T; 6000
 N REF8 !
  PARAMETER G(LIQUID,CO,CR;1)           298.15 -5836.4696+1.1402*T; 6000 N
 REF8 !
  PARAMETER G(LIQUID,CO,TA;0)           298.15 -171992+35*T; 6000 N REF10 !
  PARAMETER G(LIQUID,CO,TA;1)           298.15 -2958; 6000 N REF10 !
  PARAMETER G(LIQUID,CO,TA;2)           298.15 +24975; 6000 N REF10 !
  PARAMETER G(LIQUID,CR,TA;0)           298.15 -18600+6.2*T; 6000 N REF13 !
  PARAMETER G(LIQUID,CR,TA;1)           298.15 +12600-4.2*T; 6000 N REF13 !
```

```
TYPE_DEFINITION & GES A_P_D A1 MAGNETIC  -3.0    2.80000E-01 !
PHASE A1  %&  2 1   1 !
   CONSTITUENT A1  :CO%,CR,TA : VA% :  !

  PARAMETER G(A1,CO:VA;0)                298.15 +GFCCCO#; 6000 N REF2 !
  PARAMETER TC(A1,CO:VA;0)               298.15 +1396; 6000 N REF2 !
  PARAMETER BMAGN(A1,CO:VA;0)            298.15 +1.35; 6000 N REF2 !
  PARAMETER G(A1,CR:VA;0)                298.15 +GFCCCR#; 6000 N REF2 !
  PARAMETER TC(A1,CR:VA;0)               298.15 -1109; 6000 N REF2 !
  PARAMETER BMAGN(A1,CR:VA;0)            298.15 -2.46; 6000 N REF2 !
  PARAMETER G(A1,TA:VA;0)                298.15 +GFCCTA#; 6000 N REF2 !
  PARAMETER G(A1,CO,CR:VA;0)             298.15 -24052.09+8.1884*T; 6000 N
 REF8 !
  PARAMETER G(A1,CO,CR:VA;1)             298.15 +5331.8252-6.9059*T; 6000 N
 REF8 !
  PARAMETER TC(A1,CO,CR:VA;0)            298.15 -9392.5259; 6000 N REF8 !
  PARAMETER TC(A1,CO,CR:VA;1)            298.15 +8383.0424; 6000 N REF8 !
  PARAMETER G(A1,CO,CR,TA:VA;0)          298.15 -70000; 6000 N REF24 !
  PARAMETER G(A1,CO,CR,TA:VA;1)          298.15 -70000; 6000 N REF24 !
  PARAMETER G(A1,CO,CR,TA:VA;2)          298.15 -70000; 6000 N REF24 !
  PARAMETER G(A1,CO,TA:VA;0)             298.15 -80000+38*T; 6000 N REF5 !
  PARAMETER G(A1,CO,TA:VA;1)             298.15 -60000; 6000 N REF5 !
  PARAMETER TC(A1,CO,TA:VA;0)            298.15 -2200; 6000 N REF11 !
  PARAMETER TC(A1,CO,TA:VA;1)            298.15 -804; 6000 N REF11 !
  PARAMETER G(A1,CR,TA:VA;0)             298.15 +ZERO#; 6000 N REF5 !


TYPE_DEFINITION ' GES A_P_D A2 MAGNETIC  -1.0    4.00000E-01 !
PHASE A2  %'  2 1   3 !
   CONSTITUENT A2  :CO,CR%,TA%,VA : VA% :  !

  PARAMETER G(A2,CO:VA;0)                298.15 +GBCCCO#; 6000 N REF2 !
  PARAMETER TC(A2,CO:VA;0)               298.15 +1450; 6000 N REF2 !
  PARAMETER BMAGN(A2,CO:VA;0)            298.15 +1.35; 6000 N REF2 !
  PARAMETER G(A2,CR:VA;0)                298.15 +GHSERCR#; 6000 N REF2 !
  PARAMETER TC(A2,CR:VA;0)               298.15 -311.5; 6000 N REF2 !
  PARAMETER BMAGN(A2,CR:VA;0)            298.15 -.008; 6000 N REF2 !
  PARAMETER G(A2,TA:VA;0)                298.15 +GHSERTA#; 6000 N REF2 !
  PARAMETER G(A2,VA:VA;0)                298.15 +.2*RGAS#*T; 6000 N REF24 !
  PARAMETER G(A2,CO,VA:VA;0)             298.15 +126184-.2*RGAS#*T; 6000 N
 REF26 !
  PARAMETER G(A2,CO,CR:VA;0)             298.15 +1033.2829-1.4808*T; 6000 N
 REF8 !
```

```
  PARAMETER G(A2,CO,CR:VA;1)              298.15 +11971.5008-15*T; 6000 N
 REF8 !
  PARAMETER G(A2,CO,CR,TA:VA;0)           298.15 -170000; 6000 N REF24 !
  PARAMETER G(A2,CO,CR,TA:VA;1)           298.15 -180000; 6000 N REF24 !
  PARAMETER G(A2,CO,CR,TA:VA;2)           298.15 -180000; 6000 N REF24 !
  PARAMETER G(A2,CO,TA:VA;0)              298.15 -59084+5.334*T; 6000 N REF5 !
  PARAMETER G(A2,CO,TA:VA;1)              298.15 -20000+10*T; 6000 N REF5 !
  PARAMETER G(A2,CR,VA:VA;0)              298.15 +100000-.2*RGAS#*T; 6000 N
 REF3 !
  PARAMETER G(A2,CR,TA:VA;0)              298.15 +46800-11.4*T; 6000 N REF13 !
  PARAMETER G(A2,CR,TA:VA;1)              298.15 +37200-17.2*T; 6000 N REF13 !
  PARAMETER G(A2,CR,TA:VA;2)              298.15 +16200-5.4*T; 6000 N REF13 !
  PARAMETER G(A2,TA,VA:VA;0)              298.15 +100000-.2*RGAS#*T; 6000 N
 REF24 !


TYPE_DEFINITION ( GES A_P_D A3 MAGNETIC  -3.0    2.80000E-01 !
PHASE A3  %(  2 1   .5 !
   CONSTITUENT A3  :CO%,CR,TA : VA% :  !

  PARAMETER G(A3,CO:VA;0)                 298.15 +GHSERCO#; 6000 N REF2 !
  PARAMETER TC(A3,CO:VA;0)                298.15 +1396; 6000 N REF2 !
  PARAMETER BMAGN(A3,CO:VA;0)             298.15 +1.35; 6000 N REF2 !
  PARAMETER G(A3,CR:VA;0)                 298.15 +GHCPCR#; 6000 N REF2 !
  PARAMETER TC(A3,CR:VA;0)                298.15 -1109; 6000 N REF2 !
  PARAMETER BMAGN(A3,CR:VA;0)             298.15 -2.46; 6000 N REF2 !
  PARAMETER G(A3,TA:VA;0)                 298.15 +GHCPTA#; 6000 N REF2 !
  PARAMETER G(A3,CO,CR:VA;0)              298.15 -28500+15.5105*T; 6000 N
 REF8 !
  PARAMETER G(A3,CO,CR:VA;1)              298.15 +12673.5606-14.8392*T; 6000
 N REF8 !
  PARAMETER TC(A3,CO,CR:VA;0)             298.15 -5828.677; 6000 N REF8 !
  PARAMETER TC(A3,CO,CR:VA;1)             298.15 +4873.9533; 6000 N REF8 !
  PARAMETER G(A3,CO,CR,TA:VA;0)           298.15 -86000+27*T; 6000 N REF24 !
  PARAMETER G(A3,CO,CR,TA:VA;1)           298.15 -86000+27*T; 6000 N REF24 !
  PARAMETER G(A3,CO,CR,TA:VA;2)           298.15 -86000+27*T; 6000 N REF24 !
  PARAMETER G(A3,CO,TA:VA;0)              298.15 -102000+15*T; 6000 N REF5 !
  PARAMETER G(A3,CR,TA:VA;0)              298.15 +ZERO#; 6000 N REF5 !


PHASE AL2CU_TY  %  2 2   1 !
   CONSTITUENT AL2CU_TY  :CO,CR,TA% : CO%,CR,TA :  !

  PARAMETER G(AL2CU_TY,CO:CO;0)           298.15 +30000+3*GHSERCO#; 6000 N
```

```
REF5 !
 PARAMETER G(AL2CU_TY,CR:CO;0)          298.15 +2*GHSERCR#+GHSERCO#; 6000
N REF24 !
 PARAMETER G(AL2CU_TY,TA:CO;0)          298.15 -94343+10*T+GHSERCO#
+2*GHSERTA#; 6000 N REF5 !
 PARAMETER G(AL2CU_TY,CO:CR;0)          298.15 +2*GHSERCO#+GHSERCR#; 6000
N REF24 !
 PARAMETER G(AL2CU_TY,CR:CR;0)          298.15 +30000+3*GHSERCR#; 6000 N
REF24 !
 PARAMETER G(AL2CU_TY,TA:CR;0)          298.15 +GHSERCR#+2*GHSERTA#; 6000
N REF24 !
 PARAMETER G(AL2CU_TY,CO:TA;0)          298.15 +90000+9*T+2*GHSERCO#
+GHSERTA#; 6000 N REF5 !
 PARAMETER G(AL2CU_TY,CR:TA;0)          298.15 +2*GHSERCR#+GHSERTA#; 6000
N REF24 !
 PARAMETER G(AL2CU_TY,TA:TA;0)          298.15 +152640+3*GHSERTA#; 6000 N
REF7 !
 PARAMETER G(AL2CU_TY,CO,TA:CO;0)       298.15 -100000; 6000 N REF5 !
 PARAMETER G(AL2CU_TY,CR,TA:CO;0)       298.15 -90000; 6000 N REF24 !
 PARAMETER G(AL2CU_TY,CR,TA:CO;1)       298.15 +30000; 6000 N REF24 !
 PARAMETER G(AL2CU_TY,TA:CO,TA;0)       298.15 +20000; 6000 N REF5 !
 PARAMETER G(AL2CU_TY,TA:CO,CR;0)       298.15 -19500; 6000 N REF24 !


PHASE C14  %  2 1   2 !
   CONSTITUENT C14  :CO,CR,TA% : CO%,CR%,TA :  !

 PARAMETER G(C14,CO:CO;0)               298.15 +3*GC14CO#; 6000 N REF24 !
 PARAMETER G(C14,CR:CO;0)               298.15 +10000+2*GC14CO#+GC14CR#;
6000 N REF9 !
 PARAMETER G(C14,TA:CO;0)               298.15 -179988+26*T+2*GC14CO#
+GC14TA#; 6000 N REF24 !
 PARAMETER G(C14,CO:CR;0)               298.15 +15970+10*T+2*GC14CR#
+GC14CO#; 6000 N REF9 !
 PARAMETER G(C14,CR:CR;0)               298.15 +3*GC14CR#; 6000 N REF4 !
 PARAMETER G(C14,TA:CR;0)               298.15 -30750+.999*T+2*GHSERCR#
+GHSERTA#; 6000 N REF25 !
 PARAMETER G(C14,CO:TA;0)               298.15 +2*GC14TA#+GC14CO#; 6000 N
REF5 !
 PARAMETER G(C14,CR:TA;0)               298.15 +229050+.112*T+2*GHSERTA#
+GHSERCR#; 6000 N REF25 !
 PARAMETER G(C14,TA:TA;0)               298.15 +3*GC14TA#; 6000 N REF4 !
 PARAMETER G(C14,CR,TA:CO;0)            298.15 -145000; 6000 N REF24 !
 PARAMETER G(C14,CR,TA:CO;1)            298.15 -34000; 6000 N REF24 !
```

```
  PARAMETER G(C14,CR,TA:CO,CR;0)          298.15 -24000; 6000 N REF24 !
  PARAMETER G(C14,TA:CO,TA;0)             298.15 -54700; 6000 N REF24 !
  PARAMETER G(C14,TA:CO,CR;0)             298.15 -104365+5*T; 6000 N REF24 !
  PARAMETER G(C14,TA:CO,CR;1)             298.15 +15000; 6000 N REF24 !
  PARAMETER G(C14,CO,TA:CR;0)             298.15 -243000; 6000 N REF24 !
  PARAMETER G(C14,CR,TA:CR;0)             298.15 -35000-9.85*T; 6000 N REF25 !
  PARAMETER G(C14,CR:CR,TA;0)             298.15 +79000; 6000 N REF25 !
  PARAMETER G(C14,TA:CR,TA;0)             298.15 +35100+14.95*T; 6000 N
 REF24 !
  PARAMETER G(C14,CR,TA:TA;0)             298.15 +79000; 6000 N REF25 !


PHASE C15  %  2 1   2 !
   CONSTITUENT C15  :CO,CR,TA% : CO%,CR%,TA :  !

  PARAMETER G(C15,CO:CO;0)                298.15 +3*GC15CO#; 6000 N REF4 !
  PARAMETER G(C15,CR:CO;0)                298.15 +24000+2*GC15CO#+GC15CR#;
 6000 N REF9 !
  PARAMETER G(C15,TA:CO;0)                298.15 -189440+26.15*T+2*GC15CO#
 +GC15TA#; 6000 N REF24 !
  PARAMETER G(C15,CO:CR;0)                298.15 +2*GC15CR#+GC15CO#; 6000 N
 REF9 !
  PARAMETER G(C15,CR:CR;0)                298.15 +3*GC15CR#; 6000 N REF4 !
  PARAMETER G(C15,TA:CR;0)                298.15 -33870+2.53*T+2*GHSERCR#
 +GHSERTA#; 6000 N REF25 !
  PARAMETER G(C15,CO:TA;0)                298.15 +138000+26.15*T+GC15CO#
 +2*GC15TA#; 6000 N REF5 !
  PARAMETER G(C15,CR:TA;0)                298.15 +223170-.65*T+2*GHSERTA#
 +GHSERCR#; 6000 N REF25 !
  PARAMETER G(C15,TA:TA;0)                298.15 +3*GC15TA#; 6000 N REF4 !
  PARAMETER G(C15,CO,TA:CO;0)             298.15 -61500; 6000 N REF24 !
  PARAMETER G(C15,CR,TA:CO;0)             298.15 -135000; 6000 N REF24 !
  PARAMETER G(C15,TA:CO,CR;0)             298.15 -45000; 6000 N REF24 !
  PARAMETER G(C15,CR,TA:CR;0)             298.15 -2500-23.4*T; 6000 N REF25 !
  PARAMETER G(C15,CR:CR,TA;0)             298.15 +240000; 6000 N REF25 !
  PARAMETER G(C15,TA:CR,TA;0)             298.15 +80400-10.3*T; 6000 N REF25 !
  PARAMETER G(C15,CR,TA:TA;0)             298.15 +240000; 6000 N REF25 !


PHASE C36  %  2 1   2 !
   CONSTITUENT C36  :CO,CR,TA% : CO%,CR,TA :  !

  PARAMETER G(C36,CO:CO;0)                298.15 +3*GC36CO#; 6000 N REF5 !
  PARAMETER G(C36,CR:CO;0)                298.15 -30000+2*GC36CO#+GC36CR#;
```

```
6000 N REF24 !
 PARAMETER G(C36,TA:CO;0)                298.15 -180090+27.2*T+2*GC36CO#
+GC36TA#; 6000 N REF24 !
 PARAMETER G(C36,CO:CR;0)                298.15 -30000+GC36CO#+2*GC36CR#;
6000 N REF24 !
 PARAMETER G(C36,CR:CR;0)                298.15 +3*GC36CR#; 6000 N REF24 !
 PARAMETER G(C36,TA:CR;0)                298.15 -45000+2*GC36CR#+GC36TA#;
6000 N REF24 !
 PARAMETER G(C36,CO:TA;0)                298.15 +137000+27.2*T+GC36CO#
+2*GC36TA#; 6000 N REF5 !
 PARAMETER G(C36,CR:TA;0)                298.15 +GC36CR#+2*GC36TA#; 6000 N
REF24 !
 PARAMETER G(C36,TA:TA;0)                298.15 +3*GC36TA#; 6000 N REF5 !
 PARAMETER G(C36,CO,TA:CO;0)             298.15 -69200; 6000 N REF24 !
 PARAMETER G(C36,CR,TA:CO;0)             298.15 -75000; 6000 N REF24 !
 PARAMETER G(C36,TA:CO,CR;0)             298.15 -115000; 6000 N REF24 !



PHASE MOPT2_TY  %  2 1   2 !
   CONSTITUENT MOPT2_TY  :CR% : CR :  !

 PARAMETER G(MOPT2_TY,CR:CR;0)           298.15 +3*GBCCCR#+500; 6000 N
REF12 !


PHASE MOSI2_TY  %  2 1   2 !
   CONSTITUENT MOSI2_TY  :CR,TA% : CR%,TA :  !

 PARAMETER G(MOSI2_TY,CR:CR;0)           298.15 +10000+3*GHSERCR#; 6000 N
REF6 !
 PARAMETER G(MOSI2_TY,TA:CR;0)           298.15 +50000+GHSERTA#+2*GHSERCR#;
6000 N REF5 !
 PARAMETER G(MOSI2_TY,CR:TA;0)           298.15 +50000+GHSERCR#+2*GHSERTA#;
6000 N REF5 !
 PARAMETER G(MOSI2_TY,TA:TA;0)           298.15 +31470+3*GHSERTA#; 6000 N
REF7 !


PHASE MU4  %  4 4   2   1   6 !
   CONSTITUENT MU4  :TA% : CO,CR,TA% : CO%,CR,TA : CO%,CR,TA :  !

 PARAMETER G(MU4,TA:CO:CO:CO;0)          298.15 +GMTACO#+GMCOTA2#
```

```
+9*GHSERCO#+4*GHSERTA#; 6000 N REF5 !
 PARAMETER G(MU4,TA:CR:CO:CO;0)          298.15 +7*GMU4CO#+2*GMU4CR#
+4*GMU4TA#; 6000 N REF0 !
 PARAMETER G(MU4,TA:TA:CO:CO;0)          298.15 -523319+62*T+7*GHSERCO#
+6*GHSERTA#; 6000 N REF5 !
 PARAMETER G(MU4,TA:CO:CR:CO;0)          298.15 +8*GMU4CO#+GMU4CR#
+4*GMU4TA#; 6000 N REF0 !
 PARAMETER G(MU4,TA:CR:CR:CO;0)          298.15 +6*GMU4CO#+3*GMU4CR#
+4*GMU4TA#; 6000 N REF0 !
 PARAMETER G(MU4,TA:TA:CR:CO;0)          298.15 +6*GMU4CO#+GMU4CR#
+6*GMU4TA#; 6000 N REF0 !
 PARAMETER G(MU4,TA:CO:TA:CO;0)          298.15 +GMTACO#+GMCOTA2#+GMTACO3#
+8*GHSERCO#+5*GHSERTA#; 6000 N REF5 !
 PARAMETER G(MU4,TA:CR:TA:CO;0)          298.15 +6*GMU4CO#+2*GMU4CR#
+5*GMU4TA#; 6000 N REF0 !
 PARAMETER G(MU4,TA:TA:TA:CO;0)          298.15 -467000+38*T+6*GHSERCO#
+7*GHSERTA#; 6000 N REF5 !
 PARAMETER G(MU4,TA:CO:CO:CR;0)          298.15 +3*GMU4CO#+6*GMU4CR#
+4*GMU4TA#; 6000 N REF0 !
 PARAMETER G(MU4,TA:CR:CO:CR;0)          298.15 +GMU4CO#+8*GMU4CR#
+4*GMU4TA#; 6000 N REF0 !
 PARAMETER G(MU4,TA:TA:CO:CR;0)          298.15 -439635+GMU4CO#+6*GMU4CR#
+6*GMU4TA#; 6000 N REF0 !
 PARAMETER G(MU4,TA:CO:CR:CR;0)          298.15 +2*GMU4CO#+7*GMU4CR#
+4*GMU4TA#; 6000 N REF0 !
 PARAMETER G(MU4,TA:CR:CR:CR;0)          298.15 +9*GMU4CR#+4*GMU4TA#; 6000
N REF5 !
 PARAMETER G(MU4,TA:TA:CR:CR;0)          298.15 +7*GMU4CR#+6*GMU4TA#; 6000
N REF5 !
 PARAMETER G(MU4,TA:CO:TA:CR;0)          298.15 +2*GMU4CO#+6*GMU4CR#
+5*GMU4TA#; 6000 N REF0 !
 PARAMETER G(MU4,TA:CR:TA:CR;0)          298.15 +8*GMU4CR#+5*GMU4TA#; 6000
N REF5 !
 PARAMETER G(MU4,TA:TA:TA:CR;0)          298.15 -316995+15*T+6*GMU4CR#
+7*GMU4TA#; 6000 N REF24 !
 PARAMETER G(MU4,TA:CO:CO:TA;0)          298.15 +GMTACO#+GMCOTA2#+GMTACO4#
+3*GHSERCO#+10*GHSERTA#; 6000 N REF5 !
 PARAMETER G(MU4,TA:CR:CO:TA;0)          298.15 +GMU4CO#+2*GMU4CR#
+10*GMU4TA#; 6000 N REF0 !
 PARAMETER G(MU4,TA:TA:CO:TA;0)          298.15 +GMTACO#+GMTACO4#+GHSERCO#
+12*GHSERTA#; 6000 N REF5 !
 PARAMETER G(MU4,TA:CO:CR:TA;0)          298.15 +2*GMU4CO#+GMU4CR#
+10*GMU4TA#; 6000 N REF0 !
 PARAMETER G(MU4,TA:CR:CR:TA;0)          298.15 +3*GMU4CR#+10*GMU4TA#; 6000
```

```
N REF5 !
 PARAMETER G(MU4,TA:TA:CR:TA;0)          298.15 +GMU4CR#+12*GMU4TA#; 6000 N
REF5 !
 PARAMETER G(MU4,TA:CO:TA:TA;0)          298.15 +GMTACO#+GMCOTA2#+GMTACO3#
+GMTACO4#+2*GHSERCO#+11*GHSERTA#; 6000 N REF5 !
 PARAMETER G(MU4,TA:CR:TA:TA;0)          298.15 +2*GMU4CR#+11*GMU4TA#; 6000
N REF5 !
 PARAMETER G(MU4,TA:TA:TA:TA;0)          298.15 +13*GMU4TA#; 6000 N REF1 !
 PARAMETER G(MU4,TA:TA:CO:CO,CR;0)       298.15 -230000; 6000 N REF24 !
 PARAMETER G(MU4,TA:TA:TA:CO,CR;0)       298.15 -293730+10*T; 6000 N REF24 !
 PARAMETER G(MU4,TA:TA:TA:CR,TA;0)       298.15 -112000; 6000 N REF24 !



PHASE SIGMA3  %  3 2   8   5 !
   CONSTITUENT SIGMA3  :CO,CR%,TA : CO,CR%,TA : CO%,CR,TA :  !

 PARAMETER G(SIGMA3,CO:CO:CO;0)          298.15 +15*GSIGMACO#; 6000 N REF1 !
 PARAMETER G(SIGMA3,CR:CO:CO;0)          298.15 -100000+10*T+13*GSIGMACO#
+2*GSIGMACR#; 6000 N REF5 !
 PARAMETER G(SIGMA3,TA:CO:CO;0)          298.15 +13*GSIGMACO#+2*GSIGMATA#;
6000 N REF5 !
 PARAMETER G(SIGMA3,CO:CR:CO;0)          298.15 +100000+7*GSIGMACO#
+8*GSIGMACR#; 6000 N REF5 !
 PARAMETER G(SIGMA3,CR:CR:CO;0)          298.15 -263000+24.5*T+5*GSIGMACO#
+10*GSIGMACR#; 6000 N REF5 !
 PARAMETER G(SIGMA3,TA:CR:CO;0)          298.15 -180000+5*GSIGMACO#
+8*GSIGMACR#+2*GSIGMATA#; 6000 N REF0 !
 PARAMETER G(SIGMA3,CO:TA:CO;0)          298.15 +7*GSIGMACO#+8*GSIGMATA#;
6000 N REF5 !
 PARAMETER G(SIGMA3,CR:TA:CO;0)          298.15 +5*GSIGMACO#+2*GSIGMACR#
+8*GSIGMATA#; 6000 N REF0 !
 PARAMETER G(SIGMA3,TA:TA:CO;0)          298.15 +5*GSIGMACO#+10*GSIGMATA#;
6000 N REF5 !
 PARAMETER G(SIGMA3,CO:CO:CR;0)          298.15 +268000+10*GSIGMACO#
+5*GSIGMACR#; 6000 N REF5 !
 PARAMETER G(SIGMA3,CR:CO:CR;0)          298.15 -100000+10*T+8*GSIGMACO#
+7*GSIGMACR#; 6000 N REF5 !
 PARAMETER G(SIGMA3,TA:CO:CR;0)          298.15 +8*GSIGMACO#+5*GSIGMACR#
+2*GSIGMATA#; 6000 N REF0 !
 PARAMETER G(SIGMA3,CO:CR:CR;0)          298.15 +100000+2*GSIGMACO#
+13*GSIGMACR#; 6000 N REF5 !
 PARAMETER G(SIGMA3,CR:CR:CR;0)          298.15 +15*GSIGMACR#; 6000 N REF1 !
 PARAMETER G(SIGMA3,TA:CR:CR;0)          298.15 +13*GSIGMACR#+2*GSIGMATA#;
```

```
6000 N REF5 !
 PARAMETER G(SIGMA3,CO:TA:CR;0)          298.15 +2*GSIGMACO#+5*GSIGMACR#
+8*GSIGMATA#; 6000 N REF0 !
 PARAMETER G(SIGMA3,CR:TA:CR;0)          298.15 +7*GSIGMACR#+8*GSIGMATA#;
6000 N REF5 !
 PARAMETER G(SIGMA3,TA:TA:CR;0)          298.15 +5*GSIGMACR#+10*GSIGMATA#;
6000 N REF5 !
 PARAMETER G(SIGMA3,CO:CO:TA;0)          298.15 +10*GSIGMACO#+5*GSIGMATA#;
6000 N REF5 !
 PARAMETER G(SIGMA3,CR:CO:TA;0)          298.15 +8*GSIGMACO#+2*GSIGMACR#
+5*GSIGMATA#; 6000 N REF0 !
 PARAMETER G(SIGMA3,TA:CO:TA;0)          298.15 +8*GSIGMACO#+7*GSIGMATA#;
6000 N REF5 !
 PARAMETER G(SIGMA3,CO:CR:TA;0)          298.15 +2*GSIGMACO#+8*GSIGMACR#
+5*GSIGMATA#; 6000 N REF0 !
 PARAMETER G(SIGMA3,CR:CR:TA;0)          298.15 +10*GSIGMACR#+5*GSIGMATA#;
6000 N REF5 !
 PARAMETER G(SIGMA3,TA:CR:TA;0)          298.15 +8*GSIGMACR#+7*GSIGMATA#;
6000 N REF5 !
 PARAMETER G(SIGMA3,CO:TA:TA;0)          298.15 +2*GSIGMACO#+13*GSIGMATA#;
6000 N REF5 !
 PARAMETER G(SIGMA3,CR:TA:TA;0)          298.15 +2*GSIGMACR#+13*GSIGMATA#;
6000 N REF5 !
 PARAMETER G(SIGMA3,TA:TA:TA;0)          298.15 +15*GSIGMATA#; 6000 N REF1 !
 PARAMETER G(SIGMA3,CR,TA:CR:CO;0)       298.15 -270000; 6000 N REF0 !
 PARAMETER G(SIGMA3,CR:CR:CO,CR;0)       298.15 -130000; 6000 N REF14 !


PHASE TA2CO7_TY  %  2 2   7 !
   CONSTITUENT TA2CO7_TY  :TA : CO,CR :  !

 PARAMETER G(TA2CO7_TY,TA:CO;0)          298.15 -309000+66.5*T+7*GHCPCO#
+2*GBCCTA#; 6000 N REF5 !
 PARAMETER G(TA2CO7_TY,TA:CR;0)          298.15 -65730+10*T+7*GHSERCR#
+2*GHSERTA#; 6000 N REF24 !
 PARAMETER G(TA2CO7_TY,TA:CO,CR;0)       298.15 -198285+45*T; 6000 N REF24 !
 PARAMETER G(TA2CO7_TY,TA:CO,CR;1)       298.15 -60000; 6000 N REF24 !

LIST_OF_REFERENCES
NUMBER  SOURCE
 REF2     ' Alan Dinsdale, SGTE Data for Pure Elements, Calphad Vol
         15(1991) p 317-425 and following updates'
 REF8     ' 2002Oikawa Co-Cr'
 REF10    ' 1999Liu Co-Ta'
```

```
 REF13    ' 1993Dupin Cr-Ta'
 REF5     ' SuperCo_6-0'
 REF11    ' 2014Shinagawa Co-Ta'
 REF24    'THIS WORK'
 REF26    '2013STEIN AL-CO'
 REF3     ' PARAM A2 Co,VA o CR,VA'
 REF7     ' 2009Zhou Ni-Ta'
 REF9     ' From AFLOW database'
 REF4     ' 2006Sluiter ab initio elements'
 REF25    '2009PAV REASSESSMENT OF CR-TA'
 REF1     ' FROM SUPERCO DATABASE'
 REF12    ''
 REF6     ' 2013 Hu, Al-Cr'
 REF14    ' after SuperCo_6-0'
!
```

Appendix B The thermodynamic dataset of the Al-Co-Cr-Ni-Y system

```
ELEMENT /-   ELECTRON_GAS              0.0000E+00  0.0000E+00  0.0000E+00!
ELEMENT VA   VACUUM                    0.0000E+00  0.0000E+00  0.0000E+00!
ELEMENT AL   A1                        2.6982E+01  4.5773E+03  2.8322E+01!
ELEMENT CO   A3                        5.8933E+01  0.0000E+00  0.0000E+00!
ELEMENT CR   A2                        5.1996E+01  4.0500E+03  2.3560E+01!
ELEMENT NI   A1                        5.8690E+01  4.7870E+03  2.9796E+01!
ELEMENT Y    A3                        8.8906E+01  0.0000E+00  0.0000E+00!


FUNCTION GHSERAL   298.15 -7976.15+137.093038*T-24.3671976*T*LN(T)
    -.001884662*T**2-8.77664E-07*T**3+74092*T**(-1); 700 Y
     -11276.24+223.048446*T-38.5844296*T*LN(T)+.018531982*T**2
    -5.764227E-06*T**3+74092*T**(-1); 933.47 Y
     -11278.361+188.684136*T-31.748192*T*LN(T)-1.230622E+28*T**(-9); 2900 N
    !
FUNCTION GHSERNI   298.15 -5179.159+117.854*T-22.096*T*LN(T)-.0048407*T**2;
    1728 Y
     -27840.62+279.134977*T-43.1*T*LN(T)+1.12754E+31*T**(-9); 3000 N !
FUNCTION GHSERYY   100 -8011.09379+128.572856*T-25.6656992*T*LN(T)
    -.00175716414*T**2-4.17561786E-07*T**3+26911.509*T**(-1); 1000 Y
     -7179.74574+114.497104*T-23.4941827*T*LN(T)-.0038211802*T**2
    -8.2534534E-08*T**3; 1795.15 Y
     -67480.7761+382.124727*T-56.9527111*T*LN(T)+.00231774379*T**2
    -7.22513088E-08*T**3+18077162.6*T**(-1); 3700 N !
FUNCTION GHSERCR   298.15 -8856.94+157.48*T-26.908*T*LN(T)+.00189435*T**2
    -1.47721E-06*T**3+139250*T**(-1); 2180 Y
     -34869.344+344.18*T-50*T*LN(T)-2.88526E+32*T**(-9); 6000 N !
FUNCTION GHSERCO   298.15 +310.241+133.36601*T-25.0861*T*LN(T)
    -.002654739*T**2-1.7348E-07*T**3+72527*T**(-1); 1768 Y
     -17197.666+253.28374*T-40.5*T*LN(T)+9.3488E+30*T**(-9); 6000 N !
FUNCTION GLIQAL    298.15 +GHSERAL#+11005.045-11.84185*T+7.9337E-20*T**7;
    933.47 Y
     -795.991+177.430209*T-31.748192*T*LN(T); 2900 N !
FUNCTION GLIQCO    298.15 +GHSERCO#+15085.037-8.931932*T-2.19801E-21*T**7;
    1768 Y
     -846.61+243.599944*T-40.5*T*LN(T); 6000 N !
FUNCTION GLIQCR    298.15 +GHSERCR#+24339.955-11.420225*T+2.37615E-21*T**7;
    2180 Y
     -16459.984+335.616316*T-50*T*LN(T); 6000 N !
FUNCTION GLIQNI    298.15 +GHSERNI#+16414.686-9.397*T-3.82318E-21*T**7;
    1728 Y
     -9549.817+268.597977*T-43.1*T*LN(T); 3000 N !
FUNCTION GLIQYY    100 +2098.50738+119.41873*T-24.6467508*T*LN(T)
    -.00347023463*T**2-8.12981167E-07*T**3+23713.7332*T**(-1); 1000 Y
     +7386.44846+19.4520171*T-9.0681627*T*LN(T)-.0189533369*T**2
    +1.7595327E-06*T**3; 1795.15 Y
     -12976.5957+257.400783*T-43.0952*T*LN(T); 3700 N !
FUNCTION GFCCCO    298.15 +GHSERCO#+427.591-.615248*T; 6000 N !
FUNCTION GFCCCR    298.15 +GHSERCR#+7284+.163*T; 6000 N !
FUNCTION GFCCYY    100 +GHSERYY#+6000; 3700 N !
FUNCTION GBCCAL    298.15 +GHSERAL#+10083-4.813*T; 2900 N !
FUNCTION GBCCCO    298.15 +GHSERCO#+2938-.7138*T; 6000 N !
FUNCTION GBCCNI    298.15 +GHSERNI#+8715.084-3.556*T; 3000 N !
```

```
FUNCTION GBCCYY    100 -833.658863+123.667346*T-25.5832578*T*LN(T)
    -.00237175965*T**2+9.10372497E-09*T**3+27340.0687*T**(-1); 1000 Y
     -1297.79829+134.528352*T-27.3038477*T*LN(T)-5.41757644E-04*T**2
    -3.05012175E-07*T**3; 1795.15 Y
     +15389.4975+.981325399*T-8.88296647*T*LN(T)-.00904576576*T**2
    +4.02944768E-07*T**3-2542575.96*T**(-1); 3700 N !
FUNCTION GASCON    298.15 +8.3144621; 6000 N !
FUNCTION B2ALVA    298.15 +10000-T-.2*GASCON#*T; 6000 N !
FUNCTION LB2ALVA   298.15 +150000; 6000 N !
FUNCTION B2NIVA    298.15 +162397.3-27.40575*T-.2*GASCON#*T; 6000 N !
FUNCTION LB2NIVA   298.15 -64024.38+26.49419*T; 6000 N !
FUNCTION B2ALCO    298.15 -138247+29.92*T; 6000 N !
FUNCTION LB2ALCO   298.15 +43040-27.4*T; 6000 N !
FUNCTION LB2ALNI   298.15 -52440.88+11.30117*T; 6000 N !
FUNCTION B2ALNI    298.15 -152397.3+26.40575*T; 6000 N !
FUNCTION GHCPAL    298.15 +GHSERAL#+5481-1.8*T; 2900 N !
FUNCTION GHCPCR    298.15 +GHSERCR#+4438; 6000 N !
FUNCTION GHCPNI    298.15 +GHSERNI#+1046+1.2552*T; 3000 N !
FUNCTION ALCO3     298.15 +3*U1ALCO#; 6000 N !
FUNCTION AL3CO     298.15 +3*U1ALCO#; 6000 N !
FUNCTION AL2CO2    298.15 +4*U1ALCO#; 6000 N !
FUNCTION L04ALCO   298.15 +U3ALCO#; 6000 N !
FUNCTION L14ALCO   298.15 +U4ALCO#; 6000 N !
FUNCTION ALCR3     298.15 +3*U1ALCR#; 6000 N !
FUNCTION AL3CR     298.15 +3*U1ALCR#; 6000 N !
FUNCTION AL2CR2    298.15 +4*U1ALCR#; 6000 N !
FUNCTION L04ALCR   298.15 +U3ALCR#; 6000 N !
FUNCTION L14ALCR   298.15 +U4ALCR#; 6000 N !
FUNCTION ALNI3     298.15 +3*U1ALNI#; 6000 N !
FUNCTION AL3NI     298.15 +3*U1ALNI#; 6000 N !
FUNCTION AL2NI2    298.15 +4*U1ALNI#; 6000 N !
FUNCTION L04ALNI   298.15 +U3ALNI#; 6000 N !
FUNCTION L14ALNI   298.15 +U4ALNI#; 6000 N !
FUNCTION CO3NI     298.15 +3*U1CONI#; 6000 N !
FUNCTION CONI3     298.15 +3*U1CONI#; 6000 N !
FUNCTION CO2NI2    298.15 +4*U1CONI#; 6000 N !
FUNCTION L04CONI   298.15 +U3CONI#; 6000 N !
FUNCTION L14CONI   298.15 +U4CONI#; 6000 N !
FUNCTION CO3CR     298.15 +3*U1COCR#; 6000 N !
FUNCTION COCR3     298.15 +3*U1COCR#; 6000 N !
FUNCTION CO2CR2    298.15 +4*U1COCR#; 6000 N !
FUNCTION L04COCR   298.15 +U3COCR#; 6000 N !
FUNCTION L14COCR   298.15 +U4COCR#; 6000 N !
FUNCTION CRNI3     298.15 +3*U1CRNI#; 6000 N !
FUNCTION CR3NI     298.15 +3*U1CRNI#; 6000 N !
FUNCTION CR2NI2    298.15 +4*U1CRNI#; 6000 N !
FUNCTION L04CRNI   298.15 +U3CRNI#; 6000 N !
FUNCTION L14CRNI   298.15 +U4CRNI#; 6000 N !
FUNCTION ALCO2CR   298.15 +2*U1ALCO#+U1ALCR#+2*U1COCR#+U2ALCOCR#; 6000 N !
FUNCTION AL2COCR   298.15 +2*U1ALCO#+2*U1ALCR#+U1COCR#+U3ALCOCR#; 6000 N !
FUNCTION ALCOCR2   298.15 +U1ALCO#+2*U1ALCR#+2*U1COCR#+U1ALCOCR#; 6000 N !
FUNCTION ALCO2NI   298.15 +2*U1ALCO#+U1ALNI#+2*U1CONI#+U2ALCONI#; 6000 N !
FUNCTION AL2CONI   298.15 +2*U1ALCO#+2*U1ALNI#+U1CONI#+U3ALCONI#; 6000 N !
FUNCTION ALCONI2   298.15 +U1ALCO#+2*U1ALNI#+2*U1CONI#+U1ALCONI#; 6000 N !
FUNCTION COCRNI2   298.15 +U1COCR#+2*U1CONI#+2*U1CRNI#+U1COCRNI#; 6000 N !
FUNCTION COCR2NI   298.15 +2*U1COCR#+U1CONI#+2*U1CRNI#+U2COCRNI#; 6000 N !
FUNCTION CO2CRNI   298.15 +2*U1COCR#+2*U1CONI#+U1CRNI#+U3COCRNI#; 6000 N !
```

```
FUNCTION U1ALNI    298.15 -14808.67+2.93067*T; 6000 N !
FUNCTION U1CRNI    298.15 -1510; 6000 N !
FUNCTION ALCR2NI   298.15 +2*U1ALCR#+2*U1CRNI#+U1ALNI#; 3000 N !
FUNCTION AL2CRNI   298.15 +2*U1ALCR#+2*U1ALNI#+U1CRNI#; 3000 N !
FUNCTION U1ALCR    298.15 -630; 6000 N !
FUNCTION ALCRNI2   298.15 +U1ALCR#+2*U1ALNI#+2*U1CRNI#+6650; 3000 N !
FUNCTION ALCOCRNI  298.15 +U1ALCO#+U1ALCR#+U1ALNI#+U1COCR#+U1CONI#+U1CRNI#;
    6000 N !
FUNCTION UBALCO    298.15 +.125*B2ALCO#-.125*LB2ALCO#; 6000 N !
FUNCTION GB2CONI   298.15 -7874; 6000 N !
FUNCTION GB2COCR   298.15 -11000+5*T; 6000 N !
FUNCTION GB2ALY    298.15 -8000; 6000 N !
FUNCTION GB2COY    298.15 -8000; 6000 N !
FUNCTION BCOCRMAL  298.15 -22138; 6000 N !
FUNCTION BALCOMCR  298.15 -73790; 6000 N !
FUNCTION GCONICR   298.18 +0.0; 6000 N !
FUNCTION GSIGMAAL  298.15 +6500+GHSERAL#; 6000 N !
FUNCTION GSIGMACO  298.15 +4700+.25*T+GFCCCO#; 6000 N !
FUNCTION GSIGMANI  298.15 +16600+GHSERNI#; 6000 N !
FUNCTION GSIGMACR  298.15 +13200+GHSERCR#; 6000 N !
FUNCTION GC15AL    298.15 +15100+GHSERAL#; 6000 N !
FUNCTION GC15YY    298.15 +24430+GHSERYY#; 6000 N !
FUNCTION GC15CO    298.15 +19600+GHSERCO#; 6000 N !
FUNCTION GC15NI    298.15 +21300+GHSERNI#; 6000 N !
FUNCTION U3ALCO    298.15 +0.0; 6000 N !
FUNCTION U4ALCO    298.15 +2903; 6000 N !
FUNCTION U1ALCO    298.15 -5200; 6000 N !
FUNCTION U3ALCR    298.15 +0.0; 6000 N !
FUNCTION U4ALCR    298.15 +0.0; 6000 N !
FUNCTION U3ALNI    298.15 +0.0; 6000 N !
FUNCTION U4ALNI    298.15 +7203.60609-3.7427303*T; 6000 N !
FUNCTION U3CONI    298.15 +0.0; 6000 N !
FUNCTION U4CONI    298.15 +0.0; 6000 N !
FUNCTION U1CONI    298.15 -1323.6+3.06*T; 6000 N !
FUNCTION U3COCR    298.15 +0.0; 6000 N !
FUNCTION U4COCR    298.15 +0.0; 6000 N !
FUNCTION U1COCR    298.15 -4616+9.2*T; 6000 N !
FUNCTION U3CRNI    298.15 +0.0; 6000 N !
FUNCTION U4CRNI    298.15 +0.0; 6000 N !
FUNCTION U1ALCOCR  298.15 +0.0; 6000 N !
FUNCTION U2ALCOCR  298.15 +0.0; 6000 N !
FUNCTION U3ALCOCR  298.15 +0.0; 6000 N !
FUNCTION U1ALCONI  298.15 +0.0; 6000 N !
FUNCTION U2ALCONI  298.15 +0.0; 6000 N !
FUNCTION U3ALCONI  298.15 +0.0; 6000 N !
FUNCTION U1COCRNI  298.15 +0.0; 6000 N !
FUNCTION U2COCRNI  298.15 +0.0; 6000 N !
FUNCTION U3COCRNI  298.15 +0.0; 6000 N !
FUNCTION UN_ASS 298.15 +0; 300 N !

TYPE_DEFINITION % SEQ *!
DEFINE_SYSTEM_DEFAULT ELEMENT 2 !
DEFAULT_COMMAND DEF_SYS_ELEMENT VA /- !


TYPE_DEFINITION & GES A_P_D A1 MAGNETIC  -3.0    2.80000E-01 !
PHASE A1  %&  1  1.0  !
```

```
  CONSTITUENT A1  :AL,CO,CR,NI,Y :  !

 PARAMETER G(A1,AL;0)                    298.15 +GHSERAL#; 6000 N REF28 !
 PARAMETER G(A1,CO;0)                    298.15 +GFCCCO#; 6000 N REF23 !
 PARAMETER TC(A1,CO;0)                   298.15 +1396; 6000 N REF23 !
 PARAMETER BMAGN(A1,CO;0)                298.15 +1.35; 6000 N REF23 !
 PARAMETER G(A1,CR;0)                    298.15 +GFCCCR#; 6000 N REF27 !
 PARAMETER TC(A1,CR;0)                   298.15 -1109; 6000 N REF27 !
 PARAMETER BMAGN(A1,CR;0)                298.15 -2.46; 6000 N REF27 !
 PARAMETER G(A1,NI;0)                    298.15 +GHSERNI#; 3000 N REF29 !
 PARAMETER TC(A1,NI;0)                   298.15 +633; 3000 N REF27 !
 PARAMETER BMAGN(A1,NI;0)                298.15 +.52; 3000 N REF27 !
 PARAMETER G(A1,Y;0)                     100 +GFCCYY#; 3700 N REF30 !
 PARAMETER G(A1,AL,CO;0)                 298.15 -124200+17.24*T; 6000 N
REF4 !
 PARAMETER G(A1,AL,CO;2)                 298.15 +28740; 6000 N REF4 !
 PARAMETER TC(A1,AL,CO;0)                298.15 -1500; 6000 N REF4 !
 PARAMETER TC(A1,AL,CO;1)                298.15 +650; 6000 N REF4 !
 PARAMETER BMAGN(A1,AL,CO;0)             298.15 +10; 6000 N REF4 !
 PARAMETER G(A1,AL,CO,CR;0)              298.15 +10000; 3000 N REF1 !
 PARAMETER G(A1,AL,CO,CR;1)              298.15 +10000; 3000 N REF1 !
 PARAMETER G(A1,AL,CO,CR;2)              298.15 +10000; 3000 N REF1 !
 PARAMETER G(A1,AL,CO,NI;0)              298.15 +20560-9.113*T; 6000 N REF1 !
 PARAMETER G(A1,AL,CO,NI;1)              298.15 -25000; 6000 N REF1 !
 PARAMETER G(A1,AL,CO,NI;2)              298.15 -22000; 6000 N REF1 !
 PARAMETER G(A1,AL,CR;0)                 298.15 -42491.57; 6000 N REF3 !
 PARAMETER G(A1,AL,CR,NI;0)              298.15 -4845+15*T; 6000 N REF1 !
 PARAMETER G(A1,AL,CR,NI;1)              298.15 -4845+15*T; 6000 N REF1 !
 PARAMETER G(A1,AL,CR,NI;2)              298.15 -4845+15*T; 6000 N REF1 !
 PARAMETER TC(A1,AL,NI;0)                298.15 -1112; 6000 N REF11 !
 PARAMETER TC(A1,AL,NI;1)                298.15 +1745; 6000 N REF11 !
 PARAMETER G(A1,AL,NI;0)                 298.15 -162407.75+16.212965*T;
6000 N REF11 !
 PARAMETER G(A1,AL,NI;1)                 298.15 +73417.798-34.914168*T;
6000 N REF11 !
 PARAMETER G(A1,AL,NI;2)                 298.15 +33471.014-9.8373558*T;
6000 N REF11 !
 PARAMETER G(A1,AL,NI;3)                 298.15 -30758.01+10.25267*T; 6000
N REF11 !
 PARAMETER G(A1,CO,CR;0)                 298.15 -24052.09+8.1884*T; 6000 N
REF22 !
 PARAMETER G(A1,CO,CR;1)                 298.15 +5331.8252-6.9059*T; 6000 N
REF22 !
 PARAMETER TC(A1,CO,CR;0)                298.15 -9392.5259; 6000 N REF22 !
 PARAMETER TC(A1,CO,CR;1)                298.15 +8383.0424; 6000 N REF22 !
 PARAMETER G(A1,CO,CR,NI;0)              298.15 -55000; 6000 N REF1 !
 PARAMETER G(A1,CO,CR,NI;1)              298.15 -10000; 6000 N REF1 !
 PARAMETER G(A1,CO,CR,NI;2)              298.15 -30000; 6000 N REF1 !
 PARAMETER G(A1,CO,NI;0)                 298.15 -800+1.2629*T; 6000 N REF19 !
 PARAMETER TC(A1,CO,NI;0)                298.15 +411; 6000 N REF19 !
 PARAMETER TC(A1,CO,NI;1)                298.15 -99; 6000 N REF19 !
 PARAMETER BMAGN(A1,CO,NI;0)             298.15 +1.046; 6000 N REF19 !
 PARAMETER BMAGN(A1,CO,NI;1)             298.15 +.165; 6000 N REF19 !
 PARAMETER G(A1,CR,NI;0)                 298.15 +8347-12.1038*T; 6000 N
REF20 !
 PARAMETER G(A1,CR,NI;1)                 298.15 +29895-16.3838*T; 6000 N
REF20 !
```

```
  PARAMETER TC(A1,CR,NI;0)                298.15 -3605; 6000 N REF20 !
  PARAMETER G(A1,CR,Y;0)                  298.15 +10000; 6000 N REF1 !


TYPE_DEFINITION ' GES A_P_D A2 MAGNETIC  -1.0    4.00000E-01 !
PHASE A2  %'  1  1.0  !
   CONSTITUENT A2  :AL,CO,CR,NI,VA,Y :  !

  PARAMETER G(A2,AL;0)                    298.15 +GBCCAL#; 2900 N REF27 !
  PARAMETER G(A2,CO;0)                    298.15 +GBCCCO#; 6000 N REF27 !
  PARAMETER TC(A2,CO;0)                   298.15 +1450; 6000 N REF27 !
  PARAMETER BMAGN(A2,CO;0)                298.15 +1.35; 6000 N REF27 !
  PARAMETER G(A2,CR;0)                    298.15 +GHSERCR#; 6000 N REF28 !
  PARAMETER TC(A2,CR;0)                   298.15 -311.5; 6000 N REF27 !
  PARAMETER BMAGN(A2,CR;0)                298.15 -.008; 6000 N REF27 !
  PARAMETER G(A2,NI;0)                    298.15 +GBCCNI#; 6000 N REF29 !
  PARAMETER TC(A2,NI;0)                   298.15 +575; 6000 N REF27 !
  PARAMETER BMAGN(A2,NI;0)                298.15 +.85; 6000 N REF27 !
  PARAMETER G(A2,VA;0)                    298.15 +.2*GASCON#*T; 6000 N REF18 !
  PARAMETER G(A2,Y;0)                     100 +GBCCYY#; 3700 N REF27 !
  PARAMETER G(A2,AL,VA;0)                 298.15 +B2ALVA#+LB2ALVA#; 2900 N
 REF14 !
  PARAMETER G(A2,AL,CO;0)                 298.15 +B2ALCO#+LB2ALCO#; 6000 N
 REF4 !
  PARAMETER G(A2,AL,CO,CR;0)              298.15 +32453-25*T; 6000 N REF1 !
  PARAMETER G(A2,AL,CO,CR;1)              298.15 +5000; 6000 N REF1 !
  PARAMETER G(A2,AL,CO,CR;2)              298.15 +54000-20*T; 6000 N REF1 !
  PARAMETER G(A2,AL,CR;0)                 298.15 -52970.7-10.836*T; 3000 N
 REF3 !
  PARAMETER G(A2,AL,CR;1)                 298.15 -3655.89; 3000 N REF3 !
  PARAMETER G(A2,AL,CR,NI;0)              298.15 +80000; 3000 N REF1 !
  PARAMETER G(A2,AL,CR,NI;1)              298.15 +120000; 3000 N REF1 !
  PARAMETER G(A2,AL,CR,NI;2)              298.15 +61500; 3000 N REF1 !
  PARAMETER G(A2,AL,NI;0)                 298.15 +B2ALNI#+LB2ALNI#; 6000 N
 REF14 !
  PARAMETER G(A2,CO,VA;0)                 298.15 +126184-.2*GASCON#*T; 6000
 N REF4 !
  PARAMETER G(A2,CO,CR;0)                 298.15 +1033.2829-1.4808*T; 6000 N
 REF22 !
  PARAMETER G(A2,CO,CR;1)                 298.15 +11971.5008-13.3741*T; 6000
 N REF22 !
  PARAMETER G(A2,CO,CR,NI;0)              298.15 -55000; 6000 N REF1 !
  PARAMETER G(A2,CO,CR,NI;1)              298.15 -42000; 6000 N REF1 !
  PARAMETER G(A2,CO,CR,NI;2)              298.15 -20000; 6000 N REF1 !
  PARAMETER G(A2,CO,NI;0)                 298.15 +2000; 6000 N REF19 !
  PARAMETER TC(A2,CO,NI;0)                298.15 +556; 6000 N REF19 !
  PARAMETER TC(A2,CO,NI;1)                298.15 -288; 6000 N REF19 !
  PARAMETER BMAGN(A2,CO,NI;0)             298.15 +.474; 6000 N REF19 !
  PARAMETER G(A2,CR,VA;0)                 298.15 +145683-.2*GASCON#*T; 2900
 N REF1 !
  PARAMETER G(A2,CR,NI;0)                 298.15 +21310-13.6585*T; 6000 N
 REF20 !
  PARAMETER G(A2,CR,NI;1)                 298.15 +25800-7.8927*T; 6000 N
 REF20 !
  PARAMETER TC(A2,CR,NI;0)                298.15 +2373; 6000 N REF20 !
  PARAMETER TC(A2,CR,NI;1)                298.15 +617; 6000 N REF20 !
  PARAMETER BMAGN(A2,CR,NI;0)             298.15 +4; 6000 N REF20 !
```

```
  PARAMETER G(A2,CR,Y;0)                  298.15 +69000; 6000 N REF1 !
  PARAMETER G(A2,CR,Y;1)                  298.15 +10000; 6000 N REF1 !
  PARAMETER G(A2,NI,VA;0)                 298.15 +B2NIVA#+LB2NIVA#; 2900 N
 REF14 !
  PARAMETER G(A2,VA,Y;0)                  298.15 +130000-.2*GASCON#*T; 2900
 N REF1 !


TYPE_DEFINITION ( GES A_P_D A3 MAGNETIC  -3.0    2.80000E-01 !
PHASE A3  %(  2 1   .5 !
   CONSTITUENT A3  :AL,CO,CR,NI,Y : VA :  !

  PARAMETER G(A3,AL:VA;0)                 298.15 +GHCPAL#; 2900 N REF27 !
  PARAMETER G(A3,CO:VA;0)                 298.15 +GHSERCO#; 6000 N REF28 !
  PARAMETER TC(A3,CO:VA;0)                298.15 +1396; 6000 N REF27 !
  PARAMETER BMAGN(A3,CO:VA;0)             298.15 +1.35; 6000 N REF27 !
  PARAMETER G(A3,CR:VA;0)                 298.15 +GHCPCR#; 6000 N REF27 !
  PARAMETER TC(A3,CR:VA;0)                298.15 -1109; 6000 N REF27 !
  PARAMETER BMAGN(A3,CR:VA;0)             298.15 -2.46; 6000 N REF27 !
  PARAMETER G(A3,NI:VA;0)                 298.15 +GHCPNI#; 3000 N REF29 !
  PARAMETER TC(A3,NI:VA;0)                298.15 +633; 3000 N REF27 !
  PARAMETER BMAGN(A3,NI:VA;0)             298.15 +.52; 3000 N REF27 !
  PARAMETER G(A3,Y:VA;0)                  100 +GHSERYY#; 3700 N REF27 !
  PARAMETER G(A3,CO,CR:VA;0)              298.15 -28763.6824+15.5105*T; 6000
 N REF22 !
  PARAMETER G(A3,CO,CR:VA;1)              298.15 +12673.5606-14.8392*T; 6000
 N REF22 !
  PARAMETER TC(A3,CO,CR:VA;0)             298.15 -5828.677; 6000 N REF22 !
  PARAMETER TC(A3,CO,CR:VA;1)             298.15 +4873.9533; 6000 N REF22 !
  PARAMETER G(A3,CO,CR,NI:VA;0)           298.15 -30000; 6000 N REF1 !
  PARAMETER G(A3,CO,CR,NI:VA;1)           298.15 -74393.6; 6000 N REF1 !
  PARAMETER G(A3,CO,CR,NI:VA;2)           298.15 -40000; 6000 N REF1 !
  PARAMETER G(A3,CO,NI:VA;0)              298.15 -1620-.385*T; 6000 N REF19 !
  PARAMETER TC(A3,CO,NI:VA;0)             298.15 +411; 6000 N REF19 !
  PARAMETER TC(A3,CO,NI:VA;1)             298.15 -99; 6000 N REF19 !
  PARAMETER BMAGN(A3,CO,NI:VA;0)          298.15 +1.046; 6000 N REF19 !
  PARAMETER BMAGN(A3,CO,NI:VA;1)          298.15 +.165; 6000 N REF19 !
  PARAMETER G(A3,CR,NI:VA;0)              298.15 +8374; 6000 N REF20 !
  PARAMETER G(A3,CR,NI:VA;1)              298.15 +10000; 6000 N REF20 !
  PARAMETER G(A3,CR,Y:VA;0)               298.15 +63000; 6000 N REF9 !


PHASE AAL3Y  %  2 3   1 !
   CONSTITUENT AAL3Y  :AL : Y :  !

  PARAMETER G(AAL3Y,AL:Y;0)               298.15 -197645.6+21.16384*T
 +3*GHSERAL#+GHSERYY#; 6000 N REF6 !


PHASE AL11CR4  %  2 4   11 !
   CONSTITUENT AL11CR4  :CR : AL :  !

  PARAMETER G(AL11CR4,CR:AL;0)            298.15 +11*GHSERAL#+4*GHSERCR#
 -292000; 6000 N REF1 !


PHASE AL13CO4  %  2 13   4 !
```

```
   CONSTITUENT AL13CO4  :AL : CO,NI :  !

  PARAMETER G(AL13CO4,AL:CO;0)            298.15 -659420.5+124.5*T
 +13*GHSERAL#+4*GHSERCO#; 6000 N REF1 !
  PARAMETER G(AL13CO4,AL:NI;0)            298.15 -565000+10*T+13*GHSERAL#
 +4*GHSERNI#; 6000 N REF1 !
  PARAMETER G(AL13CO4,AL:CO,NI;0)         298.15 -19000; 6000 N REF1 !

 PHASE AL2OCR2Y %  4  18 2 1 2!
   CONSTITUENT AL2OCR2Y  :AL:CR:Y:AL,CR:  !
  PARAM G(AL2OCR2Y,AL:CR:Y:AL;0)  298.15 -383000+20*GHSERAL
                +2*GHSERCR+GHSERYY; 6000 N REF1 !
  PARAM G(AL2OCR2Y,AL:CR:Y:CR;0)  298.15 -503000+18*GHSERAL
                +4*GHSERCR+GHSERYY; 6000 N REF1 !
  PARAM G(AL2OCR2Y,AL:CR:Y:AL,CR;0)  298.15 -44000; 6000 N REF1 !

PHASE AL23NI6Y4  %  3 23   6   4 !
   CONSTITUENT AL23NI6Y4  :AL : NI : Y :  !
  PARAMETER G(AL23NI6Y4,AL:NI:Y;0)        298.15 -1669800+23*GHSERAL#
 +6*GHSERNI#+4*GHSERYY#; 6000 N REF1 !

PHASE AL2NI6Y3  %  3 2   6   3 !
   CONSTITUENT AL2NI6Y3  :AL : NI : Y :  !

  PARAMETER G(AL2NI6Y3,AL:NI:Y;0)         298.15 -520000+2*GHSERAL#
 +6*GHSERNI#+3*GHSERYY#; 6000 N REF1 !

PHASE AL2NIY  %  3 2   1   1 !
   CONSTITUENT AL2NIY  :AL : NI : Y :  !

  PARAMETER G(AL2NIY,AL:NI:Y;0)           298.15 -240000+2*GHSERAL#+GHSERNI#
 +GHSERYY#; 6000 N REF1 !

PHASE AL2Y3  %  2 2   3 !
   CONSTITUENT AL2Y3  :AL : Y :  !

  PARAMETER G(AL2Y3,AL:Y;0)               298.15 -242031.5+24.1472*T
 +2*GHSERAL#+3*GHSERYY#; 6000 N REF6 !

PHASE AL3CO1  %  2 3   1 !
   CONSTITUENT AL3CO1  :AL : CO,NI :  !

  PARAMETER G(AL3CO1,AL:CO;0)             298.15 -164946+32.725*T+3*GHSERAL#
 +GHSERCO#; 6000 N REF4 !
  PARAMETER G(AL3CO1,AL:NI;0)             298.15 -142300+17.803*T+3*GHSERAL#
 +GHSERNI#; 6000 N REF1 !
  PARAMETER G(AL3CO1,AL:CO,NI;0)          298.15 -26000; 6000 N REF1 !

PHASE AL3NI1  %  2 3   1 !
   CONSTITUENT AL3NI1  :AL : CO,NI :  !

  PARAMETER G(AL3NI1,AL:CO;0)             298.15 -143924+18*T+3*GHSERAL#
 +GHSERCO#; 6000 N REF1 !
  PARAMETER G(AL3NI1,AL:NI;0)             298.15 -193934.92+49.19652*T
 +3*GHSERAL#+GHSERNI#; 6000 N REF11 !
  PARAMETER G(AL3NI1,AL:CO,NI;0)          298.15 -29200+7*T; 6000 N REF1 !
```

```
PHASE AL3NI2  %  3 3   2   1 !
   CONSTITUENT AL3NI2  :AL : AL,CO,CR,NI% : CO,NI,VA% :  !

  PARAMETER G(AL3NI2,AL:AL:CO;0)          298.15 +5*GBCCAL#+GBCCCO#; 6000 N
 REF1 !
  PARAMETER G(AL3NI2,AL:CO:CO;0)          298.15 +3*GBCCAL#+3*GBCCCO#; 6000
 N REF1 !
  PARAMETER G(AL3NI2,AL:CR:CO;0)          298.15 +3*GBCCAL#+2*GHSERCR#
 +GBCCCO#; 6000 N REF1 !
  PARAMETER G(AL3NI2,AL:NI:CO;0)          298.15 +3*GBCCAL#+2*GBCCNI#
 +GBCCCO#; 6000 N REF1 !
  PARAMETER G(AL3NI2,AL:AL:NI;0)          298.15 +5*GBCCAL#+GBCCNI#
 -39465.978+7.89525*T; 3000 N REF10 !
  PARAMETER G(AL3NI2,AL:CO:NI;0)          298.15 -250000+3*GBCCAL#+2*GBCCCO#
 +GBCCNI#; 6000 N REF1 !
  PARAMETER G(AL3NI2,AL:CR:NI;0)          298.15 +3*GBCCAL#+2*GHSERCR#
 +GBCCNI#; 3000 N REF1 !
  PARAMETER G(AL3NI2,AL:NI:NI;0)          298.15 +3*GBCCAL#+3*GBCCNI#
 -427191.9+79.21725*T; 3000 N REF10 !
  PARAMETER G(AL3NI2,AL:AL:VA;0)          298.15 +5*GBCCAL#+30000-3*T; 3000
 N REF10 !
  PARAMETER G(AL3NI2,AL:CO:VA;0)          298.15 -268535+85*T+3*GBCCAL#
 +2*GBCCCO#; 6000 N REF1 !
  PARAMETER G(AL3NI2,AL:CR:VA;0)          298.15 +3*GBCCAL#+2*GHSERCR#
 -160000+120*T; 3000 N REF1 !
  PARAMETER G(AL3NI2,AL:NI:VA;0)          298.15 +3*GBCCAL#+2*GBCCNI#
 -357725.92+68.322*T; 3000 N REF10 !
  PARAMETER G(AL3NI2,AL:CO,NI:VA;0)       298.15 -158428+86*T; 6000 N REF1 !
  PARAMETER G(AL3NI2,AL:CR,NI:VA;0)       298.15 -80000+30*T; 3000 N REF1 !
  PARAMETER G(AL3NI2,AL:AL,NI:*;0)        298.15 -193484.18+131.79*T; 3000 N
 REF10 !
  PARAMETER G(AL3NI2,AL:*:NI,VA;0)        298.15 -22001.7+7.0332*T; 3000 N
 REF10 !

PHASE AL3NI2Y  %  3 3   2   1 !
   CONSTITUENT AL3NI2Y  :AL : NI : Y :  !
  PARAMETER G(AL3NI2Y,AL:NI:Y;0)          298.15 -360000+3*GHSERAL#
 +2*GHSERNI#+GHSERYY#; 6000 N REF1 !

PHASE AL3NI5  %  2 .375   .625 !
   CONSTITUENT AL3NI5  :AL : NI :  !
  PARAMETER G(AL3NI5,AL:NI;0)             298.15 +.375*GHSERAL#
 +.625*GHSERNI#-55507.7594+7.2648103*T; 6000 N REF11 !

PHASE AL3NIY  %  3 3   1   1 !
   CONSTITUENT AL3NIY  :AL : NI : Y :  !
  PARAMETER G(AL3NIY,AL:NI:Y;0)           298.15 -321390+30*T+3*GHSERAL#
 +GHSERNI#+GHSERYY#; 6000 N REF1 !

PHASE AL45CR7  %  2 45   7 !
   CONSTITUENT AL45CR7  :AL : CR,NI :  !
  PARAMETER G(AL45CR7,AL:CR;0)            298.15 +45*GHSERAL#+7*GHSERCR#
 -671997.04+49.8576*T; 6000 N REF3 !
  PARAMETER G(AL45CR7,AL:NI;0)            298.15 +45*GHSERAL#+7*GHSERNI#
 -900000+120*T; 6000 N REF1 !
  PARAMETER G(AL45CR7,AL:CR,NI;0)         298.15 -210000; 6000 N REF1 !
```

```
PHASE AL4CR  %  2 1   4 !
   CONSTITUENT AL4CR  :CR : AL,VA :  !
  PARAMETER G(AL4CR,CR:AL;0)             298.15 +4*GHSERAL#+GHSERCR#
 -84930.41+3.892*T; 6000 N REF3 !
  PARAMETER G(AL4CR,CR:VA;0)             298.15 +25000+GHSERCR#; 6000 N
 REF3 !
  PARAMETER G(AL4CR,CR:AL,VA;0)          298.15 +28225.77; 6000 N REF3 !

PHASE AL4NI3  %  2 4   3 !
   CONSTITUENT AL4NI3  :AL : CO,NI :  !
  PARAMETER G(AL4NI3,AL:CO;0)            298.15 -400020+110*T+4*GHSERAL#
 +3*GHSERCO#; 3000 N REF1 !
  PARAMETER G(AL4NI3,AL:NI;0)            298.15 +4*GHSERAL#+3*GHSERNI#
 -455326+74*T; 3000 N REF1 !
  PARAMETER G(AL4NI3,AL:CO,NI;0)         298.15 -119050+50*T; 3000 N REF1 !
  PARAMETER G(AL4NI3,AL:CO,NI;1)         298.15 -36000; 3000 N REF1 !

PHASE AL4NIY  %  3 4   1   1 !
   CONSTITUENT AL4NIY  :AL : NI : Y :  !
  PARAMETER G(AL4NIY,AL:NI:Y;0)          298.15 -348095+15*T+4*GHSERAL#
 +GHSERNI#+GHSERYY#; 6000 N REF1 !

PHASE AL5CO2  %  2 5   2 !
   CONSTITUENT AL5CO2  :AL : CO,NI :  !
  PARAMETER G(AL5CO2,AL:CO;0)            298.15 -329990+73.45*T+5*GHSERAL#
 +2*GHSERCO#; 6000 N REF4 !
  PARAMETER G(AL5CO2,AL:NI;0)            298.15 -282419+22.88*T+5*GHSERAL#
 +2*GHSERNI#; 6000 N REF1 !
  PARAMETER G(AL5CO2,AL:CO,NI;0)         298.15 -70002+32*T; 6000 N REF1 !
  PARAMETER G(AL5CO2,AL:CO,NI;1)         298.15 -30325+25*T; 6000 N REF1 !

PHASE AL5CR  %  2 5   1 !
   CONSTITUENT AL5CR  :AL : CR :  !
  PARAMETER G(AL5CR,AL:CR;0)             298.15 +5*GHSERAL#+GHSERCR#
 -91003.14+4.5348*T; 6000 N REF3 !

PHASE AL7NI3Y2  %  3 7   3   2 !
   CONSTITUENT AL7NI3Y2  :AL : NI : Y :  !
  PARAMETER G(AL7NI3Y2,AL:NI:Y;0)        298.15 -699000+7*GHSERAL#
 +3*GHSERNI#+2*GHSERYY#; 6000 N REF1 !

PHASE AL8CR4Y  %  3 8   4   1 !
   CONSTITUENT AL8CR4Y  :AL : CR : Y :  !
  PARAMETER G(AL8CR4Y,AL:CR:Y;0)         298.15 -440000+8*GHSERAL#
 +4*GHSERCR#+GHSERYY#; 6000 N REF1 !

PHASE AL8CRY  %  3 8   1   1 !
   CONSTITUENT AL8CRY  :AL : CR : Y :  !
  PARAMETER G(AL8CRY,AL:CR:Y;0)          298.15 -282500+8*GHSERAL#+GHSERCR#
 +GHSERYY#; 6000 N REF1 !

PHASE AL9CO2  %  2 9   2 !
   CONSTITUENT AL9CO2  :AL : CO,NI :  !
  PARAMETER G(AL9CO2,AL:CO;0)            298.15 -329830+53.14*T+9*GHSERAL#
 +2*GHSERCO#; 6000 N REF1 !
  PARAMETER G(AL9CO2,AL:NI;0)            298.15 -314521+27*T+9*GHSERAL#
```

```
 +2*GHSERNI#; 6000 N REF1 !
  PARAMETER G(AL9CO2,AL:CO,NI;0)          298.15 -36321+15.5*T; 6000 N REF1 !
  PARAMETER G(AL9CO2,AL:CO,NI;1)          298.15 -95414+70*T; 6000 N REF1 !

 PHASE AL9NI3Y  %  3 9   3   1 !
    CONSTITUENT AL9NI3Y  :AL : NI : Y :  !
  PARAMETER G(AL9NI3Y,AL:NI:Y;0)          298.15 -666190+30*T+9*GHSERAL#
 +3*GHSERNI#+GHSERYY#; 6000 N REF1 !

 PHASE ALCR2  %  2 1   2 !
    CONSTITUENT ALCR2  :AL,CR : AL,CR :  !
  PARAMETER G(ALCR2,AL:AL;0)              298.15 +10000+3*GHSERAL#; 6000 N
 REF3 !
  PARAMETER G(ALCR2,CR:AL;0)              298.15 +GHSERCR#+2*GHSERAL#
 +56515.3161+16.836*T; 6000 N REF3 !
  PARAMETER G(ALCR2,AL:CR;0)              298.15 +GHSERAL#+2*GHSERCR#
 -36515.316-16.836*T; 6000 N REF3 !
  PARAMETER G(ALCR2,CR:CR;0)              298.15 +10000+3*GHSERCR#; 6000 N
 REF3 !
  PARAMETER G(ALCR2,*:AL,CR;0)            298.15 -47773.242; 6000 N REF3 !
  PARAMETER G(ALCR2,AL,CR:*;0)            298.15 -11851.395; 6000 N REF3 !

 PHASE ALNI2Y2  %  3 1   2   2 !
    CONSTITUENT ALNI2Y2  :AL : NI : Y :  !
  PARAMETER G(ALNI2Y2,AL:NI:Y;0)          298.15 -240000+GHSERAL#+2*GHSERNI#
 +2*GHSERYY#; 6000 N REF1 !

 PHASE ALNI3Y2  %  3 1   3   2 !
    CONSTITUENT ALNI3Y2  :AL : NI : Y :  !
  PARAMETER G(ALNI3Y2,AL:NI:Y;0)          298.15 -275000+GHSERAL#+3*GHSERNI#
 +2*GHSERYY#; 6000 N REF1 !

 PHASE ALNI8Y3  %  3 1   8   3 !
    CONSTITUENT ALNI8Y3  :AL : NI : Y :  !

  PARAMETER G(ALNI8Y3,AL:NI:Y;0)          298.15 -456000+GHSERAL#+8*GHSERNI#
 +3*GHSERYY#; 6000 N REF1 !

 PHASE ALNIY  %  3 1   1   1 !
    CONSTITUENT ALNIY  :AL : NI : Y :  !

  PARAMETER G(ALNIY,AL:NI:Y;0)            298.15 -185095+15*T+GHSERAL#
 +GHSERNI#+GHSERYY#; 6000 N REF1 !

 PHASE ALY2  %  2 1   2 !
    CONSTITUENT ALY2  :AL : Y :  !

  PARAMETER G(ALY2,AL:Y;0)                298.15 -134659.8+22.18698*T
 +GHSERAL#+2*GHSERYY#; 6000 N REF6 !

$ THIS PHASE HAS A DISORDERED CONTRIBUTION FROM A2
 TYPE_DEFINITION ) GES AMEND_PHASE_DESCRIPTION B2 DIS_PART A2,,,!
 PHASE B2  %)  2 .5   .5 !
    CONSTITUENT B2  :AL,CO,CR,NI,VA,Y : AL,CO,CR,NI,VA,Y :  !
       PARA G(B2,AL:AL;0) 298.15 +0; 6000 N!
   PARAMETER G(B2,CO:AL;0)                298.15 +4*UBALCO#; 6000 N REF4 !
   PARAMETER TC(B2,CO:AL;0)               298.15 -1400; 6000 N REF4 !
```

```
 PARAMETER G(B2,CR:AL;0)                298.15 -4000; 6000 N REF1 !
 PARAMETER G(B2,NI:AL;0)                298.15 +.5*B2ALNI#-.5*LB2ALNI#;
6000 N REF14 !
 PARAMETER G(B2,VA:AL;0)                298.15 +.5*B2ALVA#-.5*LB2ALVA#;
6000 N REF10 !
 PARAMETER G(B2,Y:AL;0)                 298.15 +.5*GB2ALY#; 6000 N REF1 !
 PARAMETER G(B2,AL:CO;0)                298.15 +4*UBALCO#; 6000 N REF4 !
 PARAMETER TC(B2,AL:CO;0)               298.15 -1400; 6000 N REF4 !
     PARA G(B2,CO:CO;0) 298.15 +0; 6000 N!
 PARAMETER G(B2,CR:CO;0)                298.15 +.5*GB2COCR#; 6000 N REF16 !
 PARAMETER G(B2,NI:CO;0)                298.15 +.5*GB2CONI#; 6000 N REF1 !
     PARA G(B2,VA:CO;0) 298.15 +0; 6000 N!
 PARAMETER G(B2,Y:CO;0)                 298.15 +.5*GB2COY#; 6000 N REF1 !
 PARAMETER G(B2,AL:CR;0)                298.15 -4000; 6000 N REF1 !
 PARAMETER G(B2,CO:CR;0)                298.15 +.5*GB2COCR#; 6000 N REF16 !
     PARA G(B2,CR:CR;0) 298.15 +0; 6000 N!
 PARAMETER G(B2,NI:CR;0)                298.15 +1000; 6000 N REF1 !
     PARA G(B2,VA:CR;0) 298.15 +0; 6000 N!
     PARA G(B2,Y:CR;0) 298.15 +0; 6000 N!
 PARAMETER G(B2,AL:NI;0)                298.15 +.5*B2ALNI#-.5*LB2ALNI#;
6000 N REF14 !
 PARAMETER G(B2,CO:NI;0)                298.15 +.5*GB2CONI#; 6000 N REF1 !
 PARAMETER G(B2,CR:NI;0)                298.15 +1000; 6000 N REF1 !
     PARA G(B2,NI:NI;0) 298.15 +0; 6000 N!
 PARAMETER G(B2,VA:NI;0)                298.15 +.5*B2NIVA#-.5*LB2NIVA#;
6000 N REF10 !
     PARA G(B2,Y:NI;0) 298.15 +0; 6000 N!
 PARAMETER G(B2,AL:VA;0)                298.15 +.5*B2ALVA#-.5*LB2ALVA#;
6000 N REF10 !
     PARA G(B2,CO:VA;0) 298.15 +0; 6000 N!
     PARA G(B2,CR:VA;0) 298.15 +0; 6000 N!
 PARAMETER G(B2,NI:VA;0)                298.15 +.5*B2NIVA#-.5*LB2NIVA#;
6000 N REF10 !
     PARA G(B2,VA:VA;0) 298.15 +0; 6000 N!
     PARA G(B2,Y:VA;0) 298.15 +0; 6000 N!
 PARAMETER G(B2,AL:Y;0)                 298.15 +.5*GB2ALY#; 6000 N REF1 !
 PARAMETER G(B2,CO:Y;0)                 298.15 +.5*GB2COY#; 6000 N REF1 !
     PARA G(B2,CR:Y;0) 298.15 +0; 6000 N!
     PARA G(B2,NI:Y;0) 298.15 +0; 6000 N!
     PARA G(B2,VA:Y;0) 298.15 +0; 6000 N!
     PARA G(B2,Y:Y;0) 298.15 +0; 6000 N!
 PARAMETER G(B2,CO,VA:AL;0)             298.15 -41000; 2900 N REF1 !
 PARAMETER G(B2,CO,CR:AL;0)             298.15 +.5*BCOCRMAL#; 6000 N REF16 !
 PARAMETER G(B2,CO,NI:AL;0)             298.15 -19717+4.002*T; 6000 N REF1 !
 PARAMETER G(B2,CO:AL,NI;0)             298.15 -13863+13*T; 6000 N REF1 !
 PARAMETER G(B2,CR:AL,CO;0)             298.15 +.5*BALCOMCR#; 6000 N REF16 !
 PARAMETER G(B2,NI:AL,CO;0)             298.15 -45855+15*T; 6000 N REF1 !
 PARAMETER G(B2,NI:AL,CO;1)             298.15 -29011; 6000 N REF1 !
 PARAMETER G(B2,AL,NI:CO;0)             298.15 -13863+13*T; 6000 N REF1 !
 PARAMETER G(B2,AL:CO,VA;0)             298.15 -41000; 2900 N REF1 !
 PARAMETER G(B2,AL:CO,CR;0)             298.15 +.5*BCOCRMAL#; 6000 N REF16 !
 PARAMETER G(B2,AL:CO,NI;0)             298.15 -19717+4.002*T; 6000 N REF1 !
 PARAMETER G(B2,CR:CO,NI;0)             298.15 +.5*GCONICR#; 6000 N REF1 !
 PARAMETER G(B2,AL,CO:CR;0)             298.15 +.5*BALCOMCR#; 6000 N REF16 !
 PARAMETER G(B2,CO,NI:CR;0)             298.15 +.5*GCONICR#; 6000 N REF1 !
 PARAMETER G(B2,AL,CO:NI;0)             298.15 -45855+15*T; 6000 N REF1 !
 PARAMETER G(B2,AL,CO:NI;1)             298.15 -29011; 6000 N REF1 !
```

```
PHASE BAL3Y  %  2 3   1 !
   CONSTITUENT BAL3Y  :AL : Y :  !
  PARAMETER G(BAL3Y,AL:Y;0)              298.15 -196945.6+20.4*T+3*GHSERAL#
 +GHSERYY#; 6000 N REF1 !

PHASE CO3Y2  %  2 3   2 !
   CONSTITUENT CO3Y2  :CO : Y :  !
  PARAMETER G(CO3Y2,CO:Y;0)              298.15 -149808+35.051*T+3*GHSERCO#
 +2*GHSERYY#; 6000 N REF7 !

PHASE CO3Y4  %  2 3   4 !
   CONSTITUENT CO3Y4  :CO : Y :  !

  PARAMETER G(CO3Y4,CO:Y;0)              298.15 -202856+71.233*T+3*GHSERCO#
 +4*GHSERYY#; 6000 N REF7 !

PHASE CO5Y8  %  2 5   8 !
   CONSTITUENT CO5Y8  :CO : Y :  !

  PARAMETER G(CO5Y8,CO:Y;0)              298.15 -339960+112.711*T
 +5*GHSERCO#+8*GHSERYY#; 6000 N REF7 !

PHASE CO7Y6  %  2 7   6 !
   CONSTITUENT CO7Y6  :CO : Y :  !
  PARAMETER G(CO7Y6,CO:Y;0)              298.15 -387550+105.08535*T
 +7*GHSERCO#+6*GHSERYY#; 6000 N REF1 !

PHASE DALCONI  %  3 14   1   5 !
   CONSTITUENT DALCONI  :AL : AL,CO,NI : CO,NI :  !

  PARAMETER G(DALCONI,AL:AL:CO;0)        298.15 -808032+166*T+15*GHSERAL#
 +5*GHSERCO#; 6000 N REF1 !
  PARAMETER G(DALCONI,AL:CO:CO;0)        298.15 -648000+14*GHSERAL#
 +6*GHSERCO#; 6000 N REF1 !
  PARAMETER G(DALCONI,AL:NI:CO;0)        298.15 -973233+185.75*T
 +14*GHSERAL#+GHSERNI#+5*GHSERCO#; 6000 N REF1 !
  PARAMETER G(DALCONI,AL:AL:NI;0)        298.15 -699936+52*T+15*GHSERAL#
 +5*GHSERNI#; 6000 N REF1 !
  PARAMETER G(DALCONI,AL:CO:NI;0)        298.15 -872968+80*T+14*GHSERAL#
 +GHSERCO#+5*GHSERNI#; 6000 N REF1 !
  PARAMETER G(DALCONI,AL:NI:NI;0)        298.15 -1048162+244*T+14*GHSERAL#
 +6*GHSERNI#; 6000 N REF1 !
  PARAMETER G(DALCONI,AL:AL,CO:CO;0)     298.15 -10500; 6000 N REF1 !
  PARAMETER G(DALCONI,AL:AL,NI:CO;0)     298.15 -7000; 6000 N REF1 !
  PARAMETER G(DALCONI,AL:AL:CO,NI;0)     298.15 -303293+112*T; 6000 N REF1 !
  PARAMETER G(DALCONI,AL:CO,NI:CO;0)     298.15 -12500; 6000 N REF1 !
  PARAMETER G(DALCONI,AL:CO,NI:CO,NI;0)  298.15 -90000; 6000 N REF1 !
  PARAMETER G(DALCONI,AL:CO:CO,NI;0)     298.15 -55000; 6000 N REF1 !
  PARAMETER G(DALCONI,AL:NI:CO,NI;0)     298.15 -88030+10*T; 6000 N REF1 !
  PARAMETER G(DALCONI,AL:AL,CO:NI;0)     298.15 -85000; 6000 N REF1 !
  PARAMETER G(DALCONI,AL:AL,NI:NI;0)     298.15 -87755+65*T; 6000 N REF1 !
  PARAMETER G(DALCONI,AL:CO,NI:NI;0)     298.15 -85500; 6000 N REF1 !

PHASE DELTA  %  2 1   1 !
   CONSTITUENT DELTA  :CO,NI : Y :  !
```

```
  PARAMETER G(DELTA,CO:Y;0)              298.15 -47095+15*T+GHSERCO#
+GHSERYY#; 6000 N REF1 !
  PARAMETER G(DELTA,NI:Y;0)              298.15 -48000+GHSERNI#+GHSERYY#;
6000 N REF1 !
  PARAMETER G(DELTA,CO,NI:Y;0)           298.15 -50739+10*T; 6000 N REF1 !

PHASE GAMMAH  %  4 2   3   2   6 !
   CONSTITUENT GAMMAH  :AL,CR : AL,CR,NI : CR,NI : AL :  !
  PARAMETER G(GAMMAH,AL:AL:CR:AL;0)      298.15 +11*GHSERAL#+2*GHSERCR#
-124435.301; 6000 N REF3 !
  PARAMETER G(GAMMAH,CR:AL:CR:AL;0)      298.15 +9*GHSERAL#+4*GHSERCR#;
6000 N REF3 !
  PARAMETER G(GAMMAH,AL:CR:CR:AL;0)      298.15 +8*GHSERAL#+5*GHSERCR#
-243589.915-43.004*T; 6000 N REF3 !
  PARAMETER G(GAMMAH,CR:CR:CR:AL;0)      298.15 +6*GHSERAL#+7*GHSERCR#
+2357.3095-103.7686*T; 6000 N REF3 !
  PARAMETER G(GAMMAH,AL:NI:CR:AL;0)      298.15 +8*GHSERAL#+2*GHSERCR#
+3*GHSERNI#-200000-110*T; 6000 N REF1 !
  PARAMETER G(GAMMAH,CR:NI:CR:AL;0)      298.15 +6*GHSERAL#+4*GHSERCR#
+3*GHSERNI#-300000; 6000 N REF1 !
  PARAMETER G(GAMMAH,AL:AL:NI:AL;0)      298.15 +11*GHSERAL#+2*GHSERNI#;
6000 N REF1 !
  PARAMETER G(GAMMAH,CR:AL:NI:AL;0)      298.15 +9*GHSERAL#+2*GHSERCR#
+2*GHSERNI#; 6000 N REF1 !
  PARAMETER G(GAMMAH,AL:CR:NI:AL;0)      298.15 +8*GHSERAL#+3*GHSERCR#
+2*GHSERNI#; 6000 N REF1 !
  PARAMETER G(GAMMAH,CR:CR:NI:AL;0)      298.15 +6*GHSERAL#+5*GHSERCR#
+2*GHSERNI#; 6000 N REF1 !
  PARAMETER G(GAMMAH,AL:NI:NI:AL;0)      298.15 +8*GHSERAL#+5*GHSERNI#;
6000 N REF1 !
  PARAMETER G(GAMMAH,CR:NI:NI:AL;0)      298.15 +6*GHSERAL#+2*GHSERCR#
+5*GHSERNI#; 6000 N REF1 !
  PARAMETER G(GAMMAH,AL,CR:*:CR:AL;0)    298.15 -181214.621; 6000 N REF3 !
  PARAMETER G(GAMMAH,*:AL,CR:CR:AL;0)    298.15 -63956.7903-25.6399*T; 6000
N REF3 !

PHASE GAMMAL  %  4 12   5   5   4 !
   CONSTITUENT GAMMAL  :AL : CR,NI : AL,CR,NI : AL,CR :  !
  PARAMETER G(GAMMAL,AL:CR:AL:AL;0)      298.25 +21*GHSERAL#+5*GHSERCR#
-356964.301+19.3388*T; 6000 N REF3 !
  PARAMETER G(GAMMAL,AL:NI:AL:AL;0)      298.25 +21*GHSERAL#+5*GHSERNI#
-500000; 6000 N REF1 !
  PARAMETER G(GAMMAL,AL:CR:CR:AL;0)      298.25 +16*GHSERAL#+10*GHSERCR#
-336946.667-53.7443*T; 6000 N REF3 !
  PARAMETER G(GAMMAL,AL:NI:CR:AL;0)      298.25 +16*GHSERAL#+5*GHSERCR#
+5*GHSERNI#; 6000 N REF1 !
  PARAMETER G(GAMMAL,AL:CR:NI:AL;0)      298.25 +16*GHSERAL#+5*GHSERCR#
+5*GHSERNI#-1025100+200*T; 6000 N REF1 !
  PARAMETER G(GAMMAL,AL:NI:NI:AL;0)      298.25 +16*GHSERAL#+10*GHSERNI#;
6000 N REF1 !
  PARAMETER G(GAMMAL,AL:CR:AL:CR;0)      298.25 +17*GHSERAL#+9*GHSERCR#
-340950.194-39.12769*T; 6000 N REF3 !
  PARAMETER G(GAMMAL,AL:NI:AL:CR;0)      298.25 +17*GHSERAL#+4*GHSERCR#
+5*GHSERNI#; 6000 N REF1 !
  PARAMETER G(GAMMAL,AL:CR:CR:CR;0)      298.25 +12*GHSERAL#+14*GHSERCR#
-320932.56-112.2108*T; 6000 N REF3 !
  PARAMETER G(GAMMAL,AL:NI:CR:CR;0)      298.25 +12*GHSERAL#+9*GHSERCR#
```

```
  +5*GHSERNI#; 6000 N REF1 !
   PARAMETER G(GAMMAL,AL:CR:NI:CR;0)      298.25 +12*GHSERAL#+9*GHSERCR#
  +5*GHSERNI#-1025100+200*T; 6000 N REF1 !
   PARAMETER G(GAMMAL,AL:NI:NI:CR;0)      298.25 +16*GHSERAL#+4*GHSERCR#
  +10*GHSERNI#; 6000 N REF1 !
   PARAMETER G(GAMMAL,AL:CR:AL,CR:AL;0)   298.25 -351144.694+16.15033*T;
  6000 N REF3 !
   PARAMETER G(GAMMAL,AL:CR:AL,NI:AL;0)   298.15 -310000; 6000 N REF1 !
   PARAMETER G(GAMMAL,AL:CR:AL:AL,CR;0)   298.25 -280915.756+12.92027*T;
  6000 N REF3 !
   PARAMETER G(GAMMAL,AL:CR:CR:AL,CR;0)   298.25 -280915.756+12.92027*T;
  6000 N REF3 !
   PARAMETER G(GAMMAL,AL:CR:AL,CR:CR;0)   298.25 -351144.694+16.15033*T;
  6000 N REF3 !

$ THIS PHASE HAS A DISORDERED CONTRIBUTION FROM A1
 TYPE_DEFINITION * GES AMEND_PHASE_DESCRIPTION L12 DIS_PART A1,,,!
 TYPE_DEFINITION + GES A_P_D L12 MAGNETIC  -3.0    2.80000E-01 !
 PHASE L12  %*+  2 .75   .25 !
    CONSTITUENT L12  :AL,CO,CR,NI%,Y : AL,CO,CR,NI%,Y :  !

       PARA G(L12,AL:AL;0) 298.15 +0; 6000 N!
   PARAMETER G(L12,CO:AL;0)               298.15 +ALCO3#; 6000 N REF10 !
   PARAMETER G(L12,CR:AL;0)               298.15 +ALCR3#; 6000 N REF10 !
   PARAMETER G(L12,NI:AL;0)               298.15 +ALNI3#; 6000 N REF10 !
       PARA G(L12,Y:AL;0) 298.15 +0; 6000 N!
   PARAMETER G(L12,AL:CO;0)               298.15 +AL3CO#; 6000 N REF10 !
       PARA G(L12,CO:CO;0) 298.15 +0; 6000 N!
   PARAMETER G(L12,CR:CO;0)               298.15 +COCR3#; 6000 N REF1 !
   PARAMETER G(L12,NI:CO;0)               298.15 +CONI3#; 6000 N REF1 !
       PARA G(L12,Y:CO;0) 298.15 +0; 6000 N!
   PARAMETER G(L12,AL:CR;0)               298.15 +AL3CR#; 6000 N REF10 !
   PARAMETER G(L12,CO:CR;0)               298.15 +CO3CR#; 6000 N REF1 !
       PARA G(L12,CR:CR;0) 298.15 +0; 6000 N!
   PARAMETER G(L12,NI:CR;0)               298.15 +CRNI3#; 6000 N REF10 !
       PARA G(L12,Y:CR;0) 298.15 +0; 6000 N!
   PARAMETER G(L12,AL:NI;0)               298.15 +AL3NI#; 6000 N REF10 !
   PARAMETER G(L12,CO:NI;0)               298.15 +CO3NI#; 6000 N REF1 !
   PARAMETER G(L12,CR:NI;0)               298.15 +CR3NI#; 6000 N REF10 !
       PARA G(L12,NI:NI;0) 298.15 +0; 6000 N!
       PARA G(L12,Y:NI;0) 298.15 +0; 6000 N!
       PARA G(L12,AL:Y;0) 298.15 +0; 6000 N!
       PARA G(L12,CO:Y;0) 298.15 +0; 6000 N!
       PARA G(L12,CR:Y;0) 298.15 +0; 6000 N!
       PARA G(L12,NI:Y;0) 298.15 +0; 6000 N!
       PARA G(L12,Y:Y;0) 298.15 +0; 6000 N!
   PARAMETER G(L12,AL,CO:AL;0)            298.15 -1.5*ALCO3#+1.5*AL2CO2#
  +1.5*AL3CO#; 6000 N REF10 !
   PARAMETER G(L12,AL,CO:AL;1)            298.15 +.5*ALCO3#-1.5*AL2CO2#
  +1.5*AL3CO#; 6000 N REF10 !
   PARAMETER G(L12,AL,CO,CR:AL;0)         298.15 -1.5*ALCOCR2#-1.5*ALCO2CR#
  +ALCO3#+ALCR3#+6*AL2COCR#-1.5*AL2CO2#-1.5*AL2CR2#-1.5*AL3CO#-1.5*AL3CR#;
  6000 N REF10 !
   PARAMETER G(L12,AL,CO,NI:AL;0)         298.15 -1.5*ALCONI2#-1.5*ALCO2NI#
  +ALCO3#+ALNI3#+6*AL2CONI#-1.5*AL2CO2#-1.5*AL2NI2#-1.5*AL3CO#-1.5*AL3NI#;
  6000 N REF31 !
   PARAMETER G(L12,AL,CR:AL;0)            298.15 -1.5*ALCR3#+1.5*AL2CR2#
```

```
+1.5*AL3CR#; 6000 N REF10 !
 PARAMETER G(L12,AL,CR:AL;1)             298.15 +.5*ALCR3#-1.5*AL2CR2#
+1.5*AL3CR#; 6000 N REF10 !
 PARAMETER G(L12,AL,CR,NI:AL;0)          298.15 -7.5*U1ALCR#-7.5*U1ALNI#
-1.5*ALCRNI2#-1.5*ALCR2NI#+6*AL2CRNI#; 3000 N REF10 !
 PARAMETER G(L12,AL,NI:AL;0)             298.15 -1.5*ALNI3#+1.5*AL2NI2#
+1.5*AL3NI#; 6000 N REF10 !
 PARAMETER G(L12,AL,NI:AL;1)             298.15 +.5*ALNI3#-1.5*AL2NI2#
+1.5*AL3NI#; 6000 N REF10 !
 PARAMETER G(L12,C0,CR:AL;0)             298.15 +1.5*ALC0CR2#+1.5*ALC02CR#
-1.5*ALC03#-1.5*ALCR3#; 6000 N REF10 !
 PARAMETER G(L12,C0,CR:AL;1)             298.15 -1.5*ALC0CR2#+1.5*ALC02CR#
-.5*ALC03#+.5*ALCR3#; 6000 N REF10 !
 PARAMETER G(L12,C0,CR,NI:AL;0)          298.15 +ALC03#+ALCR3#+ALNI3#
-1.5*ALC0CR2#-1.5*ALC02CR#-1.5*ALC0NI2#-1.5*ALC02NI#-1.5*ALCRNI2#
-1.5*ALCR2NI#+6*ALC0CRNI#; 3000 N REF10 !
 PARAMETER G(L12,C0,NI:AL;0)             298.15 +1.5*ALC0NI2#+1.5*ALC02NI#
-1.5*ALC03#-1.5*ALNI3#; 6000 N REF31 !
 PARAMETER G(L12,C0,NI:AL;1)             298.15 -1.5*ALC0NI2#+1.5*ALC02NI#
-.5*ALC03#+.5*ALNI3#; 6000 N REF31 !
 PARAMETER G(L12,CR,NI:AL;0)             298.15 -4.5*U1ALCR#-4.5*U1ALNI#
+1.5*ALCRNI2#+1.5*ALCR2NI#; 3000 N REF10 !
 PARAMETER G(L12,CR,NI:AL;1)             298.15 -1.5*U1ALCR#+1.5*U1ALNI#
-1.5*ALCRNI2#+1.5*ALCR2NI#; 3000 N REF10 !
 PARAMETER G(L12,AL,C0:C0;0)             298.15 +1.5*ALC03#+1.5*AL2C02#
-1.5*AL3C0#; 6000 N REF10 !
 PARAMETER G(L12,AL,C0:C0;1)             298.15 -1.5*ALC03#+1.5*AL2C02#
-.5*AL3C0#; 6000 N REF10 !
 PARAMETER G(L12,AL,C0,CR:C0;0)          298.15 -1.5*ALC0CR2#+6*ALC02CR#
-1.5*ALC03#-1.5*AL2C0CR#-1.5*AL2C02#+AL3C0#+C0CR3#-1.5*C02CR2#-1.5*C03CR#;
6000 N REF10 !
 PARAMETER G(L12,AL,C0,NI:C0;0)          298.15 -1.5*ALC0NI2#+6*ALC02NI#
-1.5*ALC03#-1.5*AL2C0NI#-1.5*AL2C02#+AL3C0#+C0NI3#-1.5*C02NI2#-1.5*C03NI#;
6000 N REF31 !
 PARAMETER G(L12,AL,CR:C0;0)             298.15 +1.5*ALC0CR2#+1.5*AL2C0CR#
-1.5*AL3C0#-1.5*C0CR3#; 6000 N REF10 !
 PARAMETER G(L12,AL,CR:C0;1)             298.15 -1.5*ALC0CR2#+1.5*AL2C0CR#
-.5*AL3C0#+.5*C0CR3#; 6000 N REF10 !
 PARAMETER G(L12,AL,CR,NI:C0;0)          298.15 +AL3C0#+C0CR3#+C0NI3#
-1.5*ALC0CR2#-1.5*AL2C0CR#-1.5*ALC0NI2#-1.5*AL2C0NI#-1.5*C0CRNI2#
-1.5*C0CR2NI#+6*ALC0CRNI#; 3000 N REF10 !
 PARAMETER G(L12,AL,NI:C0;0)             298.15 +1.5*ALC0NI2#+1.5*AL2C0NI#
-1.5*AL3C0#-1.5*C0NI3#; 6000 N REF31 !
 PARAMETER G(L12,AL,NI:C0;1)             298.15 -1.5*ALC0NI2#+1.5*AL2C0NI#
-.5*AL3C0#+.5*C0NI3#; 6000 N REF31 !
 PARAMETER G(L12,C0,NI:C0;0)             298.15 -1.5*C0NI3#+1.5*C02NI2#
+1.5*C03NI#; 6000 N REF10 !
 PARAMETER G(L12,C0,NI:C0;1)             298.15 +.5*C0NI3#-1.5*C02NI2#
+1.5*C03NI#; 6000 N REF10 !
 PARAMETER G(L12,C0,CR:C0;0)             298.15 -1.5*C0CR3#+1.5*C02CR2#
+1.5*C03CR#; 6000 N REF1 !
 PARAMETER G(L12,C0,CR:C0;1)             298.15 +.5*C0CR3#-1.5*C02CR2#
+1.5*C03CR#; 6000 N REF1 !
 PARAMETER G(L12,C0,CR,NI:C0;0)          298.15 -1.5*C0CRNI2#-1.5*C0CR2NI#
+C0CR3#+C0NI3#+6*C02CRNI#-1.5*C02CR2#-1.5*C02NI2#-1.5*C03CR#-1.5*C03NI#;
6000 N REF10 !
 PARAMETER G(L12,CR,NI:C0;0)             298.15 +1.5*C0CRNI2#+1.5*C0CR2NI#
```

-1.5*COCR3#-1.5*CONI3#; 6000 N REF10 !
 PARAMETER G(L12,CR,NI:CO;1)   298.15 -1.5*COCRNI2#+1.5*COCR2NI#
-.5*COCR3#+.5*CONI3#; 6000 N REF10 !
 PARAMETER G(L12,AL,CR:CR;0)   298.15 +1.5*ALCR3#+1.5*AL2CR2#
-1.5*AL3CR#; 6000 N REF10 !
 PARAMETER G(L12,AL,CR:CR;1)   298.15 -1.5*ALCR3#+1.5*AL2CR2#
-.5*AL3CR#; 6000 N REF10 !
 PARAMETER G(L12,AL,CR,NI:CR;0)   298.15 -7.5*U1ALCR#-7.5*U1CRNI#
-1.5*ALCRNI2#+6*ALCR2NI#-1.5*AL2CRNI#; 3000 N REF10 !
 PARAMETER G(L12,AL,CO:CR;0)   298.15 +1.5*ALCO2CR#+1.5*AL2COCR#
-1.5*AL3CR#-1.5*CO3CR#; 6000 N REF10 !
 PARAMETER G(L12,AL,CO:CR;1)   298.15 -1.5*ALCO2CR#+1.5*AL2COCR#
-.5*AL3CR#+.5*CO3CR#; 6000 N REF10 !
 PARAMETER G(L12,AL,CO,CR:CR;0)   298.15 +6*ALCOCR2#-1.5*ALCO2CR#
-1.5*ALCR3#-1.5*AL2COCR#-1.5*AL2CR2#+AL3CR#-1.5*COCR3#-1.5*CO2CR2#+CO3CR#;
6000 N REF10 !
 PARAMETER G(L12,AL,CO,NI:CR;0)   298.15 +AL3CR#+CO3CR#+CRNI3#
-1.5*ALCO2CR#-1.5*AL2COCR#-1.5*ALCRNI2#-1.5*AL2CRNI#-1.5*COCRNI2#
-1.5*CO2CRNI#+6*ALCOCRNI#; 3000 N REF10 !
 PARAMETER G(L12,AL,NI:CR;0)   298.15 -4.5*U1ALCR#-4.5*U1CRNI#
+1.5*ALCRNI2#+1.5*AL2CRNI#; 3000 N REF10 !
 PARAMETER G(L12,AL,NI:CR;1)   298.15 -1.5*U1ALCR#+1.5*U1CRNI#
-1.5*ALCRNI2#+1.5*AL2CRNI#; 3000 N REF10 !
 PARAMETER G(L12,CO,CR:CR;0)   298.15 +1.5*COCR3#+1.5*CO2CR2#
-1.5*CO3CR#; 6000 N REF1 !
 PARAMETER G(L12,CO,CR:CR;1)   298.15 -1.5*COCR3#+1.5*CO2CR2#
-.5*CO3CR#; 6000 N REF1 !
 PARAMETER G(L12,CO,CR,NI:CR;0)   298.15 -1.5*COCRNI2#+6*COCR2NI#
-1.5*COCR3#-1.5*CO2CRNI#-1.5*CO2CR2#+CO3CR#+CRNI3#-1.5*CR2NI2#-1.5*CR3NI#;
6000 N REF10 !
 PARAMETER G(L12,CO,NI:CR;0)   298.15 +1.5*COCRNI2#+1.5*CO2CRNI#
-1.5*CO3CR#-1.5*CRNI3#; 6000 N REF10 !
 PARAMETER G(L12,CO,NI:CR;1)   298.15 -1.5*COCRNI2#+1.5*CO2CRNI#
-.5*CO3CR#+.5*CRNI3#; 6000 N REF10 !
 PARAMETER G(L12,CR,NI:CR;0)   298.15 -1.5*CRNI3#+1.5*CR2NI2#
+1.5*CR3NI#; 6000 N REF10 !
 PARAMETER G(L12,CR,NI:CR;1)   298.15 +.5*CRNI3#-1.5*CR2NI2#
+1.5*CR3NI#; 6000 N REF10 !
 PARAMETER G(L12,AL,NI:NI;0)   298.15 +1.5*ALNI3#+1.5*AL2NI2#
-1.5*AL3NI#; 6000 N REF10 !
 PARAMETER G(L12,AL,NI:NI;1)   298.15 -1.5*ALNI3#+1.5*AL2NI2#
-.5*AL3NI#; 6000 N REF10 !
 PARAMETER G(L12,AL,CO:NI;0)   298.15 +1.5*ALCO2NI#+1.5*AL2CONI#
-1.5*AL3NI#-1.5*CO3NI#; 6000 N REF31 !
 PARAMETER G(L12,AL,CO:NI;1)   298.15 -1.5*ALCO2NI#+1.5*AL2CONI#
-.5*AL3NI#+.5*CO3NI#; 6000 N REF31 !
 PARAMETER G(L12,AL,CO,NI:NI;0)   298.15 +6*ALCONI2#-1.5*ALCO2NI#
-1.5*ALNI3#-1.5*AL2CONI#-1.5*AL2NI2#+AL3NI#-1.5*CONI3#-1.5*CO2NI2#+CO3NI#;
6000 N REF31 !
 PARAMETER G(L12,AL,CO,CR:NI;0)   298.15 +AL3NI#+CO3NI#+CR3NI#
-1.5*ALCO2NI#-1.5*AL2CONI#-1.5*ALCR2NI#-1.5*COCR2NI#-1.5*AL2CRNI#
-1.5*CO2CRNI#+6*ALCOCRNI#; 3000 N REF10 !
 PARAMETER G(L12,AL,CR:NI;0)   298.15 -4.5*U1ALNI#-4.5*U1CRNI#
+1.5*ALCR2NI#+1.5*AL2CRNI#; 3000 N REF10 !
 PARAMETER G(L12,AL,CR:NI;1)   298.15 -1.5*U1ALNI#+1.5*U1CRNI#
-1.5*ALCR2NI#+1.5*AL2CRNI#; 3000 N REF10 !
 PARAMETER G(L12,AL,CR,NI:NI;0)   298.15 -7.5*U1ALNI#-7.5*U1CRNI#

```
 +6*ALCRNI2#-1.5*ALCR2NI#-1.5*AL2CRNI#; 3000 N REF10 !
  PARAMETER G(L12,CO,NI:NI;0)            298.15 +1.5*CONI3#+1.5*CO2NI2#
 -1.5*CO3NI#; 6000 N REF10 !
  PARAMETER G(L12,CO,NI:NI;1)            298.15 -1.5*CONI3#+1.5*CO2NI2#
 -.5*CO3NI#; 6000 N REF10 !
  PARAMETER G(L12,CO,CR:NI;0)            298.15 +1.5*COCR2NI#+1.5*CO2CRNI#
 -1.5*CO3NI#-1.5*CR3NI#; 6000 N REF10 !
  PARAMETER G(L12,CO,CR:NI;1)            298.15 -1.5*COCR2NI#+1.5*CO2CRNI#
 -.5*CO3NI#+.5*CR3NI#; 6000 N REF10 !
  PARAMETER G(L12,CO,CR,NI:NI;0)         298.15 +6*COCRNI2#-1.5*COCR2NI#
 -1.5*CONI3#-1.5*CO2CRNI#-1.5*CO2NI2#+CO3NI#-1.5*CRNI3#-1.5*CR2NI2#+CR3NI#;
 6000 N REF10 !
  PARAMETER G(L12,CR,NI:NI;0)            298.15 +1.5*CRNI3#+1.5*CR2NI2#
 -1.5*CR3NI#; 6000 N REF10 !
  PARAMETER G(L12,CR,NI:NI;1)            298.15 -1.5*CRNI3#+1.5*CR2NI2#
 -.5*CR3NI#; 6000 N REF10 !
  PARAMETER G(L12,AL,CO:*;0)             298.15 +3*L04ALCO#; 6000 N REF10 !
  PARAMETER G(L12,AL,CO:*;1)             298.15 +3*L14ALCO#; 6000 N REF10 !
  PARAMETER G(L12,AL,CR:*;0)             298.15 +3*L04ALCR#; 6000 N REF10 !
  PARAMETER G(L12,AL,CR:*;1)             298.15 +3*L14ALCR#; 6000 N REF10 !
  PARAMETER G(L12,AL,NI:*;0)             298.15 +3*L04ALNI#; 6000 N REF10 !
  PARAMETER G(L12,AL,NI:*;1)             298.15 +3*L14ALNI#; 6000 N REF10 !
  PARAMETER G(L12,*:AL,CO;0)             298.15 +L04ALCO#; 6000 N REF10 !
  PARAMETER G(L12,*:AL,CO;1)             298.15 +L14ALCO#; 6000 N REF10 !
  PARAMETER G(L12,*:AL,CR;0)             298.15 +L04ALCR#; 6000 N REF10 !
  PARAMETER G(L12,*:AL,CR;1)             298.15 +L14ALCR#; 6000 N REF10 !
  PARAMETER G(L12,*:AL,NI;0)             298.15 +L04ALNI#; 6000 N REF10 !
  PARAMETER G(L12,*:AL,NI;1)             298.15 +L14ALNI#; 6000 N REF10 !
  PARAMETER G(L12,CO,NI:*;0)             298.15 +3*L04CONI#; 6000 N REF1 !
  PARAMETER G(L12,CO,NI:*;1)             298.15 +3*L14CONI#; 6000 N REF1 !
  PARAMETER G(L12,CO,CR:*;0)             298.15 +3*L04COCR#; 6000 N REF1 !
  PARAMETER G(L12,CO,CR:*;1)             298.15 +3*L14COCR#; 6000 N REF1 !
  PARAMETER G(L12,*:CO,NI;0)             298.15 +L04CONI#; 6000 N REF1 !
  PARAMETER G(L12,*:CO,NI;1)             298.15 +L14CONI#; 6000 N REF1 !
  PARAMETER G(L12,*:CO,CR;0)             298.15 +L04COCR#; 6000 N REF1 !
  PARAMETER G(L12,*:CO,CR;1)             298.15 +L14COCR#; 6000 N REF1 !
  PARAMETER G(L12,CR,NI:*;0)             298.15 +3*L04CRNI#; 6000 N REF10 !
  PARAMETER G(L12,CR,NI:*;1)             298.15 +3*L14CRNI#; 6000 N REF10 !
  PARAMETER G(L12,*:CR,NI;0)             298.15 +L04CRNI#; 6000 N REF10 !
  PARAMETER G(L12,*:CR,NI;1)             298.15 +L14CRNI#; 6000 N REF10 !

PHASE LIQUID  %  1  1.0  !
   CONSTITUENT LIQUID  :AL,CO,CR,NI,Y :  !
  PARAMETER G(LIQUID,AL;0)               298.15 +GLIQAL#; 2900 N REF27 !
  PARAMETER G(LIQUID,CO;0)               298.15 +GLIQCO#; 6000 N REF27 !
  PARAMETER G(LIQUID,CR;0)               298.15 +GLIQCR#; 6000 N REF27 !
  PARAMETER G(LIQUID,NI;0)               298.15 +GLIQNI#; 3000 N REF29 !
  PARAMETER G(LIQUID,Y;0)                100 +GLIQYY#; 3700 N REF27 !
  PARAMETER G(LIQUID,AL,CO;0)            298.15 -150510+33.729*T; 6000 N
 REF4 !
  PARAMETER G(LIQUID,AL,CO;1)            298.15 -54090+26.8*T; 6000 N REF4 !
  PARAMETER G(LIQUID,AL,CO;2)            298.15 +65430-22.4*T; 6000 N REF4 !
  PARAMETER G(LIQUID,AL,CO,CR;0)         298.15 +40000; 6000 N REF1 !
  PARAMETER G(LIQUID,AL,CO,CR;1)         298.15 +40000; 6000 N REF1 !
  PARAMETER G(LIQUID,AL,CO,CR;2)         298.15 +40000; 6000 N REF1 !
  PARAMETER G(LIQUID,AL,CO,NI;0)         298.15 -225383+12.244*T; 6000 N
 REF1 !
```

```
 PARAMETER G(LIQUID,AL,CO,NI;1)          298.15 +11080+27.616*T; 6000 N
REF1 !
 PARAMETER G(LIQUID,AL,CO,NI;2)          298.15 +59143+26.207*T; 6000 N
REF1 !
 PARAMETER G(LIQUID,AL,CO,Y;0)           298.15 +40000; 3000 N REF1 !
 PARAMETER G(LIQUID,AL,CO,Y;1)           298.15 +90000; 3000 N REF1 !
 PARAMETER G(LIQUID,AL,CO,Y;2)           298.15 +90000; 3000 N REF1 !
 PARAMETER G(LIQUID,AL,CR;0)             298.15 -27622.19-19.3*T; 3000 N
REF3 !
 PARAMETER G(LIQUID,AL,CR;1)             298.15 -2851.66-4.1778*T; 3000 N
REF3 !
 PARAMETER G(LIQUID,AL,CR,NI;0)          298.15 -40000+41*T; 3000 N REF1 !
 PARAMETER G(LIQUID,AL,CR,NI;1)          298.15 -20000+45*T; 3000 N REF1 !
 PARAMETER G(LIQUID,AL,CR,NI;2)          298.15 -10000+41*T; 3000 N REF1 !
 PARAMETER G(LIQUID,AL,NI;0)             298.15 -207109.28+41.31501*T; 6000
N REF11 !
 PARAMETER G(LIQUID,AL,NI;1)             298.15 -10185.79+5.8714*T; 6000 N
REF11 !
 PARAMETER G(LIQUID,AL,NI;2)             298.15 +81204.81-31.95713*T; 6000
N REF11 !
 PARAMETER G(LIQUID,AL,NI;3)             298.15 +4365.35-2.51632*T; 6000 N
REF11 !
 PARAMETER G(LIQUID,AL,NI;4)             298.15 -22101.64+13.16341*T; 6000
N REF11 !
 PARAMETER G(LIQUID,AL,NI,Y;0)           298.15 +70000; 3000 N REF1 !
 PARAMETER G(LIQUID,AL,NI,Y;1)           298.15 +70000; 3000 N REF1 !
 PARAMETER G(LIQUID,AL,NI,Y;2)           298.15 +70000; 3000 N REF1 !
 PARAMETER G(LIQUID,AL,Y;0)              298.15 -192571.2+29.03622*T; 6000
N REF6 !
 PARAMETER G(LIQUID,AL,Y;1)              298.15 -46742.9-.46159*T; 6000 N
REF6 !
 PARAMETER G(LIQUID,AL,Y;2)              298.15 +70259-28.9999*T; 6000 N
REF6 !
 PARAMETER G(LIQUID,AL,Y;3)              298.15 +9002.8; 6000 N REF6 !
 PARAMETER G(LIQUID,CO,CR;0)             298.15 -12008.6239+2.2019*T; 6000
N REF22 !
 PARAMETER G(LIQUID,CO,CR;1)             298.15 -5836.4696+1.1402*T; 6000 N
REF22 !
 PARAMETER G(LIQUID,CO,CR,NI;0)          298.15 -47000; 6000 N REF1 !
 PARAMETER G(LIQUID,CO,CR,NI;1)          298.15 -24500; 6000 N REF1 !
 PARAMETER G(LIQUID,CO,CR,NI;2)          298.15 -21000; 6000 N REF1 !
 PARAMETER G(LIQUID,CO,NI;0)             298.15 +1331; 6000 N REF19 !
 PARAMETER G(LIQUID,CO,Y;0)              298.15 -92420+15.247*T; 6000 N
REF1 !
 PARAMETER G(LIQUID,CO,Y;1)              298.15 +18310-21.879*T; 6000 N
REF1 !
 PARAMETER G(LIQUID,CO,Y;2)              298.15 +48750-21.547*T; 6000 N
REF1 !
 PARAMETER G(LIQUID,CR,NI;0)             298.15 -1276-5.3873*T; 6000 N
REF20 !
 PARAMETER G(LIQUID,CR,NI;1)             298.15 +2699; 6000 N REF20 !
 PARAMETER G(LIQUID,CR,Y;0)              298.15 +32000; 6000 N REF9 !
 PARAMETER G(LIQUID,CR,Y;1)              298.15 +8500; 6000 N REF9 !
 PARAMETER G(LIQUID,NI,Y;0)              298.15 -155496+38.932*T; 6000 N
REF12 !
 PARAMETER G(LIQUID,NI,Y;1)              298.15 -52904+6.785*T; 6000 N
REF12 !
```

```
TYPE_DEFINITION - GES A_P_D M17Y2 MAGNETIC  -3.0    2.80000E-01 !
PHASE M17Y2  %-  2 17   2 !
   CONSTITUENT M17Y2  :AL,CO%,NI%,Y : CO,NI,Y% :  !

  PARAMETER G(M17Y2,AL:CO;0)             298.15 +17*GHSERAL#+2*GHSERCO#;
 6000 N REF1 !
  PARAMETER G(M17Y2,CO:CO;0)             298.15 +19*GHSERCO#+160000; 6000 N
 REF1 !
  PARAMETER G(M17Y2,NI:CO;0)             298.15 +17*GHSERNI#+2*GHSERCO#
 +80000; 6000 N REF1 !
  PARAMETER G(M17Y2,Y:CO;0)              298.15 +2*GHSERCO#+17*GHSERYY#;
 6000 N REF1 !
  PARAMETER G(M17Y2,AL:NI;0)             298.15 +17*GHSERAL#+2*GHSERNI#;
 6000 N REF1 !
  PARAMETER G(M17Y2,CO:NI;0)             298.15 +17*GHSERCO#+2*GHSERNI#
 +80000; 6000 N REF1 !
  PARAMETER G(M17Y2,NI:NI;0)             298.15 +19*GHSERNI#+150000; 6000 N
 REF1 !
  PARAMETER G(M17Y2,Y:NI;0)              298.15 +17*GHSERYY#+2*GHSERNI#;
 6000 N REF1 !
  PARAMETER G(M17Y2,AL:Y;0)              298.15 -352000+17*GHSERAL#
 +2*GHSERYY#; 6000 N REF1 !
  PARAMETER G(M17Y2,CO:Y;0)              298.15 +17*GHSERCO#+2*GHSERYY#
 -317400+70*T; 6000 N REF1 !
  PARAMETER TC(M17Y2,CO:Y;0)             298.15 +1138.5; 6000 N REF8 !
  PARAMETER BMAGN(M17Y2,CO:Y;0)          298.15 +1.45185; 6000 N REF8 !
  PARAMETER G(M17Y2,NI:Y;0)              298.15 -386087+61.742*T
 +17*GHSERNI#+2*GHSERYY#; 6000 N REF12 !
  PARAMETER G(M17Y2,Y:Y;0)               298.15 +19*GHSERYY#+120000; 6000 N
 REF1 !
  PARAMETER G(M17Y2,CO:CO,Y;0)           298.15 -100000; 6000 N REF1 !
  PARAMETER G(M17Y2,AL,CO:Y;0)           298.15 -1310000; 6000 N REF1 !
  PARAMETER G(M17Y2,AL,CO:Y;1)           298.15 +255000; 6000 N REF1 !
  PARAMETER G(M17Y2,AL,NI:Y;0)           298.15 -1910000; 6000 N REF1 !
  PARAMETER G(M17Y2,CO,Y:Y;0)            298.15 -348000; 6000 N REF1 !
  PARAMETER G(M17Y2,CO,NI:Y;0)           298.15 +108620-42*T; 6000 N REF1 !
  PARAMETER G(M17Y2,CO,NI:Y;1)           298.15 +8825-25*T; 6000 N REF1 !
  PARAMETER G(M17Y2,CO,NI:Y;2)           298.15 +25000; 6000 N REF1 !

PHASE M1Y1  %  2 1   1 !
   CONSTITUENT M1Y1  :AL,CO : Y :  !
  PARAMETER G(M1Y1,AL:Y;0)               298.15 -109823.8+10.9631*T
 +GHSERAL#+GHSERYY#; 6000 N REF6 !
  PARAMETER G(M1Y1,CO:Y;0)               298.15 -58981+17.075*T+GHSERCO#
 +GHSERYY#; 6000 N REF1 !
  PARAMETER G(M1Y1,AL,CO:Y;0)            298.15 +38000; 6000 N REF1 !


PHASE M2Y  %  2 2   1 !
   CONSTITUENT M2Y  :AL,CO,NI : Y :  !

  PARAMETER G(M2Y,AL:Y;0)                298.15 -254214+28.28928*T
 +2*GC15AL#+GC15YY#; 6000 N REF1 !
  PARAMETER G(M2Y,CO:Y;0)                298.15 -147072+12.8*T+2*GC15CO#
 +GC15YY#; 6000 N REF1 !
  PARAMETER G(M2Y,NI:Y;0)                298.15 -168766+8.988*T+2*GC15NI#
```

```
 +GC15YY#; 6000 N REF12 !
  PARAMETER G(M2Y,AL,CO:Y;0)              298.15 -18497-15*T; 6000 N REF1 !
  PARAMETER G(M2Y,AL,CO:Y;1)              298.15 -8000; 6000 N REF1 !
  PARAMETER G(M2Y,AL,NI:Y;0)              298.15 -44000; 6000 N REF1 !
  PARAMETER G(M2Y,AL,NI:Y;1)              298.15 -16000; 6000 N REF1 !
  PARAMETER G(M2Y,CO,NI:Y;0)              298.15 +14000; 6000 N REF1 !

PHASE M3Y  %  2 3   1 !
   CONSTITUENT M3Y  :AL,CO,NI : Y :  !
  PARAMETER G(M3Y,AL:Y;0)                 298.15 -123700+3*GHSERAL#+GHSERYY#;
  6000 N REF1 !
  PARAMETER G(M3Y,CO:Y;0)                 298.15 -103300+15.074*T+3*GHSERCO#
 +GHSERYY#; 6000 N REF1 !
  PARAMETER G(M3Y,NI:Y;0)                 298.15 -134358+16.477*T+3*GHSERNI#
 +GHSERYY#; 6000 N REF12 !
  PARAMETER G(M3Y,AL,CO:Y;0)              298.15 -252384+8*T; 6000 N REF1 !

TYPE_DEFINITION . GES A_P_D M5Y MAGNETIC  -3.0    2.80000E-01 !
PHASE M5Y  %.  2 5   1 !
   CONSTITUENT M5Y  :AL,CO%,NI%,Y : CO,NI,Y% :  !

  PARAMETER G(M5Y,AL:CO;0)                298.15 +5*GHSERAL#+GHSERCO#; 6000
 N REF1 !
  PARAMETER G(M5Y,CO:CO;0)                298.15 +6*GHSERCO#+42000; 6000 N
 REF1 !
  PARAMETER G(M5Y,NI:CO;0)                298.15 +5*GHSERNI#+GHSERCO#+20000;
 6000 N REF1 !
  PARAMETER G(M5Y,Y:CO;0)                 298.15 +GHSERCO#+5*GHSERYY#+50000;
 6000 N REF1 !
  PARAMETER G(M5Y,AL:NI;0)                298.15 +5*GHSERAL#+GHSERNI#; 6000
 N REF1 !
  PARAMETER G(M5Y,CO:NI;0)                298.15 +5*GHSERCO#+GHSERNI#+25000;
 6000 N REF1 !
  PARAMETER G(M5Y,NI:NI;0)                298.15 +6*GHSERNI#+49000; 6000 N
 REF1 !
  PARAMETER G(M5Y,Y:NI;0)                 298.15 +5*GHSERYY#+GHSERNI#+80000;
 6000 N REF1 !
  PARAMETER G(M5Y,AL:Y;0)                 298.15 -173500+5*GHSERAL#+GHSERYY#;
  6000 N REF1 !
  PARAMETER G(M5Y,CO:Y;0)                 298.15 +5*GHSERCO#+GHSERYY#-121650
 +19*T; 6000 N REF1 !
  PARAMETER TC(M5Y,CO:Y;0)                298.15 +976; 6000 N REF8 !
  PARAMETER BMAGN(M5Y,CO:Y;0)             298.15 +1.221667; 6000 N REF8 !
  PARAMETER G(M5Y,NI:Y;0)                 298.15 -186706+31.187*T+5*GHSERNI#
 +GHSERYY#; 6000 N REF12 !
  PARAMETER G(M5Y,Y:Y;0)                  298.15 +6*GHSERYY#+49000; 6000 N
 REF1 !
  PARAMETER G(M5Y,CO:CO,Y;0)              298.15 -36000; 6000 N REF1 !
  PARAMETER G(M5Y,AL,CO:Y;0)              298.15 -391000; 6000 N REF1 !
  PARAMETER G(M5Y,AL,NI:Y;0)              298.15 -520000; 6000 N REF1 !
  PARAMETER G(M5Y,CO,Y:Y;0)               298.15 -100000; 6000 N REF1 !

PHASE M7Y2  %  2 7   2 !
   CONSTITUENT M7Y2  :AL,CO%,NI% : Y :  !
  PARAMETER G(M7Y2,AL:Y;0)                298.15 -330000+7*GHSERAL#
 +2*GHSERYY#; 6000 N REF1 !
  PARAMETER G(M7Y2,CO:Y;0)                298.15 -224500+36.281*T+7*GHSERCO#
```

```
 +2*GHSERYY#; 6000 N REF1 !
  PARAMETER G(M7Y2,NI:Y;0)                298.15 -294966+38.77*T+7*GHSERNI#
 +2*GHSERYY#; 6000 N REF12 !
  PARAMETER G(M7Y2,AL,CO:Y;0)             298.15 -524000+40*T; 6000 N REF1 !
  PARAMETER G(M7Y2,AL,CO:Y;1)             298.15 +20000; 6000 N REF1 !

PHASE MOPT2_TY  %  2 1   2 !
   CONSTITUENT MOPT2_TY  :CR%,NI : CR,NI% :  !

  PARAMETER G(MOPT2_TY,CR:CR;0)           298.15 +3*GHSERCR#+500; 6000 N
 REF2 !
  PARAMETER G(MOPT2_TY,NI:CR;0)           298.15 +22530+6*T+2*GHSERCR#
 +GHSERNI#; 6000 N REF2 !
  PARAMETER G(MOPT2_TY,CR:NI;0)           298.15 -22530+6*T+2*GHSERCR#
 +GHSERNI#; 6000 N REF2 !
  PARAMETER G(MOPT2_TY,NI:NI;0)           298.15 +3*GBCCNI#+100; 6000 N REF2 !
  PARAMETER G(MOPT2_TY,CR,NI:CR;0)        298.15 +69140; 6000 N REF2 !
  PARAMETER G(MOPT2_TY,CR,NI:CR,NI;0)     298.15 -57780; 6000 N REF2 !
  PARAMETER G(MOPT2_TY,CR:CR,NI;0)        298.15 +62480; 6000 N REF2 !
  PARAMETER G(MOPT2_TY,NI:CR,NI;0)        298.15 -43700; 6000 N REF2 !
  PARAMETER G(MOPT2_TY,CR,NI:NI;0)        298.15 -2760; 6000 N REF2 !

PHASE MY3  %  2 1   3 !
   CONSTITUENT MY3  :CO,NI : Y :  !

  PARAMETER G(MY3,CO:Y;0)                 298.15 -66881+13.541*T+GHSERCO#
 +3*GHSERYY#; 6000 N REF1 !
  PARAMETER G(MY3,NI:Y;0)                 298.15 -84446+14.05*T+GHSERNI#
 +3*GHSERYY#; 6000 N REF12 !

PHASE NI2Y3  %  2 2   3 !
   CONSTITUENT NI2Y3  :NI : Y :  !

  PARAMETER G(NI2Y3,NI:Y;0)               298.15 -168600+37.482*T+2*GHSERNI#
 +3*GHSERYY#; 6000 N REF12 !

PHASE NI4Y  %  2 4   1 !
   CONSTITUENT NI4Y  :CO,NI : Y :  !

  PARAMETER G(NI4Y,CO:Y;0)                298.15 -105460+20*T+4*GHSERCO#
 +GHSERYY#; 6000 N REF1 !
  PARAMETER G(NI4Y,NI:Y;0)                298.15 -160555+22.979*T+4*GHSERNI#
 +GHSERYY#; 6000 N REF12 !
  PARAMETER G(NI4Y,CO,NI:Y;0)             298.15 -19000; 6000 N REF1 !

PHASE NIY  %  2 1   1 !
   CONSTITUENT NIY  :CO,NI : Y :  !

  PARAMETER G(NIY,CO:Y;0)                 298.15 -36984+8*T+GHSERCO#
 +GHSERYY#; 6000 N REF1 !
  PARAMETER G(NIY,NI:Y;0)                 298.15 -67908+6.11*T+GHSERNI#
 +GHSERYY#; 6000 N REF12 !
  PARAMETER G(NIY,CO,NI:Y;0)              298.15 -20284+8*T; 6000 N REF1 !

PHASE SIGMA3  %  3 2   8   5 !
   CONSTITUENT SIGMA3  :AL,CO,CR%,NI : AL,CO,CR%,NI : AL,CO%,CR,NI% :  !
```

```
 PARAMETER G(SIGMA3,AL:AL:AL;0)          298.15 +15*GSIGMAAL#; 6000 N REF1 !
 PARAMETER G(SIGMA3,CO:AL:AL;0)          298.15 +2*GSIGMACO#+13*GSIGMAAL#;
6000 N REF1 !
 PARAMETER G(SIGMA3,CR:AL:AL;0)          298.15 +2*GSIGMACR#+13*GSIGMAAL#;
6000 N REF1 !
 PARAMETER G(SIGMA3,NI:AL:AL;0)          298.15 +2*GSIGMANI#+13*GSIGMAAL#;
6000 N REF1 !
 PARAMETER G(SIGMA3,AL:CO:AL;0)          298.15 +8*GSIGMACO#+7*GSIGMAAL#;
6000 N REF1 !
 PARAMETER G(SIGMA3,CO:CO:AL;0)          298.15 +10*GSIGMACO#+5*GSIGMAAL#;
6000 N REF1 !
 PARAMETER G(SIGMA3,CR:CO:AL;0)          298.15 -500000+2*GSIGMACR#
+8*GSIGMACO#+5*GSIGMAAL#; 6000 N REF1 !
 PARAMETER G(SIGMA3,NI:CO:AL;0)          298.15 +2*GSIGMANI#+8*GSIGMACO#
+5*GSIGMAAL#; 6000 N REF1 !
 PARAMETER G(SIGMA3,AL:CR:AL;0)          298.15 +8*GSIGMACR#+7*GSIGMAAL#;
6000 N REF1 !
 PARAMETER G(SIGMA3,CO:CR:AL;0)          298.15 +2*GSIGMACO#+8*GSIGMACR#
+5*GSIGMAAL#; 6000 N REF1 !
 PARAMETER G(SIGMA3,CR:CR:AL;0)          298.15 +10*GSIGMACR#+5*GSIGMAAL#;
6000 N REF1 !
 PARAMETER G(SIGMA3,NI:CR:AL;0)          298.15 +2*GSIGMANI#+8*GSIGMACR#
+5*GSIGMAAL#; 6000 N REF1 !
 PARAMETER G(SIGMA3,AL:NI:AL;0)          298.15 +8*GSIGMANI#+7*GSIGMAAL#;
6000 N REF1 !
 PARAMETER G(SIGMA3,CO:NI:AL;0)          298.15 +2*GSIGMACO#+8*GSIGMANI#
+5*GSIGMAAL#; 6000 N REF1 !
 PARAMETER G(SIGMA3,CR:NI:AL;0)          298.15 +2*GSIGMACR#+8*GSIGMANI#
+5*GSIGMAAL#; 6000 N REF1 !
 PARAMETER G(SIGMA3,NI:NI:AL;0)          298.15 +10*GSIGMANI#+5*GSIGMAAL#;
6000 N REF1 !
 PARAMETER G(SIGMA3,AL:AL:CO;0)          298.15 +5*GSIGMACO#+10*GSIGMAAL#;
6000 N REF1 !
 PARAMETER G(SIGMA3,CO:AL:CO;0)          298.15 +7*GSIGMACO#+8*GSIGMAAL#;
6000 N REF1 !
 PARAMETER G(SIGMA3,CR:AL:CO;0)          298.15 -686000+2*GSIGMACR#
+8*GSIGMAAL#+5*GSIGMACO#; 6000 N REF1 !
 PARAMETER G(SIGMA3,NI:AL:CO;0)          298.15 +2*GSIGMANI#+8*GSIGMAAL#
+5*GSIGMACO#; 6000 N REF1 !
 PARAMETER G(SIGMA3,AL:CO:CO;0)          298.15 +13*GSIGMACO#+2*GSIGMAAL#;
6000 N REF1 !
 PARAMETER G(SIGMA3,CO:CO:CO;0)          298.15 +15*GSIGMACO#; 6000 N REF1 !
 PARAMETER G(SIGMA3,CR:CO:CO;0)          298.15 -100000+10*T+13*GSIGMACO#
+2*GSIGMACR#; 6000 N REF1 !
 PARAMETER G(SIGMA3,NI:CO:CO;0)          298.15 +13*GSIGMACO#+2*GSIGMANI#;
6000 N REF1 !
 PARAMETER G(SIGMA3,AL:CR:CO;0)          298.15 +2*GSIGMAAL#+8*GSIGMACR#
+5*GSIGMACO#; 6000 N REF1 !
 PARAMETER G(SIGMA3,CO:CR:CO;0)          298.15 -50000+5*T+7*GSIGMACO#
+8*GSIGMACR#; 6000 N REF1 !
 PARAMETER G(SIGMA3,CR:CR:CO;0)          298.15 -266000+24.5*T+5*GSIGMACO#
+10*GSIGMACR#; 6000 N REF1 !
 PARAMETER G(SIGMA3,NI:CR:CO;0)          298.15 +2*GSIGMANI#+8*GSIGMACR#
+5*GSIGMACO#; 6000 N REF1 !
 PARAMETER G(SIGMA3,AL:NI:CO;0)          298.15 +2*GSIGMAAL#+8*GSIGMANI#
+5*GSIGMACO#; 6000 N REF1 !
 PARAMETER G(SIGMA3,CO:NI:CO;0)          298.15 +7*GSIGMACO#+8*GSIGMANI#;
```

6000 N REF1 !
 PARAMETER G(SIGMA3,CR:NI:CO;0)   298.15 -210000+75*T+2*GSIGMACR#
+8*GSIGMANI#+5*GSIGMACO#; 6000 N REF1 !
 PARAMETER G(SIGMA3,NI:NI:CO;0)   298.15 +5*GSIGMACO#+10*GSIGMANI#;
6000 N REF1 !
 PARAMETER G(SIGMA3,AL:AL:CR;0)   298.15 +5*GSIGMACR#+10*GSIGMAAL#;
6000 N REF1 !
 PARAMETER G(SIGMA3,CO:AL:CR;0)   298.15 +2*GSIGMACO#+8*GSIGMAAL#
+5*GSIGMACR#; 6000 N REF1 !
 PARAMETER G(SIGMA3,CR:AL:CR;0)   298.15 +7*GSIGMACR#+8*GSIGMAAL#;
6000 N REF1 !
 PARAMETER G(SIGMA3,NI:AL:CR;0)   298.15 +2*GSIGMANI#+8*GSIGMAAL#
+5*GSIGMACR#; 6000 N REF1 !
 PARAMETER G(SIGMA3,AL:CO:CR;0)   298.15 +2*GSIGMAAL#+8*GSIGMACO#
+5*GSIGMACR#; 6000 N REF1 !
 PARAMETER G(SIGMA3,CO:CO:CR;0)   298.15 +266000+10*GSIGMACO#
+5*GSIGMACR#; 6000 N REF1 !
 PARAMETER G(SIGMA3,CR:CO:CR;0)   298.15 -100000+10*T+8*GSIGMACO#
+7*GSIGMACR#; 6000 N REF1 !
 PARAMETER G(SIGMA3,NI:CO:CR;0)   298.15 +180000+2*GSIGMANI#
+8*GSIGMACO#+5*GSIGMACR#; 6000 N REF1 !
 PARAMETER G(SIGMA3,AL:CR:CR;0)   298.15 +13*GSIGMACR#+2*GSIGMAAL#;
6000 N REF1 !
 PARAMETER G(SIGMA3,CO:CR:CR;0)   298.15 +100000+2*GSIGMACO#
+13*GSIGMACR#; 6000 N REF1 !
 PARAMETER G(SIGMA3,CR:CR:CR;0)   298.15 +15*GSIGMACR#; 6000 N REF1 !
 PARAMETER G(SIGMA3,NI:CR:CR;0)   298.15 +13*GSIGMACR#+2*GSIGMANI#;
6000 N REF1 !
 PARAMETER G(SIGMA3,AL:NI:CR;0)   298.15 +2*GSIGMAAL#+8*GSIGMANI#
+5*GSIGMACR#; 6000 N REF1 !
 PARAMETER G(SIGMA3,CO:NI:CR;0)   298.15 +180000+2*GSIGMACO#
+8*GSIGMANI#+5*GSIGMACR#; 6000 N REF1 !
 PARAMETER G(SIGMA3,CR:NI:CR;0)   298.15 -175000+7*GSIGMACR#
+8*GSIGMANI#; 6000 N REF1 !
 PARAMETER G(SIGMA3,NI:NI:CR;0)   298.15 +5*GSIGMACR#+10*GSIGMANI#;
6000 N REF1 !
 PARAMETER G(SIGMA3,AL:AL:NI;0)   298.15 +5*GSIGMANI#+10*GSIGMAAL#;
6000 N REF1 !
 PARAMETER G(SIGMA3,CO:AL:NI;0)   298.15 +2*GSIGMACO#+8*GSIGMAAL#
+5*GSIGMANI#; 6000 N REF1 !
 PARAMETER G(SIGMA3,CR:AL:NI;0)   298.15 +2*GSIGMACR#+8*GSIGMAAL#
+5*GSIGMANI#; 6000 N REF1 !
 PARAMETER G(SIGMA3,NI:AL:NI;0)   298.15 +7*GSIGMANI#+8*GSIGMAAL#;
6000 N REF1 !
 PARAMETER G(SIGMA3,AL:CO:NI;0)   298.15 +2*GSIGMAAL#+8*GSIGMACO#
+5*GSIGMANI#; 6000 N REF1 !
 PARAMETER G(SIGMA3,CO:CO:NI;0)   298.15 +10*GSIGMACO#+5*GSIGMANI#;
6000 N REF1 !
 PARAMETER G(SIGMA3,CR:CO:NI;0)   298.15 -180000+2*GSIGMACR#
+8*GSIGMACO#+5*GSIGMANI#; 6000 N REF1 !
 PARAMETER G(SIGMA3,NI:CO:NI;0)   298.15 +8*GSIGMACO#+7*GSIGMANI#;
6000 N REF1 !
 PARAMETER G(SIGMA3,AL:CR:NI;0)   298.15 +2*GSIGMAAL#+8*GSIGMACR#
+5*GSIGMANI#; 6000 N REF1 !
 PARAMETER G(SIGMA3,CO:CR:NI;0)   298.15 +2*GSIGMACO#+8*GSIGMACR#
+5*GSIGMANI#; 6000 N REF1 !
 PARAMETER G(SIGMA3,CR:CR:NI;0)   298.15 -105200-120*T+10*GSIGMACR#

```
+5*GSIGMANI#; 6000 N REF1 !
 PARAMETER G(SIGMA3,NI:CR:NI;0)          298.15 +8*GSIGMACR#+7*GSIGMANI#;
6000 N REF1 !
 PARAMETER G(SIGMA3,AL:NI:NI;0)          298.15 +13*GSIGMANI#+2*GSIGMAAL#;
6000 N REF1 !
 PARAMETER G(SIGMA3,CO:NI:NI;0)          298.15 +2*GSIGMACO#+13*GSIGMANI#;
6000 N REF1 !
 PARAMETER G(SIGMA3,CR:NI:NI;0)          298.15 +20000-91*T+2*GSIGMACR#
+13*GSIGMANI#; 6000 N REF1 !
 PARAMETER G(SIGMA3,NI:NI:NI;0)          298.15 +15*GSIGMANI#; 6000 N REF1 !
 PARAMETER G(SIGMA3,CR:CO,NI:CO;0)       298.15 -190000; 6000 N REF1 !
 PARAMETER G(SIGMA3,CR:CR,NI:CO;0)       298.15 -120000; 6000 N REF1 !
 PARAMETER G(SIGMA3,CR:CR:CO,CR;0)       298.15 -130000; 6000 N REF1 !

PHASE TAOA  %  3 8   2   1 !
   CONSTITUENT TAOA  :AL,CR,NI : AL,CR,NI : AL,CR,NI :  !
 PARAMETER G(TAOA,AL:AL:AL;0)            298.15 +11*GHSERAL#+50000; 6000 N
REF1 !
 PARAMETER G(TAOA,CR:AL:AL;0)            298.15 +3*GHSERAL#+8*GHSERCR#;
6000 N REF1 !
 PARAMETER G(TAOA,NI:AL:AL;0)            298.15 +3*GHSERAL#+8*GHSERNI#;
6000 N REF1 !
 PARAMETER G(TAOA,AL:CR:AL;0)            298.15 +9*GHSERAL#+2*GHSERCR#
-142500-18*T; 6000 N REF1 !
 PARAMETER G(TAOA,CR:CR:AL;0)            298.15 +GHSERAL#+10*GHSERCR#; 6000
N REF1 !
 PARAMETER G(TAOA,NI:CR:AL;0)            298.15 +GHSERAL#+2*GHSERCR#
+8*GHSERNI#; 6000 N REF1 !
 PARAMETER G(TAOA,AL:NI:AL;0)            298.15 +9*GHSERAL#+2*GHSERNI#;
6000 N REF1 !
 PARAMETER G(TAOA,CR:NI:AL;0)            298.15 +GHSERAL#+8*GHSERCR#
+2*GHSERNI#; 6000 N REF1 !
 PARAMETER G(TAOA,NI:NI:AL;0)            298.15 +GHSERAL#+10*GHSERNI#; 6000
N REF1 !
 PARAMETER G(TAOA,AL:AL:CR;0)            298.15 +10*GHSERAL#+GHSERCR#; 6000
N REF1 !
 PARAMETER G(TAOA,CR:AL:CR;0)            298.15 +2*GHSERAL#+9*GHSERCR#;
6000 N REF1 !
 PARAMETER G(TAOA,NI:AL:CR;0)            298.15 +2*GHSERAL#+GHSERCR#
+8*GHSERNI#; 6000 N REF1 !
 PARAMETER G(TAOA,AL:CR:CR;0)            298.15 +8*GHSERAL#+3*GHSERCR#
-204100; 6000 N REF1 !
 PARAMETER G(TAOA,CR:CR:CR;0)            298.15 +11*GHSERCR#+55000; 6000 N
REF1 !
 PARAMETER G(TAOA,NI:CR:CR;0)            298.15 +3*GHSERCR#+8*GHSERNI#;
6000 N REF1 !
 PARAMETER G(TAOA,AL:NI:CR;0)            298.15 +8*GHSERAL#+2*GHSERNI#
+GHSERCR#; 6000 N REF1 !
 PARAMETER G(TAOA,CR:NI:CR;0)            298.15 +9*GHSERCR#+2*GHSERNI#
+55000; 6000 N REF1 !
 PARAMETER G(TAOA,NI:NI:CR;0)            298.15 +GHSERCR#+10*GHSERNI#; 6000
N REF1 !
 PARAMETER G(TAOA,AL:AL:NI;0)            298.15 +10*GHSERAL#+GHSERNI#
-130500; 6000 N REF1 !
 PARAMETER G(TAOA,CR:AL:NI;0)            298.15 +2*GHSERAL#+8*GHSERCR#
+GHSERNI#; 6000 N REF1 !
 PARAMETER G(TAOA,NI:AL:NI;0)            298.15 +2*GHSERAL#+9*GHSERNI#;
```

```
 6000 N REF1 !
  PARAMETER G(TAOA,AL:CR:NI;0)            298.15 +8*GHSERAL#+2*GHSERCR#
 +GHSERNI#-324000+23.024*T; 3000 N REF1 !
  PARAMETER G(TAOA,CR:CR:NI;0)            298.15 +10*GHSERCR#+GHSERNI#+55000;
  6000 N REF1 !
  PARAMETER G(TAOA,NI:CR:NI;0)            298.15 +2*GHSERCR#+9*GHSERNI#;
 6000 N REF1 !
  PARAMETER G(TAOA,AL:NI:NI;0)            298.15 +8*GHSERAL#+3*GHSERNI#
 -330000; 6000 N REF1 !
  PARAMETER G(TAOA,CR:NI:NI;0)            298.15 +8*GHSERCR#+3*GHSERNI#
 +55000; 6000 N REF1 !
  PARAMETER G(TAOA,NI:NI:NI;0)            298.15 +11*GHSERNI#+55000; 6000 N
 REF1 !
  PARAMETER G(TAOA,AL:AL,CR:NI;0)         298.15 -20000; 6000 N REF1 !

PHASE TAOB  %  3 .8   .11   .09 !
   CONSTITUENT TAOB  :AL : CR : NI :  !
  PARAMETER G(TAOB,AL:CR:NI;0)            298.15 +.8*GHSERAL#+.11*GHSERCR#
 +.09*GHSERNI#-25200+2.3*T; 3000 N REF1 !

PHASE TAOC  %  3 .82   .15   .03 !
   CONSTITUENT TAOC  :AL : CR : NI :  !
  PARAMETER G(TAOC,AL:CR:NI;0)            298.15 +.82*GHSERAL#+.15*GHSERCR#
 +.03*GHSERNI#-17520; 3000 N REF1 !


PHASE TAOFIV  %  2 3   2 !
   CONSTITUENT TAOFIV  :AL,CO : Y :  !
  PARAMETER G(TAOFIV,AL:Y;0)              298.15 -268325+25*T+3*GHSERAL#
 +2*GHSERYY#; 6000 N REF1 !
  PARAMETER G(TAOFIV,CO:Y;0)              298.15 -141090+30*T+3*GHSERCO#
 +2*GHSERYY#; 6000 N REF1 !
  PARAMETER G(TAOFIV,AL,CO:Y;0)           298.15 -92000; 6000 N REF1 !

PHASE TAOFOUR  %  2 2   1 !
   CONSTITUENT TAOFOUR  :AL,CO : Y :  !

  PARAMETER G(TAOFOUR,AL:Y;0)             298.15 -176941+17*T+2*GHSERAL#
 +GHSERYY#; 6000 N REF1 !
  PARAMETER G(TAOFOUR,CO:Y;0)             298.15 -76995+15*T+2*GHSERCO#
 +GHSERYY#; 6000 N REF1 !
  PARAMETER G(TAOFOUR,AL,CO:Y;0)          298.15 -80000; 6000 N REF1 !
  PARAMETER G(TAOFOUR,AL,CO:Y;1)          298.15 -12000; 6000 N REF1 !

PHASE TAOONE  %  3 7   2   1 !
   CONSTITUENT TAOONE  :AL : CO : Y :  !
  PARAMETER G(TAOONE,AL:CO:Y;0)           298.15 -468998+7.33*T+7*GHSERAL#
 +2*GHSERCO#+GHSERYY#; 6000 N REF1 !

PHASE TAOTHR  %  3 2   1   1 !
   CONSTITUENT TAOTHR  :AL : CO : Y :  !
  PARAMETER G(TAOTHR,AL:CO:Y;0)           298.15 -260217+42*T+2*GHSERAL#
 +GHSERCO#+GHSERYY#; 6000 N REF1 !

PHASE TAOTWO  %  3 9   3   2 !
   CONSTITUENT TAOTWO  :AL : CO : Y :  !
  PARAMETER G(TAOTWO,AL:CO:Y;0)           298.15 -822988+56*T+9*GHSERAL#
```

```
 +3*GHSERCO#+2*GHSERYY#; 6000 N REF1 !

PHASE XALCONI  %  3 9   2   2 !
   CONSTITUENT XALCONI  :AL : CO : CO,NI :  !
  PARAMETER G(XALCONI,AL:CO:CO;0)         298.15 -510081.2+110.4*T
 +9*GHSERAL#+4*GHSERCO#; 6000 N REF1 !
  PARAMETER G(XALCONI,AL:CO:NI;0)         298.15 -679003.5+122.65*T
 +9*GHSERAL#+2*GHSERCO#+2*GHSERNI#; 6000 N REF1 !
  PARAMETER G(XALCONI,AL:CO:CO,NI;0)      298.15 -163374; 6000 N REF1 !
  PARAMETER G(XALCONI,AL:CO:CO,NI;1)      298.15 -70000; 6000 N REF1 !

PHASE Y2ALCONI  %  2 3   1 !
   CONSTITUENT Y2ALCONI  :AL : CO,NI :  !
  PARAMETER G(Y2ALCONI,AL:CO;0)           298.15 -153140.9+28.3*T+3*GHSERAL#
 +GHSERCO#; 6000 N REF1 !
  PARAMETER G(Y2ALCONI,AL:NI;0)           298.15 -163790+35*T+3*GHSERAL#
 +GHSERNI#; 6000 N REF1 !
  PARAMETER G(Y2ALCONI,AL:CO,NI;0)        298.15 -65170+14.5*T; 6000 N REF1 !
  PARAMETER G(Y2ALCONI,AL:CO,NI;1)        298.15 -10700; 6000 N REF1 !

PHASE YAL13CO4  %  2 15.1   4.9 !
   CONSTITUENT YAL13CO4  :AL : CO,NI :  !
  PARAMETER G(YAL13CO4,AL:CO;0)           298.15 -808189.2+157.6*T
 +15.1*GHSERAL#+4.9*GHSERCO#; 6000 N REF1 !
  PARAMETER G(YAL13CO4,AL:NI;0)           298.15 -712069+30*T+15.1*GHSERAL#
 +4.9*GHSERNI#; 6000 N REF1 !
  PARAMETER G(YAL13CO4,AL:CO,NI;0)        298.15 -109507+59*T; 6000 N REF1 !

LIST_OF_REFERENCES
NUMBER  SOURCE
  REF1     ' THIS WORK'
  REF27    'PURE3 - SGTE Pure Elements (Unary) Database (Version 3.0),
           developed by SGTE (Scientific Group Thermodata Europe), 1991-1996,
            and provided by TCSAB (Aug. 1996). '
  REF29    'PURE5 - SGTE Pure Elements (Unary) Database (Version 5.1),
           developed by SGTE (Scientific Group Thermodata Europe), 1991-2010,
            and provided by TCSAB (Jun. 2010). '
  REF4     ' 2013STEIN REASSESSMENT OF AL-CO'
  REF3     ' 2013HU ASSESSMENT OF AL-CR'
  REF11    'N. Dupin, Thesis, LTPCM, France, 1995; Al-Ni, also in I. Ansara,
            N. Dupin, H.L. Lukas, B. SUndman J. Alloys Compds, 247 (1-2), 20
           -30 (1997)'
  REF22    ' 2002OIKAWA ASSESSMENT OF CO-CR'
  REF19    'A. Fernandez Guillermet, Z Metallkde, Vol 78 (1987) p 639-647
           TRITA-MAC 324B (1986); CO-NI'
  REF20    'P. Gustafson, CALPHAD 12 (1988) 277-292; Cr-W, Cr-Ni-W,
           Modified by Ursula R. Kattner, NIST, Gaithersburg, MD, USA '
  REF6     'A THERMODYNAMIC REASSESSMENT OF AL-Y BY LIU SHUHONG'
  REF9     '2009CHAN ASSESSMENT OF CR-RE INCLUDING CR-Y SYSTEM'
  REF12    ' thermodynamic assessment of the Ni-Y system Zhenmin Du,
           Weijing Zhang. J. Alloys Compds, 245,164-167 (1996)'
  REF28    'PURE1 - SGTE Pure Elements (Unary) Database (Version 1.0),
           developed by SGTE (Scientific Group Thermodata Europe), 1991-1992,
            and provided by TCSAB (Jan. 1991). Also in: Dinsdale A. (1991):
           SGTE data for pure elements, Calphad, 15, 317-425.'
  REF23    '1990DIN'
  REF30    'PURE4 - SGTE Pure Elements (Unary) Database (Version 4.6),
```

```
         developed by SGTE (Scientific Group Thermodata Europe), 1991-2008,
          and provided by TCSAB (Jan. 2008). '
 REF18    ' 2014 SUGGEST THE GIBBS ENERGY OF VA IN A2 IS 0.2RT INSTEAD OF
         100000 '
 REF14    'N. Dupin, I. Ansara, Z. metallkd., Vol 90 (1999) p 76-85'
 REF10    'N. Dupin, I. Ansara, B. Sundman Thermodynamic Re-Assessment of
         the Ternary System Al-Cr-Ni, Calphad, 25 (2), 279-298 (2001); Al
         -Cr-Ni'
 REF31    ' 2001DUPIN'
 REF16    '2016LIU SAME AS 15LIU'
 REF2     ' 2006Chan assessed cr-ni system'
 REF8     'GOLUMBFSKIE DISSERTATION ABOUT AL-CO-NI-Y'
 REF7     ' ASSESSMENT FO CO-Y WITH FP CALCULATION'
!
```

Reference

[1] S. Xiang, S. Mao, Z. Shen, H. Long, H. Wei, S. Ma, J. Zhang, Y. Chen, J. Zhang, B. Zhang, Y. Liu, Site preference of metallic elements in M23C6 carbide in a Ni-based single crystal superalloy, Materials & Design, 129 (2017) 9-14.

[2] D. Mukherji, J. Rösler, Design Considerations and Strengthening Mechanisms in Developing Co-Re-Based Alloys for Applications at + 100°C above Ni-Superalloys, Advanced Materials Research, 278 (2011) 539-544.

[3] J. Sato, T. Omori, K. Oikawa, I. Ohnuma, R. Kainuma, K. Ishida, Cobalt-Base High-Temperature Alloys, Science, 312 (2006) 90-91.

[4] G. Bozzolo, R.D. Noebe, P.B. Abel, Applied computational materials modeling: theory, simulation and experiment, Springer Science & Business Media, 2007.

[5] J.R. Nicholls, Designing oxidation-resistant coatings, JOM, 52 (2000) 28-35.

[6] L. Kaufman, H. Bemstein, Computer Calculation of Phase Diagram, Academic Press, New York, 1970.

[7] N. Saunders, A.P. Miodownik, CALPHAD (Calculation of Phase Diagrams)-A Comprehensive Guide, Elsevier Science Ltd., Great British, 1998.

[8] K.C. Hari Kumar, P. Wollants, Some guidelines for thermodynamic optimisation of phase diagrams, Journal of Alloys and Compounds, 320 (2001) 189-198.

[9] M. Aghaie-Khafri, B. Binesh, Creep behavior of MAR-M 302 Co-base superalloy, 2010.

[10] J.O. Andersson, T. Helander, L. Höglund, P. Shi, B. Sundman, Thermo-Calc & DICTRA, computational tools for materials science, Calphad, 26 (2002) 273-312.

[11] S.L. Chen, S. Daniel, F. Zhang, Y.A. Chang, X.Y. Yan, F.Y. Xie, R. Schmid-Fetzer, W.A. Oates, The PANDAT software package and its applications, Calphad, 26 (2002) 175-188.

[12] C.W. Bale, E. Bélisle, P. Chartrand, S.A. Decterov, G. Eriksson, A.E. Gheribi, K. Hack, I.H. Jung, Y.B. Kang, J. Melançon, A.D. Pelton, S. Petersen, C. Robelin, J. Sangster, P. Spencer, M.A. Van Ende, FactSage thermochemical software and databases, 2010–2016, Calphad, 54 (2016) 35-53.

[13] B. Jansson,(Thesis) Computer Operated Methods for Equilibrium Calculations and Evaluation of Thermodynamic Model Parameters, Royal Institute of Technology, Stockholm, 1984.

[14] A.T. Dinsdale, SGTE data for pure elements, CALPHAD, 15 (1991) 317-425.

[15] G. Inden, Project Meeting Calphad V, Max Plank Inst. Eisenforsch, Dusseldolf, 1976.

[16] M. Hillert, M. Jarl, A model for alloying in ferromagnetic metals, CALPHAD, 2 (1978) 227-238.

[17] I. Ansara, N. Dupin, H.L. Lukas, B. Sundman, Thermodynamic assessment of the Al-Ni system, J. Alloys Compd., 247 (1997) 20-30.

[18] I. Ansara, B. Sundman, P. Willemin, Thermodynamic modeling of ordered

phases in the nickel-aluminum system, Acta Metall., 36 (1988) 977-982.

[19] N. Dupin, B. Sundman, A thermodynamic database for Ni-base superalloys, Scandinavian journal of metallurgy, 30 (2001) 184-192.

[20] A.T. Dinsdale, A.V. Khvan, A. Watson, Critical Assessment 5: Thermodynamic data for vacancies, Materials Science and Technology, 30 (2014) 1715-1718.

[21] P. Franke, Modeling of thermal vacancies in metals within the framework of the compound energy formalism, J. Phase Equilb. Diffus., 35 (2014) 780-787.

[22] P.-W. Guan, Z.-K. Liu, A physical model of thermal vacancies within the CALPHAD approach, Scripta Materialia, 133 (2017) 5-8.

[23] J. Peng, P. Franke, D. Manara, T. Watkins, R.J.M. Konings, Experimental investigation and thermodynamic re-assessment of the Al-Mo-Ni system, J. Alloys Compd., 674 (2016) 305-314.

[24] J.M. Joubert, Crystal chemistry and Calphad modeling of the σ phase, Progress in Materials Science, 53 (2008) 528-583.

[25] J.M. Joubert, N. Dupin, Mixed site occupancies in the μ phase, Intermetallics, 12 (2004) 1373-1380.

[26] K. Shinagawa, H. Chinen, T. Omori, K. Oikawa, I. Ohnuma, K. Ishida, R. Kainuma, Phase equilibria and thermodynamic calculation of the Co–Ta binary system, Intermetallics, 49 (2014) 87-97.

[27] K. Ishida, T. Nishizawa, The Co-Cr (Cobalt-Chromium) system, Bulletin of Alloy Phase Diagrams, 11 (1990) 357-370.

[28] C. Allibert, C. Bernard, N. Valignat, M. Dombre, Co-Cr binary system: experimental re-determination of the phase diagram and comparison with the diagram calculated from the thermodynamic data, Journal of the Less Common Metals, 59 (1978) 211-228.

[29] K. Oikawa, G.-W. Qin, T. Ikeshoji, R. Kainuma, K. Ishida, Direct evidence of magnetically induced phase separation in the fcc phase and thermodynamic calculations of phase equilibria of the Co–Cr system, Acta Materialia, 50 (2002) 2223-2232.

[30] A. Kusoffsky, B. Jansson, A thermodynamic evaluation of the Co-Cr and the C-Co-Cr systems, Calphad, 21 (1997) 321-333.

[31] J. Vreštál, J. Houserová, M. Šob, ENERGETICS AND PHASE DIAGRAMS OF Fe-Cr AND Co-Cr SYSTEMS FROM FIRST PRINCIPLES, Journal of Mining and Metallurgy B, 38 (2002) 205-211.

[32] Z. Li, H. Mao, P.A. Korzhavyi, M. Selleby, Thermodynamic re-assessment of the Co–Cr system supported by first-principles calculations, Calphad, 52 (2016) 1-7.

[33] A. Fernandez-Guillermet, Assessment of the thermodynamic properties of the nickel-cobalt system, Z. Metallkd, 78 (1987) 639-647.

[34] W. Xiong,(Thesis) Thermodynamic and kinetic investigation of the Fe-Cr-Ni systems driven by engineering applications, KTH Royal Institute of Technology, Stockholm, Sweden, 2012.

[35] P. Gustafson, A thermodynamic evalution of the Cr-Ni-W system,

CALPHAD, 12 (1988) 277-292.

[36] B.J. Lee, On the stability of Cr carbides, CALPHAD, 16 (1992) 121-149.

[37] P.E.A. Turchi, L. Kaufman, Z.K. Liu, Modeling of Ni-Cr-Mo based alloys: Part I - phase stability, CALPHAD, 30 (2006) 70-87.

[38] K.S. Chan, Y.M. Pan, Y.D. Lee, Computation of Ni-Cr phase diagram via a combined first-principles quantum mechanical and CALPHAD approach, Metall. Mater. Trans. A 37A (2006) 2039-2050.

[39] S.P. Garg, Phase diagrams of binary tantalum alloys, Indian Institute of Metals, Calcutta, 1996.

[40] Z.-K. Liu, Y.A. Chang, Thermodynamic assessment of the Co-Ta system, Calphad, 23 (1999) 339-356.

[41] M.H.F. Sluiter, Ab initio lattice stabilities of some elemental complex structures, Calphad, 30 (2006) 357-366.

[42] M. Venkatraman, J.P. Neumann, Cr-Ta (Chromium-Tantalum), Bull Alloy Phase Diagr., 8 (1987) 112-116.

[43] N. Dupin, I. Ansara, Thermodynamic assessment of the Cr-Ta system, Journal of Phase Equilibria, 14 (1993) 451-456.

[44] M.H.F. Sluiter, Lattice stability prediction of elemental tetrahedrally close-packed structures, Acta Materialia, 55 (2007) 3707-3718.

[45] A.R. Elsea, C.C. McBride, The Effects of Nitrogen, Iron, or Nickel Upon the Alpha-Beta Transformation and Gama Precipitation in Cobalt-Chromium Alloys, Trans. AIME, 188 (1950) 154-161.

[46] S. Rideout, W.D. Manly, E.L. Kamen, B.S. Lement, P.A. Beck, Intermediate Phases in Ternary Alloy Systems of Transition Elements, Trans. AIME, 191 (1951) 872-876.

[47] H.H. Xu, Z.P. Jin, The determination of the isothermal section at 1200K of the Cr-Ni-Ti phase diagram, Scripta Materialia, 37 (1997) 147-150.

[48] G.P. Zhmurko, E.G. Kabanova, V.N. Kuznetsov, A.V. Leonov, Phase equilibria in the Co-Cr-Ni system, Moscow University Chemistry Bulletin, 63 (2008) 234-235.

[49] T. Omori, J. Sato, K. Shinagawa, I. Ohnuma, K. Oikawa, R. Kainuma, K. Ishida, Experimental Determination of Phase Equilibria in the Co-Cr-Ni System, Journal of Phase Equilibria and Diffusion, 35 (2014) 178-185.

[50] O. Kubaschewski, K. Hack, Heats of formation and of transformation in the system Nickel-Cobalt-Chromium, Z. Metallkde, 70 (1979) 789-791.

[51] S. Yang, M. Jiang, H. Li, Y. Liu, L. Wang, Assessment of Co-Cr-Ni ternary system by CALPHAD technique, Rare Metals, 31 (2012) 75-80.

[52] X.L. Liu, G. Lindwall, T. Gheno, Z.K. Liu, Thermodynamic modeling of Al-Co-Cr, Al-Co-Ni, Co-Cr-Ni ternary systems towards a description for Al-Co-Cr-Ni, CALPHAD, 52 (2016) 125-142.

[53] J.M. Drapier, J.L.D. Brouwer, D. Coutsouradis, Refractory metals and intermetallic precipitates in cobalt-chromium alloys, Cobalt. , 27 (1965) 59-72.

[54] G. Haour, F. Mollard, B. Lux, I.G. Wright, New eutectics based on Fe, Co, and Ni. Pt. 2, Z. Fuer Met. , 69 (1978) 69-74.

[55] C.C. Zhao, S.Y. Yang, X.J. Liu, C.P. Wang, Experimental determination of the phase equilibria in the Co–Cr–Ta ternary system, Journal of Alloys and Compounds, 608 (2014) 118-125.

[56] B. Kaplan,(Thesis) Experimental and theoretical study of carbides in the Co-Cr-C system, 2014.

[57] A.V. Khvan, B. Hallstedt, K. Chang, Thermodynamic assessment of Cr–Nb–C and Mn–Nb–C systems, Calphad, 39 (2012) 54-61.

[58] A. Gabriel, C. Chatillon, I. Ansara, Thermochemical and phase diagram analysis of the Ni-C, Co-C, and Co-Ni-C systems, High temperature science, 25 (1988) 17-54.

[59] K. Frisk, A. Fernández Guillermet, Gibbs energy coupling of the phase diagram and thermochemistry in the tantalum-carbon system, Journal of Alloys and Compounds, 238 (1996) 167-179.

[60] P. Gustafson, A Thermodynamic Evaluation of the C-Cr-Fe-W System, Metallurgical Transactions A, 19 (1988) 2547-2554.

[61] B. Kaplan, A. Blomqvist, M. Selleby, S. Norgren, Thermodynamic analysis of the W-Co-Cr system supported by ab initio calculations and verified with quaternary data, Calphad: Computer Coupling of Phase Diagrams and Thermochemistry, 50 (2015) 59-67.

[62] S.H. Zhou, Y. Wang, L.Q. Chen, Z.K. Liu, R.E. Napolitano, Solution-based thermodynamic modeling of the Ni-Ta and Ni-Mo-Ta systems using first-principle calculations, Calphad: Computer Coupling of Phase Diagrams and Thermochemistry, 33 (2009) 631-641.

[63] A.F. Guillermet, L. Östlund, Experimental and theoretical study of the phase equilibria in the Fe-Ni-W system, Metallurgical and Materials Transactions A, 17 (1986) 1809-1823.

[64] C. Guo, C. Li, S. Shang, Z. Du, Thermodynamic description of the Ta–W–Zr system, International Journal of Materials Research, 105 (2014) 1048-1056.

[65] B. Kaplan, A. Markström, A. Blomqvist, S. Norgren, M. Selleby, Thermodynamic analysis of the Co-Cr-C system, Calphad: Computer Coupling of Phase Diagrams and Thermochemistry, 46 (2014) 226-236.

[66] A. Fernández Guillermet, Thermodynamic Properties of the Fe-Co-Ni-C System, Zeitschrift für Metallkunde, 79 (1988) 524-536.

[67] L.F.S. Dumitrescu, M. Ekroth, B. Jansson, Thermodynamic assessment of the Me-Co-C systems (Me=Ti, Ta, or Nb), Metallurgical and Materials Transactions A, 32 (2001) 2167-2174.

[68] A. Markström, B. Sundman, K. Frisk, A Revised Thermodynamic Description of the Co-W-C System, Journal of Phase Equilibria & Diffusion, 26 (2005) 152-160.

[69] R. Luoma, A thermodynamic analysis of the system Fe-Cr-Ni-C-O, Finnish Academies of Technololgy, Espoo, 2002.

[70] C. Sha, M. Bu, H. Xu, Y. Du, S. Wang, G. Wen, A thermodynamic modeling of the C–Cr–Ta ternary system, Journal of Alloys and Compounds, 509 (2011) 5996-6003.

[71] Y. Cui, Z. Jin, Assessment of the Re–Ta binary system, Journal of Alloys and Compounds, 285 (1999) 150-155.

[72] Y. Wang, C. Chen, Z. Zhang, J. Long, T. Xu, X. Liu, L. Zhang, Y. Peng, P. Zhou, Y. Du, Phase equilibria in the Al-C-Ni-W quaternary system, International Journal of Refractory Metals and Hard Materials, 46 (2014) 43-51.

[73] K. Frisk, A thermodynamic analysis of the Ta-W-C and the Ta-W-C-N systems, Zeitschrift für Metallkunde, 90 (1999) 704-711.

[74] J. Zhu, M.S. Titus, T.M. Pollock, Experimental Investigation and Thermodynamic Modeling of the Co-Rich Region in the Co-Al-Ni-W Quaternary System, Journal of Phase Equilibria and Diffusion, 35 (2014) 595-611.

[75] N. Dupin, I. Ansara, Thermodynamic assessment of the Cr-Ni-Ta system, Zeitschrift fuer Metallkunde, 87 (1996) 555-561.

[76] P. Gustafson, A THERMODYNAMIC EVALUATION OF THE Cr-Ni-W SYSTEM, Calphad, 12 (1988) 277-292.

[77] L. Kaufman, P.E.A. Turchi, W. Huang, Z.-K. Liu, Thermodynamics of the Cr-Ta-W system by combining the Ab Initio and CALPHAD methods, Calphad, 25 (2001) 419-433.

[78] E. Vacchieri, A. Costa, G. Roncallo, G. Cacciamani, Service induced fcc→ hcp martensitic transformation in a Co-based superalloy, Materials Science and Technology, 33 (2017) 1100-1107.

[79] B. Grushko, G. Cacciamani, Al-Co (Aliminium-Cobalt), in: G. Effenberg (Ed.), Materials Science International Services GmbH, Stuttgart, 2003.

[80] A.J. McAlister, The Al-Co(aluminum-cobalt) system, Bull Alloy Phase Diagr, 10 (1989) 646-650.

[81] N. Dupin, I. Ansara, Évaluation thermodynamique du système Al-Co, Rev. Met. Paris, 95 (1998) 1121-1130.

[82] F. Stein, C. He, N. Dupin, Melting behaviour and homogeneity range of B2 CoAl and updated thermodynamic description of the Al–Co system, Intermetallics, 39 (2013) 58-68.

[83] P. Priputen, M. Kusý, M. Drienovský, D. Janičkovič, R. Čička, I. Černičková, J. Janovec, Experimental reinvestigation of Al–Co phase diagram in vicinity of $Al_{13}Co_4$ family of phases, J. Alloys Compd., 647 (2015) 486-497.

[84] Y. Wang, G. Cacciamani, Thermodynamic modeling of the Al-Cr-Ni system over the entire composition and temperature range, J. Alloys Compd., 688, Part B (2016) 422-435.

[85] B. Grushko, B. Przepiorzynski, E. Kowalska-Strzeciwilk, M. Surowiec, New phase in the high-Al region of Al-Cr, J. Alloys Compd., 420 (2006) L1-L4.

[86] B. Hu, W.W. Zhang, Y.B. Peng, Y. Du, S.H. Liu, Y.L. Zhang, Thermodynamic reassessment of the Al-Cr-Si system with the refined description of the Al-Cr system, Thermochimica Acta, 561 (2013) 77-90.

[87] H. Wu, M. Zhang, B.J. Xu, G.P. Ling, Preparation and characterization of $Al_{11}Cr_4$ phase by diffusion of Al/Cr composite film, J. Alloys Compd., 610 (2014) 492-497.

[88] B. Grushko, W. Kowalski, D. Pavlyuchkov, B. Przepiorzynski, M. Surowiec,

A contribution to the Al-Cr-Ni phase diagram, J. Alloys Compd., 460 (2008) 299-304.

[89] B. Grushko, W. Kowalski, D. Pavlyuchkov, S. Mi, M. Surowiec, Al-rich region of the Al-Ni-Cr alloy system below 900 ^{O}C, J. Alloys Compd., 485 (2009) 132-138.

[90] H.L. Chen,(Thesis) Phase diagram measurement and thermodynamic modeling of the Al-Cr-Si, Al-Cr-Ti, Al-Cu-Fe, Al-Cu-Ni and Nb-Ni systems, Central South University, China, 2008.

[91] N. Saunders, V.G. Rivlin, Thermodynamic characterization of Al-Cr, Al-Zr and Al-Cr-Zr alloy systems, Mater. Sci. Technol., 2 (1986) 520-527.

[92] I. Ansara, A.T. Dinsdale, M.H. Rand, COST507: Thermochemical Database for Light Metal Alloys, Office for Official Publications of the European Communities, Luxembourg, 1998.

[93] T. Tokunaga, H. Ohtani, M. Hasebe, Thermodynamic assessment of the Al-Cr system by combining the first-principles and CALPHAD methods, Mater. Sci. Forum, 539-543 (2007) 2407-2412.

[94] Y. Liang, C. Guo, C. Li, Z.M. Du, Thermodynamic modeling of the Al-Cr system, J. Alloys Compd., 460 (2008) 314-319.

[95] N. Dupin, I. Ansara, B. Sundman, Thermodynamic re-assessment of the ternary system Al-Cr-Ni, Calphad, 25 (2001) 279-298.

[96] P. Saltykov, L. Cornish, G. Cacciamani, Al-Ni (Aluminium-Nickel), in: G. Effenberg (Ed.), Stuttgart, 2003.

[97] H.L. Chen, E. Doernberg, P. Svoboda, R. Schmid-Fetzer, Thermodynamics of the Al_3Ni phase and revision of the Al-Ni system, Thermochi. Acta, 512 (2011) 189-195.

[98] Y. Du, N. Clavaguera, Thermodynamic assessment of the Al-Ni system, J. Alloys Compd., 237 (1996) 20-32.

[99] W. Huang, Y.A. Chang, A thermodynamic analysis of the Ni-Al system, Intermetallics, 6 (1998) 487-498.

[100] F. Zhang, Y.A. Chang, Y. Du, S.L. Chen, W.A. Oates, Application of the cluster-site approximation (CSA) model to the fcc phase in the Ni-Al system, Acta Mater., 51 (2003) 207-216.

[101] W.A. Oates, S.L. Chen, W. Cao, F. Zhang, Y.A. Chang, L. Bencze, E. Doernberg, R. Schmid-Fetzer, Vacancy thermodynamics for intermediatie phases using the compound energy formalism, Acta Mater., 56 (2008) 5255-5262.

[102] M. Ellner, S. Kek, B. Predel, Ni_3Al_4 - A phase with ordered vacanies isotypic to Ni_3Ga_4, J. Less-Common Met., 154 (1989) 207-215.

[103] S. Kek,(Thesis), University Stuttgart, Germany, 1991.

[104] T. Gödecke, M. Scheffer, R. Lück, S. Ritsch, C. Beeli, Formation and Phase Boundaries of $(Co, Ni)_3Al_4$ and the Ternary X Phase in the Al-AlCo-AlNi System, Z. Metallkd., 88 (1997) 687-697.

[105] D.M. Shi, B. Wen, R. Melnik, S. Yao, T.J. Li, First-principles studies of Al-Ni intermetallic compounds, J. Solid State Chem., 182 (2009) 2664-2669.

[106] K.A. Gschneidner, F.W. Calderwood, The Al-Y (Aluminum-Yttrium) System, Bull. Alloy Phase Diagr., 10 (1989) 44-47.

[107] S. Liu, Y. Du, H. Xu, C. He, J.C. Schuster, Experimental investigation of the Al–Y phase diagram, Journal of Alloys and Compounds, 414 (2006) 60-65.

[108] Q. Ran, H. Leo Lukas, G. Effenberg, G. Petzow, A thermodynamic optimization of the Al-Y system, Journal of the Less Common Metals, 146 (1989) 213-222.

[109] S. Liu, Y. Du, H. Chen, A thermodynamic reassessment of the Al–Y system, Calphad, 30 (2006) 334-340.

[110] Y.-B. Kang, A.D. Pelton, P. Chartrand, C.D. Fuerst, Critical evaluation and thermodynamic optimization of the Al–Ce, Al–Y, Al–Sc and Mg–Sc binary systems, Calphad, 32 (2008) 413-422.

[111] T.B. Massalski, P.R. Subramanian, H. Okamoto, L. Kacprzak, Binary Alloy Phase Diagram, ASM International Materials Park, OH, 1990.

[112] H. Okamoto, Co-Y (Cobalt-Yttrium), J. Phase Equilb., 13 (1992) 326-328.

[113] C.H. Wu, Y.C. Chuang, X.P. Su, Re-Investigation of the Y-Co Binary System, Z. Metallkd., 82 (1991) 73-79.

[114] H. Okamoto, Co-Y (Cobalt-Yttrium), J. Phase Equilb. Diffus., 27 (2006) 309-310.

[115] Z. Du, D. Lü, Thermodynamic modelling of the Co–Y system, Journal of Alloys and Compounds, 373 (2004) 171-178.

[116] W. Golumbfskie, Z.-K. Liu, CALPHAD/first-principles re-modeling of the Co–Y binary system, Journal of Alloys and Compounds, 407 (2006) 193-200.

[117] H. Okamoto, Cr-Y (Chromium-Yttrium), J. Phase Equilb., 13 (1992) 100-101.

[118] V.F. Terekhova, I.A. Markova, E.M. Savitskii, Equilibrium Diagram of the Chromium-Yttrium System, Russ. J. Inorg. Chem., 6 (1961) 641-642.

[119] W. Chan, M.C. Gao, Ö.N. Doğan, P. King, A.D. Rollett, Thermodynamic Assessment of Cr-Rare Earth Systems, Journal of Phase Equilibria and Diffusion, 30 (2009) 578.

[120] Z. Du, W. Zhang, Thermodynamic assessment of the Ni-Y system, Journal of Alloys and Compounds, 245 (1996) 164-167.

[121] M. Mezbahul-Islam, M. Medraj, A critical thermodynamic assessment of the Mg–Ni, Ni–Y binary and Mg–Ni–Y ternary systems, Calphad, 33 (2009) 478-486.

[122] E.S. Moskvitina, V.N. Kuznetsov, L.S. Guzei, Refinement of the Co-Cr-Al Phase-Diagram, Moscow Univ Chem Bull, 33 (1992) 373-374.

[123] K. Ishikawa, M. Ise, I. Ohnuma, R. Kainuma, K. Ishida, Phase equilibria and stability of the bcc aluminide in the Co-Cr-Al system, Berichte der Bunsengesellschaft für physikalische Chemie, 102 (1998) 1206-1210.

[124] X.L. Liu, T. Gheno, B.B. Lindahl, G. Lindwall, B. Gleeson, Z.-K. Liu, First-Principles Calculations, Experimental Study, and Thermodynamic Modeling of the Al-Co-Cr System, PLOS ONE, 10 (2015) e0121386.

[125] N. Dupin, I. Ansara, Thermodynamic assessment of the system Al-Co Rev Metall, 95 (1998) 1121-1129.

[126] T. Velikanova, K. Korniyenko, V. Sidorko, Aluminium-Cobalt-Nickel, 2004.

[127] J. Schramm, The ternary system Nickel-Cobalt-Aluminium, Z. Metallkd., 33 (1941) 403-412.

[128] C.C. Jia, K. Ishida, T. Nishizawa, Partition of alloying elements between γ(A1), γ'($L1_2$), and β(B2) phases in Ni-Al base systems, Metall. Mater. Trans. A, 25 (1994) 473-485.

[129] R. Kainuma, M. Ise, C.C. Jia, H. Ohtani, K. Ishida, Phase equilibria and microstructural control in the Ni-Co-Al system, Intermetallics, 4 (1996) S151-S158.

[130] M. Albers, D. Kath, K. Hilpert, Thermodynamic activities and phase boundaries for the alloys of the solid solution of Co in Ni_3AI, Metall. Mater. Trans. A, 28 (1997) 2183-2188.

[131] W.L. Bai,(Thesis) Thermodynamic modeling and investigation experimental superalloys, University of Genoa, Genoa, 2016.

[132] L. Zhu, C. Wei, H. Qi, L. Jiang, Z. Jin, J.-C. Zhao, Experimental investigation of phase equilibria in the Co-rich part of the Co-Al-X (X=W, Mo, Nb, Ni, Ta) ternary systems using diffusion multiples, J. Alloys Compd., 691 (2017) 110-118.

[133] T. Gödecke, M. Scheffer, R. Lück, S. Ritsch, C. Beeli, Isothermal sections of phase equilibria in the Al-AlCo-AlNi system, Z. Metallkd., 89 (1998) 687-698.

[134] K. Hiraga, T. Ohsuna, S. Nishimura, A new crystalline phase related to an Al–Ni–Co decagonal phase, J. Alloys Compd., 325 (2001) 145-150.

[135] S. Katrych, W. Steurer, Stability range of the ternary W-phase in the system Al–Co–Ni, J. Alloys Compd., 481 (2009) 258-263.

[136] T. Gödecke, M. Ellner, Phase equilibria in the Al-rich portion of the ternary system Co-Ni-Al at 75 and 78 at.% Al, Z. Metallkd., 88 (1997) 382-389.

[137] T. Gödecke, Liquidus projection surface and phase equilibria with liquid of the Al-AlCo-AlNi ternary subsystem, Z. Metallkd., 88 (1997) 557-569.

[138] M. Scheffer, T. Gödecke, R. Lück, S. Ritsch, C. Beeli, Phase equilibria of the decagonal AlCoNi phase, Z. Metallkd., 89 (1998) 270-278.

[139] K. Rzyman, Formation enthalpy of Ni_3Al-based alloys with cobalt additions vs their mechanical properties, J. Chim. Phys., 94 (1997) 1133-1142.

[140] S. Kek, K. Rzyman, F. Sommer, Determination of the enthalpy of formation of ternary Ni_3Al-based alloys, An. Fis., B86 (1990) 31-38.

[141] A. Grün, E.T. Henig, F. Sommer, Calorimetric determination of the enthalpy of formation and the description of the constitu-tional defects of the ordered $(Ni, Co)_{1-y}Al_y$ phase, Z. Metallkd., 89 (1998) 591-597.

[142] N. Dupin,(Thesis) Contribution a l'evaluation Thermodynamique des Alliages Polyconstitutes a Base de Nickel, Institut National Polytechnique de Grenoble, france, 1995.

[143] Y. Wang, P. Zhou, Y. Peng, Y. Du, B. Sundman, J. Long, T. Xu, Z. Zhang, A thermodynamic description of the Al–Co–Ni system and site occupancy in Co + $AlNi_3$ composite binder phase, J. Alloys Compd., 687 (2016) 855-866.

[144] I. Ansara, N. Dupin, H.L. Lukas, B. Sundman, Thermodynamic assessment of the Al-Ni system, J. Alloys Compd., 247 (1997) 20-30.

[145] B. Sundman, N. Dupin, Development of multicomponent thermodynamic

databases for use in process modelling and simulations, XXIXèmes JEEP, Journées d'Etude des Equilibres entre Phases, Lyon, France, (2003) 25-26.

[146] Y. Kitajima, S. Hayashi, T. Narita, Phase equilibria of the nickel-aluminum-chromium system at 1150°C, Mater. Sci. Forum 522-523 (2006) 103-110.

[147] R.W. Culter,(Thesis) The 1200 ^{O}C isothermal sections of the Ni-Al-Cr and the Ni-Al-Mo ternary phase diagrams, The Ohio State University, United States, 2011.

[148] A. Sato, A. Yamamoto, X.Z. Li, K. Hiraga, T. Haibach, W. Steuree, A New Hexagonal K phase of Al-Cr-Ni, Acta Cryst., C53 (1997) 1531-1533.

[149] F. Weitzer, W. Xiong, N. Krendelsberger, S.H. Liu, Y. Du, J.C. Schuster, Reaction scheme and liquidus surface in the Al-rich section of the Al-Cr-Ni system, Metall. Mater. Trans. A 39A (2008) 2363-2369.

[150] S.M. Merchant, M.R. Notis, A Review: constitution of the Al-Cr-Ni system, Mater. Sci. Eng., 66 (1984) 47-60.

[151] I.I. Kornilov, R.S. Mints, Phase diagram of the Cr-Ni-Al system, Izv. Sekt. Fiz. -Khim. Anal, 22 (1953) 111-116.

[152] P. Rogl, Aluminum-Chromium-Nickel, stuttgart, Germany, 1993.

[153] Y.A. Bagaryatskiy, The Cr corner of the Cr-Ni-Al system and the Cr-NiAl pseudobinary section, Zh. Neorg. Khim., 3 (1958) 722-728.

[154] T. Velikanova, K. Korniyenko, V. Sidorko, Aluminum-Chromium-Nickel, Landolt-Bornstein New Series IV, 11A1 (2004) 371-410.

[155] W. Huang, Y.A. Chang, Thermdynamic properties of the Ni-Al-Cr system, Intermetallics, 7 (1999) 863-874.

[156] W. Cao, J. Zhu, Y. Yang, F. Zhang, S. Chen, W.A. Oates, Y.A. Chang, Application of the cluster/site approximation to fcc phases in Ni-Al-Cr system, Acta Mater., 53 (2005) 4189-4197.

[157] T. Maciag, K. Rzyman, Calorimetric studies of the enthalpies of formation of alloys from Ni075Al25-Ni75Cr25 and $Ni_{75}Al_{25}$-$Ni_{85}Cr_{15}$ sections at 873 K, JAMME, 55 (2012) 275-279.

[158] T. Maciag, K. Rzyman, New possibilities of recently constructed high-temperature solution calorimeter, J Therm Anal Calorim, 113 (2013) 189-197.

[159] A. Taylor, R.W. Floyd, The constitution of Nickel-rich alloys of the Nickel-Chromium-Aluminium system, J. Inst. Met., 81 (1952) 451-464.

[160] S. Ochiai, Y. Oya, T. Suzuki, Solubility data in Ni_3Al with ternary addition, Bul. P.M.E., 52 (1983) 1-16.

[161] Y.M. Hong, H. Nakayama, Y. Mishima, T. Suzuki, The γ-Solvus Surface in Ni-Al-X (X=Cr, Mo and W) Ternary Systems, Mat. Res. Soc. Symp. Proc., 133 (1989) 429.

[162] D. David,(Thesis), Institut National Polytechnique de Grenoble, France, 1990.

[163] P. Saltykov, V.T. Witusiewicz, I. Arpshofen, O. Fabrichnaya, H.J. Seifert, F. Aldinger, Thermodynamics of liquid and undercooled liquid Al-Cr-Ni alloys, Scand. J. Metall., 30 (2001) 297-301.

[164] S. Kek, C. Rzyman, F. Sommer, An. Fis. B, 86 (1990) 31-38.

[165] N.C. Oforka, B.B. Argent, Thermodynamics of Ni-Cr-Al alloys, J. Less-Common Met., 114 (1985) 97-109.

[166] G.P. Goretsky, Study of alloys of binary eutectics α+γ and α+β in the Ni-Cr-Al systems, Metally, (1992) 199-202.

[167] C.C. Jia, K. Ishida, T. Nishizawa, Partition of alloying elements between γ(Al), γ'($L1_2$) and β(B2) phases in Ni-Al base systems, Metall. Mater. Trans. A, 25 (1994) 473-485.

[168] P. Brozh, M. Svoboda, J. Bursik, A. Kroupa, J. Havrankova, Theoretical and experimental study of the influence of Cr on the γ+γ' phase field boundary in the Ni-Al-Cr system, Mater. Sci. Eng., A 325 (2002) 59-65.

[169] N. DeLanerolle, L.L. Seigle, State University of New York at Stony Brook, USA, 1983.

[170] L.A. Carol,(Thesis) A Study of Interdiffusion in β+γ/γ+γ' Ni-Cr-Al alloys at 1200^{o}C, Michigan Technological University, USA, 1984.

[171] C.W. Yeung, W.D. Hopfe, J.E. Morral, A.D. Romig, experimental methods of phase diagram determination, 1994.

[172] M.S. Qiao,(Thesis) Interdiffusion microstructure in γ+β/γ+γ'diffusion couples, University of Connecticut, 1998.

[173] I.I. Kornilov, R.S. Mints, The Fusibility Diagram of the Ni-Cr-NiAl System, Dolk. Akad. Nauk. SSSR, 94 (1954) 1085-1088.

[174] P.K. Sung, D.R. Poirier, Liquid-solid partition rations in Nickel-base alloys, Metall. Mater. Trans. A, 30A (1999) 2173.

[175] M. Ellner, K. Kolatschek, B. Predel, On the partial atomic volume and the partial molar enthalpy of aluminium in some phases with Cu and Cu_3Au structures, J. Less-Common Met., 170 (1991) 171-184.

[176] R.M. Rykhal, O.S. Zarechnyuk, Y-Co-Al Ternary System in the Region 0-33.3 at.% Y, Dop. Akad. Nauk Ukr. RSR A, Fiz-Mat. Tekh., 33 (1971) 854-956.

[177] Y. Jiang, X. Li, Y. Jiang, S. Huang, X. Shi, C. Mao, L. Zhang, L. Liu, F. Zheng, Experimental investigation of phase relations in Al-Co-Y ternary system, Calphad, 56 (2017) 1-9.

[178] O. Bodak, Al-Co-Y (Aluminium - Cobalt - Yttrium), in: G. Effenberg, S. Ilyenko (Eds.) Light Metal Systems. Part 1: Selected Systems from Ag-Al-Cu to Al-Cu-Er, Springer Berlin Heidelberg, Berlin, Heidelberg, 2004, pp. 303-309.

[179] L. Guzei, Aluminium-Chromium-Yttrium, stuttgart, 1991.

[180] O.S. Zarechnyuk, P.M. Rykhal, N.V. Herman, X-ray investigation of the Aluminium-rich alloys of the systems Yttrium-Vanadium-Aluminium and Yttrium-Chromium-Aluminium, Visn. L'viv. Univ. Ser. Khim, 12 (1971) 10-12.

[181] R. Ferro, G. Zanicchi, R. Marazza, Aluminium - Nickel - Yttrium, stuttgart, Germany, 1993.

[182] S. Rosen, J.A. Goebel, Phase equilibria in the nickel-aluminium-yttrium system at 1000 °C, Journal of the Less Common Metals, 16 (1968) 285-287.

[183] R.M. Rykhal, O.S. Zarechnyuk, sothermal 800 ^{o}C Section of the Ternary System Y-Ni-Al in the Range 0-33.3 at.% Y, Dop. Akad. Nauk Ukr. RSR A, Fiz-Mat. Tekh., 4 (1977) 375.

[184] R. Raggio, G. Borzone, R. Ferro, The Al-rich region in the Y–Ni–Al system: microstructures and phase equilibria, Intermetallics, 8 (2000) 247-257.

[185] P. Nash, H.N. Su, O. Kleppa, Enthalpies of Formation of Compounds in the Al-Ni-Y System, Trans. Nonferr. Met. Soc., 12 (2002) 754-758.

[186] W.J. Golumbfskie, R. Arroyave, D. Shin, Z.K. Liu, Finite-temperature thermodynamic and vibrational properties of Al–Ni–Y compounds via first-principles calculations, Acta Materialia, 54 (2006) 2291-2304.

[187] D. Shin, W.J. Golumbfskie, E.R. Ryba, Z.-K. Liu, First-principles study of Al–Ni–Y ternary compounds for crystal structure validation, Journal of Alloys and Compounds, 462 (2008) 262-266.

[188] O. Matselko, S. Pukas, Y. Lutsyshyn, R. Gladyshevskii, D. Kaczorowski, Ternary aluminides R0.67Ni2Al6 (R=Sc, Y, Gd–Lu) with partly disordered structures, Journal of Solid State Chemistry, 198 (2013) 50-56.

[189] C. Benndorf, H. Eckert, O. Janka, Ternary rare-earth aluminium intermetallics $RE_{10}TAl_3$ (RE = Y, Ho, Tm, Lu; T = Fe, Co, Ni, Ru, Rh, Pd, Os, Ir, Pt) with an ordered anti-Co_2Al_5 structure, Dalton Transactions, 46 (2017) 1083-1092.

[190] J. Huang, B. Yang, H. Chen, H. Wang, Thermodynamic Optimisation of the Ni-Al-Y Ternary System, Journal of Phase Equilibria and Diffusion, 36 (2015) 357-365.

[191] Z. Du, D. Lü, Thermodynamic modeling of the Co–Ni–Y system, Intermetallics, 13 (2005) 586-595.

[192] O.I. Kharchenko, O.I. Bodak, E.I. Glady-Shevskii, Interactions of Yttrium with Metals of the Iron Group, Metalli, 1 (1977) 200-205.

[193] W.B. Xue, G.Q. Liu, W.J. Zhang, Y. Zhang, H.S. Shen, Experimental Study of 1000 ^{O}C Isothermal Section of Y-Co-Ni System J. Univ. Sci. Technol., Beijing, 17 (1995) 243-248.

[194] W.B. Xue, G.Q. Liu, W.J. Zhang, Y. Zhang, H.S. Shen, Experimental Study of 1175 ^{O}C Isothermal Section of Y-Co-Ni System J Rare Metals, 19 (1995) 281-285.

[195] P. Brož, J. Buršík, M. Svoboda, A. Kroupa, Theoretical and experimental study of the γ and γ′ equilibrium in Ni-based superalloys, Materials Science and Engineering: A, 324 (2002) 28-33.

[196] P. Brož, J. Buršík, R. Picha, Theoretical and experimental study of the γ and γ′ equilibrium in the Ni–Al–Cr–Co system, Intermetallics, 10 (2002) 635-639.

[197] J. Buršík, P. Brož, J. Popovič, Microstructure and phase equilibria in Ni–Al–Cr–Co alloys, Intermetallics, 14 (2006) 1257-1261.

[198] T. Gheno, X.L. Liu, G. Lindwall, Z.-K. Liu, B. Gleeson, Experimental study and thermodynamic modeling of the Al–Co–Cr–Ni system, Science and Technology of Advanced Materials, 16 (2015) 055001.

[199] X. Liu,(Thesis) Design of Ni-base superalloys and MCrAlY coatings from first-principles and computional thermodynamics The Pennsylvania State University, 2015.